Université de Montréal

THE ROLE OF EPHB6 AND EPHRINBS IN BLOOD PRESSURE REGULATION

par
Zenghui Wu

Département de Sciences Biomédicales
Faculté de Médecine

Thèse présentée à la faculté des études supérieures
en vue de l'obtention du grade de
Philosophiae Doctor (Ph.D.)
en sciences biomédicales

Décembre 2012

Université de Montréal

Faculté des études supérieures

Cette thèse intitulée:

<<THE ROLE OF EPHB6 AND EPHRINBS IN BLOOD PRESSURE REGULATION>>

Présentée par:

Zenghui Wu

a été évaluée par un jury composé des personnes suivantes:

Dr Edward Bradley

……

Président du jury

Dr Jiangping Wu

……

Directeur de recherche

Dr Hongyu Luo

……

Directeur de recherche

Dr Jonathan Ledoux

……

Membre du jury

Dr Serge Lemay

……

Examinateur externe

Dr Marie-Josée Hébert

……

Repésentante de la doyenne

Résumé

L'hypertension artérielle est le facteur de risque le plus important dans les maladies cardiovasculaires (MCV) et les accidents vasculaires cérébraux (AVC). L'hypertension artérielle essentielle est une maladie complexe, multifactorielle et polygénique. Même si on a identifié de nombreux facteurs de risque de l'hypertension artérielle, on ne comprend pas encore clairement les mécanismes qui la régissent.

Les kinases hépatocytes produisant l'érythropoïétine (Eph) constituent la plus grande famille des récepteurs tyrosine kinase qui se lient à des ligands de surface cellulaire appelés éphrines sur les cellules avoisinantes. On sait que les interactions de Eph et des éphrines sont essentielles aussi bien dans les processus de développement que dans le fonctionnement des organes et des tissus adultes. Cependant on n'a pas encore étudié la relation entre Eph/éphrines et l'hypertension artérielle.

Nous avons créé des modèles de souris knockout (K.O.) Ephb6$^{-/-}$, Efnb1$^{-/-}$ et Efnb3$^{-/-}$ pour cette étude. Dans le modèle EphB6$^{-/-}$, nous avons observé que les souris K.O. Ephb6 castrées, mais pas les femelles, ainsi que les souris mâles non castrées présentaient une tension artérielle élevée (TA) par rapport à leurs homologues de type sauvage (TS). Ceci suggère que Ephb6 doit agir de concert avec l'hormone sexuelle mâle pour réguler la TA. Les petites artères des mâles castrés Ephb6$^{-/-}$ présentaient une augmentation de la contractilité, une activation de RhoA et une phosphorylation constitutive de la chaîne légère de la myosine (CLM) lorsque comparées à celles de leurs homologues TS. Ces deux derniers résultats indiquent que la phosphorylation de CLM et de RhoA passe par la voie de signalisation de Ephb6 dans les cellules du muscle lisse de la paroi vasculaire (CMLV). Nous avons démontré que la réticulation de Efnbs mais non celle de Ephb6 aboutit à une réduction de la contractilité des CMLV. Ceci montre que l'effet de Ephb6 passe par la signalisation inversée à travers Efnb.

Dans le modèle Efnb1$^{-/-}$ conditionnel spécifique au muscle lisse, nous n'avons observé aucune différence entre Efnb1$^{-/-}$ et les souris de TS concernant la mesure de la TA dans des conditions normales. Cependant, la TA des souris K.O. Efnb1 lors d'un stress d'immobilisation est supérieure à celle des souris de TS. Dans les petites artères des souris K.O. Efnb1, le rétrécissement et la phosphorylation de CLM étaient élevés. In vitro, la contractilité et

l'activation RhoA de la CMLV des souris TS étaient augmentées quand leur Efnb1 était réticulé. Ces résultats corroborent ceux des souris KO Ephb6 et prouvent que l'effet de Ephb6 dans le contrôle de la TA se produit au moins par l'intermédiaire d'un de ses ligands Efnb1 dans les CMLV.

Dans le modèle Efnb3$^{-/-}$, on a observé une augmentation de la TA et du rétrécissement des vaisseaux chez les femelles Efnb3$^{-/-}$, mais non chez les mâles; l'échographie a aussi révélé une résistance accrue au débit sanguin des souris K.O. femelles. Cependant la mutation de Efnb3 ne modifie pas la phosphorylation de la CLM ou l'activation de RhoA in vivo. Dans l'expérience in vitro, les CMLV des souris femelles Efnb3$^{-/-}$ ont présenté une augmentation de la contractilité mais pas celle des souris mâles Efnb3$^{-/-}$. La réticulation des CMLV chez les mâles ou les femelles de TS avec solide anti-Efnb3 Ab peut réduire leur contractilité.

Notre étude est la première à évaluer le rôle de Eph/éphrines dans la régulation de la TA. Elle montre que les signalisations Eph/éphrines sont impliquées dans le contrôle de la TA. La signalisation inverse est principalement responsable du phénotype élevé de la TA. Bien que les Efnb1, Efnb3 appartiennent à la même famille, leur fonction et leur efficacité dans la régulation de la TA pourraient être différentes. La découverte de Eph/Efnb nous permet d'explorer plus avant les mécanismes qui gouvernent la TA.

Mots-clés : Eph; Efnb; hypertension; cellule du muscle lisse vasculaire; tension artérielle

Abstract

Hypertension is the most important risk factor for the cardiovascular diseases (CVD) and strokes. The essential hypertension is a complex, multifactorial and polygenic disease. Although many hypertension risk factors have been identified, the comprehensive understanding of mechanisms remains elusive.

Erythropoietin-producing hepatocyte kinases (Ephs) are the largest family of receptor tyrosine kinases, which bind to cell surface ligands called ephrins on neighboring cells. Eph and ephrin interactions are known to be essential in developmental processes, as well as in functions of adult organs and tissues. However the relationship between Ephs/ephrins and hypertension has not been studied.

Ephb6$^{-/-}$, Efnb1$^{-/-}$ and Efnb3$^{-/-}$knockout mice models were established for this study. In the EphB6$^{-/-}$ model, we observed that the castrated Ephb6 KO mice but not female or uncastrated male mice presented heightened blood pressure (BP) compared to the wild type (WT) counterparts. This suggests that Ephb6 needs to act in concert with sex hormone to regulate blood pressure. Small arteries from castrated Ephb6$^{-/-}$ males showed increased contractility, RhoA activation and constitutive myosin light chain (MLC) phosphorylation compared to their WT counterparts. The latter two findings indicate that RhoA and MLC phosphorylation are in the signaling pathway of Ephb6 in vascular smooth muscle cell (VSMC). We demonstrated that, crosslinking of Efnbs but not Ephb6 resulted in reduced VSMC contractility. This indicates that the effect of Ephb6 is via reverse signaling through Efnbs.

In smooth muscle-specific conditional Efnb1$^{-/-}$ model, no difference was observed between Efnb1$^{-/-}$ and WT mice in BP measurement under a normal condition. However, the BP of Efnb1 KO mice during immobilization stress were higher than that of WT mice. In the small arteries from Efnb1 KO mice, the constriction and MLC phosphorylation were elevated. In vitro, the contractility and RhoA activation of WT VSMC were augmented when their Efnb1 was crosslinked. These results corroborate the findings from Ephb6 KO mice, and prove that the effect of Ephb6 in BP control is at least via one of its ligand Efnb1 in VSMC.

In the Efnb3$^{-/-}$ model the heightened BP and increased vessel constriction were observed in Efnb3$^{-/-}$females but not males; the echography also revealed the increased blood flow resistance of female KO mice. However the mutation of Efnb3 doesn't alter the MLC phosphorylation or

RhoA activation in vivo. In in vitro experiment, VSMCs from Efnb3$^{-/-}$ female mice showed increased contractility but did not Efnb3$^{-/-}$ male mice. Crosslinking of VSMCs from WT males or females with solid anti-Efnb3 Ab can reduce their contractility.

Our study is the first to assess the role of Eph/ephrins in BP regulation. Eph/ephrins signalings are involved in the regulation of BP. The reverse signaling is mainly responsible for the elevated BP phenotype. Although the Efnb1, Efnb3 belongs to the same family, their function and effectiveness in the regulation of BP might be different. The discovery of Eph/Efnbs allows us to further explore the mechanism in BP.

Keywords: Eph; Efnb; hypertension; vascular smooth muscle cell; blood pressure

INDEX

List of figures and tables

INTRODUCTION

ARTICLE 1

ARTICLE 2

ARTICLE 3

DISCUSSION

List of abbreviations

Ab	Antibody
ACE	Angiotensin-converting enzyme
Akt	Protein kinase B
AMPAR	AMPA receptor
Ang II	Angiotensin II
AP	Arterial pressure
ApoER2	Apolipoprotein E receptor 2
AT1	Angiotensin receptor type 1
AT2	Angiotensin receptor type2
ATIP1	AT_2R interacting protein-1
ATRAP	AT_1R-associated protein
BM	Bone marrow
BM progenitors	Bone marrow progenitors
BP	Blood pressure
CDC42	Cell division control protein 42 homolog
CFNS	Craniofrontonasal syndrome
cGMP	Cyclic guanosine 3', 5'-monophosphate
CIL	Contact inhibition of locomotion
COX2	Cyclo-oxygenase 2
CRC	Colorectal cancers
CS	Cyclic stretch
CVD	Cardiovascular disease
CXCL	Chemokine (C-X-C motif) ligand
DP	Diastolic pressure
ECM	Extracellular matrix
eGFP	Enhanced green fluorescent protein

GEPR	G protein-coupled estrogen receptor
ENAC	Epithelial sodium channel
eNOS	Endothelial nitric oxide synthase
Eph	Erythropoietin-producing hepatocellular
ERE	Estrogen response element
ERK	Extracellular signal-regulated kinases
ERs	Estrogen receptors
FAK	Focal adhesion kinase
FGF	Fibroblast growth factor
FGFR1	Fibroblast growth factor receptor 1
GAP	GTPase activating protein
GEFs	Guanine nucleotide exchange factors
GEPR	G protein-coupled estrogen receptor 1
GDI	Guanosine nucleotide dissociation inhibitor
GPCRs	G-protein-coupled receptors
GPI	Glycosylphosphatidylinositol
GPI-ANCHOR	Glycosylphosphatidylinositol anchor
GRIP 1	Glutamate receptor-interacting protein 1
Grb2	Growth factor receptor-bound protein 2
GTP	Guanosine triphosphate
HR	Heart rate
Hsp90	Heat shock protein 90
IgD	Immunoglobulin D
IgG	Immunoglobulin G
IP3	Inositol triphosphate
iNOS	Inducible NOS
KO	Knockout
LARG	Leukemia associated Rho guanine nucleotide exchange factor
LECs	Lymphatic endothelial cells
LO	Lipoxygenase

LTP	Long term depression
MAP	Mean arterial pressure
MAPK	Mitogen-activated protein kinase
MET	Mesenchymal-epithelial transition
MHC	Major histocompatibility complex
miRNA	MicroRNA
MLC_{20}	Myosin light chain
MLCK	Myosin light chain kinase
MLCP	Myosin light chain phosphatase
MMP-2	Matrix metalloprotease 2
MYPT1	Myosin-targeting subunit 1
MR	Mineralocorticoid receptor
NC	Neural crest
NCC	Neural crest cell
NMDA	N-methyl-D-aspartate
NMDAR	N-methyl-D-aspartate receptor
NO	Nitric oxide
NOS	Nitric oxide synthase
NSCLC	Non-small-cell lung cancer
O_2^-	Superoxide
$ONOO^-$	Peroxynitrite
PAK	P21 protein-activated kinase
PARP	Poly-ADP-ribose polymerase
PDAC	Pancreatic ductal adenocarcinoma
PDGF	Platelet-derived growth factor
PI3K	Phosphatidylinositide 3-kinases
PLC	Phospholipase C
PDZ	Psd-95,DlgA and ZO1
PICK1	PKC-intracting protein 1
PP2A	Protein phosphatase 2

PRR	Pro-renin receptor
PYK2	Protein tyrosine kinase 2
RAAS	Rennin-angiotensin aldosterone system
RACK1	Receptor activated C-kinase 1
RANKL	Receptor activator of NF-κB ligand
RAS	Rennin-angiotensin system
RBD	Receptor-binding domain
RELN	Secreted glycoprotein reelin
ROS	Reactive oxygen species
RNA	Ribonucleic acid
RTK	Receptor tyrosine kinase
RT-qPCR	Reverse transcription quantitative polymerase chain reactioin
SAM	Serile α-motif
SH2	Src Homology 2
sGC	Soluble guanylate cyclase
SOC	Store-operated Ca2+ channels
SR	Sarcoplasmic reticulum
TCR	T cell receptor
Tg	Transgenic
TRP	Transient receptor potential
VEGF	Vascular endothelial growth factor
VEGFR	Vascular endothelial growth factor receptor
VLDLR	Very-low density lipoprotein receptor
VSMCs	Vascular smooth muscle cells
WT	Wild type

Acknowledgements

I would like to express my sincere gratitude to my supervisor Dr. Jiangping Wu and Dr. Hongyu Luo for their scientific guidance and encouragement throughout my study and during the preparation of thesis.

I would like to thank all the colleagues in the lab for their kindly cooperation.
Thanks also extended to all my friends and those who always support me in different ways.

Finally, I would like to thank all of my family members for their understanding, patience, and their great support, which were critically important for me to complete this study.

I. INTRODUCTION

Part I

Structure and function of Eph/ephrin family members

Receptor tyrosine kinases (RTKs) are trans-membrane glycoproteins [1, 2], which are the key components of signaling pathways involved in cell proliferation[3], differentiation, migration and metabolism [4, 5]. The activation of RTKs is due to the binding of their cognate ligands, by which they transduce the extracellular signal to cytoplasm through auto-phosphorylation process. The receptor tyrosine kinases are widely spread among different organs, and are involved in different kinds of cellular processes. More than 90 tyrosine kinase genes have been identified in human genome. 58 are cell surface receptors, which are divided into 20 subfamilies [6, 7].

The Eph receptors are the largest family of receptor tyrosine kinases[8], which are successfully isolated from the cDNA of erythropoietin-producing hepatocellular carcinoma cell line[9]. Since then, the Eph receptors have been identified in affecting the physiological and pathological processes in many cell types and organs[10], such as axon guidance, angiogenesis, tissue border formation, cell adhesion and cell migration [11-14]. As the Eph receptor-interacting proteins[15], ephrins also involve in many aspects of cell survival, differentiation, proliferation, and migration[16].

The initial subdivision of Ephs into EphA and EphB classes was based on similarities in extracellular sequences[8], and a corresponding binding preference to either the glycosylphosphatidylinositol anchored ephrin-A ligands or the three transmembrane ephrin-B ligands. Eph-ephrin interactions are promiscuous, but EphA members preferentially bind to ephrinAs, and EphBs bind to ephrinBs.

There are 16 members of Eph receptors identified in mammals[17]. EphA1-EphA10 bind to 5 ephrinAs; EphB1-EphB6 bind to 3 ephrinBs. As stated above, ten EphA (EphA1-A10) members promiscuously interact with 5 A-ephrins (EfnA1-A5) and six different EphBs (EphB1-B6) promiscuously interact with 3 B-ephrins (EfnbB1-B3). However, EphB2 can also bind to ephrinA5, and EphA4 binds to ephrinB2 [18].

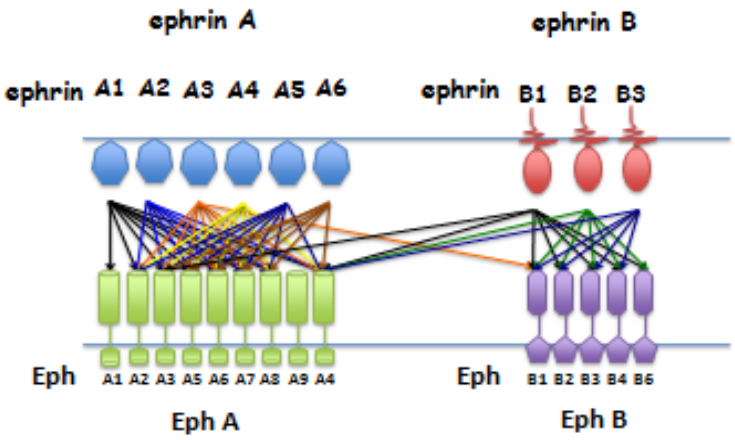

Figure 1 the family of Eph/ephrin proteins

1.1 Structure and signaling mechanism of Eph/ephrins

Like all RTKs, Eph receptors are type I trans-membrane protein. The functional domains can be divided into extracellular and intracellular region. The extracellular region contains ligand-binding globular domain of a highly conserved N-terminal sequence, which is both necessary and sufficient for ligand recognition and binding. The binding domain is followed by a cysteine-rich region and two fibronectin type III repeats[19], which might be involved in receptor-receptor dimerization interactions or other proteins such as the NMDA receptors.

The cytoplasmic part of Eph receptors can be divided into four functional units: the juxtamembrane domain containing two conserved tyrosine residues; a classical protein tyrosine kinase domain, a serile α-motif (SAM) and a PDZ-domain-binding motif. The resolved structure of SAM domain (around 70 amino acids) indicates that Eph receptor could form dimers and oligomers. The PDZ-binding motif is located in the carboxy-terminal with 4-5 amino acid residues, which contains a consensus binding sequence that includes a hydrophobic residue (usually valine or isoleucine).

As ligands of Eph receptors, ephrins are membrane-anchored proteins or transmembrane proteins. EphrinAs have an extracellular Eph receptor-binding domain; and they directly attach to the cell surface without the intracellular tail. EphrinBs are transmembrane proteins. The extracellular Eph receptor-binding domain is located at its N-terminus, and about 3 amino-acid PDZ-binding motifs are at the carboxy terminus.

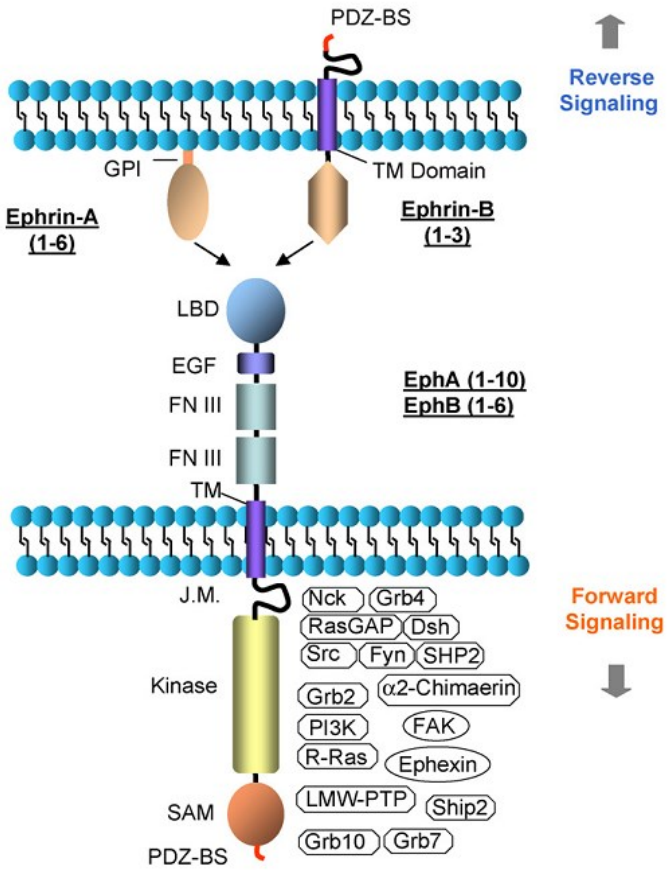

Figure 2 structure of Eph/ephrin proteins [20]

As Ephs and ephrins are membrane proteins, they can only interact within short distance. Eph receptors are activated once they are bound by clustered ephrins on membrane between two neighboring cells, which express Ephs and ephrins respectively.

The first step in the formation of an Eph/ephrin "signaling cluster" is the monovalent interaction between Eph and ephrin in juxtaposed cell surface, which occurs with nanomolar affinity[21]. The Eph/ephrin complexes can progressively aggregate into larger

clusters, the size of which depend on the densities of Eph receptors and ephrins on the cell surface[21].

The significant characteristics of Eph/ephrin signaling pathway is bi-directionality [22]. The forward signals depend on Eph kinase activity in receptor-expressing cell, in which Eph/ephrin complex induces the initiation of Eph signaling through auto-phosphorylation, such as phosphorylation of juxtamembrane domain and downstream target proteins [23]. The reverse signal depends on Src family kinases in eprhin-expressing cells [22].

Several years of studies have revealed that Ephs/ephrins have many effects on different aspects of cell activities and broad roles in normal physiology and in pathogenesis: such as angiogenesis [24], the development of neurons [25], cardiovascular development [26, 27] and tumorigenesis [28] et al.

1.2 Ephs/ephrins in nervous system

In the literature, many papers show that Eph/ephrin signaling plays an essential role during the process of synapse formation and neuronal plasticity[29]. It is known that Ephs are expressed in developing and mature nervous system, with classic functions of mediating axon guidance and target recognition[30].

The roles of Eph receptors in spine morphogenesis have been widely studied. As small protrusions, the dendritic spines are located on the surface of dendrite, which receive the excitatory synapses and are responsible for synaptic transmission and long-term memory. N-methyl-D-aspartate (NMDA)-type glutamate receptors are essential for activity-dependent synaptic plasticity[31] and memory formation[32].

Eph forward signaling has effects on spine and synapse formation[31]. It is known that dynamic formation and retraction of spines is one of features underlying synaptic plasticity and possibly long-term memory [33].

Eph receptors expressed on dendrites are activated by ephrins, which are expressed on axons or astrocytes and regulate spine and synapse formation. Eph/ephrin complex participates in activity-induced long-term changes in synaptic strength[34].

In hippocampus, several Ephs have been localized to dendrites and spines[33, 34]. The experiment of null mutant mice has clearly indicated a functionally redundant requirement of three EphB receptors in dendritic spine morphogenesis[33]. For example EphB2-deficient

mice show modestly reduced hippocampal long-term potentiation. In this model, EphB2 receptors associate with NMDA receptors at synaptic sites and play a role in synaptogenesis. Eph/ephrin complex induces the clustering of NMDA receptors and promotes morphogenesis of dendritic spines; in the meantime forward signaling can stabilize clustering of NMDAR to further enhance NMDAR-dependent Ca^{2+} flux [35]. Although normal hippocampus synapse morphology still exists, the deletion of EphB2 drastically impairs long-lasting LTP and leads to extinguish LTD and depotentiation [33].

EphB2 interacts with Syndecan-2 of trans-membrane heparin sulfate proteoglycan to induce mature spine morphology in mouse brain [36]. EphB2 also plays an important role in the regulation of AMPAR, which mediates most fast excitatory synaptic transmission [37]. Under the stimulation of ephrinB, the EphB2 co-clusters with Glu2 and Glu3 subunits of AMPAR, mediates the interaction between AMPAR binding protein and PKC-intracting protein 1 (PICK1) or GRIP1 through PDZ motif [38].

As mentioned before, EphB2 controls AMPA-type glutamate receptor localization through PDZ binding domain interactions and triggers presynaptic differentiation via its ephrin binding domain. However, not all the EphBs exhibit equal effects during the spine and synapse formation. Triple null mutation of EphB1-3 leads to synapse number reduction; double mutants (EphB1/EphB2, EphB1/EphB3, EphB2/EphB3) show obvious defects in spine formation; however, the EphB1/EphB2 mutant leads severe defects than other mutants in spine formation [39]. The re-expression of EphB2 is sufficient to rescue phenotype and support normal function of spine in $EphB2^{-/-}$ mice.

In cultured hippocampal neurons, EphB receptors regulate spine morphology by modulating the activity of Rho family GTPases. This process involves the activation of focal adhesion kinase (FAK) [40], Src, Grb2 and paxillin, among which FAK is a non-receptor tyrosine kinase that is widely expressed in different cells and is typically activated after assembly of integrin-mediated focal adhesions. Spine morphogenesis is shown to depend on signaling of kalinrin/Rac1 and intersectin/Cdc42/N-WASP to promote filamentous actin formation [41]. EphA binds and activates ephexin, which is a member of Dbl family of exchange factors that activate RhoA and suppress Cdc42 [42]. In the meanwhile, the EphBs appear to be linked to GEFs, such as the kalinrin and intersectin, with exchange activity towards Rac1 and Cdc42 respectively.

EphrinBs are also essential in regulation of neuronal migration and plasticity in brain during the process of neuronal migration and proper functional maintenance. The secreted glycoprotein reelin (RELN) guides migration of neurons by binding to two lipoprotein receptors, the very-low density lipoprotein receptor (VLDLR) and apolipoprotein E receptor 2 (ApoER2). Loss of reelin function in humans results in a severe developmental disorder lissencephaly and other neurological disorders such as Alzheimer's disease and schizophrenia[43]. Compound mouse mutants ($Reln^{+/-}$/$EphrinB3^{-/-}$, $Reln^{+/-}$ /$EphrinB2^{-/-}$) and triple EphrinB1, B2, B3 knockout mice show neuronal migration defects. Clustering of ephrinBs recruit and phosphorylate Dab1, which is necessary for the activation of Reelin signaling [44]. Therefore, the lack of EphrinBs in neurons causes interruption between Reelin and Dab1, leading to a reduced phosphorylation of Dab1 then neuronal migration defects.

In humans, mutations in ephrinB1 lead to the craniofrontonasal syndrome (CFNS) by disturbing the crest/mesoderm boundary formation [45]. CFNS is an X-linked developmental disorder that different gender shows the different phenotypes: females have frontonasal dysplasia and cornal craniosynostosis (fusion of the coronal sutures); in males, hypertenlorism is the only typical manifestation. PDZ-dependent reverse ephrinB1 signaling is also critical for the formation of a major commissural axon tract and the corpus callosum[46]. The miR-124 of an abundant brain microRNA (miRNA) acts as a posttranscriptional effector to regulate ephrinB1 reverse signaling[47] in development of neural tube[48].

Plasticity is essential for maintaining memory and learning. AMPA receptors, which are the main transducers of rapid excitatory transmission in the brain, are pivotal in this process. EphrinB2 signaling is critical for the stabilization of AMPA receptors on cellular membrane. The lack of ephrinB2 enhances internalization of AMPA receptors on cell membrane and reduces synaptic transmission [49].

EphrinB3 regulates the morphogenesis of postsynaptic compartment by transducing the tyrosine phosphorylation/SH2-dependent and PDZ-dependent reverse signaling [50]. It is reported that $ephrinB3^{-/-}$ mice exhibit peculiar hopping gaits, which are correlated to the loss of unilateral motor control. As a midline repulsive barrier, EphrinB3 prevents corticospinal tract axons from re-crossing once they enter the spinal gray matter[51]. EphrinB3 also induces axon pruning by binding the sytoplasmic SH2/SH3 adaptor protein

Grb4, which functions as a molecular bridge to connect activated tyrosine-phosphorylated intracellular domain of ephrinB3 with Dock180, Rac/Cdc 42, and PAK[52].

1.3 Ephs/ephrins in immune system

Ephs and ephrins are widely expressed in lymphoid organs[53-55] as well as lymphocytes [56]. Study shows that Eph/Ephrin signaling is essential for thymus migration during the organogenesis and lymphocyte maturation [57, 58]. Thymus organogenesis requires coordinated interactions of multiple cell types, such as neural crest (NC) cells, mesenchymal cells and thymic epithelial cells [59]. EphB2$^{-/-}$, EphB3$^{-/-}$, EphB2$^{-/-}$/EphB3$^{-/-}$ mice show significantly decreased thymic cellularity compared to WT mice [60]

The formation, separation, and subsequent migration are critical for the development of thymus[59]. EphrinB2 plays an important role in correct position of thymus on NC-derived cells. The conditional mutation of ephrinB2 in the NC-derived cell leads to abnormal anatomical location of thymus [57]. However, deletion of ephrinB2 doesn't disturb separation of thymus. EphA4 also influences the development of thymus through alternations of epithelial network development. The EphA4$^{-/-}$ mice show smaller thymuses compared to wild-type controls [54].

The migration of lymphoid progenitors from fetal liver or bone marrow (BM) into thymic parenchyma is the first step of intrathymic T cell development, and following steps are essential for immature thymocytes, which develop their proper function through distinct thymic epithelial environment [61]. EphB2 regulates the response of BM progenitors to extracellular matrix (ECM) ligand and chemokine. Deletion of EphB2 in BM progenitors exhibits a decreased migratory response to ECM ligands and chemokines (CXCL12, CXCL21, and CXCL25) [62]. EphA1, EphA4 regulate the migration of CD4$^+$ T lymphocyte and induce tyrosine phosphorylation of PYK2, which associates with Src family kinase members [63, 64].

Binding of ephrinA1 and EphA receptors stimulates migration on CD4$^+$and CD8$^+$ T cell [65, 66]. However, ephrinA1 induced migration is mainly found in CD45RO$^+$ memory subset cells [67]. Stimulation of Eph receptors leads to migration involving activation of Lck, Pyk2, PI3K, Vav1 and Rho GTPase in CD8$^+$ CCR7 T cells [67].

T cell receptor (TCR), located on the cell surface with a highly diverse repertoire of αβ chains, is responsible for recognizing antigens and bounding to major histocompatibility complex (MHC) molecules[68]. This recognition process is crucial for T cell differentiation and maturation [68]. Studies have shown that Eph receptors modulate responses mediated by TCR [69]. Under suboptimal condition, EphB6 cross-linked with EphB6 Ab leads to drastic T cell proliferation; $EphB6^+$ T cell has stronger response to anti-CD3 and anti-CD28 activation than $EphB6^-$ T cell. EphB6 is aggregated and co-localized with TCR to enhance the following response through the activation of p38 MAPK signaling pathway[69, 70]. EphrinB1 and ephrinB2 are involved in thymocyte development and peripheral T cell differentiation [71, 72]. EphB3/EphB6 induced reverse signaling of ephrinB1/ephrinB2 strongly suppresses Fas-induced apoptosis in Malignant T lymphocytes, in which the activation is associated with promotion of Akt activation and the inhibition of the Fas receptor-initiated caspase proteolytic cascade [73]. EphrinB1/B2 also interacts with IL 7Rα to promote the IL7-indeuced internalization in T cell [74, 75].

EphA receptors inhibit TCR-induced (anti-CD3) apoptosis of $CD4^+CD8^+$ thymocytes in culture and selection process in vivo [76]. The immobilized EphB2-Fc and EfnB1-Fc fusion protein, at certain concentration can modulate anti-CD3 Ab induced apoptosis of $CD4^+CD8^+$ thymocytes [58].

Eph/ephrin signaling is also involved in the regulation of B cell[77]. EphA4 and EphA7 are expressed on B cells [77]. The activated human B lymphocytes express ephrinA4 [78]. EphrinB3 specifically binds to B lymphocytes in blood through the sulphated cell surface receptor [79], in which the binding of ephrinB3 and B cell induces migration of IgD^- memory B cell subpopulation [79].

1.4 Ephs/ephrins in bone homeostasis

Bone homeostasis is strictly controlled by proper cellular communication between osteoclasts and osteoblasts [80, 81] and balance of bone formation and resorption [82, 83]. The mutation of ephrinB1 in mice leads to severe defects, including the neural crest cell (NCC)-derived tissues, incomplete body wall closure, and abnormal skeletal patterning and embryonic lethality [84].

The bone formation and resorption is regulated by the EphB4/ephrinB2 bidirectional signaling pathway[85]. The osteoclasts express ephrinB2 and osteoblasts express the EphB4 respectively. Reverse signaling of ephrinB2 leads to the suppression of osteoclast differentiation by inhibiting the osteoclastogenic c-Fos-NFATc1 cascade, while the EphB4 forward signaling stimulates osteogenic differentiation [86]. Osteoclast precursors[87] express EphA2/ephrinA2, which is induced by receptor activator of NF-κB ligand (RANKL) [88, 89]. EphA2/ephrinA2 up-regulates RhoA in osteoclast precursors to suppress osteoblast differentiation[89].

1.5 Eph/ephrin signaling in cancer

Numerous studies implicate the role of Eph/ephrin signaling in cancer progression and neovascularization such as cancer cell migration and invasion, in which Eph/ephrins were thought to play an oncogenic role [3, 90, 91]. In recent years, the aberrant expression of Eph and ephrin genes has been identified in a wide range of human tumors [92] such as colorectal cancers (CRCs), lung cancer, myeloid cancer, breast carcinoma cells [93]and prostate cancer et al [94].

CRC is one of the most common cancers in the world. Strong relationship is observed between Ephs/ephrins and CRC. The mRNA level of EphA1 and EphA2 are highly elevated in CRC cell lines[95] and down-regulated EphA1 expression in colorectal cancer is correlated with poor survival [96] indicating that down regulation of EphA1 correlates with invasion and metastasis in colorectal carcinomas [97].

Human gastric cancer has strong relationship with expression level of EphA4. The overexpression of EphA4 are observed in 55 tumor specimen [98], which correlates with overexpression of FGFR1. Patients with EphA4-positive cancers have significantly lower survival rate than the patients with EphA4-negative cancers [98].

EphA4/ephrinA signaling also regulates cancer cell proliferation in pancreatic ductal adenocarcinoma (PDAC) carcinogenesis and development. Suppressing expression of EphA4/ephrinA3 drastically attenuates PDAC cell viability. Conversely, overexpression of EphA4 increases growth rate in PDAC cells [99].

EphB/ephrinBs have been reported to promote mesenchymal-epithelial transition (MET), which is a critical mechanism for acquisition of malignant phenotypes by epithelial cell[100,

[101]. Interaction of EphB3/ephrinBs promotes MET through inactivation of CrkL-Rac1 signaling pathway: Overexpression of EphB3 inactivates both CrkL and Rac1; the knockdown of EphB3 activates CrkL by decreasing its phosphorylation. In CRCs, the expression level of EphB3 is decreased. Overexpression of EphB3 results in tumor suppression in HT29 CRC cell line [102].

However, opposite results are also observed in other cancer cell line, such as non-small-cell lung cancer (NSCLC). In NSCLC cells, expression level of EphB3 is elevated comparing normal cells; the tyrosine phosphorylation of EphB3 is reduced; the migration is inhibited under the stimulation of ephrinB1-Fc/ephrinB2-Fc; the silencing of EphB3 shows suppression of tumor growth and metastasis in vivo [73, 103]. The possible signaling pathway is that the activation of EphB3 forms the protein complex of RACK1, PP2A and Akt to inhibit cell migration; Silencing of EphB3 disassociates complex of AKT and RACK1, leading to cell migration[103].

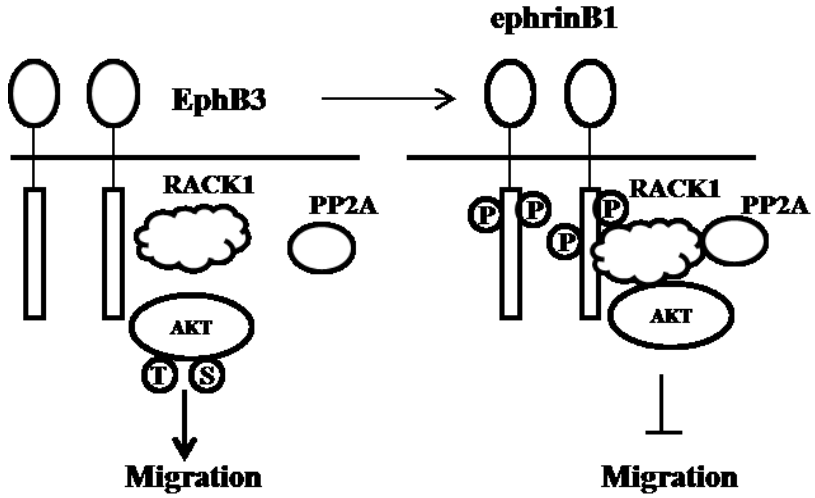

Figure 3 the signaling pathway of EphB3 /ephrinB1 in cell migration[103]

EphB4/ephrinB2 signaling has been linked to breast cancer. The breast cancer cells grow faster in EphB4ΔC-EGFP mouse xenograft model, where EphB4 kinase dominant negative form is overexpressed in recipients [104]. Through the reverse signaling way, ephrinB2 increases blood content in tumor by enhancing the angiogenesis. EphB4 is expressed in human breast cancer; however its function is unclear. EphB4 induces migration of tumor cells and promotes tumor growth/survival. On the contrary, EphB4 also activates an antioncogenic Abl-Crk pathway in MDA-MB-435c breast cancer cells. EphB4 enhances

the phosphorylation of Crk on Tyr221 to inhibit breast cancer cell of viability, proliferation, motility, invasion and down-regulation of pro-invasive matrix metalloprotease (MMP-2)[105].

In prostate cancer, ephrinB2 induces migration of Pc-3 prostate cancer cells and activates their Cdc42 by regulating the contact inhibition of locomotion (CIL), a process of stopping the continual locomotion of a cell in the same direction after collision with another cell [106]. Through the Eph-Rho-ROCK pathway, Pc-3 prostate cancer cells switch from restrained state to invasive state[107].

EphA2/ephrinA1 interaction also promotes tumor growth and metastasis of breast cancer cells [108]. In a tumor xenografts mouse model with the MDA-MB-435 human breast cancer cells or KS1767 human Kaposi's sarcoma cells, EphA2 shows continuous tyrosine phosphorylation throughout tumor vasculature [109]. EphB2 is also important for the growth, migration and invasiveness in colon cancer cell. As the target gene of Wnt signaling pathway, EphB2 is related to early stage of colorectal cancer[110].

1.6 Eph/ephrin in cardiovascular system

1.6.1 Eph/ephrin in angiogenesis

In vertebrate circulatory system, most of arteries and veins are formed in early stage of embryonic development [111]. The remodeling and formation of vessels, through angiogenesis or the outgrowth of the new sprouts, perform complex cascade processes, in which Eph/ephrins are extensively involved [53, 112].

Angiogenesis is a highly orchestrated process that plays an essential role in physiological and pathophysiological development. Through angiogenesis, the pre-existing vessels sprout new vessels to complete the vascular formation and remodeling. EphB4/ephrinB2 is the first pair of genes which are found differentially expressed in arterial and venous endothelium[113]. According to the literature, EphB4/ephrinB2 plays an important role in embryonic vessel development and vascular remodeling [114]. EphB4 marks venous endothelial cells and its ligand ephrinB2 marks arterial endothelial cells [115]. Disruption of EphB4 or miss-expression of ephrinB2 results in intersomitic veins growing abnormally into the adjacent somatic tissue[116].

Vascular endothelial growth factor (VEGF) signaling plays a crucial role in development and remodeling of blood vessels during embryogenesis[117]. VEGF is also involved in pathogenic angiogenesis, such as the recruitment and maintenance of tumor vasculature[118]. It is reported that VEGF can induce the expression of ephrinA1 in endothelial cells and subsequently activate EphA receptor signaling to promote angiogenesis through a juxtacrine mechanism. The soluble EphA2-Fc receptors inhibit VEGF-mediated endothelial cell survival, migration, sprouting, and assembly in vitro; however, it has no effect on FGF-induced angiogenesis [119].

Vascular endothelial growth factor receptor (VEGFR), the ligand of VEGF, is a receptor tyrosine kinase and a key regulator in blood vessel growth and homeostasis[117]. It is produced by endothelial, hematopoietic, and stromal cells. The VEGFR can be classified as three main subtypes, VEGFR-1, -2, and -3 [120].

EphrinB2 regulates the internalization and signaling activity of VEGFR2. Through PDZ domain, ephrinB2 regulates VEGFR2 trafficking and controls endothelial tip-cell-mediated vessel sprouting[121]. EphrinB2 also regulates internalization of VEGFR3 in cultured lymphatic endothelial cells [122]. However, the mutation of ephrinB2 only affects VEGFR but shows no effect on other angiogenic regulator receptors such as fibroblast growth factor receptors [123]. Normal development of lymphatic vasculature needs the ephrinB2, in which PDZ motif plays the essential role[124, 125]. EphrinB2 regulates the remodeling of lymphatic vasculature through the interaction of PDZ-binding motif and PDZ-RGS3 and Dvl2 [124, 125].

Slit/roundabout (Robo) proteins with three different members have emerged as key regulators of vascular remodeling and homeostasis[126]. The cooperation between Slit2 and ephrinA1 regulates a balance between angiogenesis and angiostasis. Slit2 stimulates angiogenesis through mRORC2-dependent activation of Akt and Rac GTPase. EphrinA1 down-regulates the activation of Slit2 and inhibits angiogenesis [127]. EphrinB2 induces migration of endothelial cells by induction of Akt phosphorylation through the phosphorylatidylinositol-3 kinase pathway and promotes angiogenesis in adult vasculature [128]. The dominant negative form of EphA2 inhibits capillary tube-like formation in human umbilical vein endothelial cells [109]. EphA2 also promotes tight junction formation and impairs angiogenesis in brain endothelial cells [129].

1.6.2 Eph/ephrins in VSMCs

Eph/ephrin participates in the regulation of migration, spreading, contraction and attachment in VSMCs [130]. EphrinA1 inhibits the activated Rac1 of Rac/PAK pathway to impair VSMC migration [131]. EphrinB2 is involved in the spreading, migration [132] and attachment [133] of VSMC. During the blood-vessel-wall formation process, interaction of ephrinB2 and Crk-p130 (CAS) is required for directional migration and cell-matrix association in VSMC [53]. Mice of ehprinB2 tissue-specific mutation in epithelium show vascular defects in skin, lung and gastrointestinal tract[53].

EphA4 increases the activated RhoA via Vsm-RhoGEF to regulate VSMC contractility[134]. The EphB6 activated reverse signaling pathway regulates VSMC contractility through RhoA-ROCK-MLCP signaling pathway[135, 136]. In EphB6 knockout mice model, EphB6 knockout female and castrated male VSMCs show increased phosphorylated MLC and contractility[135] and castrated male KO mice show elevated BP.

Part II

Blood pressure regulation and hypertension

Cardiovascular disease (CVD) is the lead cause of death worldwide, responsible for 30% of all death[137]. Increased blood pressure is the most-important risk factor for CVD. It is demonstrated that persistent hypertension is involved in stroke, ischemic heart diseases, kidney failure, and metabolic syndrome [138].

Hypertension is a medical condition, in which the blood pressure is chronically elevated According to *"Reports of the joint national committee on prevention, detection, evaluation and treatment", the diagnosis of hypertension in adults will be made when the average of 2 or more diastolic BP measurements on at least 2 subsequent visits is over 90mmHg or when the average of multiple systolic BP readings on 2 or more subsequent visits is consistently over 140mmHg. Isolated systolic hypertension is defined as systolic BP >140mmHg and diastolic BP<90mmHg* [139], 15% to 30% of adult population as well as more than half of elderly population suffer from high blood pressure in most countries.

Normally, hypertension can be classified into two categories: the secondary hypertension and essential hypertension[139]. The secondary hypertension indicates that the elevated BP is a result of other conditions, such as reno-vascular disease [140], renal failure, pheochromocytoma, aldosteronism, et al. On the contrary, essential hypertension, also called idiopathic hypertension, accounting for 95% of all cases of hypertension, indicates that no specific medical cause is responsible for the elevated BP. Until now, the etiological of essential hypertension is still unclear. Genetic variations, gene malfunction, and disease conditions may be involved in essential hypertension, such as obesity and insulin resistance. Certain physiological status and life styles also involve in essential hypertension, such as high alcohol intake, high salt uptake, aging and stress[139].

2.1 The physiology of vascular smooth muscle

In vasculature, small arteries and arterioles are main contributors to blood flow resistance in circulation[141].Small arteries are composed of three layers: tunica adventitia, tunica media and tunica intima. The outer and inner layers are composed of mainly connective tissues and endothelial cells respectively; tunica media is composed of smooth muscle cells [142].

Two opposite effects tightly control homeostasis of VSMC tone: generation of force (contraction) and release of force (relaxation) [143], in which circulating neurotransmitters, hormones, and endothelium-1derived factors are involved.

Contraction and relaxation of smooth muscle cells are regulated by the phosphorylation and de-phosphorylation of myosin light chain (MLC_{20}), which is controlled by myosin light chain kinase (MLCK) [144, 145] and myosin light chain phosphatase (MLCP) [146] separately. Upon stimulating of smooth muscle cell, Ca^{2+} is transiently elevated in the cytoplasm through extracellular fluid Ca^{2+} and intracellular stores. Ca^{2+} combines calmodulin to form the Ca^{2+}/calmodulin complex, which binds and provokes MLCK to phosphorylate MLC_{20} at Ser 19 and Thr18 [147]. The activation of myosin ATPase promotes interaction of actin and myosin then leading to muscle contraction.

De-phosphorylated MLC_{20} is responsible for vessel relaxation, which is regulated by MLCP. MLCP is a heterotrimer, consisting of a catalytic subunit PP1cδ, a 20kDa subunit (M_{20}) and Myosin-targeting subunit (MYPT1)[148, 149]. MLCP dephosphorylates MLC_{20} and induces VSMC relaxation.

2.2 Duality phenotypes of VSMC (contractile and synthetic phenotypes)

Under physiological condition, VSMC keep the quiescent “contractile” phenotype state and maintain appropriate vessel tone[150]. However VSMC shifts “contractile” to “synthetic” phenotypes [151] in response to certain circumstances such as stretch, injury, atherosclerosis and inflammation, in which VSMC enhances migration, proliferation and secretion but suppresses contraction [151]. VSMC of synthetic phenotype changes morphology from “spindle” to “rhomboid” shape (Figure 4) and decreases expression level of contractile marker proteins (Figure 5), such as α-smooth muscle actin, smooth muscle myosin heavy chain, smoothelin-A/B[152].

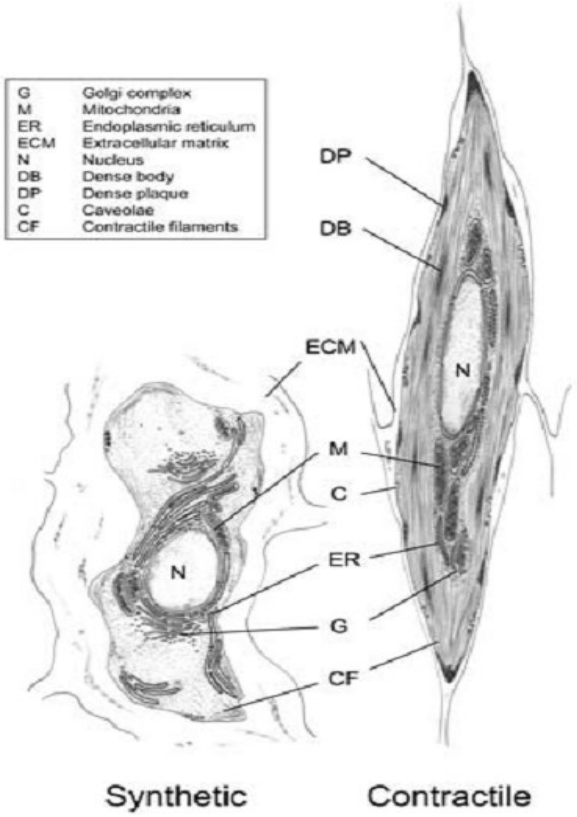

Figure 4 the morphology of VSMC in different phenotypes[152]

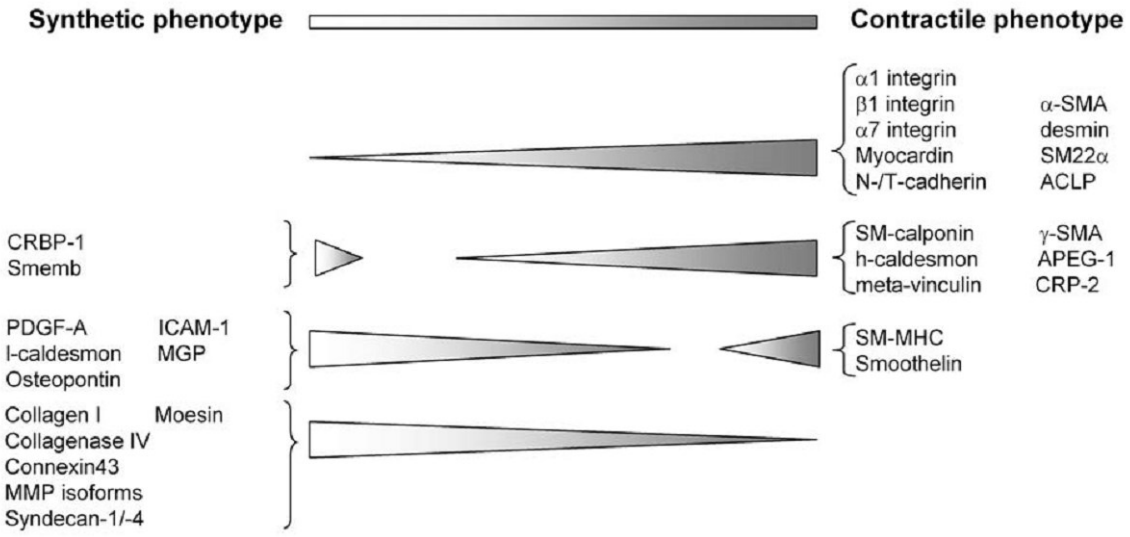

Figure 5 the expression level of contractile and synthetic protein marker[152]

2.3 The renin-angiotensin-aldosterone system (RAAS)

The RAAS is essential in physiological and pathophysiological processes of cardiovascular system, and involved in the renal or non-renal complications of hypertension. Traditionally, RAAS plays the function of regulating renal sodium and water excretion [153], and body sodium-fluid balance[154]. With further understating of RAAS, its function is also recognized in endocrine systems and multiple hormonal systems, such as endocrine, paracrine and intracrine [155].

2.4 Angiotensin II in RAAS

Angiotensin II (Ang II), produced from the liver, is the active component of renin-angiotensin system (RAS)[156]. Ang II is the key effector to maintain systemic blood pressure through various mechanisms in cardiovascular and renal systems[157]. In classic RAAS, circulating renal-derived renin cleaves hepatic-derived angiotensinogen to form the deca-peptide angiotensin I (Ang I), which is converted by angiotensin-converting enzyme (ACE) to the Ang II. Besides the renin enzymetic pathway, Ang I and Ang II also can be produced through a nonrenin enzymetic pathway. For example the tonin and cathepsin convert angiotensinogen to Ang I then Trypsin, cathepsin and chymase convert Ang I to Ang II [158]. As the cleavage product of Ang I, Ang II has potent effects on RAAS system. Ang II elevates blood pressure and retains salt and water in body. Ang II induces the secretion of aldosterone from zona glomerulosa of adrenal gland cortex. Ang II also stimulates vasoconstriction through AT1R-mediated activation of RhoA/Rho kinase-dependent myosin light chain (MLC) phosphorylation.

There are two subtypes of Ang II receptors, AT_1 and AT_2[159]. Both of them belong to the super-family of G-protein-coupled receptors (GPCRs). AT_1 receptor is expressed ubiquitously and involved in most of the biological functions of Ang II, such as vasoconstriction, cardiac contractility, renal tubular sodium re-absorption, cell proliferation, vascular and cardiac hypertrophy, inflammatory responses, and oxidative stress[160]. In rodents, the AT_1 can be classified into two isoforms, AT_{1a} and AT_{1b}. The AT_{1a} is main activator of many signaling pathways in vascular smooth muscle cells. AT_1R presents a basal activity in VSMC and may bind to GPCR kinases and β-arrestins. GPCR kinases can desensitize AT_1R through a phosphorylation process. The AT_1R-associated

protein (ATRAP) binds to AT_1R and negatively regulates its signaling pathway. Inositol triphosphate (IP3) is the fast signaling factor in response to Ang II, leading to contraction of VSMCs [161], in which IP3 induces intracellular stores to release calcium and increases intracellular calcium concentration. AT_1R is also involved in the inflammation process[162]. AT_1R activates the NADPH oxidase, which generates superoxide anions and activates NF-κB in response to the induction of expression of pro-inflammatory molecules VCAM-1, MCP-1 and IL-6 [163].

AT_2R promotes different signaling pathway and works opposite to that of AT_1R [164]. AT_2R is only highly expressed in fetal tissues[164]. Its expression dramatically decreases after birth and is restricted to a few organs mainly in cardiovascular system[165]. However, the AT_2R is re-expressed in adult after cardiac and vascular injury. AT_2R binds to AT_2R-interacting protein-1 (ATIP1) to relax vascular smooth muscle cells through NO/cGMP signaling pathway [166].

Pro-renin receptor (PRR) [167] can be classified into three different molecular forms: a full-length integral TM protein (transmembrane), a soluble PRR, existing in plasma and urine, and a truncated form [168]. The activation of PRR triggers the phosphorylation of mitogen-activated protein kinases (MAPKs), the intracellular signaling of extracellular signal regulated kinase 1/2 (ERK1/2) [169], up-regulation of cyclo-oxygenase 2 (COX2) and the activation of p38 MAPK/hsp27 [170]. PRR also regulates the Wnt/β-catenin signaling pathway of cell proliferation, migration and polarity[171].

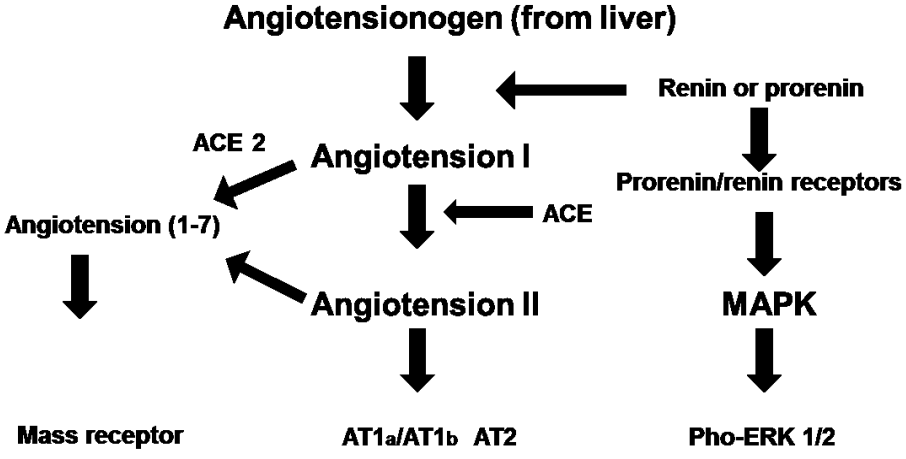

Figure 6 the Angiotensin system[165]

2.5 Aldosterone in RAAS

Numerous studies have shown that aldosterone, a steroid hormone, is widely involved in physiological and pathological processes in blood pressure regulation [172].

As downstream molecule of Ang II in RAAS, aldosterone is produced by the outer-section of adrenal cortex in adrenal gland in response to Ang II and affects renal distal tubules and collecting ducts of nephron[173]. Besides regulating salt homeostasis, aldosterone is now considered as a key factor of performing profibrotic and proinflammatory effects in cardiovascular diseases and metabolic diseases, such as hypertension, insulin resistance and dyslipidemia et al [174]. Elevated level of aldosterone in patients with heart failure is related to a high risk of mortality[175].

The mineralocorticoid receptor (MR), receptor of aldosterone, has two ligands, aldosterone and cortisol [176]. MR is widely expressed on extra-renal tissues such as cardiomyocytes [177, 178], endothelial cells [179, 180] and VSMCs [181, 182]. Through MR, aldosterone performs actions in renal distal convoluted tubules for fluid and electrolyte balance. The MR blockers (apironolactone and eplerenone) restrain action of aldosterone at the level of the receptor and effectively suppress blood pressure [173].

2.5.1 Aldosterone and endothelial cells

Endothelial cells are critical for vessel homeostasis [183]. Aldosterone is broadly involved in physiological and pathophysiological process of endothelial cells. Aldosterone induces the early stage swelling and stiffness of endothelial cells by stimulating the epithelial sodium channel (ENAC) [184-186], ENAC decreases production of nitric oxide by down regulating endothelial nitric oxide synthase (eNOS) in endothelial cell [187, 188]. Aldosterone also inhibits morphogenesis and angiogenesis of endothelial through down-regulating vascular endothelial growth factor receptor-2 (VEGFR-2) expression[189].

2.5.2 Aldosterone and vascular smooth muscle cells

Aldosterone has been shown to induce vascular damage, proliferation [190]. There are two ways to regulate VSMC by aldosterone. One is through MR, the other is through another proteins such as GPR30[191].

Aldosterone mediates VSMC apoptosis by activating intermediate signaling pathways including PI3 kinase, ERK, GPR30 [191] and MR [192]. Aldosterone influences migration and

proliferation of VSMCs through IGF-I signaling pathway, which enhances the VSMC proliferation under the stimulation of αVβ3 integrin [193, 194]. Aldosterone modulates 12-/15-lipoxygenase (LO) atherogenesis in VSMC. VSMCs, treated with aldosterone, show elevated hydroxyeicosatetraenoic acid level and mRNA expression of platelet type 12-LO. In rat VSMC, uniaxial cyclic stretch (CS) promotes aldosterone synthesis and cytochrome p450 aldosterone synthase (CYP11B2) through ERK1/2 phosphorylation signaling [195].

2.6 Calcium in VSMCs

Plenty of ion channels are expressed in the plasma membrane of VSMCs, which form the walls of resistance arteries and regulate vascular tone[196]. Four types of K^+ channels [197, 198], Ca^{2+} channel[199] and two Cl^- channels[200] are expressed on the membrane of VSMC. Ca^{2+} is the key factor to trigger VSMC contraction[196, 201]. Four Ca^{2+} channels are shown as follows: the voltage-gated Ca^{2+} channels, receptor-operated Ca^{2+}, the store-operated Ca^{2+} channels (SOC) and the Ca^{2+} permeable nonselective cation channels [202].

Voltage-gated Ca^{2+} channel is essential for influx of extracellular Ca^{2+} in vascular smooth muscles[203]. The channel is regulated by the membrane potential [204]. Under physiological conditions, the channel is activated by depolarization and shut off by hyper polarization[205]. Voltage-gated Ca^{2+} channels can be classified into five different types, L-type, P-type, N-type, R-type and T-type channels. Through two basic modes of low-activity and high-activity of Ca^{2+} sparklets[199, 206, 207], L-type Ca^{2+} channel primarily mediates Ca^{2+} influx in VSMC among five type channels [208].

The store-operated Ca^{2+} channels, being ATP and bradykinin sensitive, are highly selective for calcium [209]. Store-operated Ca^{2+} channels are activated when intracellular calcium stores are empty [210]. Store-operated Ca^{2+} channels are involved not only in the cell contraction but also proliferation[211] and apoptosis [212]. In smooth muscle cells, IP3-mediated Ca^{2+} release induces the mitogen or growth factor depletion of the sarcoplasmic reticulum (SR) [213] and results in the subsequent activation of transient receptor potential (TRP) cation channels that triggers Ca^{2+} entry into the cell. Platelet-derived growth factor (PDGF), an indicator in the development of pulmonary hypertension, enhances the store-operated Ca^{2+} entry by up-regulating STIM1/Orai1 through activation of Akt/mTOR[211].

2.7 NO and NOS in the cardiovascular system

Nitric oxide (NO) is a gaseous molecule, which has broad functions in cardiovascular system[214]. NO works as a cofactor to interact with many molecules, such as NADPH, FMN, FAD, Calmodulin, Heme and tetrahydrobiopterin (BH4) to fulfill its functions. As a key signaling messenger, NO inhibits platelet aggregation and vascular smooth muscle proliferation to maintain vascular integrity. As an endothelium-derived relaxation factor, NO inhibits L-type Ca^{2+} channels and promotes Ca^{2+} re-uptake of SR to induce vasodilation in VSMC [215].

NO is produced by nitric oxide synthase (NOS). There are three distinct isoforms of NOS: inducible NOS (NOS-II), neuronal NOS (NOS-I) and endothelial NOS (NOS-III). NOS-III and NOS-I are constitutively produced by cardiomyocytes and NOS-II is induced under certain stress conditions[216]. Three isoforms are found in cardiac myocytes, VSMCs and vascular endothelial cells. Besides these three isoforms of NOS, there is a constitutively active NOS in mitochondria, which is the mtNOS [217, 218].

One of the most important functions for NO is to activate the soluble guanylate cyclase (sGC) signaling pathway via a complex interplay between NO and sGC of heme /non-heme sites [219]. sGC, a heterodimer with α and β subunits acts as the biosensor of NO and leads to the production of intracellular cyclic guanosine 3', 5'-monophosphate (cGMP), which is a ubiquitous intracellular secondary messenger, mediating VSMC proliferation, differentiation, cell growth, apoptosis, cellular mobility and contractility [220]. In vasculature, NO up-regulates cGMP production, activates NO-dependent relaxation of vascular smooth muscles and leads to vasodilation [221]. As a neurotransmitter in the autonomic nervous system, NO plays a role in the gastrointestinal tract, urinary tract, and mediates the smooth muscle relaxation of these tissues by increasing cGMP production.

NO can also be a modulator of oxidative stress in cells [222], where the NO interacts with superoxide (O_2^-) to form peroxynitrite ($ONOO^-$). Large amounts of NO can directly inhibit mitochondrial complexes I, IV and activate poly-ADP-ribose polymerase (PARP) [223], lead to the depletion of cellular energy stores.

2.8 G proteins in the regulation of VSMCs

Guanine nucleotide regulatory proteins (G proteins) are a family of guanosine triphosphate (GTP)-binding proteins that play a key regulatory role as transducers in a variety of signal transduction systems. G proteins are heterotrimetric proteins, composed of three distinct subunits: α, β, γ [224].

Different sets of G proteins couple with their receptors to regulate the vasoconstriction through the phosphorylation of MLC via Ca^{2+}/MLCK- or Rho/ROCK-mediated signaling pathways. A typical example is regulation of VSMCs through G_q-G_{11} and G_{12}-G_{13}[225, 226]. $G_{q/11}$ plays the role of maintaining basal tone in VSMC. G_q family induces the activation of β isoforms of phospholipase C (PLC) and forms inositol-1, 4, 5-trisphosphate, which leads to MLC_{20} phosphorylation through elevated Ca^{2+} concentration and complex of Ca^{2+} and calmodulin in the cytosol[227]. As one of RhoA-specific GEFs, P63RhoGEF selectively couples $G_{q/11}$to activation of RhoA in blood vessel to regulate Ca^{2+} sensitization [228].

The injection of $G_{12/13}$-expressing plasmids induces VSMC contraction within 3 hours, in which the signaling pathway might go through the Rho/ROCK pathway [226]. In salt-induced hypertension mice, $G_{12/13}$ activates RhoA/ROCK signaling pathway through Leukemia-associated Rho guanine nucleotide exchange factor (LARG) to regulate VSMC contractility [225].

2.9 The Rho/ROCK signaling pathway in VSMCs

Rho and Rac are two members of the Ras-related superfamily of small GTPases, which have diverse functions in eukaryotic cells, such as assembly of actin cytoskeleton [229], cell polarity and cell migration [230]. GTPases are molecule switchers controlling complex cellular processes [231, 232]. There is a cycle of Rho/Rac between two conformational states: they bind to GTP, they are in active state; they hydrolyze GTP to GDP and bind to it, they are in inactive state. The guanine nucleotide exchanger factors (GEFs) can switch GDP-bound Rho/Rac from inactive state to active GTP-bound state. The guanosine nucleotide dissociation inhibitors (GDI) work as inhibitors to maintain small GTPases in off-state and GTPase activating proteins (GAP) enhance GTP hydrolysis [233].

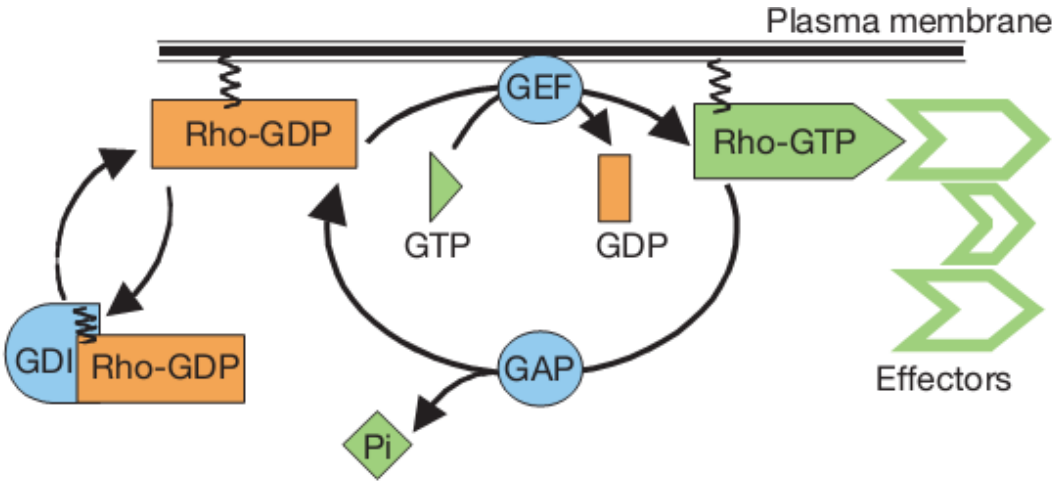

Figure 7 the signaling pathway of Rho family [233]

Rho GTPases control signaling transduction pathways that link cell surface receptors to a variety of intracellular processes. There are evidences showing that Rho/Rho kinase signaling plays important physiological and pathological roles in cardiovascular system[234, 235]. The Rho family proteins are classified into five subfamilies: Rho, Cdc42, Rac, Rnd and RhoBTB subfamilies [236]. More than 20 genes encoding Rho-like small GTPase proteins with a GTPase domain have been found in human[229].

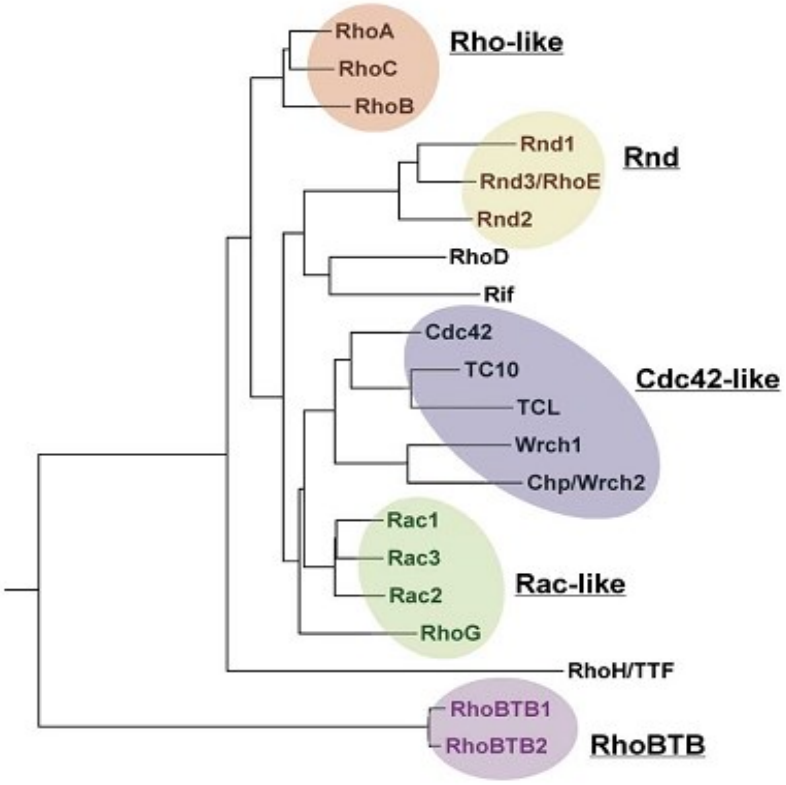

Figure 8 the distribution of Rho family [229]

In VSMC, Rho not only directly interacts with MLC kinase which phosphorylates the regulatory MLC, but inhibits MLC phosphatase as well [237]. Cdc42, Rac1 and RhoA are the most studied family members of Rho GTPase. They are well known as regulators of actin cytoskeleton, cell contractility, cell polarity, gene expression, microtubule dynamics and vesicular trafficking [238, 239]. It is reported that recombinant RhoA increases Ca^{2+} sensitivity in permeable through the activation of ROCK, which inhibits MLCP and extends phosphorylation of MLC_{20} [240] .

As specific ROCK inhibitor, Y-27632, can consistently suppresses the function of p160 ROCK, resulting in reduced Ca^{2+} sensitization in smooth muscle cells. It can thus reduce blood pressure in rat hypertensive model, in which p160 ROCK plays the role in formation of stress fibers in smooth muscle cell [235].

2.10 Hormones in the cardiovascular system

Catecholamines, produced by the medulla of the adrenal glands and postganglionic fibers of sympathetic nervous system are molecules, which include adrenaline, dopamine and

noradrenaline. Studies have shown that catecholamine bind to plasma proteins in bloodstream in response to stress [241]. The different sympathetic reactivity is associated with elevated cardiovascular responses and plasma catecholamine [242]. Increased catecholamine levels contribute to the elevated blood pressure in TRPM4-deficient and Ephb6-deficient mice [135, 243].

Endogenous estrogens are important blood pressure regulation molecules [244]; however the mechanism is still unclear[245]. Normally estrogens are thought as a vasodilator to reduce vascular tone in various arteries [246, 247]. Estrogens act via three different estrogen receptors (ERs) affecting both gene transcription and the rapid signaling pathways in a complex interplay. ERs can be classified into estrogen receptor α (ER α) [248], the estrogen receptor β (ERβ) and the GPR30.

ERs are ligand-activated transcription factors. Once binding to the estrogen, ERs change the conformation of their protein structure, which triggers their dissociation from 90-kDa heat shock protein to allow dimerization of receptors. The dimerized receptors then interact with estrogen response element (ERE), a specific regulatory DNA sequence present in the promoter region of target genes. As the transcriptional regulators, ERα and ERβ mediate vasodilation [249]. Through ERβ, the estrogen rescues severe pulmonary hypertension in a rat model [250]; on the other hand, ERβ-deficient mice show sustained systolic and diastolic hypertension [244]. Estrogen also interacts with G protein on cell membrane. 17β-estradiol has been shown to modulate the process of vasodilation through the phosphatidylinositol 3-kinase-Akt pathway [251].

The G protein-coupled estrogen receptor 1 (GEPR), a cell membrane protein formally named GPR30, is widely expressed in the brain, heart, bone and vasculature [252]. Several studies shown GPR30 is related to the expression of Bcl-2 [253], cAMP generation [254], calcium mobilization [255] and PI3k activation [256]. In kidney, GPR30 is highly expressed in renal tubules and renal epithelial cells [257]. In $Gper^{-/-}$ mouse model, the male $Gper^{-/-}$ mice show the left ventricular dilatation and an elevation of diastolic pressure[258, 259].

Testosterone, the main male sex steroid hormone, has been implicated in cardiovascular risks, such as increased arterial BP, left ventricular hypertrophy and myocardial infarction[260, 261].

Testosterone regulates vascular remodeling by inducing VSMC migration through NADPH Oxidaseand c-Src pathways, in which testosterone promotes NADPH Oxidase expression and c-Src activation [262]. However testosterone also promotes vessel relaxation by activating NO production in endothelial cells [263] as well as suppressing of vascular smooth muscle L type voltage-gated Ca^{2+} channels [264]. In diabete rat model, testosterone showes the suppression of activated RhoA and mRNA level of ROCK1[265].

Conclusion and remarks

Our group pioneered the research on the biological functions of Eph/ephrins. Previous Eph/Efn studies are focused on the function in systems such as the central nervous system, immune system and cancer development. We investigated its roles in VSMC function and blood pressure regulation and the signaling pathways involved, by employing several Eph and ephrin gene knockout mouse models. Our results revealed the pivotal function of Eph and ephrin in blood pressure regulation. Details of our investigation are provided in the following 3 articles.

Reference List

1. Hubbard,S.R. & Till,J.H. Protein tyrosine kinase structure and function. *Annu. Rev. Biochem.* **69**, 373-398 (2000).

2. Bennasroune,A., Gardin,A., Aunis,D., Cremel,G., & Hubert,P. Tyrosine kinase receptors as attractive targets of cancer therapy. *Crit Rev. Oncol. Hematol.* **50**, 23-38 (2004).

3. Pasquale,E.B. Eph receptors and ephrins in cancer: bidirectional signalling and beyond. *Nat. Rev. Cancer* **10**, 165-180 (2010).

4. Schlessinger,J. & Ullrich,A. Growth factor signaling by receptor tyrosine kinases. *Neuron* **9**, 383-391 (1992).

5. Carmeliet,P. & Jain,R.K. Molecular mechanisms and clinical applications of angiogenesis. *Nature* **473**, 298-307 (2011).

6. Robinson,D.R., Wu,Y.M., & Lin,S.F. The protein tyrosine kinase family of the human genome. *Oncogene* **19**, 5548-5557 (2000).

7. Manning,G., Whyte,D.B., Martinez,R., Hunter,T., & Sudarsanam,S. The protein kinase complement of the human genome. *Science* **298**, 1912-1934 (2002).

8. Unified nomenclature for Eph family receptors and their ligands, the ephrins. Eph Nomenclature Committee. *Cell* **90**, 403-404 (1997).

9. Hirai,H., Maru,Y., Hagiwara,K., Nishida,J., & Takaku,F. A novel putative tyrosine kinase receptor encoded by the eph gene. *Science* **238**, 1717-1720 (1987).

10. Arvanitis,D. & Davy,A. Eph/ephrin signaling: networks. *Genes Dev.* **22**, 416-429 (2008).

11. Egea,J. & Klein,R. Bidirectional Eph-ephrin signaling during axon guidance. *Trends Cell Biol.* **17**, 230-238 (2007).

12. Muto,A. *et al.* Eph-B4 prevents venous adaptive remodeling in the adult arterial environment. *J. Exp. Med.* **208**, 561-575 (2011).

13. Gale,N.W. *et al.* Eph receptors and ligands comprise two major specificity subclasses and are reciprocally compartmentalized during embryogenesis. *Neuron* **17**, 9-19 (1996).

14. Miao,H. & Wang,B. EphA receptor signaling--complexity and emerging themes. *Semin. Cell Dev. Biol.* **23**, 16-25 (2012).

15. Daar,I.O. Non-SH2/PDZ reverse signaling by ephrins. *Semin. Cell Dev. Biol.* **23**, 65-74 (2012).

16. Salvucci,O. & Tosato,G. Essential Roles of EphB Receptors and EphrinB Ligands in Endothelial Cell Function and Angiogenesis. *Adv. Cancer Res.* **114**, 21-57 (2012).

17. Manning,G., Plowman,G.D., Hunter,T., & Sudarsanam,S. Evolution of protein kinase signaling from yeast to man. *Trends Biochem. Sci.* **27**, 514-520 (2002).

18. Pasquale,E.B. Eph receptor signalling casts a wide net on cell behaviour. *Nat. Rev. Mol. Cell Biol.* **6**, 462-475 (2005).

19. Irie,F. & Yamaguchi,Y. EPHB receptor signaling in dendritic spine development. *Front Biosci.* **9**, 1365-1373 (2004).

20. Miao,H. & Wang,B. Eph/ephrin signaling in epithelial development and homeostasis. *Int. J. Biochem. Cell Biol.* **41**, 762-770 (2009).

21. Himanen,J.P. *et al.* Crystal structure of an Eph receptor-ephrin complex. *Nature* **414**, 933-938 (2001).

22. Murai,K.K. & Pasquale,E.B. 'Eph'ective signaling: forward, reverse and crosstalk. *J. Cell Sci.* **116**, 2823-2832 (2003).

23. Bruckner,K., Pasquale,E.B., & Klein,R. Tyrosine phosphorylation of transmembrane ligands for Eph receptors. *Science* **275**, 1640-1643 (1997).

24. Salvucci,O. & Tosato,G. Essential roles of EphB receptors and EphrinB ligands in endothelial cell function and angiogenesis. *Adv. Cancer Res.* **114**, 21-57 (2012).

25. Sheffler-Collins,S.I. & Dalva,M.B. EphBs: an integral link between synaptic function and synaptopathies. *Trends Neurosci.* **35**, 293-304 (2012).

26. Adams,R.H. *et al.* Roles of ephrinB ligands and EphB receptors in cardiovascular development: demarcation of arterial/venous domains, vascular morphogenesis, and sprouting angiogenesis. *Genes Dev.* **13**, 295-306 (1999).

27. Augustin,H.G. & Reiss,Y. EphB receptors and ephrinB ligands: regulators of vascular assembly and homeostasis. *Cell Tissue Res.* **314**, 25-31 (2003).

28. Hiratsuka,S. Vasculogenensis, angiogenesis and special features of tumor blood vessels. *Front Biosci.* **16**, 1413-1427 (2011).

29. Lai,K.O. & Ip,N.Y. Synapse development and plasticity: roles of ephrin/Eph receptor signaling. *Curr. Opin. Neurobiol.* **19**, 275-283 (2009).

30. Chen,Y., Fu,A.K., & Ip,N.Y. Bidirectional signaling of ErbB and Eph receptors at synapses. *Neuron Glia Biol.* **4**, 211-221 (2008).

31. Shen,K. & Scheiffele,P. Genetics and cell biology of building specific synaptic connectivity. *Annu. Rev. Neurosci.* **33**, 473-507 (2010).

32. Pozo,K. & Goda,Y. Unraveling mechanisms of homeostatic synaptic plasticity. *Neuron* **66**, 337-351 (2010).

33. Grunwald,I.C. *et al.* Kinase-independent requirement of EphB2 receptors in hippocampal synaptic plasticity. *Neuron* **32**, 1027-1040 (2001).

34. Klein,R. Bidirectional modulation of synaptic functions by Eph/ephrin signaling. *Nat. Neurosci.* **12**, 15-20 (2009).

35. Nolt,M.J. *et al.* EphB controls NMDA receptor function and synaptic targeting in a subunit-specific manner. *J. Neurosci.* **31**, 5353-5364 (2011).

36. Ethell,I.M. *et al.* EphB/syndecan-2 signaling in dendritic spine morphogenesis. *Neuron* **31**, 1001-1013 (2001).

37. Henley,J.M., Barker,E.A., & Glebov,O.O. Routes, destinations and delays: recent advances in AMPA receptor trafficking. *Trends Neurosci.* **34**, 258-268 (2011).

38. Baer,K. *et al.* PICK1 interacts with alpha7 neuronal nicotinic acetylcholine receptors and controls their clustering. *Mol. Cell Neurosci.* **35**, 339-355 (2007).

39. Henkemeyer,M., Itkis,O.S., Ngo,M., Hickmott,P.W., & Ethell,I.M. Multiple EphB receptor tyrosine kinases shape dendritic spines in the hippocampus. *J. Cell Biol.* **163**, 1313-1326 (2003).

40. Shi,Y., Pontrello,C.G., DeFea,K.A., Reichardt,L.F., & Ethell,I.M. Focal adhesion kinase acts downstream of EphB receptors to maintain mature dendritic spines by regulating cofilin activity. *J. Neurosci.* **29**, 8129-8142 (2009).

41. Irie,F. & Yamaguchi,Y. EphB receptors regulate dendritic spine development via intersectin, Cdc42 and N-WASP. *Nat. Neurosci.* **5**, 1117-1118 (2002).

42. Zhou,L., Jones,E.V., & Murai,K.K. EphA signaling promotes actin-based dendritic spine remodeling through slingshot phosphatase. *J. Biol. Chem.* **287**, 9346-9359 (2012).

43. Chin,J. *et al.* Reelin depletion in the entorhinal cortex of human amyloid precursor protein transgenic mice and humans with Alzheimer's disease. *J. Neurosci.* **27**, 2727-2733 (2007).

44. Senturk,A., Pfennig,S., Weiss,A., Burk,K., & Acker-Palmer,A. Ephrin Bs are essential components of the Reelin pathway to regulate neuronal migration. *Nature* **472**, 356-360 (2011).

45. Twigg,S.R. *et al.* Mutations of ephrin-B1 (EFNB1), a marker of tissue boundary formation, cause craniofrontonasal syndrome. *Proc. Natl. Acad. Sci. U. S. A* **101**, 8652-8657 (2004).

46. Bush,J.O. & Soriano,P. Ephrin-B1 regulates axon guidance by reverse signaling through a PDZ-dependent mechanism. *Genes Dev.* **23**, 1586-1599 (2009).

47. Arvanitis,D.N., Jungas,T., Behar,A., & Davy,A. Ephrin-B1 reverse signaling controls a posttranscriptional feedback mechanism via miR-124. *Mol. Cell Biol.* **30**, 2508-2517 (2010).

48. Cao,X., Pfaff,S.L., & Gage,F.H. A functional study of miR-124 in the developing neural tube. *Genes Dev.* **21**, 531-536 (2007).

49. Essmann,C.L. *et al.* Serine phosphorylation of ephrinB2 regulates trafficking of synaptic AMPA receptors. *Nat. Neurosci.* **11**, 1035-1043 (2008).

50. Xu,N.J., Sun,S., Gibson,J.R., & Henkemeyer,M. A dual shaping mechanism for postsynaptic ephrin-B3 as a receptor that sculpts dendrites and synapses. *Nat. Neurosci.* **14**, 1421-1429 (2011).

51. Kullander,K. *et al.* Ephrin-B3 is the midline barrier that prevents corticospinal tract axons from recrossing, allowing for unilateral motor control. *Genes Dev.* **15**, 877-888 (2001).

52. Xu,N.J. & Henkemeyer,M. Ephrin-B3 reverse signaling through Grb4 and cytoskeletal regulators mediates axon pruning. *Nat. Neurosci.* **12**, 268-276 (2009).

53. Foo,S.S. *et al.* Ephrin-B2 controls cell motility and adhesion during blood-vessel-wall assembly. *Cell* **124**, 161-173 (2006).

54. Munoz,J.J. *et al.* Thymic alterations in EphA4-deficient mice. *J. Immunol.* **177**, 804-813 (2006).

55. Vergara-Silva,A., Schaefer,K.L., & Berg,L.J. Compartmentalized Eph receptor and ephrin expression in the thymus. *Mech. Dev.* **119 Suppl 1**, S225-S229 (2002).

56. Wu,J. & Luo,H. Recent advances on T-cell regulation by receptor tyrosine kinases. *Curr. Opin. Hematol.* **12**, 292-297 (2005).

57. Foster,K.E. *et al.* EphB-ephrin-B2 interactions are required for thymus migration during organogenesis. *Proc. Natl. Acad. Sci. U. S. A* **107**, 13414-13419 (2010).

58. Alfaro,D. *et al.* EphrinB1-EphB signaling regulates thymocyte-epithelium interactions involved in functional T cell development. *Eur. J. Immunol.* **37**, 2596-2605 (2007).

59. Blackburn,C.C. & Manley,N.R. Developing a new paradigm for thymus organogenesis. *Nat. Rev. Immunol.* **4**, 278-289 (2004).

60. Alfaro,D. *et al.* Alterations in the thymocyte phenotype of EphB-deficient mice largely affect the double negative cell compartment. *Immunology* **125**, 131-143 (2008).

61. Boehm,T. & Bleul,C.C. Thymus-homing precursors and the thymic microenvironment. *Trends Immunol.* **27**, 477-484 (2006).

62. Stimamiglio,M.A. *et al.* EphB2-mediated interactions are essential for proper migration of T cell progenitors during fetal thymus colonization. *J. Leukoc. Biol.* **88**, 483-494 (2010).

63. Berg,N.N. & Ostergaard,H.L. T cell receptor engagement induces tyrosine phosphorylation of FAK and Pyk2 and their association with Lck. *J. Immunol.* **159**, 1753-1757 (1997).

64. Franklin,R.A., Atherfold,P.A., Robinson,P.J., & Bonner,D. Regulation of Pyk2 expression by p56(Lck) in Jurkat T lymphocytes. *Cell Signal.* **13**, 65-69 (2001).

65. Aasheim,H.C., Delabie,J., & Finne,E.F. Ephrin-A1 binding to CD4+ T lymphocytes stimulates migration and induces tyrosine phosphorylation of PYK2. *Blood* **105**, 2869-2876 (2005).

66. Hjorthaug,H.S. & Aasheim,H.C. Ephrin-A1 stimulates migration of CD8+CCR7+ T lymphocytes. *Eur. J. Immunol.* **37**, 2326-2336 (2007).

67. Holen,H.L., Nustad,K., & Aasheim,H.C. Activation of EphA receptors on CD4+CD45RO+ memory cells stimulates migration. *J. Leukoc. Biol.* **87**, 1059-1068 (2010).

68. Wing,J.B. & Sakaguchi,S. TCR diversity and Treg cells, sometimes more is more. *Eur. J. Immunol.* **41**, 3097-3100 (2011).

69. Luo,H., Yu,G., Tremblay,J., & Wu,J. EphB6-null mutation results in compromised T cell function. *J. Clin. Invest* **114**, 1762-1773 (2004).

70. Luo,H., Yu,G., Wu,Y., & Wu,J. EphB6 crosslinking results in costimulation of T cells. *J. Clin. Invest* **110**, 1141-1150 (2002).

71. Yu,G., Mao,J., Wu,Y., Luo,H., & Wu,J. Ephrin-B1 is critical in T-cell development. *J. Biol. Chem.* **281**, 10222-10229 (2006).

72. Yu,G., Luo,H., Wu,Y., & Wu,J. EphrinB1 is essential in T-cell-T-cell co-operation during T-cell activation. *J. Biol. Chem.* **279**, 55531-55539 (2004).

73. Maddigan,A. *et al.* EphB receptors trigger Akt activation and suppress Fas receptor-induced apoptosis in malignant T lymphocytes. *J. Immunol.* **187**, 5983-5994 (2011).

74. Luo,H. *et al.* Efnb1 and Efnb2 proteins regulate thymocyte development, peripheral T cell differentiation, and antiviral immune responses and are essential for interleukin-6 (IL-6) signaling. *J. Biol. Chem.* **286**, 41135-41152 (2011).

75. Luo,H. *et al.* Ephrinb1 and Ephrinb2 are associated with interleukin-7 receptor alpha and retard its internalization from the cell surface. *J. Biol. Chem.* **286**, 44976-44987 (2011).

76. Freywald,A., Sharfe,N., Miller,C.D., Rashotte,C., & Roifman,C.M. EphA receptors inhibit anti-CD3-induced apoptosis in thymocytes. *J. Immunol.* **176**, 4066-4074 (2006).

77. Alonso,C. *et al.* Expression profile of Eph receptors and ephrin ligands in healthy human B lymphocytes and chronic lymphocytic leukemia B-cells. *Leuk. Res.* **33**, 395-406 (2009).

78. Aasheim,H.C. *et al.* A splice variant of human ephrin-A4 encodes a soluble molecule that is secreted by activated human B lymphocytes. *Blood* **95**, 221-230 (2000).

79. Holen,H.L. *et al.* Ephrin-B3 binds specifically to B lymphocytes in blood and induces migration. *Scand. J. Immunol.* **74**, 144-154 (2011).

80. Matsuo,K. & Irie,N. Osteoclast-osteoblast communication. *Arch. Biochem. Biophys.* **473**, 201-209 (2008).

81. Tamma,R. & Zallone,A. Osteoblast and osteoclast crosstalks: from OAF to Ephrin. *Inflamm. Allergy Drug Targets.* **11**, 196-200 (2012).

82. Matsuo,K. & Otaki,N. Bone cell interactions through Eph/ephrin: Bone modeling, remodeling and associated diseases. *Cell Adh. Migr.* **6**, 148-156 (2012).

83. Kramer,I. *et al.* Osteocyte Wnt/beta-catenin signaling is required for normal bone homeostasis. *Mol. Cell Biol.* **30**, 3071-3085 (2010).

84. Davy,A., Aubin,J., & Soriano,P. Ephrin-B1 forward and reverse signaling are required during mouse development. *Genes Dev.* **18**, 572-583 (2004).

85. Edwards,C.M. & Mundy,G.R. Eph receptors and ephrin signaling pathways: a role in bone homeostasis. *Int. J. Med. Sci.* **5**, 263-272 (2008).

86. Zhao,C. *et al.* Bidirectional ephrinB2-EphB4 signaling controls bone homeostasis. *Cell Metab* **4**, 111-121 (2006).

87. Matsuo,K. Eph and ephrin interactions in bone. *Adv. Exp. Med. Biol.* **658**, 95-103 (2010).

88. Yamashita,T. *et al.* NF-kappaB p50 and p52 regulate receptor activator of NF-kappaB ligand (RANKL) and tumor necrosis factor-induced osteoclast precursor differentiation by activating c-Fos and NFATc1. *J. Biol. Chem.* **282**, 18245-18253 (2007).

89. Irie,N. *et al.* Bidirectional signaling through ephrinA2-EphA2 enhances osteoclastogenesis and suppresses osteoblastogenesis. *J. Biol. Chem.* **284**, 14637-14644 (2009).

90. Chen,J. Regulation of tumor initiation and metastatic progression by Eph receptor tyrosine kinases. *Adv. Cancer Res.* **114**, 1-20 (2012).

91. Arvanitis,D.N. & Davy,A. Regulation and misregulation of Eph/ephrin expression. *Cell Adh. Migr.* **6**, 131-137 (2012).

92. Tang,X.X. *et al.* Implications of EPHB6, EFNB2, and EFNB3 expressions in human neuroblastoma. *Proc. Natl. Acad. Sci. U. S. A* **97**, 10936-10941 (2000).

93. Bhushan,L. & Kandpal,R.P. EphB6 receptor modulates micro RNA profile of breast carcinoma cells. *PLoS. One.* **6**, e22484 (2011).

94. Muller-Tidow,C. *et al.* Identification of metastasis-associated receptor tyrosine kinases in non-small cell lung cancer. *Cancer Res.* **65**, 1778-1782 (2005).

95. Herath,N.I. *et al.* Complex expression patterns of Eph receptor tyrosine kinases and their ephrin ligands in colorectal carcinogenesis. *Eur. J. Cancer*(2011).

96. Herath,N.I., Doecke,J., Spanevello,M.D., Leggett,B.A., & Boyd,A.W. Epigenetic silencing of EphA1 expression in colorectal cancer is correlated with poor survival. *Br. J. Cancer* **100**, 1095-1102 (2009).

97. Dong,Y. *et al.* Downregulation of EphA1 in colorectal carcinomas correlates with invasion and metastasis. *Mod. Pathol.* **22**, 151-160 (2009).

98. Oki,M. *et al.* Overexpression of the receptor tyrosine kinase EphA4 in human gastric cancers. *World J. Gastroenterol.* **14**, 5650-5656 (2008).

99. Iiizumi,M. *et al.* EphA4 receptor, overexpressed in pancreatic ductal adenocarcinoma, promotes cancer cell growth. *Cancer Sci.* **97**, 1211-1216 (2006).

100. Kalluri,R. & Weinberg,R.A. The basics of epithelial-mesenchymal transition. *J. Clin. Invest* **119**, 1420-1428 (2009).

101. Singh,A., Winterbottom,E., & Daar,I.O. Eph/ephrin signaling in cell-cell and cell-substrate adhesion. *Front Biosci.* **17**, 473-497 (2012).

102. Chiu,S.T. *et al.* Over-expression of EphB3 enhances cell-cell contacts and suppresses tumor growth in HT-29 human colon cancer cells. *Carcinogenesis* **30**, 1475-1486 (2009).

103. Li,G. *et al.* EphB3 suppresses non-small-cell lung cancer metastasis via a PP2A/RACK1/Akt signalling complex. *Nat. Commun.* **3**, 667 (2012).

104. Noren,N.K., Lu,M., Freeman,A.L., Koolpe,M., & Pasquale,E.B. Interplay between EphB4 on tumor cells and vascular ephrin-B2 regulates tumor growth. *Proc. Natl. Acad. Sci. U. S. A* **101**, 5583-5588 (2004).

105. Noren,N.K., Foos,G., Hauser,C.A., & Pasquale,E.B. The EphB4 receptor suppresses breast cancer cell tumorigenicity through an Abl-Crk pathway. *Nat. Cell Biol.* **8**, 815-825 (2006).

106. Abercrombie,M. & Turner,A.A. Contact reactions influencing cell locomotion of a mouse sarcoma in culture. *Med. Biol.* **56**, 299-303 (1978).

107. Astin,J.W. *et al.* Competition amongst Eph receptors regulates contact inhibition of locomotion and invasiveness in prostate cancer cells. *Nat. Cell Biol.* **12**, 1194-1204 (2010).

108. Beauchamp,A. & Debinski,W. Ephs and ephrins in cancer: Ephrin-A1 signalling. *Semin. Cell Dev. Biol.*(2011).

109. Ogawa,K. *et al.* The ephrin-A1 ligand and its receptor, EphA2, are expressed during tumor neovascularization. *Oncogene* **19**, 6043-6052 (2000).

110. Senior,P.V., Zhang,B.X., & Chan,S.T. Loss of cell-surface receptor EphB2 is important for the growth, migration, and invasiveness of a colon cancer cell line. *Int. J. Colorectal Dis.* **25**, 687-694 (2010).

111. Herbert,S.P. & Stainier,D.Y. Molecular control of endothelial cell behaviour during blood vessel morphogenesis. *Nat. Rev. Mol. Cell Biol.* **12**, 551-564 (2011).

112. Cowan,C.A. *et al.* Ephrin-B2 reverse signaling is required for axon pathfinding and cardiac valve formation but not early vascular development. *Dev. Biol.* **271**, 263-271 (2004).

113. Kim,Y.H. *et al.* Artery and vein size is balanced by Notch and ephrin B2/EphB4 during angiogenesis. *Development* **135**, 3755-3764 (2008).

114. Herbert,S.P. *et al.* Arterial-venous segregation by selective cell sprouting: an alternative mode of blood vessel formation. *Science* **326**, 294-298 (2009).

115. Wang,H.U., Chen,Z.F., & Anderson,D.J. Molecular distinction and angiogenic interaction between embryonic arteries and veins revealed by ephrin-B2 and its receptor Eph-B4. *Cell* **93**, 741-753 (1998).

116. Helbling,P.M., Saulnier,D.M., & Brandli,A.W. The receptor tyrosine kinase EphB4 and ephrin-B ligands restrict angiogenic growth of embryonic veins in Xenopus laevis. *Development* **127**, 269-278 (2000).

117. Ferrara,N., Gerber,H.P., & LeCouter,J. The biology of VEGF and its receptors. *Nat. Med.* **9**, 669-676 (2003).

118. Ellis,L.M. & Hicklin,D.J. VEGF-targeted therapy: mechanisms of anti-tumour activity. *Nat. Rev. Cancer* **8**, 579-591 (2008).

119. Cheng,N. *et al.* Blockade of EphA receptor tyrosine kinase activation inhibits vascular endothelial cell growth factor-induced angiogenesis. *Mol. Cancer Res.* **1**, 2-11 (2002).

120. Stuttfeld,E. & Ballmer-Hofer,K. Structure and function of VEGF receptors. *IUBMB. Life* **61**, 915-922 (2009).

121. Sawamiphak,S. *et al.* Ephrin-B2 regulates VEGFR2 function in developmental and tumour angiogenesis. *Nature* **465**, 487-491 (2010).

122. Shawber,C.J. *et al.* Notch alters VEGF responsiveness in human and murine endothelial cells by direct regulation of VEGFR-3 expression. *J. Clin. Invest* **117**, 3369-3382 (2007).

123. Wang,Y. *et al.* Ephrin-B2 controls VEGF-induced angiogenesis and lymphangiogenesis. *Nature* **465**, 483-486 (2010).

124. Makinen,T. *et al.* PDZ interaction site in ephrinB2 is required for the remodeling of lymphatic vasculature. *Genes Dev.* **19**, 397-410 (2005).

125. Nunes,S.S., Rekapally,H., Chang,C.C., & Hoying,J.B. Vessel arterial-venous plasticity in adult neovascularization. *PLoS. One.* **6**, e27332 (2011).

126. Liao,W.X., Wing,D.A., Geng,J.G., & Chen,D.B. Perspectives of SLIT/ROBO signaling in placental angiogenesis. *Histol. Histopathol.* **25**, 1181-1190 (2010).

127. Dunaway,C.M. *et al.* Cooperative signaling between Slit2 and Ephrin-A1 regulates a balance between angiogenesis and angiostasis. *Mol. Cell Biol.* **31**, 404-416 (2011).

128. Maekawa,H. *et al.* Ephrin-B2 induces migration of endothelial cells through the phosphatidylinositol-3 kinase pathway and promotes angiogenesis in adult vasculature. *Arterioscler. Thromb. Vasc. Biol.* **23**, 2008-2014 (2003).

129. Zhou,N. *et al.* Inactivation of EphA2 promotes tight junction formation and impairs angiogenesis in brain endothelial cells. *Microvasc. Res.* **82**, 113-121 (2011).

130. Zhang,J. & Hughes,S. Role of the ephrin and Eph receptor tyrosine kinase families in angiogenesis and development of the cardiovascular system. *J. Pathol.* **208**, 453-461 (2006).

131. Deroanne,C., Vouret-Craviari,V., Wang,B., & Pouyssegur,J. EphrinA1 inactivates integrin-mediated vascular smooth muscle cell spreading via the Rac/PAK pathway. *J. Cell Sci.* **116**, 1367-1376 (2003).

132. Korff,T., Braun,J., Pfaff,D., Augustin,H.G., & Hecker,M. Role of ephrinB2 expression in endothelial cells during arteriogenesis: impact on smooth muscle cell migration and monocyte recruitment. *Blood* **112**, 73-81 (2008).

133. Salvucci,O. *et al.* EphrinB reverse signaling contributes to endothelial and mural cell assembly into vascular structures. *Blood* **114**, 1707-1716 (2009).

134. Ogita,H. *et al.* EphA4-mediated Rho activation via Vsm-RhoGEF expressed specifically in vascular smooth muscle cells. *Circ. Res.* **93**, 23-31 (2003).

135. Luo,H. *et al.* Receptor tyrosine kinase ephb6 regulates vascular smooth muscle contractility and modulates blood pressure in concert with sex hormones. *J. Biol. Chem.* **287**, 6819-6829 (2012).

136. Wu,Z. *et al.* Possible role of Efnb1 protein, a ligand of Eph receptor tyrosine kinases, in modulating blood pressure. *J. Biol. Chem.* **287**, 15557-15569 (2012).

137. Ruilope,L.M. Current challenges in the clinical management of hypertension. *Nat. Rev. Cardiol.*(2011).

138. Lawes,C.M., Vander,H.S., & Rodgers,A. Global burden of blood-pressure-related disease, 2001. *Lancet* **371**, 1513-1518 (2008).

139. Carretero,O.A. & Oparil,S. Essential hypertension. Part I: definition and etiology. *Circulation* **101**, 329-335 (2000).

140. Sen,U., Mishra,P.K., Tyagi,N., & Tyagi,S.C. Homocysteine to hydrogen sulfide or hypertension. *Cell Biochem. Biophys.* **57**, 49-58 (2010).

141. Meyer,C., de,V.G., Davidge,S.T., & Mayes,D.C. Reassessing the mathematical modeling of the contribution of vasomotion to vascular resistance. *J. Appl. Physiol* **92**, 888-889 (2002).

142. Woodrum,D.A. & Brophy,C.M. The paradox of smooth muscle physiology. *Mol. Cell Endocrinol.* **177**, 135-143 (2001).

143. Fisher,S.A. Vascular smooth muscle phenotypic diversity and function. *Physiol Genomics* **42A**, 169-187 (2010).

144. Mabuchi,Y., Mabuchi,K., Stafford,W.F., & Grabarek,Z. Modular structure of smooth muscle Myosin light chain kinase: hydrodynamic modeling and functional implications. *Biochemistry* **49**, 2903-2917 (2010).

145. Stull,J.T., Lin,P.J., Krueger,J.K., Trewhella,J., & Zhi,G. Myosin light chain kinase: functional domains and structural motifs. *Acta Physiol Scand.* **164**, 471-482 (1998).

146. Ito,M., Nakano,T., Erdodi,F., & Hartshorne,D.J. Myosin phosphatase: structure, regulation and function. *Mol. Cell Biochem.* **259**, 197-209 (2004).

147. Cipolletta,E. *et al.* Calmodulin-dependent kinase II mediates vascular smooth muscle cell proliferation and is potentiated by extracellular signal regulated kinase. *Endocrinology* **151**, 2747-2759 (2010).

148. Cole,W.C. & Welsh,D.G. Role of myosin light chain kinase and myosin light chain phosphatase in the resistance arterial myogenic response to intravascular pressure. *Arch. Biochem. Biophys.* **510**, 160-173 (2011).

149. Hartshorne,D.J., Ito,M., & Erdodi,F. Role of protein phosphatase type 1 in contractile functions: myosin phosphatase. *J. Biol. Chem.* **279**, 37211-37214 (2004).

150. Owens,G.K. Molecular control of vascular smooth muscle cell differentiation and phenotypic plasticity. *Novartis. Found. Symp.* **283**, 174-191 (2007).

151. Kawai-Kowase,K. & Owens,G.K. Multiple repressor pathways contribute to phenotypic switching of vascular smooth muscle cells. *Am. J. Physiol Cell Physiol* **292**, C59-C69 (2007).

152. Rensen,S.S., Doevendans,P.A., & van Eys,G.J. Regulation and characteristics of vascular smooth muscle cell phenotypic diversity. *Neth. Heart J.* **15**, 100-108 (2007).

153. Wickelgren,I. HYPERTENSION: Mutation Points to Salt Recycling Pathway. *Science* **289**, 23b-26b (2000).

154. Brunner,H.R. *et al.* Essential hypertension: renin and aldosterone, heart attack and stroke. *N. Engl. J. Med.* **286**, 441-449 (1972).

155. Zhuo,J.L. & Li,X.C. New insights and perspectives on intrarenal renin-angiotensin system: focus on intracrine/intracellular angiotensin II. *Peptides* **32**, 1551-1565 (2011).

156. Taubman,M.B. Angiotensin II: a vasoactive hormone with ever-increasing biological roles. *Circ. Res.* **92**, 9-11 (2003).

157. Fyhrquist,F. & Saijonmaa,O. Renin-angiotensin system revisited. *J. Intern. Med.* **264**, 224-236 (2008).

158. Paul,M., Poyan,M.A., & Kreutz,R. Physiology of local renin-angiotensin systems. *Physiol Rev.* **86**, 747-803 (2006).

159. Csikos,T., Chung,O., & Unger,T. Receptors and their classification: focus on angiotensin II and the AT2 receptor. *J. Hum. Hypertens.* **12**, 311-318 (1998).

160. Wakui,H. *et al.* Enhanced Angiotensin Receptor-Associated Protein in Renal Tubule Suppresses Angiotensin-Dependent Hypertension. *Hypertension*(2013).

161. Nakayama,H. *et al.* The IP3 receptor regulates cardiac hypertrophy in response to select stimuli. *Circ. Res.* **107**, 659-666 (2010).

162. Wu,L. *et al.* Roles of angiotensin II type 2 receptor stimulation associated with selective angiotensin II type 1 receptor blockade with valsartan in the improvement of inflammation-induced vascular injury. *Circulation* **104**, 2716-2721 (2001).

163. Esteban,V. *et al.* Angiotensin II, via AT1 and AT2 receptors and NF-kappaB pathway, regulates the inflammatory response in unilateral ureteral obstruction. *J. Am. Soc. Nephrol.* **15**, 1514-1529 (2004).

164. Savoia,C., D'Agostino,M., Lauri,F., & Volpe,M. Angiotensin type 2 receptor in hypertensive cardiovascular disease. *Curr. Opin. Nephrol. Hypertens.* **20**, 125-132 (2011).

165. Santos,R.A., Ferreira,A.J., & Simoes E Silva AC Recent advances in the angiotensin-converting enzyme 2-angiotensin(1-7)-Mas axis. *Exp. Physiol* **93**, 519-527 (2008).

166. Savoia,C. *et al.* Angiotensin II/AT2 receptor-induced vasodilation in stroke-prone spontaneously hypertensive rats involves nitric oxide and cGMP-dependent protein kinase. *J. Hypertens.* **24**, 2417-2422 (2006).

167. Campbell,D.J. Critical review of prorenin and (pro)renin receptor research. *Hypertension* **51**, 1259-1264 (2008).

168. Nguyen,G. Renin, (pro)renin and receptor: an update. *Clin. Sci. (Lond)* **120**, 169-178 (2011).

169. Nguyen,G. & Muller,D.N. The biology of the (pro)renin receptor. *J. Am. Soc. Nephrol.* **21**, 18-23 (2010).

170. Saris,J.J. *et al.* Prorenin induces intracellular signaling in cardiomyocytes independently of angiotensin II. *Hypertension* **48**, 564-571 (2006).

171. Bernhard,S.M. *et al.* The (pro)renin receptor ((P)RR) can act as a repressor of Wnt signalling. *Biochem. Pharmacol.* **84**, 1643-1650 (2012).

172. Mihailidou,A.S. Aldosterone in Heart Disease. *Curr. Hypertens. Rep.*(2012).

173. Briet,M. & Schiffrin,E.L. Aldosterone: effects on the kidney and cardiovascular system. *Nat. Rev. Nephrol.* **6**, 261-273 (2010).

174. Joffe,H.V. & Adler,G.K. Effect of aldosterone and mineralocorticoid receptor blockade on vascular inflammation. *Heart Fail. Rev.* **10**, 31-37 (2005).

175. Nappi,J.M. & Sieg,A. Aldosterone and aldosterone receptor antagonists in patients with chronic heart failure. *Vasc. Health Risk Manag.* **7**, 353-363 (2011).

176. Feraco,A. *et al.* Role of mineralocorticoid receptor and renin-angiotensin-aldosterone system in adipocyte dysfunction and obesity. *J. Steroid Biochem. Mol. Biol.*(2013).

177. Lombes,M. *et al.* Immunohistochemical and biochemical evidence for a cardiovascular mineralocorticoid receptor. *Circ. Res.* **71**, 503-510 (1992).

178. Hernandez-Diaz,I. *et al.* The mineralocorticoid receptor is a constitutive nuclear factor in cardiomyocytes due to hyperactive nuclear localization signals. *Endocrinology* **151**, 3888-3899 (2010).

179. Nguyen Dinh,C.A. *et al.* The endothelial mineralocorticoid receptor regulates vasoconstrictor tone and blood pressure. *FASEB J.* **24**, 2454-2463 (2010).

180. Brown,N.J. Aldosterone and end-organ damage. *Curr. Opin. Nephrol. Hypertens.* **14**, 235-241 (2005).

181. Nguyen Dinh,C.A. *et al.* Adipocyte-derived factors regulate vascular smooth muscle cells through mineralocorticoid and glucocorticoid receptors. *Hypertension* **58**, 479-488 (2011).

182. Rautureau,Y., Paradis,P., & Schiffrin,E.L. Cross-talk between aldosterone and angiotensin signaling in vascular smooth muscle cells. *Steroids* **76**, 834-839 (2011).

183. Lamalice,L., Le,B.F., & Huot,J. Endothelial cell migration during angiogenesis. *Circ. Res.* **100**, 782-794 (2007).

184. Oberleithner,H. *et al.* Human endothelium: target for aldosterone. *Hypertension* **43**, 952-956 (2004).

185. Kusche-Vihrog,K., Callies,C., Fels,J., & Oberleithner,H. The epithelial sodium channel (ENaC): Mediator of the aldosterone response in the vascular endothelium? *Steroids* **75**, 544-549 (2010).

186. Kellenberger,S. & Schild,L. Epithelial sodium channel/degenerin family of ion channels: a variety of functions for a shared structure. *Physiol Rev.* **82**, 735-767 (2002).

187. Nagata,D. *et al.* Molecular mechanism of the inhibitory effect of aldosterone on endothelial NO synthase activity. *Hypertension* **48**, 165-171 (2006).

188. Forstermann,U. & Munzel,T. Endothelial nitric oxide synthase in vascular disease: from marvel to menace. *Circulation* **113**, 1708-1714 (2006).

189. Fujii,M. *et al.* Aldosterone inhibits endothelial morphogenesis and angiogenesis through the downregulation of vascular endothelial growth factor receptor-2 expression subsequent to peroxisome proliferator-activated receptor gamma. *J. Steroid Biochem. Mol. Biol.* **129**, 145-152 (2011).

190. Kagiyama,S., Matsumura,K., Goto,K., Otsubo,T., & Iida,M. Role of Rho kinase and oxidative stress in cardiac fibrosis induced by aldosterone and salt in angiotensin type 1a receptor knockout mice. *Regul. Pept.* **160**, 133-139 (2010).

191. Gros,R. *et al.* GPR30 expression is required for the mineralocorticoid receptor-independent rapid vascular effects of aldosterone. *Hypertension* **57**, 442-451 (2011).

192. Fraccarollo,D. *et al.* Deletion of cardiomyocyte mineralocorticoid receptor ameliorates adverse remodeling after myocardial infarction. *Circulation* **123**, 400-408 (2011).

193. Cascella,T. *et al.* Aldosterone enhances IGF-I-mediated signaling and biological function in vascular smooth muscle cells. *Endocrinology* **151**, 5851-5864 (2010).

194. Maile,L.A. *et al.* Insulin-like growth factor-I signaling in smooth muscle cells is regulated by ligand binding to the 177CYDMKTTC184 sequence of the beta3-subunit of alphaVbeta3. *Mol. Endocrinol.* **20**, 405-413 (2006).

195. Grote,K. *et al.* Mechanical stretch enhances mRNA expression and proenzyme release of matrix metalloproteinase-2 (MMP-2) via NAD(P)H oxidase-derived reactive oxygen species. *Circ. Res.* **92**, e80-e86 (2003).

196. Somlyo,A.P. & Somlyo,A.V. Signal transduction and regulation in smooth muscle. *Nature* **372**, 231-236 (1994).

197. Ko,E.A., Han,J., Jung,I.D., & Park,W.S. Physiological roles of K+ channels in vascular smooth muscle cells. *J. Smooth Muscle Res.* **44**, 65-81 (2008).

198. Jackson,W.F. Potassium channels in the peripheral microcirculation. *Microcirculation.* **12**, 113-127 (2005).

199. Hughes,A.D. Calcium channels in vascular smooth muscle cells. *J. Vasc. Res.* **32**, 353-370 (1995).

200. Forrest,A.S. *et al.* Intricate interaction between store-operated calcium entry and calcium-activated chloride channels in pulmonary artery smooth muscle cells. *Adv. Exp. Med. Biol.* **661**, 31-55 (2010).

201. Marchand,A., Abi-Gerges,A., Saliba,Y., Merlet,E., & Lompre,A.M. Calcium signaling in vascular smooth muscle cells: from physiology to pathology. *Adv. Exp. Med. Biol.* **740**, 795-810 (2012).

202. Thorneloe,K.S. & Nelson,M.T. Ion channels in smooth muscle: regulators of intracellular calcium and contractility. *Can. J. Physiol Pharmacol.* **83**, 215-242 (2005).

203. Cribbs,L.L. Vascular smooth muscle calcium channels: could "T" be a target? *Circ. Res.* **89**, 560-562 (2001).

204. Amberg,G.C., Navedo,M.F., & Santana,L.F. On the loose: uncaging Ca2+ -induced Ca2+ release in smooth muscle. *J. Gen. Physiol* **127**, 221-223 (2006).

205. Jackson,W.F. Ion channels and vascular tone. *Hypertension* **35**, 173-178 (2000).

206. Amberg,G.C., Navedo,M.F., Nieves-Cintron,M., Molkentin,J.D., & Santana,L.F. Calcium sparklets regulate local and global calcium in murine arterial smooth muscle. *J. Physiol* **579**, 187-201 (2007).

207. Navedo,M.F., Amberg,G.C., Votaw,V.S., & Santana,L.F. Constitutively active L-type Ca2+ channels. *Proc. Natl. Acad. Sci. U. S. A* **102**, 11112-11117 (2005).

208. Amberg,G.C. & Navedo,M.F. Calcium dynamics in vascular smooth muscle. *Microcirculation.*(2013).

209. Nilius,B. & Droogmans,G. Ion channels and their functional role in vascular endothelium. *Physiol Rev.* **81**, 1415-1459 (2001).

210. Berridge,M.J. Elementary and global aspects of calcium signalling. *J. Exp. Biol.* **200**, 315-319 (1997).

211. Ogawa,A., Firth,A.L., Smith,K.A., Maliakal,M.V., & Yuan,J.X. PDGF enhances store-operated Ca2+ entry by upregulating STIM1/Orai1 via activation of Akt/mTOR in human pulmonary arterial smooth muscle cells. *Am. J. Physiol Cell Physiol* **302**, C405-C411 (2012).

212. Wamhoff,B.R., Bowles,D.K., & Owens,G.K. Excitation-transcription coupling in arterial smooth muscle. *Circ. Res.* **98**, 868-878 (2006).

213. Xi,Q. *et al.* IP3 constricts cerebral arteries via IP3 receptor-mediated TRPC3 channel activation and independently of sarcoplasmic reticulum Ca2+ release. *Circ. Res.* **102**, 1118-1126 (2008).

214. Bolotina,V.M., Najibi,S., Palacino,J.J., Pagano,P.J., & Cohen,R.A. Nitric oxide directly activates calcium-dependent potassium channels in vascular smooth muscle. *Nature* **368**, 850-853 (1994).

215. Van Hove,C.E., Van der Donckt,C., Herman,A.G., Bult,H., & Fransen,P. Vasodilator efficacy of nitric oxide depends on mechanisms of intracellular calcium mobilization in mouse aortic smooth muscle cells. *Br. J. Pharmacol.* **158**, 920-930 (2009).

216. Barouch,L.A. *et al.* Nitric oxide regulates the heart by spatial confinement of nitric oxide synthase isoforms. *Nature* **416**, 337-339 (2002).

217. Brown,G.C. Cell biology. NO says yes to mitochondria. *Science* **299**, 838-839 (2003).

218. Moncada,S. & Erusalimsky,J.D. Does nitric oxide modulate mitochondrial energy generation and apoptosis? *Nat. Rev. Mol. Cell Biol.* **3**, 214-220 (2002).

219. Denninger,J.W. & Marletta,M.A. Guanylate cyclase and the .NO/cGMP signaling pathway. *Biochim. Biophys. Acta* **1411**, 334-350 (1999).

220. Tsai,E.J. & Kass,D.A. Cyclic GMP signaling in cardiovascular pathophysiology and therapeutics. *Pharmacol. Ther.* **122**, 216-238 (2009).

221. Sausbier,M. *et al.* Mechanisms of NO/cGMP-dependent vasorelaxation. *Circ. Res.* **87**, 825-830 (2000).

222. Motterlini,R., Foresti,R., Intaglietta,M., & Winslow,R.M. NO-mediated activation of heme oxygenase: endogenous cytoprotection against oxidative stress to endothelium. *Am. J. Physiol* **270**, H107-H114 (1996).

223. Luo,X. & Kraus,W.L. On PAR with PARP: cellular stress signaling through poly(ADP-ribose) and PARP-1. *Genes Dev.* **26**, 417-432 (2012).

224. Gilman,A.G. G proteins and dual control of adenylate cyclase. *Cell* **36**, 577-579 (1984).

225. Wirth,A. *et al.* G12-G13-LARG-mediated signaling in vascular smooth muscle is required for salt-induced hypertension. *Nat. Med.* **14**, 64-68 (2008).

226. Gohla,A., Schultz,G., & Offermanns,S. Role for G(12)/G(13) in agonist-induced vascular smooth muscle cell contraction. *Circ. Res.* **87**, 221-227 (2000).

227. Kai,H. *et al.* Prolonged exposure to agonist results in a reduction in the levels of the Gq/G11 alpha subunits in cultured vascular smooth muscle cells. *Mol. Pharmacol.* **49**, 96-104 (1996).

228. Momotani,K. *et al.* p63RhoGEF couples Galpha(q/11)-mediated signaling to Ca2+ sensitization of vascular smooth muscle contractility. *Circ. Res.* **109**, 993-1002 (2011).

229. Burridge,K. & Wennerberg,K. Rho and Rac take center stage. *Cell* **116**, 167-179 (2004).

230. Aspenstrom,P. The Rho GTPases have multiple effects on the actin cytoskeleton. *Exp. Cell Res.* **246**, 20-25 (1999).

231. Ng,J. *et al.* Rac GTPases control axon growth, guidance and branching. *Nature* **416**, 442-447 (2002).

232. Scheffzek,K. & Ahmadian,M.R. GTPase activating proteins: structural and functional insights 18 years after discovery. *Cell Mol. Life Sci.* **62**, 3014-3038 (2005).

233. Etienne-Manneville,S. & Hall,A. Rho GTPases in cell biology. *Nature* **420**, 629-635 (2002).

234. Hirooka,Y., Shimokawa,H., & Takeshita,A. Rho-kinase, a potential therapeutic target for the treatment of hypertension. *Drug News Perspect.* **17**, 523-527 (2004).

235. Uehata,M. *et al.* Calcium sensitization of smooth muscle mediated by a Rho-associated protein kinase in hypertension. *Nature* **389**, 990-994 (1997).

236. Sinha,S. & Yang,W. Cellular signaling for activation of Rho GTPase Cdc42. *Cell Signal.* **20**, 1927-1934 (2008).

237. Amano,M. *et al.* Phosphorylation and activation of myosin by Rho-associated kinase (Rho-kinase). *J. Biol. Chem.* **271**, 20246-20249 (1996).

238. Wirth,A. Rho kinase and hypertension. *Biochim. Biophys. Acta* **1802**, 1276-1284 (2010).

239. Barman,S.A., Zhu,S., & White,R.E. RhoA/Rho-kinase signaling: a therapeutic target in pulmonary hypertension. *Vasc. Health Risk Manag.* **5**, 663-671 (2009).

240. Otto,B., Steusloff,A., Just,I., Aktories,K., & Pfitzer,G. Role of Rho proteins in carbachol-induced contractions in intact and permeabilized guinea-pig intestinal smooth muscle. *J. Physiol* **496 (Pt 2)**, 317-329 (1996).

241. Kirsten,R. *et al.* Relationship of plasma catecholamines to blood pressure in hypertensive patients during beta-adrenoceptor blockade with and without intrinsic sympathomimetic activity. *Br. J. Clin. Pharmacol.* **13**, 397S-406S (1982).

242. Lee,J. & Harley,V.R. The male fight-flight response: A result of SRY regulation of catecholamines? *Bioessays*(2012).

243. Mathar,I. *et al.* Increased catecholamine secretion contributes to hypertension in TRPM4-deficient mice. *J. Clin. Invest* **120**, 3267-3279 (2010).

244. Zhu,Y. *et al.* Abnormal vascular function and hypertension in mice deficient in estrogen receptor beta. *Science* **295**, 505-508 (2002).

245. Umar,S., Rabinovitch,M., & Eghbali,M. Estrogen paradox in pulmonary hypertension: current controversies and future perspectives. *Am. J. Respir. Crit Care Med.* **186**, 125-131 (2012).

246. Manes,A. *et al.* [Female gender and pulmonary arterial hypertension: a complex relationship]. *G. Ital. Cardiol. (Rome)* **13**, 448-460 (2012).

247. Ma,Y. *et al.* Gender-specific reduction in contraction is associated with increased estrogen receptor expression in single vascular smooth muscle cells of female rat. *Cell Physiol Biochem.* **26**, 457-470 (2010).

248. Soloff,M.S. & Szego,C.M. Purification of estradiol receptor from rat uterus and blockade of its estrogen-binding function by specific antibody. *Biochem. Biophys. Res. Commun.* **34**, 141-147 (1969).

249. Meyer,M.R., Haas,E., & Barton,M. Gender differences of cardiovascular disease: new perspectives for estrogen receptor signaling. *Hypertension* **47**, 1019-1026 (2006).

250. Umar,S. *et al.* Estrogen rescues preexisting severe pulmonary hypertension in rats. *Am. J. Respir. Crit Care Med.* **184**, 715-723 (2011).

251. Chen,Z. *et al.* Estrogen receptor alpha mediates the nongenomic activation of endothelial nitric oxide synthase by estrogen. *J. Clin. Invest* **103**, 401-406 (1999).

252. Takada,Y., Kato,C., Kondo,S., Korenaga,R., & Ando,J. Cloning of cDNAs encoding G protein-coupled receptor expressed in human endothelial cells exposed to fluid shear stress. *Biochem. Biophys. Res. Commun.* **240**, 737-741 (1997).

253. Kanda,N. & Watanabe,S. 17beta-estradiol inhibits oxidative stress-induced apoptosis in keratinocytes by promoting Bcl-2 expression. *J. Invest Dermatol.* **121**, 1500-1509 (2003).

254. Filardo,E.J., Quinn,J.A., Frackelton,A.R., Jr., & Bland,K.I. Estrogen action via the G protein-coupled receptor, GPR30: stimulation of adenylyl cyclase and cAMP-mediated attenuation of the epidermal growth factor receptor-to-MAPK signaling axis. *Mol. Endocrinol.* **16**, 70-84 (2002).

255. Revankar,C.M., Cimino,D.F., Sklar,L.A., Arterburn,J.B., & Prossnitz,E.R. A transmembrane intracellular estrogen receptor mediates rapid cell signaling. *Science* **307**, 1625-1630 (2005).

256. Pietras,R.J., Levin,E.R., & Szego,C.M. Estrogen receptors and cell signaling. *Science* **310**, 51-53 (2005).

257. Hazell,G.G. *et al.* Localisation of GPR30, a novel G protein-coupled oestrogen receptor, suggests multiple functions in rodent brain and peripheral tissues. *J. Endocrinol.* **202**, 223-236 (2009).

258. Ullrich,N.D., Krust,A., Collins,P., & MacLeod,K.T. Genomic deletion of estrogen receptors ERalpha and ERbeta does not alter estrogen-mediated inhibition of Ca2+ influx and contraction in murine cardiomyocytes. *Am. J. Physiol Heart Circ. Physiol* **294**, H2421-H2427 (2008).

259. Deschamps,A.M. & Murphy,E. Activation of a novel estrogen receptor, GPER, is cardioprotective in male and female rats. *Am. J. Physiol Heart Circ. Physiol* **297**, H1806-H1813 (2009).

260. Svartberg,J. *et al.* Association of endogenous testosterone with blood pressure and left ventricular mass in men. The Tromso Study. *Eur. J. Endocrinol.* **150**, 65-71 (2004).

261. Hu,X., Zhang,K., & Jiang,H. Is testosterone or estrogen more important for male patients with coronary artery disease? *Eur. J. Intern. Med.* **23**, e114-e115 (2012).

262. Chignalia,A.Z. *et al.* Testosterone induces vascular smooth muscle cell migration by NADPH oxidase and c-Src-dependent pathways. *Hypertension* **59**, 1263-1271 (2012).

263. Perusquia,M. & Stallone,J.N. Do androgens play a beneficial role in the regulation of vascular tone? Nongenomic vascular effects of testosterone metabolites. *Am. J. Physiol Heart Circ. Physiol* **298**, H1301-H1307 (2010).

264. Montano,L.M. *et al.* Relaxation of androgens on rat thoracic aorta: testosterone concentration dependent agonist/antagonist L-type Ca2+ channel activity, and 5beta-dihydrotestosterone restricted to L-type Ca2+ channel blockade. *Endocrinology* **149**, 2517-2526 (2008).

265. Vignozzi,L. *et al.* Testosterone regulates RhoA/Rho-kinase signaling in two distinct animal models of chemical diabetes. *J. Sex Med.* **4**, 620-630 (2007).

II. ARTICLES

Article 1

Ephb6 Regulates Vascular Smooth Muscle Contractility and Modulates Blood Pressure in Concert with Sex Hormones

[1]Hongu Luo, [1]Zenghui Wu, [1]Johanne Tremblay, [2]Eric Thorin, [1]Junzheng Peng, [1]Julie L. Lavoie, [3]Bing Hu, [1]Ekatherina Stoyanova, [1]Guy Cloutier, [1]Shijie Qi, [1]Tao Wu, [4]Mark Cameron and [1,5]Jiangping Wu

[1]Zenghui Wu and [1]Hongyu Luo are co-first author

J Biol Chem. 2012 Feb 24; 287(9):6819-29. Epub 2012 Jan 5.

Summary: in this paper we showed the elevated blood pressure in Ephb6$^{-/-}$mice. The phosphorylation of MLC was also increased in knockout mice. The level of catecholamine was changed before and after castration in knockout mice. It was revealed that the Ephb6 forward signaling and sex hormones were involving in the regulation of blood pressure and the function of vascular smooth muscle cells.

Dr Hongyu Luo and Zenghui Wu performed the experiments and analyzed the data except the blood pressure measurement and vessel constriction. Dr Hongyu Luo made the EphB6 KO mice, in collaboration with Mark Cameron, she conducted microarray analysis which identified EphB6-regulated gene with a function in BP control. She also performed aldosterone level check in sera; Drs. Johanne Tremblay, Junzheng Peng and Julie Lavoie measured the blood pressure in vivo and analyzed the data; Dr Eric Thorin did the experiments of vessel constriction in vitro. Dr. Shijie Qi performed castration and ovariectomy and took care of animal husbandry. Drs. Stoyanova and Cloutier performed ultrasonic analysis of the cardiovascular system. Dr. Hu conducted histological analysis. Dr. Tao Wu initiated the VSMC culture protocol. Dr Jiangping Wu and Dr Hongyu Luo directed the experimental design and data analysis.

Ephb6 Regulates Vascular Smooth Muscle Contractility and Modulates Blood Pressure in Concert with Sex Hormones

[1]Hongu Luo, [1]Zenghui Wu, [1]Johanne Tremblay, [2]Eric Thorin, [1]Junzheng Peng, [1]Julie L. Lavoie, [3]Bing Hu, [1]Ekatherina Stoyanova, [1]Guy Cloutier, [1]Shijie Qi, [1]Tao Wu, [4]Mark Cameron and [1,5]Jiangping Wu

[1]Research Centre and [5]Nephrology Service, Centre hospitalier de l'Université de Montréal (CHUM), Montreal, Quebec, Canada; [2]Montreal Heart Institute, Montreal, Quebec, Canada; and [3]AmeriPath, Orlando, Florida, USA; [4]Toronto General Hospital Research Institute, Toronto, Ontario, Canada

Abstract

Background: Eph kinases constitute the largest receptor tyrosine kinase family and there is no knowledge about their function in blood pressure regulation. Results: Ephb6 regulates vascular smooth muscle cell contraction and its knockout resulted in increased blood pressure in castrated male mice. Conclusion: Ephb6 and its ligands can regulate vessel tone and blood pressure. Significance: We have identified a new group of molecules capable of regulating blood pressure. Eph kinases constitute the largest receptor tyrosine kinase family, and their ligands, ephrins (Efns), are also cell surface molecules. Our study is the first to assess the role of Ephb6 in blood pressure (BP) regulation. We observed that EphB6 and all 3 of their Efnb ligands were expressed on vascular smooth muscle cells (VSMC) in mice. We discovered that small arteries from castrated Ephb6 gene knockout (KO) males showed increased contractility, RhoA activation and constitutive myosin light chain phosphorylation ex vivo compared to their wild type (WT) counterparts. Consistent with this finding, castrated Ephb6 KO mice presented heightened BP compared to castrated WT controls. In vitro experiments in VSMC revealed that crosslinking Efnbs but not Ephb6 resulted in reduced VSMC contractions, suggesting that reverse signaling through Efnbs was responsible for the observed BP phenotype. The reverse singaling was mediated by an

adaptor protein Grip1. Additional experiments demonstrated decreased 24-h urine catecholamines in male Ephb6 KO mice, probably as a compensatory feedback mechanism to keep their BP in the normal range. After castration, however, such compensation was abolished in Ephb6 KO mice and was likely the reason why BP increased overtly in these animals. It suggests that Ephb6 has a target in the nervous/endocrine system in addition to VSMC, regulating a testosterone-dependent catecholamine compensatory mechanism. Our study discloses that Ephs and Efns, in concert with testosterone, play a critical role in regulating small artery contractility and BP.

Primary hypertension represents a high blood pressure (BP) condition that is not induced by other diseases. About 90 to 95% of hypertension cases fall into this category. As a result of numerous studies, some risk genes contributing to primary hypertension have been identified, such as genes related to the renin-angiotensin-aldosterone system[1], the sympatho-adrenal system[2], endothelial hormones[3,4] and sex steroids[5-7], to name a few. However, the etiology of primary hypertension remains incompletely understood.

Ephs, the largest family of receptor tyrosine kinases, comprise about 25% of known receptor tyrosine kinases[8]. The ligands of Ephs, ephrins (Efns), are also cell surface molecules[8] and can transduce signals into cells[9] in a phenomenon called reverse signaling. Interactions among Ephs and Efns are promiscuous. One Eph can interface with multiple Efns and vice versa. In general, EphA members interact preferentially with EfnA members, and EphB members with EfnB members[10-12]. Such interactions suggest that these molecules are so vital to biological systems that heavy redundancy is obligatory.

Various Eph and Efn members are expressed in various tissues and organs. They are important not only in embryonic development but also in physiological and pathophysiological conditions in adults. Most reported functions of Ephs occur in the central nervous system[10,11]. They are essential in the development of neuronal connections, circuit plasticity and repair. Some Ephs and Efns, expressed in endothelial cells, are vital in angiogenesis during normal embryonic development as well as in tumorigenesis[12,13]. This and other studies have reported that Ephs and Efns, particularly their B family members, as well as some A family members, are expressed in thymocytes and T cells; they are capable of modulating T-cell responses and survival[14]. It has been shown that Ephs/Efns are involved in intestinal epithelium self-renewal[15], urorectal development[16],

pancreatic α-cell insulin secretion[17], bone development, maintenance and repair[18, 19], regulation of red blood cell production in response to hypoxia[20], clotting[21], glomerular filtration[22] and ionic homeostasis of vestibular endolymph fluid in the inner ear[23].

Efnb2 and Efna1 are expressed in vascular smooth muscle cells (VSMC)[24-27]. Conditional knockout (KO) of Efnb2 in pericytes and VSMC with a platelet-derived growth factor receptor β promoter leads to perinatal lethality[24]. VSMC with Efnb2 deletion manifest compromised migration[24]. Ogita et al. showed that in long-term cultures of rat and human VSMC, Efna1 triggered Epha4 signaling and actin stress fiber assembly[28], but whether such signaling elicited changes in VSMC contractility was not investigated. Therefore, Eph and Efn function in VSMC contractility and BP regulation has not been studied to date.

Our earlier DNA microarray analysis of Ephb6 KO mouse thymocytes indicated that the expression of some genes regulating BP seems to be altered. Based on this clue, we hypothesized that Ephb6 KO mice might have abnormal BP. This hypothesis was the focus of our study.

Materials and Methods

EphB6 KO mice

EphB6 KO mice were generated in our laboratory, as described previously[29]. They have been backcrossed to the C57BL/6 background for more than 10 generations. Age- and gender-matched wild type (WT) littermates or C57BL/6 mice were used as controls and are referred to as WT mice.

We also generated transgenic (Tg) mice with human β-actin promoter-driven expression of a truncated Ephb6 (aa 1-667), whose intracellular domain was deleted, with a plasmid construct pAC-Ephb6Δ, as illustrated in Supplemental Fig. 1. The Tg mice were backcrossed to the C57BL/6 background for 10 generations and then crossed with Ephb6 KO. The resulting mice, called Ephb6Δ/KO mice, expressed tailless Ephb6 on the cell surface. Again, age- and gender-matched WT littermates or C57BL/6 mice were used as controls and are referred to as WT mice.

Reverse transcription-quantitative polymerase chain reaction (RT-qPCR)

Ephn6, Efnb1, Efnb2, Efnb3, Dishevelled, PDZ-RGS3 and Grip1 mRNA levels were measured by RT-qPCR. Total RNA from VSMC or mesenteric artery endothelial cells was

extracted with TRIzol® (Invitrogen, Carlsbad, CA, USA) and then reverse-transcribed with Superscript II™ reverse-transcriptase (Invitrogen). The primers utilized in RT-qPCR and the fragment sizes amplified are listed in Supplemental Table I. PCR conditions for the reactions were as follows: 2 min at 50°C, 2 min at 95°C, followed by 20-25 cycles of 10 s at 94°C, 20 s at 58°C and 20 s at 72°C. β-actin mRNA levels served as internal controls, and the data were expressed as signal ratios of test gene mRNA/β-actin mRNA.

VSMC isolation

Mouse VSMCs were isolated, as described by Golovina and Blaustein[30], with modifications. The aorta and mesenteric arteries, including their secondary branches, were digested with collagenase type II (347 U/ml) (Worthington Biochemical Corporation, Lakewood, NJ, USA). These vessels were washed twice, and the adventitia and endothelium were removed with fine forceps and sterile cotton-tipped applicators. They were further digested with both collagenase type II (347 U/ml) and elastase type IV (6 U/ml) (Sigma-Aldrich Corporation, St. Louis, MO, USA). The dissociated cells were cultured at 37°C in Dulbecco's modified Eagle's medium (Wisent, St-Bruno, Quebec, Canada) supplemented with 15% fetal bovine serum for 4 to 5 days before experimentation. In the studies of sex hormones, VSMC were cultured in 15% stripped fetal bovine serum (serum reacted with active charcoal for 24 h to remove bovine sex hormones).

Immunofluorescence microscopy

VSMC cultured for 4-5 days were fixed with paraformaldehyde (4%) for 15 min. The cells were blocked with 10% goat immunoglobulin G (IgG) in phosphate-buffered saline for 20 min and then incubated with various first antibodies (Abs, 2 μg/ml): goat anti-mouse Efnb1, Efnb1, Efnb3 and Ephb6 Abs (R&D Systems, Minneapolis, MN, USA). The cells were reacted overnight at 4 °C with rhodamine-conjugated donkey anti-goat Ab (0.15 μg/ml, Jackson ImmunoResearch Laboratories, West Grove, PA, USA). For intracellular α-actin staining, the cells were permeabilized with permeabilization buffer (BD Biosciences, San Jose, CA, USA) for 20 min at 4°C, and then incubated with mouse anti-human α-actin monoclonal antibodies (mAbs, 2 μg/ml, Santa Cruz Biotechnology, Santa Cruz, CA, USA) followed by FITC-conjugated goat anti-mouse IgG (0.2 μg/ml, Bethyl Laboratories, Montgomery, TX, USA). The stained cells were examined under a Zeiss microscope.

Ex vivo vessel constriction

Vessel constriction was studied ex vivo as described previously[31]. Mesenteric artery segments (2 mm in length) of third-order branches (exterior diameter 125 to 150 μm) were stripped off endothelium and mounted on 20-μm tungsten wires in small vessel myographs, stretched to optimal tension and maintained in physiological saline solution (PSS: NaCl, 130 mM; KCl, 4.7 mM; KH_2PO_4, 1.18 mM; $MgSO_4$, 1.17 mM; $NaHCO_3$, 1.17 mM; $CaCl_2$, 1.6 mM; EDTA, 0.023 mM; glucose, 10 mM; aerated with 12% O_2/5% CO_2/83% N_2; pH 7.4) at 37°C. After a 40-min stabilization period, arterial segments were challenged with 40-mM KCl PSS (KCl was substituted for an equivalent concentration of NaCl). Single cumulative concentration-response curves to the α1-adrenergic receptor agonist phenylephrine (PE, 1 nM to 100 μM, Sigma, St. Louis, MO, USA) were charted. At the end of the protocol, maximal tension (Emax) was determined by changing the PSS to a solution containing 127 mM KCl. The data are expressed as percentages of Emax. Student's *t* tests were performed to compare concentration-response curves.

Immunoblotting of myosin light chain (MLC) phosphorylation

The aorta and mesenteric arteries of WT and KO mice were isolated, washed twice with Ca^{++}-free Hank's buffered salt solution (HBSS) buffer, and then frozen in liquid nitrogen until they were used. The vessels were homogenized for 1 min at room temperature in 0.4 ml radio-immunoprecipitation assay buffer, which contained Pho-stop and Protease Inhibitor Cocktail (Roche Applied Science, Laval, QC, Canada). The samples were spun at 12,000 rpm for 15 min at 4°C, and the supernatants were collected. Twenty micrograms of proteins per sample were resolved in 12% SDS-PAGE. Proteins from the gel were transferred to PVDF membranes (Invitrogen), which were incubated in blocking buffer containing 5% (w/v) skimmed milk (for MLC, 5% BSA was used in the blocking buffer) for 1 h at room temperature, and then hybridized overnight at 4°C with mouse anti-mouse phospho-MLC mAb or rabbit anti-mouse total MLC Ab (both from Cell Signaling Technology, Danvers, MA, USA). The Abs were used at the manufacturer's recommended dilutions or at 1:1,000. The membranes were washed 3 times and reacted with corresponding second Abs, i.e., horseradish peroxidise-conjugated sheep anti-mouse IgG Ab (GE Healthcare, Baie D'Urfe, Quebec, Canada), or horseradish peroxidise-conjugated rabbit anti-goat IgG Ab (R&D Systems), for 90 min. The signals were detected with

SuperSignal West Pico Chemiluminescent Substrate (Thermo Scientific, Rockford, IL, USA).

BP measurements by radiotelemetry

The mice were anesthetized with isoflurane and implanted surgically with TA11PA-C10 radiotelemetry sensors (Data Sciences International, St. Paul, MN, USA) in the left carotid artery for direct measurement of arterial pressure (AP) and heart rate (HR), as described previously[32]. Seven days were allowed for recovery before measurement. For castrated mice, the measurement was conducted 21 days after surgery. In some experiments, male mice were castrated one week after transmitter implantation; three weeks after the castration, mice were administered with estrogen (240mg) daily subcutaneously for 7 day. Their BP and HR were measured by telemetry during the last 3 days of estrogen administration.

Arterial pressure and HR in conscious, free-moving mice were then recorded continuously for 3 days with the Dataquest acquisition 3.1 system (Data Sciences International). Individual 10-s waveforms of systolic pressure (SP), diastolic pressure (DP), mean arterial pressure (MAP) and HR were sampled every 2 min throughout the monitoring period. The raw data were processed with the Dataquest A.R.T-Analysis program[32] and presented as means ± SE. Statistically significant differences between the experimental groups were evaluated by unpaired *t* test and repeated-measures ANOVA with Statview. $P<0.05$ values were considered to be statistically significant.

Measurement of VSMC contractility

Cultured primary VSMC were washed once with HBSS and cultured in the same solution. They were placed under a Zeiss microscope with environmental controls (37ºC and 5% CO_2). The cells were stimulated with PE (20 μM), unless otherwise indicated, and photographed continuously for 15 min at a rate of 1 picture per min. Fifteen or more cells were selected randomly, and their length was measured at each time point with Zeiss Axiovision software. Percentage contraction was calculated as follows:

% contraction = (cell length at time 0 – cell length at time X) / cell length at time 0.

Student's *t* test was performed to assess statistically significant differences.

Small interfering RNA (siRNA) transfection

siRNAs of Disheveled, PDZ-RGS3 and Grip1 as well as negative control siRNAs were synthesized by Integrated DNA Technologies (Coralville, IA, USA), and their sequences shown in Supplemental Table II. VSMC were cultured for 4 to 5 days, with the last 16 h being free of antibiotics, and then transfected with a mix of 3 pairs of siRNAs of a particular gene (each pair at a final concentration of 10 nM), with FuGENE HD X-tremeGENE siRNA Transfection Reagent (Roche Applied Science). The transfected VSMC were further cultured for 24 to 36 h, and their contractility was measured upon PE [218] stimulation.

Activated RhoA assay

GTP-associated activated RhoA levels in mesenteric artery smooth muscles were determined by G-LISA RhoA Activation Assay Biochem Kit (Cytoskeleton Inc. Denver, CO, USA) according to manufacturer's instructions.

Results

Expression of Ephb6 and its ligands in VSMC

The mRNA expression of Ephb6 as well as 3 of its major ligands, Efnb1, 2 and 3, in VSMC was detectable by RT-qPCR (Fig. 1A). We assessed these 4 molecules in VSMC at the protein level by immunofluorescence (Fig. 1B). The expression of Ephb6 and its ligands in these cells suggests that Ephb6 might regulate VSMC function.

Ephb6Δ/KO mice expressed tailless Ephb6 (Ephb6 Δ) on the cell surface. Fig. 1C demonstrates the lack of Ephb6 expression in Ephb6 KO VSMC and re-expression of cell surface Ephb6 in Ephb6 Δ /KO VSMC.

Ephb6 null mutation alters blood vessel contraction

BP is controlled by cardiac output, vessel resistance and blood volume. We did not observe any difference in cardiac output between KO and WT mice according to echocardiography (data not included). We then examined small artery contractility, a major factor contributing to BP in terms of peripheral blood flow resistance. Ex vivo contractility of the mesenteric arteries from KO and WT mice was assessed after stimulation with PE. Male KO vessels showed lower contractility than male WT vessels (Fig. 2A), while female KO vessels presented higher contractility than WT vessels after PE stimulation (Fig. 2B). This raised the possibility that Ephb6 might work in concert with sex hormone to regulate vasoconstriction. To test whether such is the case, we castrated male Ephb6 KO mice.

Indeed, vessels from castrated KO males manifested increased contractility compared to castrated WT males (Figs. 2C and 2D). It is to be noted that these observed contractility phenotypes remained unchanged in the presence or absence of endothelium (Figs. 2A-2D), indicating that the nitric oxide production by the endothelium is not involved in the altered contractility in the absence of Ephb6 and male sex hormone.

Consistent with the contractility results, at the molecular level, freshly isolated mesenteric arteries without endothelium from female KO and castrated male KO, but not male KO mice presented a constitutive increase of MLC phosphorylation (Fig. 2E), reflecting the increased sensitivity of VSMC to vasoconstrictive stimuli.

As activated RhoA could increase MLC phosphorylation via the RhoA-associated kinase/myosin phosphatase pathway[33], we assessed the levels of GTP-bound RhoA in mesenteric artery smooth muscles. As shown in Fig. 2F, 5 seconds after the activation by PE, endotheliumless mesenteric arteries from castrated and female but not uncastrated male KO mice had significantly elevated activated RhoA levels, compared to their counterpart WT mice. The RhoA activity in KO mice was increased almost 15 folds after castration, much more than that of WT males after castration. Such elevation was compatible with the augmented MLC phosphorylation and constriction in female and castrated KO vessels.

Castrated KO mice show increased BP

We wondered whether heightened vasoconstriction in female and castrated KO mice led to elevated BP. The BP of Ephb6 KO and WT mice was measured by radiotelemetry. SP, DP, MAP and HR of male and female KO mice presented no significant differences from their respective WT controls (Supplemental Fig. 2). However, 3 weeks after castration, KO mice manifested increased SP, DP and MAP compared to castrated WT mice, while both groups maintained similar HR (Fig. 3A).

Was the lack of BP elevation in female KO mice due to that estrogens lowered the BP? To answer this question, we administered estrogen for 7 days to the castrated KO and WT mice. As shown in Fig. 3B, BP of castrated KO did not come down after estrogen administration and remained higher compared to the castrated WT males treated with estrogen, indicating that the lack of BP elevation in female KO mice was not due to a suppressive effect of estrogen.

We next tested whether these in vivo findings could be reproduced in a defined in vitro culture system. For this purpose, female KO VSMC were cultured in medium containing 15% strip serum, in which the bovine sex hormones had been removed by active charcoal adsorption. In this system, the female KO VSMC contractility in the absence of testosterone was significantly higher than that female KO VSMC in the presence of testosterone, while testosterone did not affect the contractility of WT female VSMC (Fig. 3C). On the other hand, an addition of estrogen to the cultured male KO or WT VSMC did not alter their contractility (Fig. 3D). The results indicate that Ephb6 and testosterone need to be removed simultaneously to elevate VSMC contractility. These in vitro results are compatible with the ex vivo vessel contraction and in vivo BP phenotype of castrated KO mice, and demonstrate that Ephb6 and testosterone are necessary to maintain normal VSMC contractility and BP, both of which will increase only when Ephb6 and testosterone are simultaneously missing.

BP-related hormone levels in Ephb6 KO mice

We questioned whether some key hormones involved in BP regulation were affected directly by or as a compensatory consequence to Ephb6 null mutation. As depicted in Supplemental Figs. 3A and 3B, plasma angiotensin II (AngII) and serum aldosterone levels in male, female and castrated KO mice were comparable to those in their WT counterparts. Twenty-four-h urine catecholamines (i.e., adrenaline, noradrenaline and dopamine) were similar in KO females and WT females during fasting (Fig. 4, second column). However, 24-h urine catecholamines under this condition were significantly lower in KO males than in WT males (Fig. 4, first column). After KO males were castrated, their 24-h urine catecholamines rose to levels comparable to those in castrated WT mice (Fig. 4, last column). This suggests that in male KO mice, there is a compensative reduction of ambient catecholamines and such compensation is abolished after castration.

Ephb6 modulates BP and VSMC contractility through Efnb reverse signaling

Ephb6 and its major ligands, Efnb1, Efnb2 and Efnb3, are capable of bidirectional signaling, i.e., Ephb6 can be stimulated by its ligands and transmit signals into cells, and Efnbs can also be stimulated by Ephb6, transmitting signals into cells. We investigated which signaling direction was responsible for the effect of Ephb6 in BP control. This was first done in primary VSMC culture.

Mouse VSMC from the mesenteric arteries and aorta after 4 to 5 days of culture were stimulated by PE. About 80% of these cells responded dose-dependently to PE stimulation (Figs. 5A and 5B), indicating that they were still mainly of the contractile phenotype at that time. We monitored the speed of VSMC contraction in terms of percentages of their original length at different time points after PE stimulation. This parameter reflects the force of VSMC contraction, which dislodges adherent VSMC from the plastic well surface. WT VSMC, whether from males, females or castrated males, were cultured in wells coated with goat anti-mouse Ephb6 Ab, so that they would receive forward signaling due to Ephb6 crosslinking by solid-phase anti-Ephb6 Ab on the wells. The contraction response of these VSMC to PE was similar to that of cells cultured in wells coated with control normal goat IgG (Fig. 5C), indicating that the forward signaling received by these cells via Ephb6 did not have any effect on their contractility. Then, these WT cells were cultured in wells coated with Ephb6-Fc (the Fc of recombinant protein is of human origin), which would crosslink Efnbs on VSMC and trigger reverse signaling through Efnbs (either single or multiple Efnbs, i.e., Efnb1, Efnb2 and/or Efnb3). The contractility of all these VSMC types (from WT males, females and castrated males) after PE stimulation was significantly decreased relative to those cultured in wells coated with control normal human IgG (Fig. 5D). The results reveal that reverse signaling from Ephb6 to Efnb(s) downregulates VSMC contractility. Possible reasons for the similarly reduced contractility of VSMC from males, females and castrated males will be discussed later. The decrease in VSMC contraction in Ephb6-Fc-coated wells was not due to Ephb6-Fc's mechanical binding to Efnbs expressed on VSMC, because similarly coated anti-EphB6 Ab did not have any influence on VSMC (Fig. 5C), which express Ephb6 on their surface.

To confirm our in vitro findings in vivo, we measured the BP of male or castrated male Ephb6 Δ KO mice, which express Tg tailless Ephb6 in the Ephb6 KO background. Male and castrated male Ephb6 Δ KO mice showed no BP increase compared to their WT counterparts (Supplemental Figs. 4A and 4B), indicating that the missing intracellular Ephb6 tail, which is needed for forward signaling from ligands to Ephb6, is not important for its function in BP regulation. In other words, this result suggests that the observed BP control phenotype of Ephb6 is the consequence of a lack of reverse signaling from Ephb6 to Efnbs.

Identification of Grip1 as a component of the Efnb reverse signaling pathway related to VSMC contraction

Efnbs have no enzymatic activity, but use adaptor proteins to link Efnb intracellular tails to various signaling pathways. To identify molecules in the Efnb reverse signaling pathway that regulate VSMC contractility, siRNAs were deployed to knock down the expression of Grip1, Disheveled and PDZ-RGS3 that are known to associate with Efnbs[34-36]. The effectiveness of mRNA knockdown was verified by RT-qPCR (Fig. 6A). The solid-phase EphB6-Fc-induced hyporesponsiveness of WT VSMC to PE stimulation could be partially negated by Grip1 siRNA, but not by Disheveled or PDZ-RGS3 siRNA (Fig. 6B). These data indicate that Grip1 is involved in the Ephb6 reverse signaling that dampens VSMC contractility.

Discussion

This study identified a previously unknown function of Eph and Efn in vasoconstriction and BP regulation. We demonstrated that 1) Ephb6 triggered reverse signaling via Efnbs, leading to hyporesponsiveness of VSMC, 2) Ephb6, in coordination with testosterone, controlled ambient catecholamine secretion, and 3) the absence of both Ephb6 and testosterone overtly increased BP.

A few words are warranted to reconcile the differences in results on VSMC contraction, small artery contraction and *in vivo* BP measurements. Increased vessel contraction (Fig. 2C), accompanied by augmented constitutive MLC phosphorylation and BP (Figs. 2D and 3), was observed consistently in castrated Ephb6 KO mice compared to castrated WT mice. On the other hand, some of the data related to VSMC contractility, small artery contraction and BP were at odds with each other. For example, VSMC, regardless of whether they were from males, females or castrated males, were susceptible to Ephb6-Fc-triggered reverse signaling, culminating in reduced contractility. However, in intact small artery contraction studies, only small arteries from KO females and castrated KO males but not males presented increased contraction. Moreover, although female KO arteries demonstrated enhanced contractility, female KO mice showed no overt BP elevation. Possible explanations are as follows.

In small arteries, VSMC are in close contact with each other, whereas under cell culture conditions, this contact is limited since cells are not confluent. In our experiments, cells

were used at about 20% confluence (see Fig. 5A), as it was difficult to conduct contraction studies if they were connected to each other. In any case, even at full confluence, VSMC were still not packed as tightly as they would be in vessels. Consequently, WT VSMC in culture lack sufficient Ephb6 stimulation from neighboring cells, and individual cells exist in a state close to Ephb6 KO cells. The lack of sufficient Ephb6 stimulation in cultured VSMC was evident from the fact that when cultured WT VSMC from males, females and castrated males were exposed to solid-phase Ephb6-Fc, which gave sufficient stimulation to Efnbs in VSMC, their response to PE was drastically reduced (Fig. 5D). This suggests that the fundamental effect of reverse signaling through Efnbs in VSMC is a diminished response to vasoconstrictive stimuli. A lack of such reverse signaling translates into ex vivo increased small artery contractility, and augmented constitutive MLC phosphorylation at the molecular level, as well as increased RhoA activity in female and castrated KO mice. Why then did KO females not show elevated BP? BP is a tightly-controlled physiological parameter with many compensatory feedback mechanisms. In KO males, reduced ambient catecholamine release seems to be one such mechanism to balance the defect caused by Ephb6 deletion. Only when this compensation is also affected by castration, is BP overtly elevated. Indeed, we have discovered that Ephb6 is highly expressed in the adrenal medulla, the major source of ambient catecholamines (Supplemental Fig. 5). In females, it is possible that there is a different in vivo compensatory mechanism irrelevant to catecholamines. As a consequence, female KO mice still maintained normal BP.

A more interesting question is why male VSMC receiving Efnb reverse signaling manifested reduced contractility, but this phenotype was not reflected in intact vessels from male KO mice. In fact, mesenteric arteries from male Ephb6 KO even showed lower contractility than those from WT males (Fig. 2A), and they presented no constitutive increase of MLC phosphorylation (Fig. 2D) or increased RhoA activity (Fig. 2F), unlike the small arteries from females and castrated male KO mice. One possible explanation is that under the influence of testosterone, a compensatory mechanism in VSMC at the vascular level (in addition to the systemic change in ambient catecholamine secretion) overreaches its goal, resulting in dampened contractility. This overcompensation is not operational without testosterone, so vessels from females and castrated males showed increased but not decreased contractility. Examples of such overcompensation do exist in

biological systems. For example, when ILK – a major signaling molecule in the integrin signaling pathway that controls hepatocyte differentiation – is null mutated in the liver, overexpression of multiple integrin chains and enzymes involved in the synthesis of collagens has a net result of putting ILK null-mutated hepatocytes in an overcompensated state[37]. In our case, such overcompensation only occurs in intact vessels and not in isolated VSMC, because in the latter, low cell density limits cell-cell contact, and most cells, regardless of whether they are KO or WT, are all in a *de facto* near-KO phenotype.

We attempted to elucidate the mechanism by which Ephb6 null mutation affects vasoconstriction and BP. We noted that neither Ephb6 null mutation nor castration affects the expression of Efnb1, Efnb2, Efnb3 and type 1a α-adrenoreceptor in VSMC at the protein level (Supplemental Figure 6A) or altered Efnb1, Efnb2, Efnb3, Ephb6, and Grip1 expression at the mRNA level (Supplemental Fig. 6B). Since endothelial cells are in close contact with VSMC, their Efn and Eph expression might influence the contractility of VSMC. We confirmed that neither Ephb6 deletion nor castration altered the expression of Efnb1, Efnb2 and Efnb3 expression in the mesenteric artery endothelial cells (Supplemental Fig. 6C). We further demonstrated that cultured VSMC in the presence or absence of testosterone or estrogen expressed similar levels of Efnb1, Efnb2, Efnb2 and Grip1 (Supplemental Figs. 6D and 6E). These data show that the mechanisms of Ephb6 in influence VSMC contraction and BP are not via modulating the expression of their ligands or Grip1.

We also examined the histology of small arteries of WT versus KO mice, and uncastrated versus castrated KO mice, but no obvious difference was observed (data not shown).

Our additional mechanistic studies established that reverse signaling from Ephb6 to Efnbs, but not forward signaling transduced by Ephb6 intracellular domains, was responsible for the observed phenotype, according to in vivo BP measurements in Ephb6Δ/KO mice and in vitro VSMC contraction with solid-phase Ephb6-Fc. This conclusion on the critical role of Efnb reverse signaling in BP regulation is corroborated by our finding that Efnb1 smooth muscle-specific conditional KO mice presented similar although not identical, abnormal BP regulation, like Ephb6 KO mice (to be reported elsewhere).

EphB6 null mutation and Efnb reverse signaling did not modulate Ca^{++} flux (Supplemental Figure 7). Thus, parameters upstream of Ca^{++} flux regulating VSMC contractility seem to

be normal. We discovered that constitutive VSMC MLC phosphorylation, a critical event controlling VSMC responsiveness to Ca^{++} influx, was increased in female KO mice and castrated male KO mice. Therefore, although there was no change in Ca^{++} flux, these VSMC became more responsive to Ca^{++} due to their increased MLC phosphorylation, and this translated into increased vessel constriction upon PE stimulation.

Although Efnbs only have short intracytoplasmic tails with no enzymatic activity, there are 5 conserved tyrosine phosphorylation sites in the tails in addition to a PDZ-binding motif at the C-terminal. The former can dock SH2 domain-containing proteins, such as Tiam1[37] and Disheveled[33], and the latter, PDZ domain-containing signaling proteins, such as Grip[34] and PDZ-RGS3[35]. We discovered that knocking down Grip1 but not Disheveled or PDZ-RGS3 expression in VSMC by siRNAs partially reversed the hyporesponsiveness induced by solid-phase Ephb6-Fc. Therefore, Grip1 is located in the Efnb reverse signaling pathway that leads to the reduced response of VSMC. We also discovered that RhoA activation in the form of GTP-associated RhoA was augmented in the mesenteric artery smooth muscles of KO females and castrated KO males but not unmanipulated KO males within 5 seconds after PE activation, compared to their WT counterparts. Activated RhoA can activate RhoA-associated kinase, which phosphorylates myosin phosphatase. The phosphorylation of the phosphatase will reduce its activity, which will then prolong the phosphorylation of MLC[33]. This might be a mechanism to increase the responsiveness of MLC to Ca^{++} flux in the VSMC of castrated and female KO small arteries. How the reverse signaling through Efnb in VSMC leads to a reduction of RhoA activity is not clear, and we can only speculate at this point. Grip1 contains 7 PDZ domains[38]. It is possible that multiple PDZ domains in Grip1 can bridge Efnbs and modulators of RhoA activity, such as GDP dissociation inhibitors (GDI) or GDP exchange factors (GEF), and influence the function of these modulators, which will in turn regulate RhoA activity. Indeed, Grip1 can associate with a Rho-GDI[39] and a Ras-GEF[40] through its PDZ domains. Validation of such hypotheses is in progress.

Based on our observations described above, we propose the following unified scheme regarding the newly discovered functions of Ephb6 and Efnbs in BP regulation. Under physiological conditions, Ephb6 on neighboring cells provides VSMC with a negative signal to dampen their contractility. Since interactions between Ephb6 and Efnbs are

constant, such a dampening effect is not regulated rapidly and likely controls constitutive vascular tone rather than fast responses to neuroendocrine stimulation. The dampening signal is transmitted reversely through Efnbs into VSMC *via* an Efnb-associating protein, Grip1. Through a so-far unknown signaling pathway which leads to the activation of RhoA, the reverse signaling modulates constitutive MLC phosphorylation, which is increased in the absence of reverse signaling and results in enhanced contraction responses to Ca^{++} flux in VSMC. Although Efnb reverse signaling can alter VSMC contractility at the cellular level regardless of gender or castration, such modulation is not always reflected in BP due to various *in vivo* compensatory mechanisms. In male KO mice, one of these mechanisms is a negative feedback loop that decreases ambient catecholamine secretion by the nervous/endocrine system. This loop depends on both Ephb6 and testosterone. When both are absent, the loop is no longer functional, and catecholamine secretion is no longer reduced. In combination with heightened VSMC responsiveness, it leads to overtly increased BP. Conceivably, defects in Ephb6 and Efnb interactions or in the Efnb reverse signaling pathway, in combination with declining testosterone levels in a subpopulation of aging males, might result in elevated BP.

Acknowledgements

This work was supported by grants from the Canadian Institutes of Health Research to J.W. (MOP57697 and MOP69089), H.L. (MOP97829), J.T., E.T. (MOP14496), and G.C. (CMI72323). It was also financed by grants from the Heart and Stroke Foundation of Quebec, the Quebec Ministry of Economic Development, Innovation and Exportation (PSR-SIIRI-069), and the J.-Louis Levesque Foundation to J.W. This study was also made possible by a group grant from Fonds de la recherche en santé du Québec for Transfusional and Hemovigilance Medical Research to J.W.

References

1 Weir MR, Bakris GL. Combination therapy with renin-angiotensin-aldosterone receptor blockers for hypertension: how far have we come? J Clin Hypertens (Greenwich) 2008;10(2):146-52.

2 Victor RG, Shafiq MM. Sympathetic neural mechanisms in human hypertension. Curr Hypertens Rep 2008;10(3):241-7.

3 Versari D, Daghini E, Virdis A, Ghiadoni L, Taddei S. Endothelium-dependent contractions and endothelial dysfunction in human hypertension. Br J Pharmacol. 2009 Jun;157(4):527-36.

4 Iglarz M, Schiffrin EL. Role of endothelin-1 in hypertension. Curr Hypertens Rep 2003;5(2):144-8.

5 Qiao X, McConnell KR, Khalil RA. Sex steroids and vascular responses in hypertension and aging. Gend Med 2008;5 Suppl A:S46-64.

6 Kienitz T, Quinkler M. Testosterone and blood pressure regulation. Kidney Blood Press Res 2008;31(2):71-9.

7 Ashraf MS, Vongpatanasin W. Estrogen and hypertension. Curr Hypertens Rep 2006;8(5):368-76.

8 Eph Nomenclature Committee. Unified nomenclature for Eph family receptors and their ligands, the ephrins. Cell 1997;90(3):403-4.

9 Pasquale EB. Eph-ephrin bidirectional signalling in physiology and disease. Cell 2008;133:38-52.

10 Wilkinson DG. Eph receptors and ephrins: regulators of guidance and assembly. Int Rev Cytol 2000;196:177-244.

11 Flanagan JG, Vanderhaeghen P. The ephrins and Eph receptors in neural development. Annu Rev Neurosci 1998;21:309-45.

12 Wang HU, Chen ZF, Anderson DJ. Molecular distinction and angiogenic interaction between embryonic arteries and veins revealed by ephrin-B2 and its receptor Eph-B4. Cell 1998;93(5):741-53.

13 Noren NK, Pasquale EB. Paradoxes of the EphB4 receptor in cancer. Cancer Res 2007;67(9):3994-7.

14 Wu J, Luo H. Recent advances on T-cell regulation by receptor tyrosine kinases. Curr Opin Hematol 2005;12(4):292-7.

15 Batlle E, Henderson JT, Beghtel H, van den Born MM, Sancho E, Huls G, Meeldijk J, Robertson J, van de Wetering M, Pawson T, Clevers H. Beta-catenin and TCF mediate cell positioning in the intestinal epithelium by controlling the expression of EphB/ephrinB. Cell 2002;111(2):251-63.

16 Dravis C, Yokoyama N, Chumley MJ, Cowan CA, Silvany RE, Shay J, Baker LA, Henkemeyer M. Bidirectional signalling mediated by ephrin-B2 and EphB2 controls urorectal development. Dev Biol 2004;271(2):272-90.

17 Konstantinova I, Nikolova G, Ohara-Imaizumi M, Meda P, Kucera T, Zarbalis K, Wurst W, Nagamatsu S, Lammert E. EphA-Ephrin-A-mediated beta cell communication regulates insulin secretion from pancreatic islets. Cell 2007;129(2):359-70.

18 Davy A, Bush JO, Soriano P. Inhibition of gap junction communication at ectopic Eph/ephrin boundaries underlies craniofrontonasal syndrome. PLoS Biol 2006;4[219]:e315.

19 Zhao C, Irie N, Takada Y, Shimoda K, Miyamoto T, Nishiwaki T, Suda T, Matsuo K. Bidirectional ephrinB2-EphB4 signaling controls bone homeostasis. Cell Metab 2006;4(2):111-21.

20 Pasquale EB. Eph receptor signalling casts a wide net on cell behaviour. Nat Rev Mol Cell Biol 2005;6(6):462-75.

21 Arvanitis D, Davy A. Eph/ephrin signaling: networks. Genes Dev 2008;22(4):416-29.

22 Hashimoto T, Karasawa T, Saito A, Miyauchi N, Han GD, Hayasaka K, Shimizu F, Kawachi H. Ephrin-B1 localizes at the slit diaphragm of the glomerular podocyte. Kidney Int 2007;72(8):954-64.

23 Dravis C, Wu T, Chumley MJ, Yokoyama N, Wei S, Wu DK, Marcus DC, Henkemeyer M. EphB2 and ephrin-B2 regulate the ionic homeostasis of vestibular endolymph. Hear Res 2007;223[220]:93-104.

24 Foo SS, Turner CJ, Adams S, Compagni A, Aubyn D, Kogata N, Lindblom P, Shani M, Zicha D, Adams RH. Ephrin-B2 controls cell motility and adhesion during blood-vessel-wall assembly. Cell 2006;124[1]:161-73.

25 Shin D, Garcia-Cardena G, Hayashi S, Gerety S, Asahara T, Stavrakis G, Isner J, Folkman J, Gimbrone MA, Jr., Anderson DJ. Expression of ephrinB2 identifies a stable

genetic difference between arterial and venous vascular smooth muscle as well as endothelial cells, and marks subsets of microvessels at sites of adult neovascularization. Dev Biol 2001;230(2):139-50.

26 Gale NW, Baluk P, Pan L, Kwan M, Holash J, DeChiara TM, McDonald DM, Yancopoulos GD. Ephrin-B2 selectively marks arterial vessels and neovascularization sites in the adult, with expression in both endothelial and smooth-muscle cells. Dev Biol 2001;230(2):151-60.

27 Deroanne C, Vouret-Craviari V, Wang B, Pouyssegur J. EphrinA1 inactivates integrin-mediated vascular smooth muscle cell spreading via the Rac/PAK pathway. J Cell Sci 2003;116(Pt 7):1367-76.

28 Ogita H, Kunimoto S, Kamioka Y. EphA4-mediated Rho activation via Vsm-RhoGEF expressed specifically in vascular smooth muscle cells. Circ Res 2003;93[1]:23-31.

29 Luo H, Yu G, Tremblay J, Wu J. EphB6-null mutation results in compromised T cell function. J Clin Invest 2004;114[221]:1762-73.

30 Golovina VA, Blaustein MP. Preparation of primary cultured mesenteric artery smooth muscle cells for fluorescent imaging and physiological studies. Nat Protoc 2006;1(6):2681-7.

31 Thorin E, Huang PL, Fishman MC, Bevan JA. Nitric oxide inhibits alpha2-adrenoceptor-mediated endothelium-dependent vasodilation. Circ Res 1998;82[222]:1323-9.

32 Lavoie JL, Lake-Bruse KD, Sigmund CD. Increased blood pressure in transgenic mice expressing both human renin and angiotensinogen in the renal proximal tubule. Am J Physiol Renal Physiol 2004;286(5):F965-71.

33. Kimura K, Ito M, Amano M, Chihara K, Fukata Y, Nakafuku M, Yamamori B, Feng J, Nakano T, Okawa K, Iwamatsu A, Kaibuchi K. Regulation of myosin phosphatase by Rho and Rho-associated kinase (Rho-kinase) Science. 1996 Jul 12;273(5272):245-8.

34. Tanaka M, Kamo T, Ota S, Sugimura H. Association of Dishevelled with Eph tyrosine kinase receptor and ephrin mediates cell repulsion. EMBO J 2003;22(4):847-58.

35. Bruckner K, Pablo LJ, Scheiffele P, Herb A, Seeburg PH, Klein R. EphrinB ligands recruit GRIP family PDZ adaptor proteins into raft membrane microdomains. Neuron 1999;22(3):511-24.

36. Lu Q, Sun EE, Klein RS, Flanagan JG. Ephrin-B reverse signaling is mediated by a novel PDZ-RGS protein and selectively inhibits G protein-coupled chemoattraction. Cell 2001;105[1]:69-79.
37. Gkretsi V, Apte U, Mars WM, Bowen WC, Luo JH, Yang Y, Yu YP, Orr A, St-Arnaud R, Dedhar S, Kaestner KH, Wu C, Michalopoulos GK. Liver-specific ablation of integrin-linked kinase in mice results in abnormal histology, enhanced cell proliferation, and hepatomegaly. Hepatology 2008;48(6):1932-41.
38. Dong H, O'Brien RJ, Fung ET, Lanahan AA, Worley PF, Huganir RL. GRIP: a synaptic PDZ domain-containing protein that interacts with AMPA receptors. Nature. 1997 Mar 20;386(6622):279-84.

39. Su LF, Wang Z, Garabedian MJ. Regulation of GRIP1 and CBP Coactivator activity by Rho GDI modulates estrogen receptor transcriptional enhancement. J Biol Chem. 2002 Oct 4;277(40):37037-44. Epub 2002 Jul 22.

40. Ye B, Liao D, Zhang X, Zhang P, Dong H, Huganir RLGRASP-1: a neuronal RasGEF associated with the AMPA receptor/GRIP complex. Neuron. 2000 Jun;26(3):603-17.

FIGURES AND LEGENDS

Figure 1 Expression of Ephb6 and Efnbs in mouse VSMC

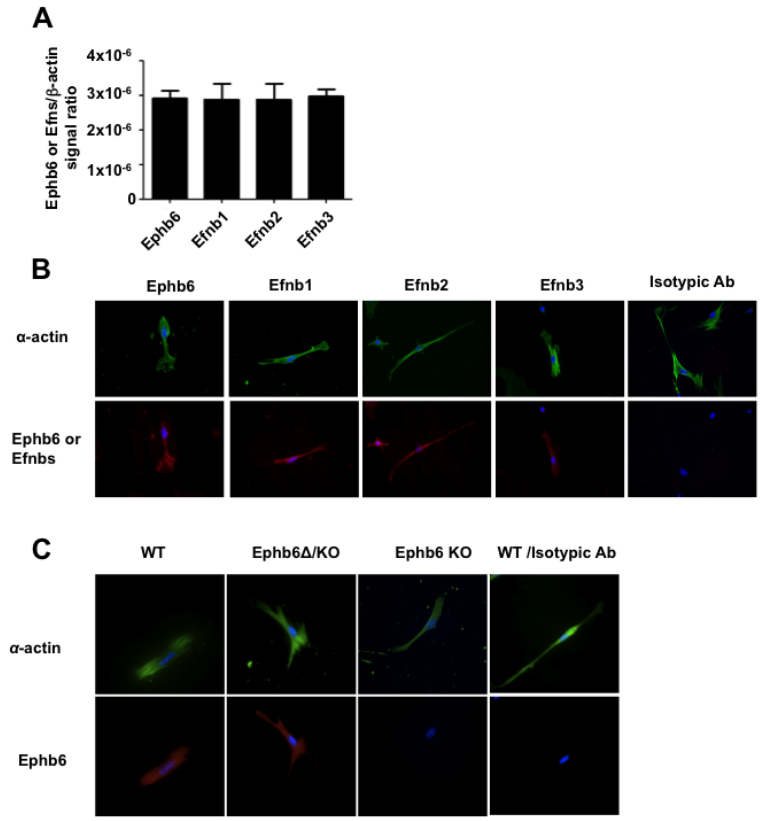

All experiments were repeated at least twice, and data from a representative experiment are reported.

A. Ephb6, Efnb1, Efnb2 and Efnb3 mRNA expression in mouse VSMC. Ephb6, Efnb1, Efnb2 and Efnb3 mRNA expression in VSMC from mesenteric arteries and aorta was measured by RT-qPCR with β-actin mRNA as internal control. Means ± SD of Ephb6 or Efnb signal/ β -actin signal ratios are shown.

B. Ephb6 and Efnb expression on VSMC according to immunofluorescence. WT VSMC cultured for 4-5 days were stained with FITC-goat anti-α-actin (in pseudo-green color) Ab and goat anti-mouse-Ephb6, Efnb1, Efnb2 and Efnb3 Abs, followed by PE-donkey anti-goat IgG (in pseudo-red color). Cells stained with control isotypic first Ab control (normal goat IgG, last column) showed no specific signal.

C. VSMC from Ephb6Δ/KO mice re-expressed cell surface Ephb6. VSMC from WT (first and last columns), Ephb6/KO and Ephb6 KO mice were stained with anti-Ephb6 Ab (first 3 columns) or isotypic control Ab (last column) and anti-α-actin Ab, as indicated, and 2-color micrographs are presented.

Figure 2 Contractility MLC phosphorylation and RhoA activation of mesenteric arteries from Ephb6 KO and WT mice.

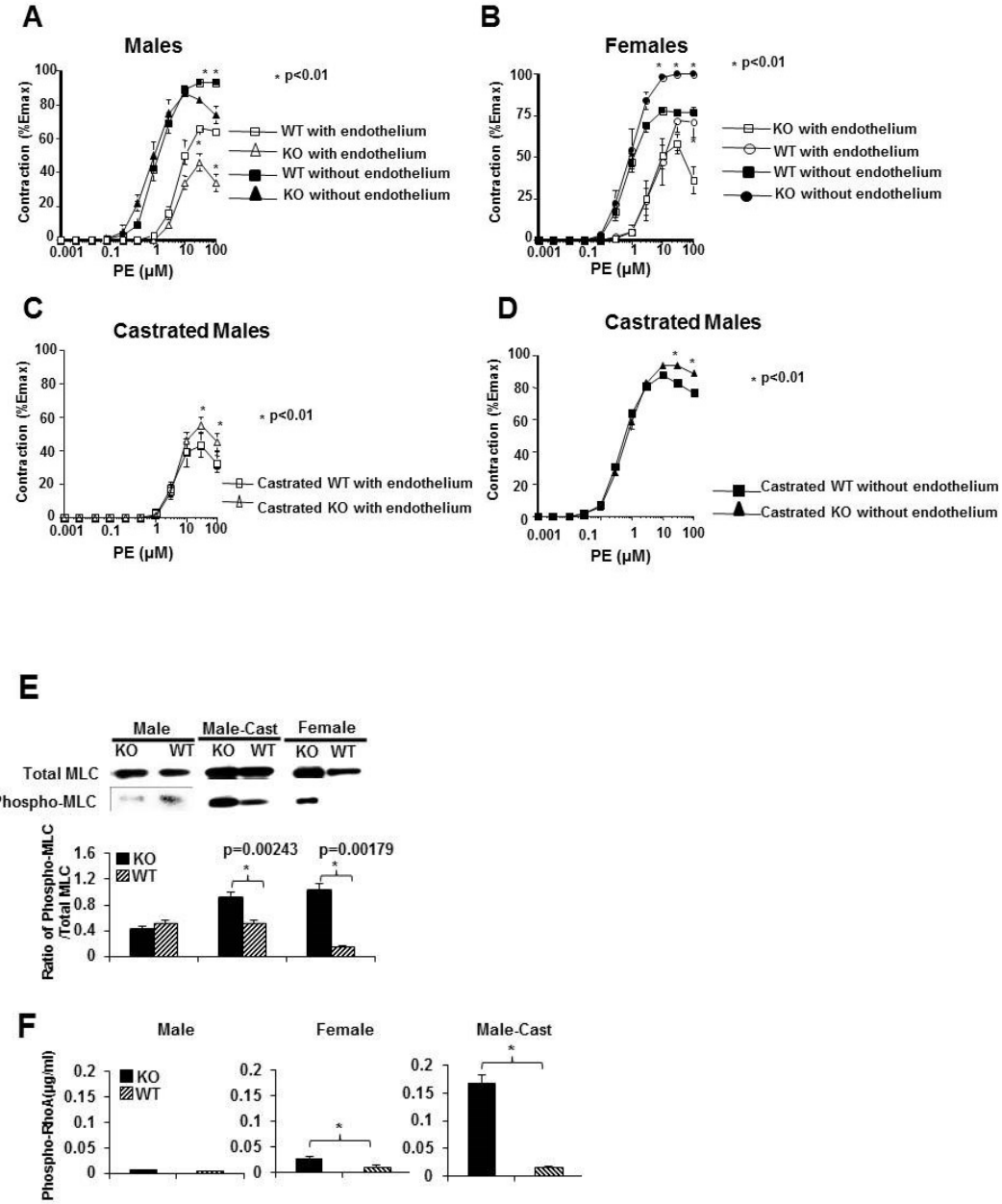

A-D: Contractility of mesenteric arteries from EphB6 KO and WT mice following PE stimulation.

Segments (2 mm) of the third-order branch of the mesenteric artery with endothelium or with endothelium removed were stimulated with PE. A single cumulative concentration-

response curve to PE [223] was obtained. The maximal tension (Emax) was determined by challenging the vessels with a physiological saline containing 127 mM KCl. Vessel contractility is expressed as percentage of the Emax. Data from three mice per group were pooled and mean + SE are shown. *: $p<0.01$ (paired Student's t test). A: vessel contractility of males; B: vessel contractility of females; C: vessel contractility with endothelium of castrated males; D: vessel contractility without endothelium of castrated males.

E. Constitutive MLC phosphorylation in Ephb6 KO arteries.

Proteins from freshly-isolated mesenteric arteries and aortas of male, castrated male (Male-Cast) and female WT and Ephb6 KO mice were analyzed for total and phosphorylated MLC by immunoblotting. The experiments were repeated 3 times, and data from representative immunoblotting are shown. The means ± SD of signal ratios of phosphorylated versus total MLC of 3 independent experiments were determined by densitometry and illustrated in the bar graph in the lower panel.

F. Activated RhoA levels in PE-stimulated smooth muscles of mesenteric arteries. Mesenteric arteries were isolated from WT and KO mice and the epithelium of the vessels was removed. The vessels were subjected to PE stimulation (20 μM) for 5 sec at room temperature and then quickly frozen in liquid nitrogen. The vessels were then homogenized and the activated RhoA (GTP associated RhoA) levels were determined in duplicate by the G-LISA RhoA Activation Assay Biochem Kit. Results of two independent experiments were pooled and Means + SD are illustrated. Data were analyzed by paired student t tests, and p values are indicated.

Figure 3 the effect of sex hormones on BP and VSMC contraction of castrated Ephb6 KO mice.

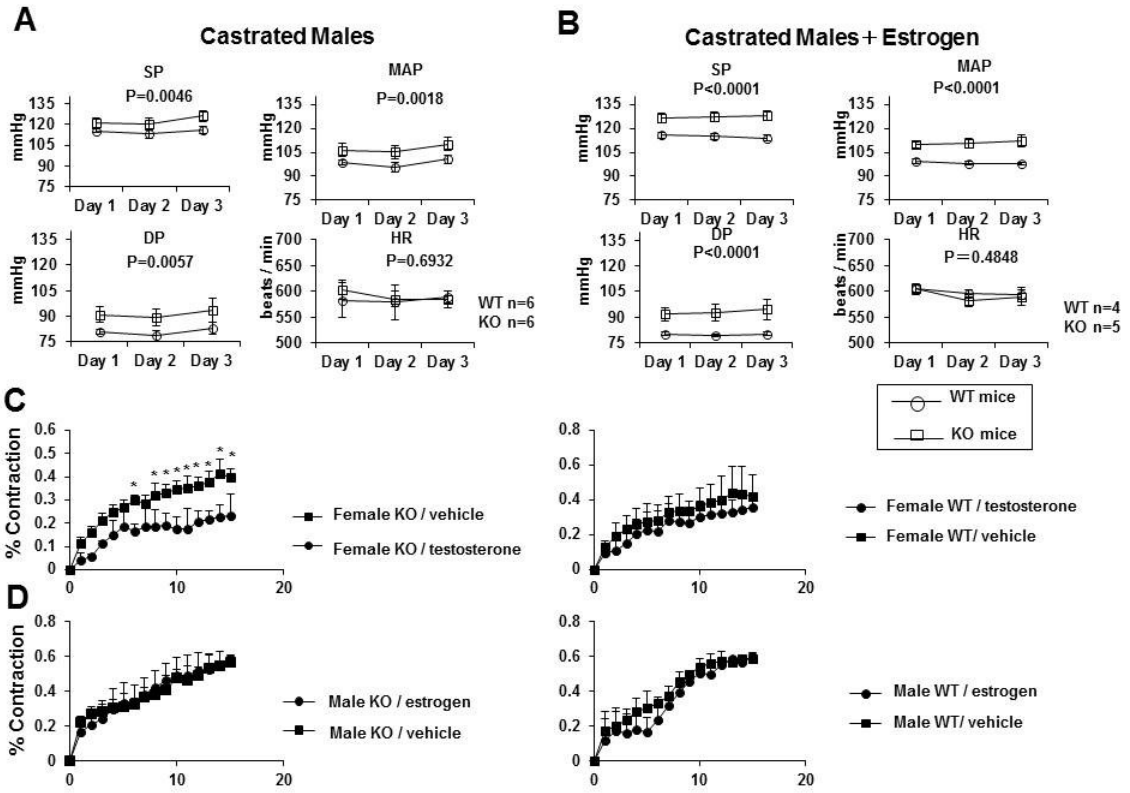

A. Increased BP in castrated Ephb6 KO mice.

Mice were implanted with telemetry transmitters, and then castrated. After 3 weeks, BP and HR were measured for 3 consecutive days.

B. Administration of estrogen to the castrated Ephb6 KO mice did not lower BP. Male mice were castrated one week after transmitter implantation; three weeks after the castration, mice were administered with estrogen (240 μg) daily s.c. for 7 days. Their BP and HR were measured by telemetry during the last 3 days of estrogen administration. For A and B, mouse numbers per group are shown. Values are expressed as means ± SE 24-h BP and HR for each day ± SE. SP: systolic pressure; DP: diastolic pressure; MAP: mean arterial pressure; HR: heart rate. Data were analyzed by repeated ANOVA, and the p values are shown.

C. Female KO VSMC showed higher contraction in the absence of exogenous testosterone. VSMC from WT and KO female mice were cultured in 15% stripped FCS for 4 days in the

presence of 10 μg/ml testosterone or vehicle. The cells were then stimulated with 20 μM PE.

D. Estrogen did not affect VSMC contraction in the absence of Ephb6.

VSMC from WT and KO male mice were cultured in 15% stripped FCS for 4 days in the presence of 10 μg/ml estrogen or vehicle. The cells were then stimulated with 20 μM PE. For C and D, each point represents the mean + SE of percentage contraction of 10 or more cells. All experiments were repeated at least twice, and data from a representative experiment are shown. *: significant differences compared to controls ($p<0.05$; paired Student's t test).

Figure 4 Twenty-four-h urine catecholamine levels in Ephb6 KO mice.

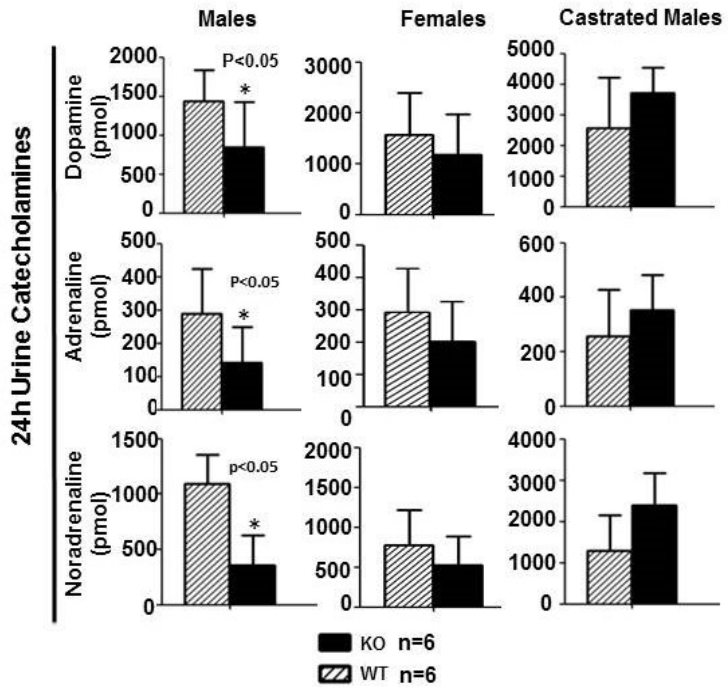

Male, female and castrated Ephb6 KO and WT mice were placed in metabolic cages. Urine was collected during a 24-h fasting period. Urine catecholamines were measured by ELISA, and means + SD of hormones excreted during the 24-h period and mouse number per groups (n) are presented.

Figure 5 Reverse but not forward signaling between Ephb6 and Efnbs dampens VSMC contractility.

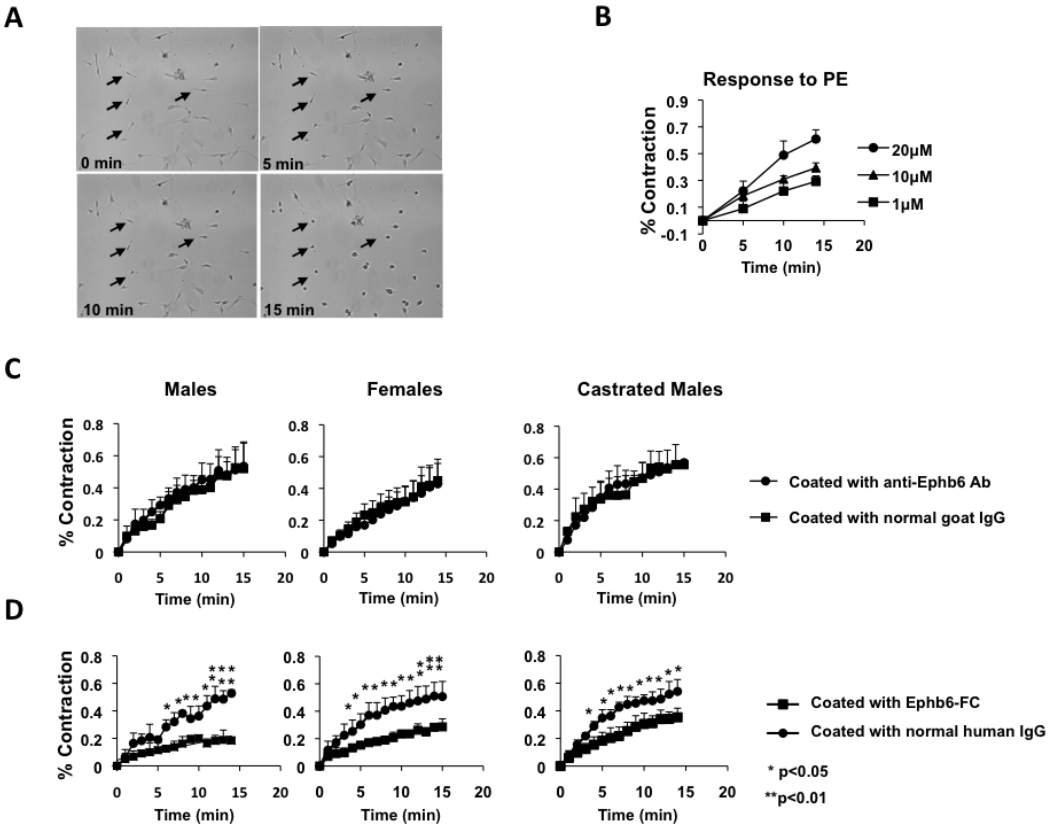

Data presentation and statistical analysis are the same as described in Fig. 4C and 4D.

A. Micrographs of VSMC contraction after PE stimulation. VSMC were stimulated with 20 μM PE and imaged every min. Images at 0, 5, 10 and 15 min are presented. Four arrows point to the same 4 cells during the 15-min imaging period, and show their contraction. The photos also reveal that about 85% of the cells are capable of contraction, indicating the purity of VSMC in such cell preparations.

B. Dose-dependent response of VSMC contractility to PE stimulation.WT VSMC was stimulated with PE at different concentrations for 15 min at 37 degree.

C. Solid-phase anti-Ephb6 Ab had no effect on VSMC contractility.

Wells were coated with goat-anti-Ephb6 Ab or normal goat IgG (2 μg/ml during coating). VSMC from WT male (left panel), WT female (middle panel) or castrated WT male (right panel) mice were cultured in these wells for 4 days and then stimulated with 20 μM PE.

D. Solid-phase Ephb6-Fc reduced VSMC contractility. Wells were coated with recombinant Ephb6-Fc or normal human IgG (2 μg/ml during coating). VSMC from WT male (left panel), WT female (middle panel) or castrated WT mice (right panel) were cultured in these wells for 4-5 days and then stimulated with 20 μM PE.

Figure 6 Grip1 in the Efnb reverse signaling pathway in VSMC

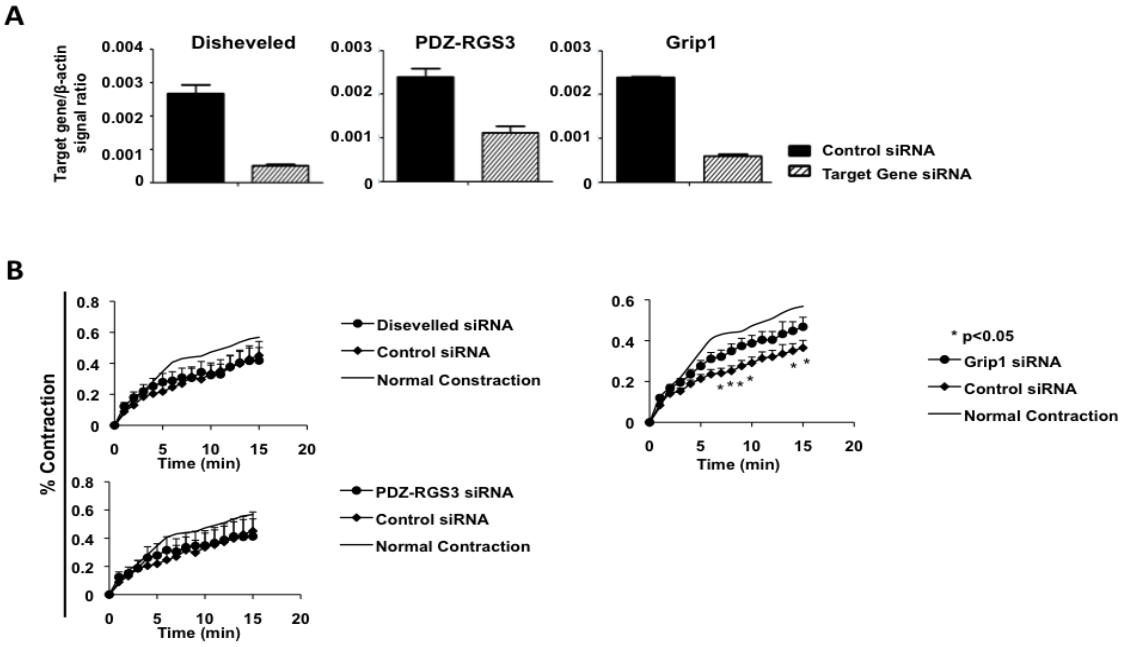

Experiments in this figure were repeated more than twice, and representative data are shown.

A. Effective mRNA knockdown of Disheveled, PDZ-RGS3 and Grip1 by siRNAs. Cultured WT VSMC were transfected with a mixture of siRNAs of a particular gene or control siRNAs, as indicated. After additional 24-h culture, the cells were harvested and the mRNA expression of each gene was determined by RT-qPCR. The data are expressed as means + SD of the ratios of the target gene signal versus the β-actin signal.

B. Grip1 knockdown by siRNAs partially reversed the inhibitory effect of solid-phase Ephb6-Fc.

VSMC from WT males were cultured in wells coated with Ephb6-Fc (2 μg/ml for coating). After 2 days, the cells were transfected with siRNAs targeting Disheveled, PDZ-RGS3 or Grip1, or with control siRNA. On day 4 of culture, they were stimulated with PE (20 μM) and their percentage contraction was registered. Means ± SD of the percentage are shown. The thin line (indicated as Normal Contraction) represents the mean percentage contraction of VSMC cultured in wells coated with normal human IgG (2 μg/ml) without siRNA transfection (for a better visual effect, the SD of each time point in this control is omitted).

*: $p < 0.05$ according to paired Student's t test, between Grip1 siRNA- and control siRNA-transfected VSMC.

SUPPLEMENTAL INFORMATION

Supplemental methods

Measurement of Ca^{++} flux

VMSC were incubated in DMEM containing 2% FBS and 5 μM Fura-2-AM for 30 min. The cells were washed in medium warmed for 15 to 20 min to remove extracellular dye. They were re-cultured in HBSS with Ca^{++} (1.26 mM) and placed under a Zeiss microscope with environmental controls (37ºC and 5% CO_2). The cells were stimulated with PE (20 μM) and were imaged for 5 min at a rate of 6 pictures per min. Excitation wavelengths were switched between 340 nm and 380 nm with illumination time of 180 ms, and emission wavelength was 510 nm. Signals from more than 15 randomly-selected cells were recorded and the results expressed as ratios of fluorescent intensity at 510 nm excited by 340 nm versus 380 nm.

Quantitative immunofluorescemce microscopy for Efnb1, Efnb2, Enb3, type 1a α adrenoreceptor and angiotensin II receptor Ia

VSMC were cultured in 24-well plates with cover glass placed at the bottom of the wells. After four to five days, the cells were washed twice with PBS and fixed with paraformaldehyde (4%) for 15 minutes. For cell surface Ag staining, cells were blocked with 10% goat IgG in PBS for 20 minutes and then incubated with various first Abs (2 μg/ml): goat anti-mouse EFNB1 Ab (R&D System, Minneapolis, MN, USA); goat anti-mouse EFNB2 Ab (R&D Systems); goat anti-mouse EFNB3 Ab (R&D Systems); rabbit anti-mouse type 1a α adrenoreceptor (α_{1a} -AR) Ab, (Abcam Inc., Cambridge, MA, USA); and rabbit anti-mouse AngII receptor Ia (ATR_{1a}) Ab (Santa Cruz Biotechnology, Santa Cruz, CA, USA) overnight at 4 ºC.

Cells were then reacted with corresponding second Abs (i.e., rhodamine-conjugated donkey anti-goat Ab, 0.15 μg/ml, (Jackson ImmunoResearch Laboratories, West Grove, PA, USA); and FITC-conjugated sheep anti-rabbit IgG, 0.2 μg/ml, (Chemicon International, Billerica, MA, USA) for overnight at 4 ºC. The stained cells were examined under a Zeiss microscope. The total fluorescent intensity of a cell and cell size were measured using software AxionVision (Zeiss) and the results are presented as arbitrary fluorescent intensity per unit cell area.

In situ hybridization (ISH)

A 1,700-bp fragment of EphB6 cDNA (positions 859 to 2,559) in the pGEM-3Z vector was used to generate sense and antisense riboprobes with SP6 and T7 RNA polymerase for both ^{35}S-UTP and ^{35}S-CTP incorporation. Tissues were frozen in -35°C isopentane and kept at -80°C until cut. ISH was performed on 10-μm cryostat sections. ISH microscopy was undertaken by photographic emulsion followed by 8-day exposure.

Supplemental tables

Supplemental Table I. Sequ1ences of primers for RT-qPCR.

Supplemental Table I. qPCR Primer Sequences

Gene	qPCR primer sequences		length of PCR products
	sense sequences	antisense sequences	
β-actin	5'-TCGTACCACAGGCATTGTGATGGA-3'	5'-TGATGTCACGCACGATTTCCCTCT-3'	200bp
Ephb6	5'-CTTTGCCTTTGTTCACCGAGCACT-3'	5'-AGCAAGGAACTTGAACCCTGAGGA-3'	111bp
Efnb1	5'-ACCAGGAAATCCGCTTCACCATCA-3'	5'-ACAGCATTTGGATCTTGCCCAACC-3'	199bp
Efnb2	5'-TTCTGCTGGATCAGCCAGGAATCA -3'	5'-TCCTGATGCGATCCCTGCGAATAA-3'	196bp
Efnb3	5'-AGTTCCGATCCCACCACGATTACT-3'	5'-AGAAGCACCTTCATGCCTCTGGTT -3'	112bp
Dishevelled 1	5'-TCTCGGCTAGTTCGGAAGCACAAA-3'	5'-TGATGTTCAGGGACATGGTGGAGT-3'	112bp
PDZ-RGS3	5'-TGGCAACAGGAGGAACAGTGGTAT-3'	5'-ATGTCTTCCAGCAGGAATGGGTCA-3'	170bp
Grip1	5'-ACAAGTCCCGTCCGGTTGTGATAA-3'	5'-TCTATCAGCAGCGTGGCTTCTTGT-3'	181bp

Supplemental Table II siRNA sequences of Dishevelled, PDZ-RGS3, Grip1 and controls

Supplemental Table II. siRNA Sequences

Gene	sets of siRNA sequences	
	sense sequences	antisense sequences
Disheveled 1	5'-rGrCrU rArGrU rUrCrG rGrArA rGrCrA rCrArA rArUrG rCrCG T-3'	5'-rArCrG rGrCrA rUrUrU rGrUrG rCrUrU rCrCrG rArArC rUrArG rCrCrG-3'
	5'-rArCrA rGrCrU rCrArA rGrUrA rUrCrU rArUrA rGrArG rUrCT T-3'	5'-rArArG rArCrU rCrUrA rUrArG rArUrA rCrUrU rGrArG rCrUrG rUrArC-3'
	5'-rCrGrC rCrUrA rCrArA rArUrU rCrUrU rCrUrU rCrArA rGrUC C-3'	5'-rGrGrA rCrUrU rGrArA rGrArA rGrArA rUrUrU rGrUrA rGrGrC rGrUrG-3'
PDZ-RGS3	5'-rGrGrG rArGrA rGrArA rCrArC rCrArA rArUrA rArArU rCrAA C-3'	5'-rGrUrU rGrArU rUrUrA rUrUrU rGrGrU rGrUrU rCrUrC rUrCrC rCrUrG-3'
	5'-rGrCrC rArCrA rUrArA rArUrC rArCrG rCrUrA rArGrA rArGC A-3'	5'-rUrGrC rUrUrC rUrUrA rGrCrG rUrGrA rUrUrU rArUrG rUrGrG rCrArG-3'
	5'-rCrCrU rArCrA rGrArG rArGrG rArArG rArArA rCrUrU rCrAC C-3'	5'-rGrGrU rGrArA rGrUrU rUrCrU rUrCrC rUrCrU rCrUrG rUrArG rGrUrG-3'
Grip1	5'-rArGrA rUrArA rCrUrC rArGrA rCrGrA rGrCrA rArGrA rGrAG T-3'	5'-rArCrU rCrUrC rUrUrG rCrUrC rGrUrC rUrGrA rGrUrU rArUrC rUrUrC-3'
	5'-rArGrC rGrUrG rGrArA rCrUrU rGrGrA rArUrA rArCrC rArUC A-3'	5'-rUrGrA rUrGrG rUrUrA rUrUrC rCrArA rGrUrU rCrCrA rCrGrC rUrGrU-3'
	5'-rArCrA rCrUrA rGrArA rArUrC rGrArG rUrUrU rGrArU rGrUT G-3'	5'-rCrArA rCrArU rCrArA rArCrU rCrGrA rUrUrU rCrUrA rGrUrG rUrGrA-3'
Control	5'-rCrUrU rCrCrU rCrUrC rUrUrU rCrUrC rUrCrC rCrUrU rGrUG A-3'	5'-rUrCrA rCrArA rGrGrG rArGrA rGrArA rArGrA rGrArG rGrArA rGrGrA-3'

Legends to supplemental figures

Supplemental Figure1 Plasmid construct used to generate β-actin promoter-driven Ephb6Δ (Ephb6 without its intracellular domain) Tg mice.

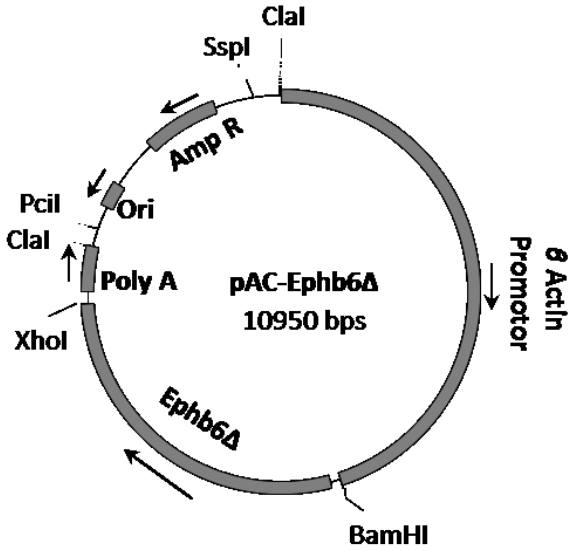

Ephb6Δ Tg mice were generated by linearized ClaI/ClaI fragment from plasmid pAC-Ephb6Δ. The fragment contained the human β-actin promoter followed by the Ephb6 coding sequence with the intracellular domain truncated, and the poly A sequence of β-actin.

Supplemental Figure2 BP and HR of male and female Ephb6 KO mice.

BP and HR were measured for 3 days by radiotelemetry, starting at least 7 days after transmitter implantation. Mouse numbers per group are shown. Values are expressed as mean 24-h BP and HR for each day ± SE. SP: systolic pressure; DP: diastolic pressure; MAP: mean arterial pressure; HR: heart rate. Data were analyzed by repeated ANOVA, and the *p* values are reported. **A**: males; **B**: females.

Supplemental Figure3 Plasma and serum hormone levels in Ephb6 KO mice.

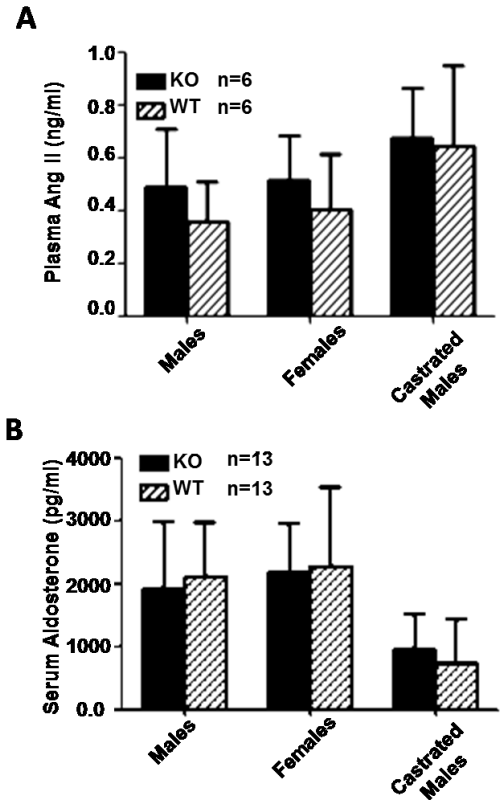

Plasma AngII (A) and serum aldosterone (B) of male, female and castrated EphB6 KO and WT mice were measured by ELISA. For castrated mice, samples were collected at more than 4 weeks after castration. Mouse numbers per group (n) are indicated. Means + SD of hormone concentrations are shown. No statistically significant differences were found (Student's *t* test).

Supplemental Figure4 Castrated Ephb6Δ/KO mice present no BP increase.

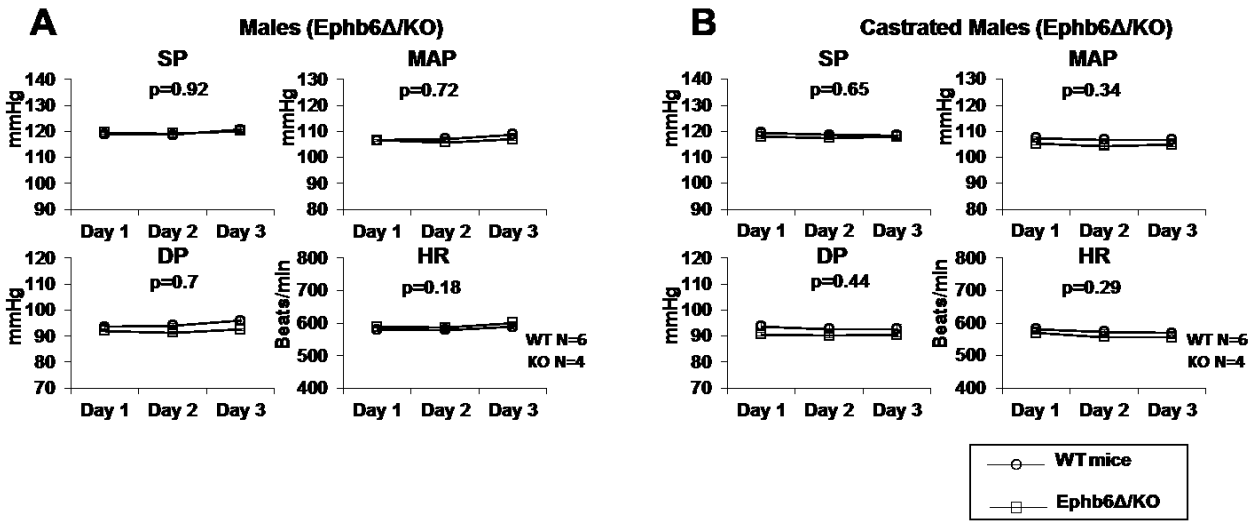

BP and HR of male (**A**) or castrated (**B**) male Ephb6Δ/KO mice were measured by radiotelemetry as described in Fig. 3. Data were analyzed by repeated ANOVA, and the *p* values are reported.

Supplemental Figure 5 Ephb6 expression in the adrenal gland medulla according to ISH

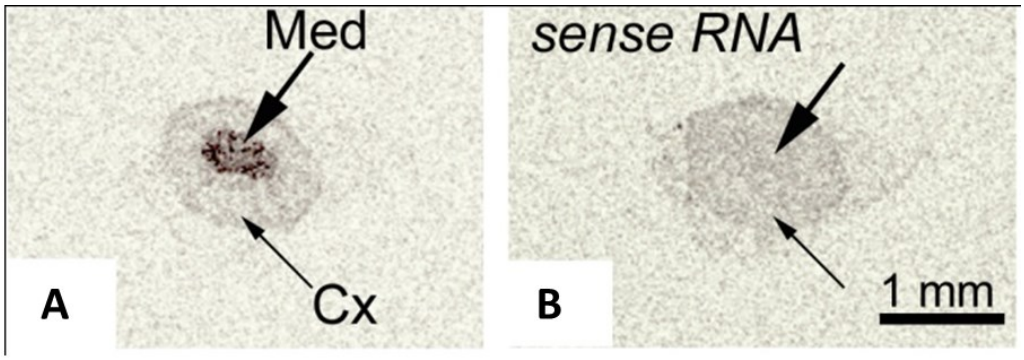

Med: medulla; Cx: cortex. Scale: 1 mm.

A. *Adult adrenal gland labeled with anti-sense probe.*

B. *Adult adrenal gland labeled with sense probe.*

Supplemental Figure 6 Expression of EFNBs, Ephb6, AR, AT1, and Grip1 in VSMC and endothelial cells

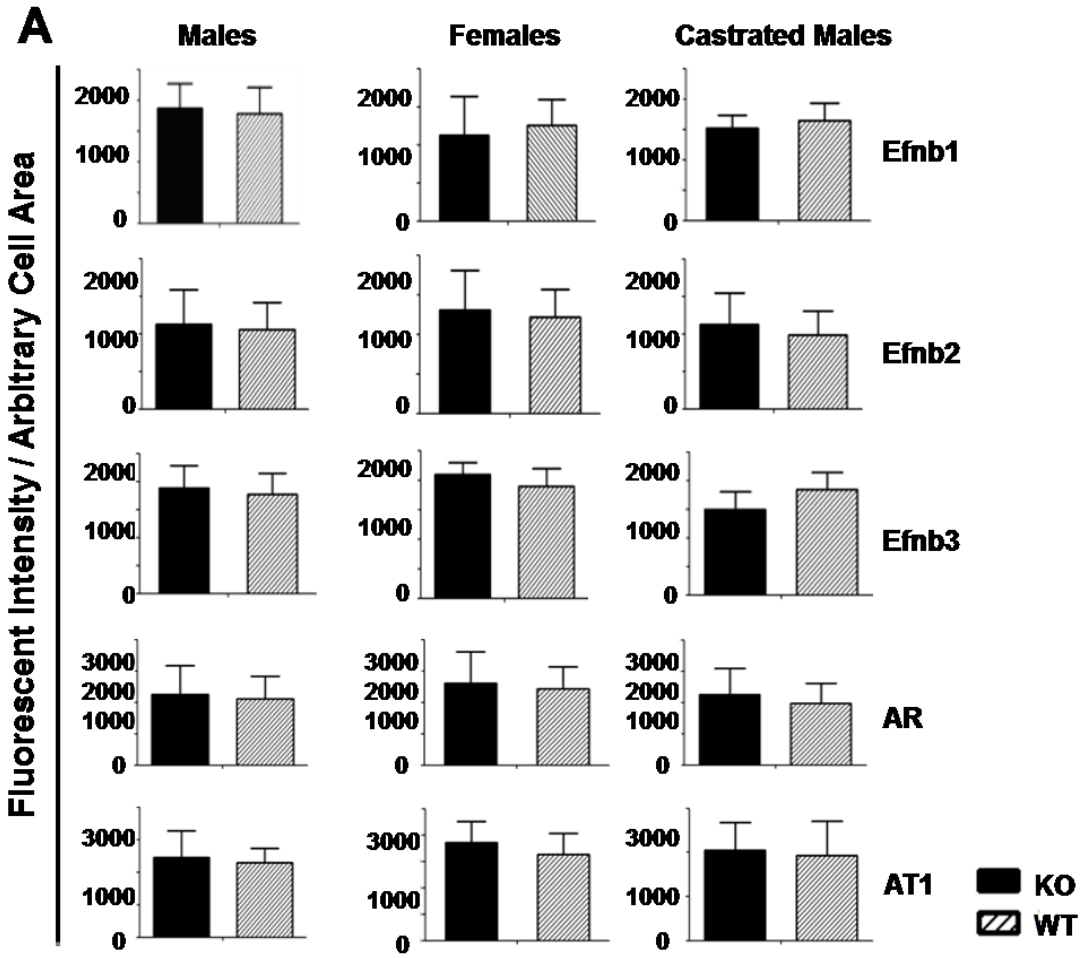

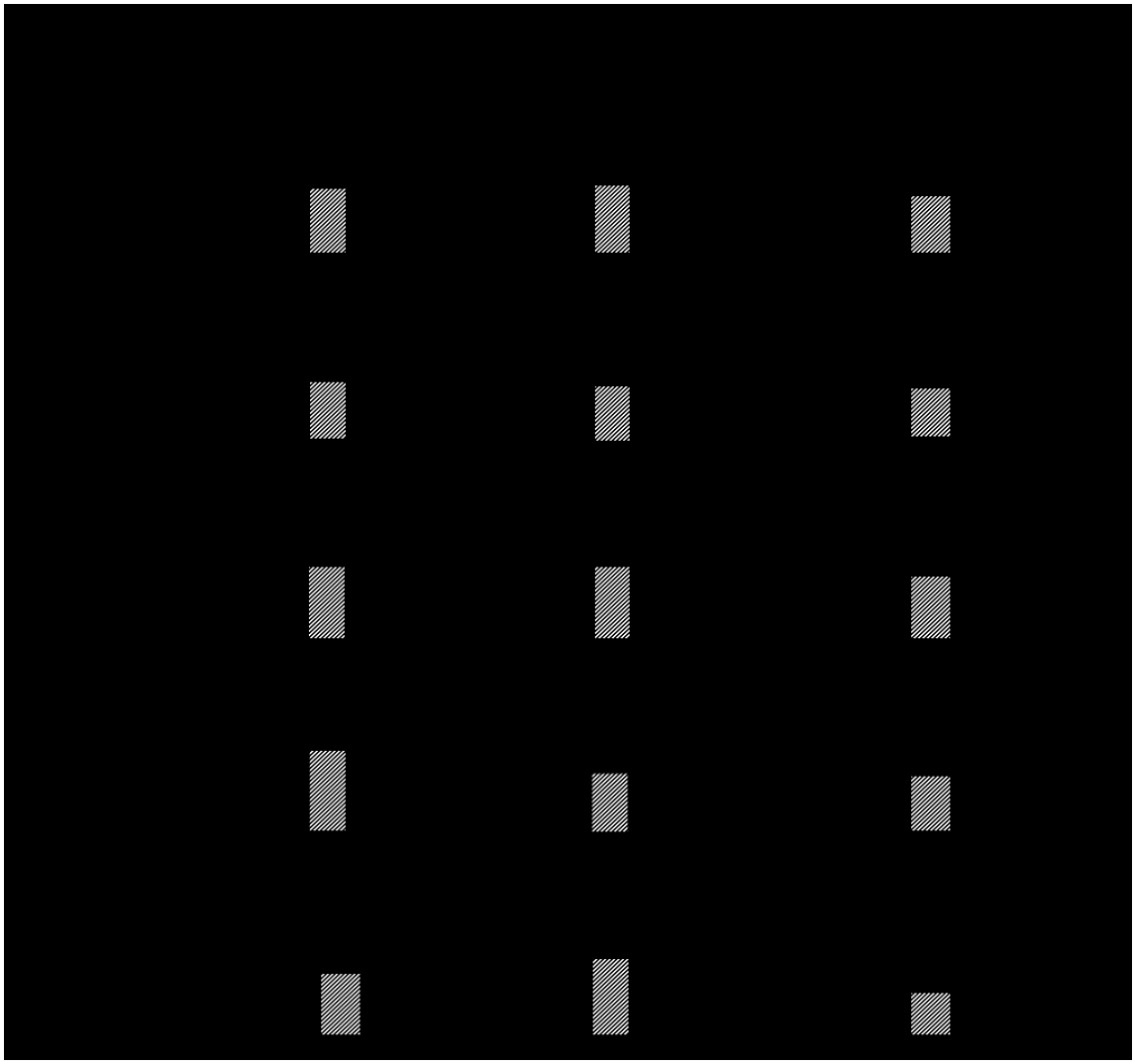

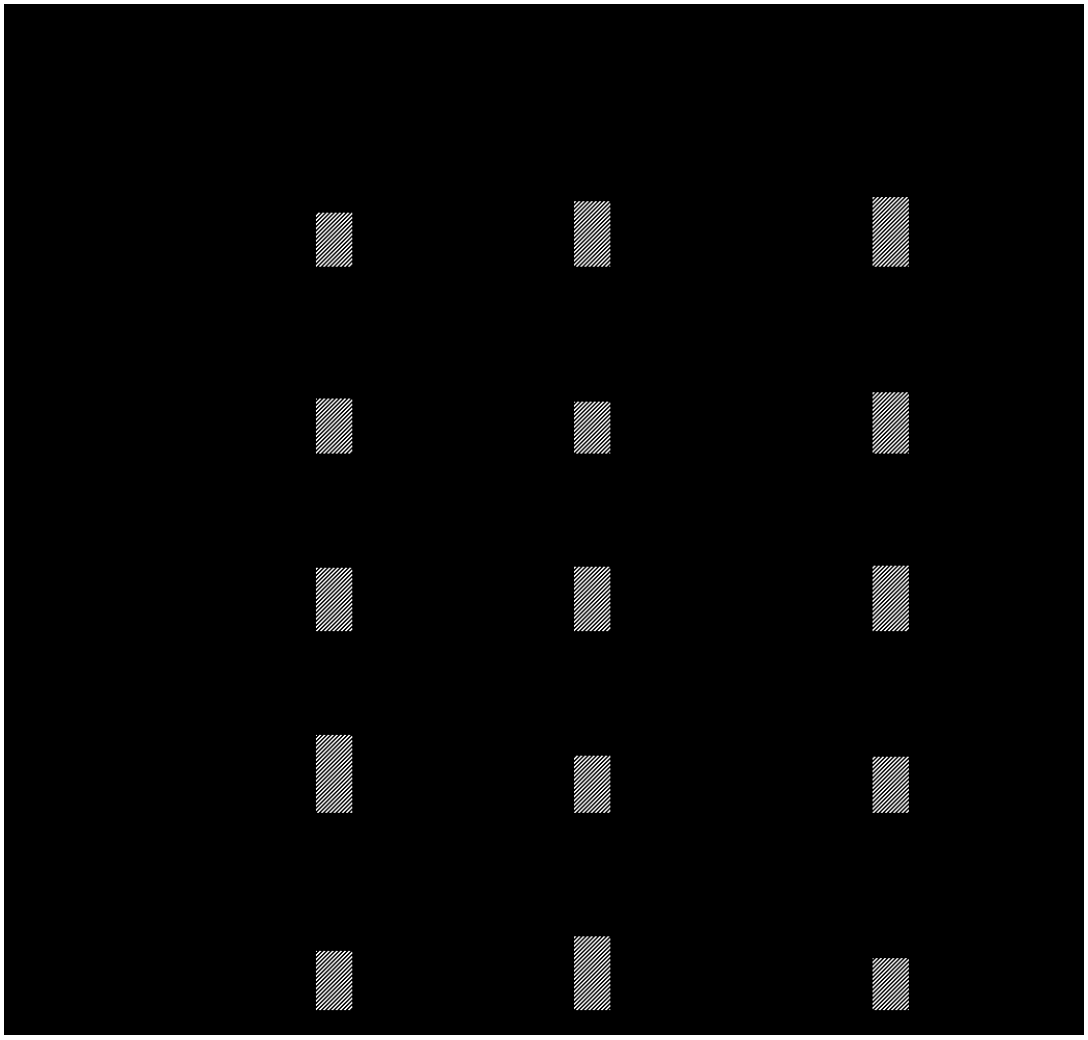

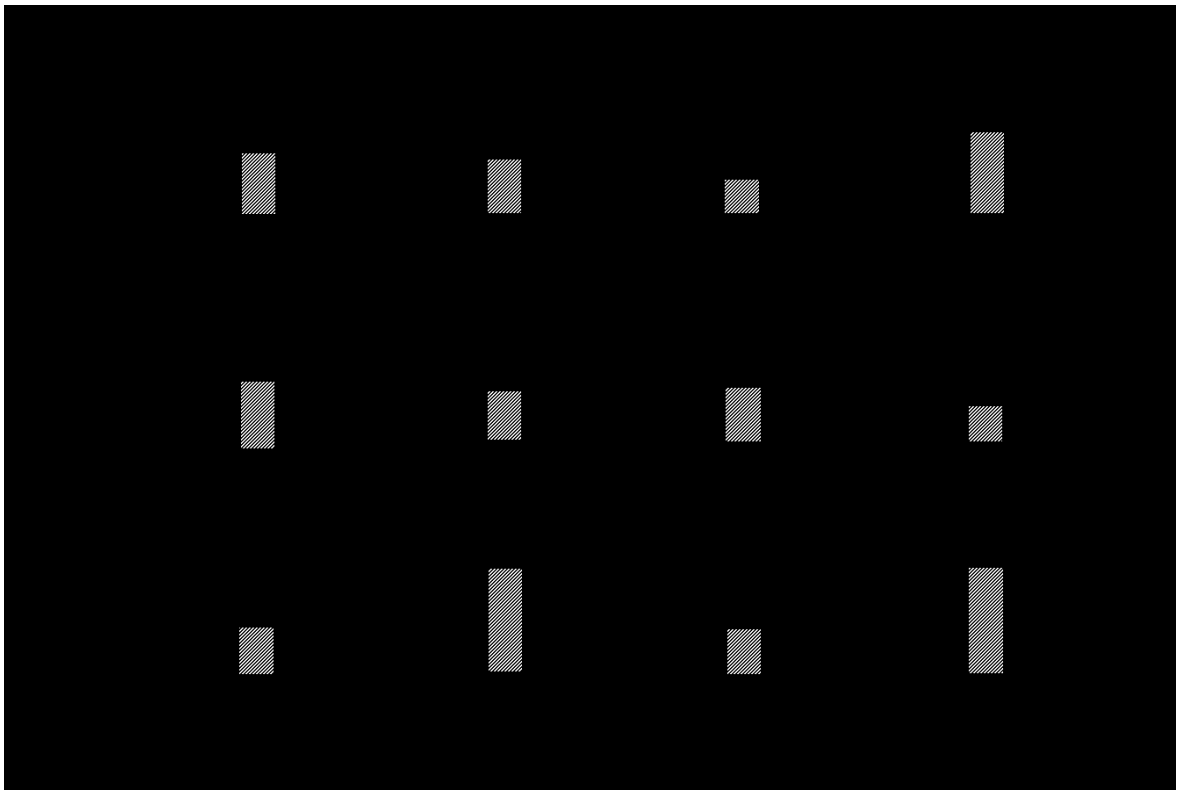

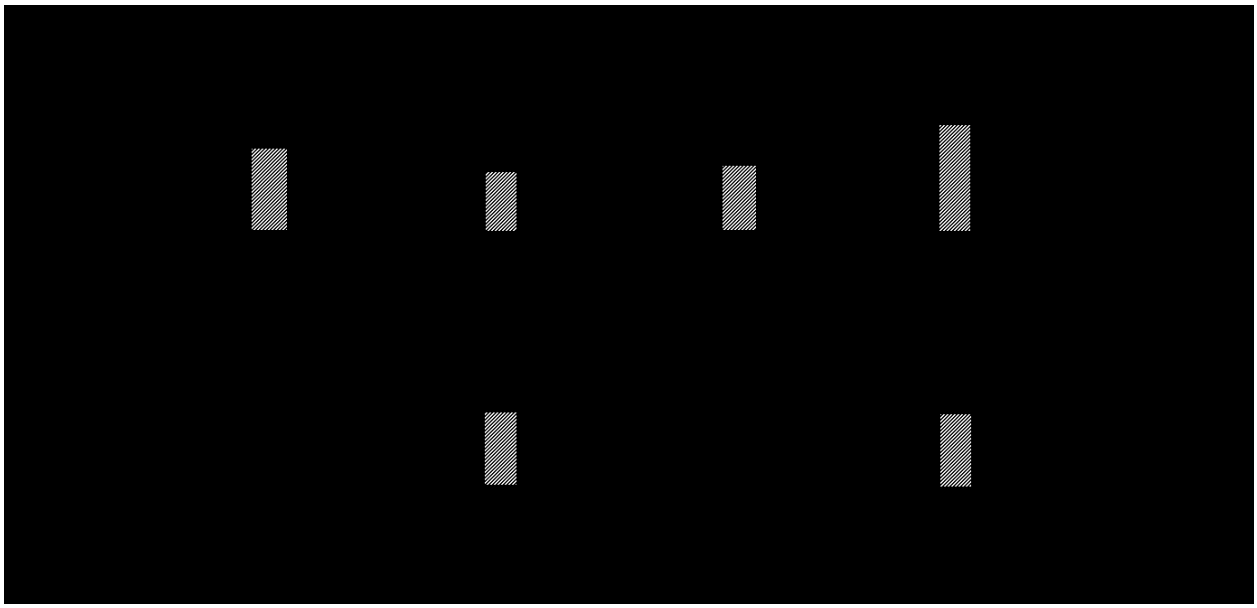

A. *Normal expression of Efnb1, Efnb2, Efnb3, type 1a* α-adrenoreceptor *(AR) and AngII receptor (AT1) in Ephb6 KO VSMC according to immunofluorescence.*

VSMC from male, female and castrated male Ephb6 KO or WT mice were stained with Abs against Efnb1, Efnb2, Efnb3, AR or AT1 as indicated. VSMC were identified with anti-α-actin Ab staining. Normal goat IgG served as isotypic control. For each staining,

more than 10 α-actin-positive cells were randomly selected and their total immunofluorescence intensity and cell size were recorded by Zeiss AxioVision software. The experiment was repeated at least twice. The means + SD of fluorescence intensity per arbitrary unit cell area of all cells examined (more than 10 per experiment) in a representative experiment are shown.

***B** and **C**. Efnbs, Ephb6 and Grip1 expression in endothelial cells according to q-PCR.*

Efnb1, Efnb2, Efnb3 Ephb6 and Grip1 mRNA levels in freshly isolated mesenteric arteries with endothelium stripped (B) or endothelial cells from mesenteric arteries (C) of males, females and castrated males of WT or KO mice were determined by RT-qPCR in triplicate. The data are expressed as means $\pm$ SD of the ratios of the target gene signal versus the β-actin signal. No significant difference between KO samples and their WT counterparts was found (Student's *t* tests), except Ephb6, which was deleted in KO mice.

***D**. Efnbs, Ephb6 and Grip1 expression according to q-PCR in VSMC after sex hormone treatment in vitro.*

VSMC from female WT mice were cultured in the presence of testosterone (10 μg/ml) for 4 days. Conversely, VSMC from male WT mice were cultured in the presence of estrogen (10 μg/ml) for 4 days. The cells were harvested and their mRNA levels of Efnb1, Efnb2, Efnb2, Ephb6 and Grip1 were determined by RT-qPCR. The data are expressed as means $\pm$ SD of the ratios of the target gene signal versus the β-actin signal. No significant difference between KO samples and their WT counterparts was found (Student's *t* tests), except Ephb6, which was deleted in KO mice.

Supplemental Figure 7 Ca^{++} flux in PE-stimulated VSMC.

The experiments in this figure were repeated more than twice, and a representative dataset is shown.

A. *Ca^{++} flux in PE-stimulated VSMC from WT and Ephb6 KO mice.*

VSMC from male (left panel), female (middle panel) or castrated male (right panel) WT or Ephb6 KO mice were cultured for 4 days and then loaded with Fura2 (5 μM). They were then placed in HBSS containing 1.26 mM Ca^{++} at 37ºC and stimulated with PE (20 μM). The ratio of emission at 510 nm triggered by 340 nm versus 380 nm excitation in each cell was registered every 10 s for 5 min, and the means + SD of the ratio of more than 15 randomly-selected VSMC are shown. Arrows indicate the time point when PE was added.

B. *Ca^{++} flux in PE-stimulated WT VSMC cultured in wells coated with Ephb6-Fc.*

VSMC from WT male, female or castrated male mice were cultured for 4 days in wells coated with Ephb6-Fc or NHIgG (2 μg/ml during coating). Ca^{++} flux after PE stimulation (20 μM) was measured as described above.

Article 2.

A possible role of Efnb1- A lligand of Eph receptor tyrosine kinases in modulating blood pressure

*Zenghui Wu[1], *Hongyu Luo[1], #Eric Thorin, *Johanne Tremblay, *Junzheng Peng, *Julie L. Lavoie, *Yujia Wang, *Shijie Qi, *^Tao Wu, and *+Jiangping Wu

J Biol Chem. 2012 May 4; 287 (19):15557-69. Epub 2012 Mar 5.

Summary: in this paper we showed the elevated blood pressure in Efnb1$^{-/-}$mice under immobilized condition. The phosphorylation of MLC was also increased in knockout mice. It was revealed that the Efnb1 reverse signaling was involving in the regulation of blood pressure and the function of vascular smooth muscle cells.

Zenghui Wu performed experiments using VSMC and data analysis. Dr. Hongyu Luo generated Efnb1 KO mice, measured the aldosterone levels and analyzed data. Drs. Johanne Tremblay, Junzheng Peng and Julie Lavoe measured BP. Dr Eric Thorin performed vessel constriction experiments in vitro. Dr. Yujia Wang constructed plasmids for Grip1 overexpression in VSMC. Dr. Tao Wu initiated VSMC culture technique. Dr. Shijie Qi conducted castration, ovariectomy and mouse husbandry. Dr Jiangping Wu and Dr Hongyu Luo directed the experimental design and data analysis.

Article 2.

A POSSIBLE ROLE OF EFNB1- A LIGAND OF EPH RECEPTOR TYROSINE KINASES - IN MODULATING BLOOD PRESSURE

*Zenghui Wu[1], *Hongyu Luo[1], #Eric Thorin, *Johanne Tremblay, *Junzheng Peng, *Julie L. Lavoie, *Yujia Wang, *Shijie Qi, *^Tao Wu, and *+Jiangping Wu

From +Nephrology Department and *Centre de recherché, Centre hospitalier de l'Université de Montréal (CRCHUM), Montreal, Quebec, Canada; #Montreal Heart Institute, Montreal, Quebec, Canada; ^and Institute of Cardiology, the First Affiliated Hospital, Medical College, Zhejiang University, Hangzhou, China

Running title: Efnb1 regulates vascular smooth muscle contractility and blood pressure

Abstract

Background: Currently, there is no knowledge about the function of ephrins in vascular smooth muscle contraction and blood pressure regulation. Results: Stimulating Efnb1 reduces vascular smooth muscle cell contraction. Efnb1 null mutation leads to increased RhoA activation and heightens blood pressure in mice. Conclusion: Efnb1 can regulate vessel tone and blood pressure. Significance: We have identified a new group of molecules capable of regulating blood pressure. Eph kinases constitute the largest receptor tyrosine kinase family and their ligands, ephrins (Efns), are also cell surface molecules. Efns, although being ligands, can transduce signals reversely into cells. We have no prior knowledge of the role played by any members of this family of kinases or their ligands in blood pressure (BP) regulation. In the present studies, we investigated the role of Efnb1 in vascular smooth muscle cell (VSMC) contractility and BP regulation. We revealed that reverse signalling through Efnb1 led to a reduction of RhoA activation and VSMC contractility in vitro. Consistent with this finding, ex vivo, there was an increase of RhoA

activity accompanied by augmented myosin light chain phosphorylation in mesenteric arteries from mice with smooth muscle-specific conditional Efnb1 gene knockout (KO). Small interfering RNA knockdown of Grip1, a molecule associated with the Efnb1 intracellular tail, partially eliminated the effect of Efnb1 on VSMC contractility and MLC phosphorylation. In supporting of these in vitro and ex vivo results, Efnb1 KO mice on a high-salt diet showed statistically significant heightened increment of BP at multiple time points during stress, compared to wild type littermates. Our results demonstrate that Efnb1 is a previously unknown negative regulator of VSMC contractility and BP, and that it exerts such effects via reverse signalling through Grip1.

Eph kinases form the largest family of receptor tyrosine kinases. Eph kinases can be divided into A and B families based on their sequence homology. There are 9 members in the EphA family and 6 members in the EphB family. Each species does not necessarily have all the members of each family. In mice, except there are only 5 members in the EphB family. The ligands of Eph kinases are also cell surface proteins (2-4), and this dictates that interactions between Ephs and ephrins (Efns) are mainly local and are restricted to neighboring cells. Efns are divided into A and B families, the former being GPI-anchored cell surface proteins, and the latter transmembrane proteins (2-4). Ephs and Efns interact promiscuously, but EphAs predominantly bind to EfnAs, and EphBs, mainly to EfnBs (2-4). Interestingly, EfnBs may also transduce signals into cells upon binding to EphBs, and this phenomenon is called reverse signaling (2-4).

The functions of Eph/Efn molecules in the central nervous system were the first to be studied in depth (3,4). In recent years, their functions have been revealed in various other tissue and organs. These molecules are involved in immune regulation (5), intestinal and urorectal tract development and function (6,7), angiogenesis (8), bone formation (9,10), insulin secretion by islet α-cells [225], kidney glumerolar filtration [226], and ionic homeostasis of vestibular endolymph fluid in the inner ear [227], to name a few.

There are a few reports showing that EfnB2 and EfnA1 are expressed in vascular smooth muscle cells (VSMC) [228], and VSMC with EfnB2 deletion manifests compromised migration [229]. One study has shown that EfnA1 could trigger EphA4 signaling and actin

stress fiber assembly [230]. However, there are no studies to date on the function of Ephs and Efns in VSMC contractility and blood pressure (BP) regulation.

In an unrelated project, our DNA microarray assay showed that some genes controlling BP were differentially expressed in Ephb6 gene knockout (KO) versus wild type (WT) thymocytes. This prompted us to investigate the roles of Ephs and Efns in BP regulation. In this report, we have demonstrated for the first time that Efnb1 regulates VSMC contractility and blood pressure in mice with conditional deletion of the Efnb1 gene.

Methods:

Generation of smooth muscle cell-specific Efnb1 KO mice

The scheme, procedures and verification of the generation of Efnb1 floxed mice are reported recently by us [231]. Efnb1 is an X-linked gene. Mice with LoxP sites flanked by the 1st Efnb1 exon were named Efnb1f/f (loxP insertions in both alleles in females) or Efnb1f (loxP insertion in one allele in males). They were backcrossed with C57BL/6 for 5 or 10 generations and then mated with smooth muscle myocin heavy chain-promoter-driven Cre transgenic (Tg) mice in the C57BL/6 background (smMHC-Cre-IRES-eGFP; ref. 19) to obtain smooth muscle cell-specific Efnb1 gene KO mice.

Reverse transcription/real-time polymerase chain reaction (RT/qPCR)

Efnb1, Grip1, Disheveled and PDZ-RGS3 mRNA levels were measured by RT/qPCR. Forward and reverse primers and the size of amplified fragments are listed in Table I. Total RNA from VSMC or spleen cells was extracted using TRIzol® (Invitrogen, Carlsbad, CA) and then reverse-transcribed with Superscript II™ reverse-transcriptase (Invitrogen). The PCR condition for the reactions were as follows: 2 min at 50^{o}C, 2 min at 95^{o}C followed by 45 cycles of 10 s at 94^{o}C, 20 s at 58^{o}C and 20 s at 72^{o}C. β-actin mRNA levels were used as internal controls and data were expressed as signal ratios of test gene mRNA/β-actin mRNA.

Immunoblotting

The aorta and mesenteric arteries of WT and KO mice were isolated, washed twice with HBSS buffer, and then frozen in liquid nitrogen until their use. The vessels were

homogenized for 1 min at room temperature in 0.4 ml radio-immunoprecipiation assay buffer, which contained Pho-stop and Protease Inhibitor Cocktail (Roche Applied Science, Laval, QC, Canada). The samples were spun at 12,000 rpm for 15 min at 4^{o}C and the supernatants were collected. Twenty micrograms of proteins per sample were resolved in 12% SDS-PAGE. Proteins from the gel were transferred to PVDF membranes (Invitrogen), which were incubated in blocking buffer containing 5% (w/v) skimmed milk (for MLC, 5% BSA was used in the blocking buffer) for 1 h at room temperature, and then hybridized overnight at 4^{o}C with goat anti-mouse Efnb1 Ab (R & D Systems, Minneapolis, MN), rabbit anti-mouse α-actin Ab, mouse anti-mouse phospho-MLC mAb, or rabbit anti-mouse total MLC Ab (all from Cell Signalling Technology, Danvers, MA). The Abs were used at the manufactures' recommended dilutions or at 1:1000. The membranes were washed 3 times and reacted with corresponding second Abs, i.e., horseradish peroxidise-conjugated donkey anti-rabbit IgG Ab (GE healthcare, Baie d'Urfe Quebec, Canada), horseradish peroxidise-conjugated sheep anti-mouse IgG Ab (GE Healthcare), or horseradish peroxidise-conjugated rabbit anti-goat IgG Ab (R & D Systems), for 90 min. The signals were detected with SuperSignal West Pico Chemiluminescent Substrate (Thermo Scientific, Rockford, IL).

VSMC isolation

Mouse VSMC isolation was conducted as described by Golovina et al. (20) with modifications. Briefly, the mesenteric arteries, including their secondary branches from the 10- to 15 week-old mice were cleaned of the adventitia with fine forceps and sterile cotton-tipped applicators under sterile conditions. The isolated blood vessels were cut into small pieces [232] and digested at 37^{o}C for 20 min in low-Ca2+ HBSS containing both collagenase type II (347 U/ml, Worthington Biochemical Corporation, Lakewood, NJ) and elastase type IV (6 U/ml) (Sigma-Aldrich, St. Louis, MO). The digestion mixture was centrifuged at 1,500 g for 5 minutes to bring down cells. The dissociated cells were suspended and plated on 12-well plates. The cells were cultured at 37^{o}C in Dulbecco's modified Eagle's medium (Wisent, St. Bruno, QC, Canada) supplemented with 15% fetal bovine serum (FBS) for 4 to 5 days before experimentation.

Immunofluorescence microscopy

VSMC were cultured in 24-well plates with cover glass placed at the bottom of the wells. After 4 to 5 days, the cells were washed twice with PBS and fixed with paraformaldehyde (4%) for 20 min. For cell surface Ag staining, cells were blocked with 10% goat IgG in PBS for 20 min and then incubated with various first Abs (2 μg/ml): goat anti-mouse Efnb1 Ab (R&D System, Minneapolis, MN); rabbit anti-mouse type 1a α adrenoreceptor (α1a-AR) Ab, (Abcam Inc., Cambridge, MA); and rabbit anti-mouse AngII receptor Ia (ATR1a) Ab (Santa Cruz Biotechnology, Santa Cruz, CA) overnight at 4ºC. Cells were then reacted with corresponding second Abs (i.e., rhodamine-conjugated donkey anti-goat Ab, 0.15 μg/ml, Jackson ImmunoResearch Laboratories, West Grove, PA, USA; and FITC-conjugated sheep anti-rabbit IgG, 0.2 μg/ml, Chemicon International, Billerica, MA) overnight at 4ºC. For intracellular Ag staining, the cells were permeabilized with permeabilization buffer (BD Biosciences, San Jose, CA) for 20 min at 4ºC, and then incubated with various first Abs: mouse anti-human α-actin mAb (2 μg/ml; Santa Cruz Biotechnology); rabbit anti-mouse myosin light chain (MLC, 0.2 μg/ml; Santa Cruz Biotechnology); and rabbit anti-mouse phospho-MLC Ab (0.2 μg/ml; Santa Cruz Biotechnology) overnight at 4 degree. Cells were then washed and reacted with, respectively, second Abs: rhodamine (TRITC)-conjugated AffiniPure F(ab')2 fragment of goat anti-mouse IgG (H+L) (0.2 μg/ml; Jackson ImmunoResearch Laboratories); FITC-conjugated goat anti-mouse IgG (0.2 μg/ml; Bethyl Laboratories, Montgomery, TX); FITC-conjugated sheep anti-rabbit IgG (0.2 μg/ml; Chemicon International) at room temperature for 2 h, and imbedded with ProLong® Gold anti-fade reagent (Invitrogen). The stained cells were examined under a Zeiss microscope. In some experiments, the total fluorescent intensity of a cell and cell size were measured using AxioVision software from Zeiss; results are then presented as fluorescent intensity per arbitrary unit of cell area [233].

Measurement of VSMC contractility

Cultured primary VMSC were washed once with Ca++-free HBSS and cultured in the same solution. They were placed under a Zeiss microscope with environmental controls (37ºC and 5% CO_2). The cells were stimulated with PE (20 μM) or Ang II [234] (both from Sigma-Aldrich). These concentrations were determined to be optimal according to pilot studies.

The cells were photographed continuously for 15 min at a rate of 1 picture per min. Fifteen or more cells were randomly selected and their length was measured at each time point with Zeiss Axiovision software. The percentage contraction was calculated as follows:
% contraction = (cell length at time 0 – cell length at time X) / cell length at time 0.

Measurement of Ca++ flux

VMSC were incubated in 2% FBS DMEM medium containing 5 μM Fura-2-AM for 30 min. The cells were washed in warmed medium for 15 to 20 min to remove extracellular dye. They were re-cultured in HBSS with Ca++ [235] and placed under a Zeiss microscope with environmental controls (37ºC and 5% CO_2). The cells were stimulated with PE (20 μM) and were imaged for 5 minutes at a rate of 6 pictures per min. The excitation wavelengths were switched between 340 nm and 380 nm with illumination time of 180 ms, and the emission wavelength was 510 nm. Signals from more than 15 randomly selected cells were registered and the results expressed as ratios of fluorescent intensity at 510 nm excited by 340 nm versus 380 nm.

Small interfering RNA (siRNA) transfection

siRNA of Grip1, Dishevelled, PDZ-RGS3 and negative control siRNA were synthesized by Integrated DNA Technologies (Coralville, IA); the sequences of these siRNAs are shown in Table II. VSMC were cultured for 4 to 5 days with the last 16 hours free of antibiotics and then transfected with a mix of 3 pairs of siRNAs of a particular gene (each pair at a final concentration of 10 nM), using FuGENE HD X-tremeGENE siRNA Transfection Reagent (Roche Applied Science). The transfected VSMC were further cultured for 24 to 36 h; contractility was measured upon PE stimulation and MLC phosphorylation was measured by immunofluorescence.

Transient Grip1 overexpression in VSMC

A Grip1 expression plasmid pCEP4-Grip1 was constructed by cloning mouse Grip1 cDNA (a NotI/HincII fragment of clone MGC80644 containing Grip1 cDNA from position 1 to 4064 according to Genbank BC072632 sequence) in the NotI/XhoI sites downstream of the CMV promoter in a mammalian cell protein expression vector pCEP4. WT VSMC

were cultured for 6 days, and then transfected with pCEP4-Grip1 or the control empty vector pCEP4 using 0.2 μg pasmid DNA mixed with FuGENE HD X-tremeGENE siRNA Transfection Reagent (Roche Applied Science) for a well VSMC in 6-well plates. Cell contraction was conducted 24 h later.

Activated RhoA assay

GTP-associated activated RhoA levels in mesenteric artery smooth muscles were determined by G-LISK RhoA Activation Assay Biochem Kit (Cytoskeleton Inc. Denver, CO, USA) according to manufacturer's instructions.

Ex vivo vessel constriction

Vessel constriction was studied ex vivo as described previously (21). Mesenteric artery segments (2 mm in length) of third-order branches (exterior diameter 125 to 150 μm) were stripped off endothelium and mounted on 20-μm tungsten wires in small vessel myographs, stretched to optimal tension and maintained in physiological saline solution (PSS: NaCl, 130 mM; KCl, 4.7 mM; KH_2PO_4, 1.18 mM; $MgSO_4$, 1.17 mM; $NaHCO_3$, 1.17 mM; $CaCl_2$, 1.6 mM; EDTA, 0.023 mM; glucose, 10 mM; aerated with 12% O_2/5% CO_2/83% N_2; pH 7.4) at 37°C. After a 40-min stabilization period, arterial segments were challenged with 40-mM KCl PSS (KCl was substituted for an equivalent concentration of NaCl). Single cumulative concentration-response curves to the α1-adrenergic receptor agonist phenylephrine (PE, 1 nM to 100 μM, Sigma, St. Louis, MO, USA) were charted. At the end of the protocol, maximal tension (Emax) was determined by changing the PSS to a solution containing 127 mM KCl. The data are expressed as percentages of Emax. Student's t tests were performed to compare concentration-response curves.

BP measurements by radiotelemetry

Mice were anesthetized with isoflurane and surgically implanted with TA11PA-C10 radiotelemetry sensors (Data Sciences International, St. Paul, MN, USA) in the left carotid artery for direct measurement of arterial pressure and HR as described previously (22). Mice were given 7 days to recover. Next, BP and HR in conscious free-moving mice were continuously recorded for 3 days using the Dataquest acquisition 3.1 system (Data Sciences International). Individual 10-s waveforms of systolic pressure (SP), diastolic pressure

(DP), mean arterial pressure (MAP) and heart rate (HR) were sampled every 2 minutes throughout the monitoring period. To assess the impact of immobilization stress on BP and HR were measured continuously during 30-min immobilization in a restraining device (IITC Life Science, Woodland Hills, CA) [236]. Raw data were processed by the Dataquest A.R.T-Analysis program (24) and then presented as means ± SE. Statistical significance of differences between the experimental groups was evaluated by unpaired t test and repeated-measures ANOVA tests with the Statview program. $P<0.05$ values were considered to be statistically significant.

ELISA for urine catecholamine and plasma AngII measurements

The 24-h urine catecholamines were assayed by catecholamine ELISA Kit (Rocky Mountain Diagnostics, Colorado Springs, CO). The plasma AngII was measured by Angiotensin ELISA Kit (Phoenix Pharmaceuticals, Burlingame, CA). The assays were conducted according to manufacturers' instructions.

Results

Generation of SMC-specific Efnb1 conditional gene KO mice

Efnb1 null mutation caused embryonic lethality (25). To study their function in VMSC, we generated conditional KO mice [237]. These mice (Efnb1f/f for females and Efnb1f for males, as Efnb1 is an X-linked gene) were crossed with smMHC-Cre-IRES-eGFP Tg mice [238]. The resulting Efnb1 conditional KO mice were named smMHC-Cre-Efnb1f/f for females and smMHC-Cre-Efnb1f for males. For reasons to be elucidated, female smMHC-Cre-Efnb1f/f mice were embryonic lethal and only male smMHC-Cre-Efnb1f could be generated. Therefore, smMHC-Cre-Efnb1f male mice (backcrossed to the C57BL/6 background for 5 or 10 generations) were used as KO mice throughout this study, while age-matched Cre-Efnb1f male mice with the same generation of backcrossing were used as controls. These mice were called Efnb1 KO and WT mice hereafter, respectively.

As shown in Fig. 1A, the SMC-specific deletion of exon 1 in the genome resulted in Efnb1 mRNA deletion in Efnb1 KO VSMC, but not in spleen cells of Efnb1 KO mice, according to RT/qPCR. The mRNA deletion in the KO arterial tissue was not complete, probably due

to the presence of a small amount of fibroblasts and endothelial cells in the vessel. Efnb1 deletion in KO VSMC at the protein level was demonstrated by immunoblotting. As shown in Fig. 1B, Efnb1 could be detected from lysates of freshly isolated WT but not in Efnb1 KO arteries.

Efnb1 deletion in VSMC at the protein level was also clearly demonstrated by immunofluorescence (Fig. 1C), as WT α-actin-positive (green) VSMC were Efnb1-positive (red), while α -actin-positive Efnb1 KO VSMC were Efnb1-negative. The result proved not only VSMC-specific deletion of Efnb1 in Efnb1 KO mice, but also the specificity of anti-Efnb1 Ab.

Efnb1 engagement in VSMC results in their decreased contractility due to Efnb1 reverse signalling

We established a method of intravital microscopy to assess the contractility of KO and WT VSMC. Isolated VSMC were cultured for 4-5 days and then stimulated with vasoconstricting agents such as phenylephrin (PE) and angiotensin II (AngII). Images of the cells were recorded for 15 min and VSMC length was measured digitally at different time points. As illustrated in Fig. 2A, the majority of the cells (more than 80%) showed drastic contraction upon PE stimulation, and the contraction reached its maximum 15 min after the stimulation. This result indicates that after 4-5 days of culture, the isolated VSMC retained their contractile phenotype. A few non-contracting cells were likely contaminating fibroblasts. By randomly selecting contracting cells and measuring their length at different time points, we were able to assess their contractility as a function of cell length and time elapsed.

The contractility of Efnb1 KO and WT VSMC was measured on the basis of their responses to PE and AngII, but both types of VSMC presented similar contractility (Fig. 2B). A possible explanation is that unlike VSMC in vivo where the cells have close contact with neighboring VSMC, allowing constant Eph/Efn engagement, the cultured VSMC had limited interaction with neighbouring cells hence limited engagement between Efn and Eph, especially in our culture conditions, where VSMC were always non-confluent. Under

such circumstances, the difference of Efn1 KO and WT in contractility, if there was any, was difficult to detect.

We reasoned that if VSMC were cultured on wells coated with anti-Efnb1 or recombinant Efnb1, they might receive sufficient reverse or forward signalling, respectively, to mimic the in vivo condition. Indeed, when cultured in wells coated with anti-Efnb1 Ab and upon PE or AngII stimulation, WT VSMC contraction reduced about 45-70% [(% contraction of WT cells in isotypic Ab-coated wells)/(% contraction of WT cells in anti-Efnb1 Ab-coated wells)] in multiple time points compared to those cultured in wells coated with isotypic control Ab (Fig. 2C). For Efnb1 KO VSMC cultured in wells coated with anti-Efnb1 Ab, their contractility upon PE and AngII stimulation showed no significant difference from that of WT VSMC cultured in well coated with isotypic Ab. This is logical, as anti-Efnb1 Ab could not react to these cells due to their null mutation of Efnb1. These results indicate that the function of Efnb1 in VSMC is to dampen their contractility through reverse signaling. As the presence of solid phase anti-Efnb1 Ab dampened the contractility of WT VSMC in response to both PE and AngII, the reverse signaling through Efnb1 was not specific to adrenoreceptor (AR) or AngII type I receptor (AT1R), but was probably on a downstream event after AR and AT1R signalling converges. The effects of solid phase anti-Efnb1 Ab in reducing WT VSMC contractility could be brought back to near-normal level (the contraction was only about 10% lower than that of the WT cells cultured in isotypic Ab-coated wells without soluble Efnb1-Fc) by soluble Efnb1-Fc (Fig. 2D), demonstrating the specificity of the interaction between anti-Efnb1Ab and Efnb1-Fc.

When WT VSMC were cultured in wells coated with recombinant Efnb1-Fc, the contractility of the cells was no different from that of cells cultured in wells coated with normal human IgG (Fc in Efnb1-Fc is of human origin) (Fig. 2E). This proves that forward signaling from Efnb1 to its receptors in VSMC is of no consequence in terms of VSMC contractility.

Normal expression of AR and AT1R in Efnb1 KO VSMC

The reduced contractility of WT VSMC in the presence of Efnb1 engagement in response to PE and AngII could be due to modulation of AR or AT1R expression by Efnb1. We therefore assessed the expression levels of AR and AT1R on VSMC by immunofluorescence microscopy. The staining was quantified using Zeiss AxioVision software by measuring the immunofluorescene intensity per arbitrary unit of cell surface area [239]. Efnb1 KO VSMCs were no different from WT VSMC in their AR and AT1R expression when cultured in uncoated wells (Fig. 3A). Although Efnb1 WT VSMC, when cultured in wells coated with anti-Efnb1 Ab, showed reduced contractility than KO VSMC, their AR and AT1R expression levels did not change (Fig. 3B). In this experiment, WT VSMC Efnb1 was stimulated by solid phase anti-Efnb1 Ab, while KO VSMC could not be stimulated by the Ab due to a lack of Efnb1. The results indicate that Efnb1 engagement or not did not alter AR and AT1R expression.

Effect of Efnb1 reverse signaling on calcium flux of VSMC

Calcium flux is an essential early signaling event common to both PE and AngII stimulation in VSMC, leading to their contraction. We investigated whether the deletion or engagement of Efnb1 in VSMC led to increased basal calcium level and/or amplitude of calcium flux, which could in turn lead to increased contractility. As shown in Fig. 3C (cells cultured in wells coated with isotypic control Abs with no Ca++ in the medium) and in Fig. 3D (cells cultured in wells coated with anti-Efnb1 Ab with no Ca++ in the medium), Efnb1 KO and control WT VSMC showed no significant difference in basal and stimulated intracellular calcium levels on PE (left panel) and AngII (right panel) stimulation. It is to be noted that in Fig. 3D, WT VSMC received stimulation from solid phase anti-EFNB1 Ab, while KO VSMC could not, due to their lack of EFNB1. In both Fig. 3C and 3D, the calcium influx seen in these cells was mobilized from intracellular Ca++ storage in sarcoplasmic reticulum.

We next cultured Efnb1 KO and WT VSMC in medium containing Ca++ and stimulated them with PE. In this case, the source of increased intracellular calcium in VSMC came from both extracellular culture medium and from intracellular sarcoplasmic reticulum. WT and KO VSMC in wells coated with isotypic control Ab (Fig. 3E, left panel) again showed

similar basal Ca++ levels and Ca++ flux. In this case, even if EFNB1 in WT VSMC received some stimulation from neighbouring cells, while KO VSMC did not, there was no difference in their Ca++ levels. We then cultured WT and KO VSMC in wells coated with anti-Efnb1 Ab in the presence of calcium in culture medium. In this case, again, WT could receive stimulation from solid phase anti-Efnb1 Ab while KO VSMC cannot due to their Efnb1 deletion. Yet, their basal Ca++ levels and Ca++ flux presented not difference (Fig. 3E, right panel).

The results from this section indicate that Efnb1 null mutation or anti-Efnb1 Ab-triggered reverse signaling in VSMC does not affect the function Ca++ ion channels related to Ca++ mobilization from either intracellular or extracellular sources. Therefore, the reduced VSMC contractility upon Efnb1 reverse signaling is not due to abnormalities of the immediate early signaling event Ca++ flux.

Effect of Efnb1 reverse signaling on VSMC MLC phosphorylation and RhoA activation

Since there was no difference in basal and flux levels of calcium in VSMC with or without Efnb1 signaling, we wondered whether Efnb1 reverse signaling altered the sensitivity of VSMC to Ca++. We evaluated these cells for their MLC phosphorylation, which is the main mechanism regulating VSMC sensitivity to Ca++ (26, 27). Levels of total MLC and phosphorylated MLC ex vivo in freshly isolated arteries (with adventitia and endothelium removed) were determined by immunoblotting. As shown in Fig. 4A, there was a significant increase in levels of constitutive MLC phosphorylation but not total MLC in Efnb1 KO vessels, compared to those in WT vessels. We next assessed constitutive MLC phosphorylation in cultured VSMC by immunofluorescence microscopy, which was employed because the amount of proteins that could possibly be obtained from these cultured VSMC was too small for immunoblotting. Consistent with the findings of immunoblotting in vessels ex vivo, WT VSMC cultured in anti-Efnb1 Ab-coated wells showed reduced levels of constitutive MLC phosphorylation (Fig. 4B, right panel), but not total MLC (Fig. 4B, left panel), compared to those without anti-Efnb1 stimulation (cultured in wells coated with isotypic control Ab. These results suggest that Efnb1 reverse signaling dampens VSMC responsiveness to Ca++ flux by reducing MLC phosphorylation.

Consistent findings between immunoblotting and quantitative immunfluorescence microscopy validated the latter as an alternative to the former.

As activated RhoA could increase MLC phosphorylation via the RhoA-associated kinase/myosin phosphatase pathway (28), we wondered whether Efnb1 reverse signaling in VSMC resulted in RhoA activation. Indeed, when WT VSMC were cultured in wells coated with anti-Efnb1 Ab, there was a significant increase of GTP-bound RhoA level, compared to cells cultured in wells coated with isotypic control Ab (normal goat IgG) (Fig. 4C).

Identification of Grip1 as a component in the Efnb1 reverse signaling pathway in controling VSMC contraction

Since we discovered that reverse signaling is critical for the effect of Efnb1 on VSMC contraction, we attempted to identify components of the Efnb1 reverse signaling pathway. The intracellular tails of Efnb1 show no direct biological activity, but it has 3 conserved tyrosine phosphorylation sites, which are known to interact with SH2-domain-containing adaptors, such as Disheveled (29). In addition, the C-terminus of Efnb1 possesses a PDZ-binding domain (2), which could interact with PDZ-containing proteins such as Grip1 (30) or PDZ-RGS3 (31). To test the relevance of these adaptor proteins in mediating Efnb1's reverse signaling in and effect on VSMC, we employed siRNA to knock down the expression of Disheveled, Grip1 and PDZ-RGS3 in WT VSMC. The expression and knockdown of these genes was confirmed at the mRNA level (Fig. 5A). When Efnb1-engaged WT VSMC (i.e., VSMC cultured in anti-Efnb1 Ab-coated wells), whose contractility was depressed about 40% in multiple time points compared to the controls, were transfected with Grip1 but not PDZ-RGS3 or Disheveled siRNA, they regained about 50% of their lost strength (Fig. 5B). On the other hand, Grip1 siRNA had no effect on VSMC without Efnb1 engagement (VSMC cultured in wells without anti-Efnb1 Ab coating, Fig. 5C). This shows that the effect of Grip1 siRNA is specific to Efnb1 reverse signaling, but does not exert its effect via other pathways by itself. These results indicate that diminished Grip1 expression blocks the negative effect of Efnb1 engagement on VSMC contraction

Conversely, when Grip1 was overexpressed in WT VSMC without anti-Efnb1 stimulation, these cells showed about 50% reduced contractility, mimicking the effect of Efnb1 reverse signalling (Fig. 5D).

These data demonstrate that Grip1 is a relevant adaptor protein that mediates Efnb1 reverse signaling in VSMC to achieve reduced VSMC contractility.

We further demonstrated that Grip1 knockdown resulted in an increased level of MLC phosphorylation but not total MLC protein in EFNB1-engaged WT VSMC (Fig. 5E); such an increase is likely a basis for the increased VSMC contractility that was caused by Grip1 siRNA transfection. This places Grip1 upstream of MLC phosphorylation in the Efnb1 reverse signaling pathway.

Ex vivo findings in mesenteric arteries from Efnb1 KO mice.

We wondered whether the reduced RhoA activation and contraction of cultured VSMC upon Efnb1 activation was reflected in freshly isolated small arteries, which control vascular resistance, hence BP. GTP-associated RhoA levels in mesenteric arteries stripped of endothelium was first assessed. As shown in Fig. 6A, the arteries from the KO mice manifested significantly heightened GTP-associated RhoA levels compared with that from WT mice. This is conversely consistent with the findings from anti-Efnb1 Ab stimulated VSMC, which had reduced RhoA activation.

However, ex vivo vessel constriction tests on freshly isolated mesenteric arteries from KO and WT mice did not reveal significant difference, with or without endothelium, upon PE stimulation (Fig. 6B). Possible reasons for this observation will be discussed later.

Efnb1 KO mice presented higher increments of BP than WT mice during immobilization stress

The above findings regarding dampening VSMC contractility by Efnb1 engagement suggests that smooth muscle cell-specific Efnb1 null mutation might augment BP. Thus, we measured the BP of male Efnb1 KO mice by telemetry. On a normal diet alone, (Fig. 7A), on a normal diet under stress alone (data not shown) or on a high-salt diet alone (Fig. 7B), Efnb1 mice and control WT mice presented no significant difference in their SP, DP, MAP or HR. BP control has multiple compensatory mechanisms. A BP phenotype might be manifested only when the compensation is stretched to the limit. Indeed, the role of Efnb1 in BP regulation was revealed when the KO mice (average age: 21 week old) were

in a condition that combined a high-salt diet and immobilization stress. At several time points, Efnb1 KO mice showed significantly higher increments of SP, DP, and MAP (SP, DP and MAP, respectively; i.e., the BP during stress minus BP of the resting status of the same animal) (Fig. 7C). Such increased BP was a reproducible phenomenon. In a separate experiment carried out on 16-week old mice, such a statistically significant phenotype was also observed, even with a small sample size (n=3) (Fig. 7D). This is the first time a role of any Efn molecules in BP control has been discovered.

We have also observed (Fig. 7C) that during stress on a high-salt diet, Efnb1 KO mice had significantly a higher HR increment (ΔHR) than WT mice. Obviously, the higher ΔHR contributed to higher stress BP in these mice, along with increased VSMC contractility, as we have proven in vitro. The reason why Efnb1 deletion heightened ΔHR in this particular experiment is not clear and is under investigation, but the phenotype does not seem to be consistent and reproducible. As seen in Fig. 7D, in a similar experiment, such a heightened ΔHR increment was not present.

Normal levels of urinary catecholamines and plasma AngII of Efnb1 KO mice

The Efnb1 KO mice employed in this study had conditional Efnb1 KO in SMC and the phenotype of the mice was attributed to the deletion of Efnb1 in SMC. To rule out the unlikely possibility that such conditional KO also affects the endocrine system, which in turn contributes to the enhanced VSMC contractility and stress BP, we assayed the 24-h urine catecholamines right after stress or without stress (Fig. 8A), and plasma AngII (Fig. 8B) of Efnb1 KO mice. The results showed no significant difference in these parameters between Efnb1 KO and control WT mice, ruling out the possible effect of conditional Efnb1 deletion on the secretion of these hormones.

Discussion

We for the first time discovered that Efnb1 is likely involved in BP control by regulating VSMC contractility. Efnb1 engagement in mouse VSMC resulted in their decreased contractility in vitro, while EFNB1 null deletion in smooth muscle cells heightened the increment of BP during stress in mice on a high-salt diet in vivo. Such regulation depended on reverse signaling of Efnb1 into VSMC and this reverse signalling modulated the levels of GTP-associated RhoA and MLC phosphorylation in VSMC. An adaptor protein Grip1

was in the Efnb1 reverse signaling pathway and it mediated the effect of Efnb1 on VSMC contractility and MLC phosphorylation. A few issues are discussed as follows.

Efnb1 is vital during embryonic development. Complete deletion of Efnb1 leads to lethality during the fetal stage (25). Although male Efnb1 KO mice could be obtained, their occurrence was below the rate expected according to Mendel's law. It is known that LoxP-Cre-mediated deletion is not an all or none event, and there is variation in Cre expression even with the same copy number of Cre genes in the Tg genome (32). Leaky Tg Cre expression outside the targeted tissue is also frequently encountered. We speculate that fetuses with stronger Cre expression might become embryonic lethal, due to either a higher degree of Efnb1 deletion in SMC or leaky Cre expression in other tissues. No female smMHC-Cre-Efnb1f/f was ever born. This might be a result of essential interaction between Efnb1 and certain molecule(s) whose necessity is different in male and female fetuses.

Intracellular Ca++ level change in VSMC is a common and early signaling event after AR and AngIIR activation. We noticed that the VSMC Ca++ occurred within 1 min after PE stimulation, a time frame compatible with that under a physiological condition in vivo, under which arteries will constrict quickly upon adrenaline stimulation. However, it took about 15 min for cultured VSMC to achieve maximal contraction. This is because that the cultured VSMC adhere to the wells, and will need to master enough force to gradually dislodge themselves from the plastic well surface to complete the contraction, while VSMC in the vessels are free-standing, and can contract without much hindrance.

The increased intracellular Ca++ in VSMC comes from the influx of Ca++ from extracellular milieu via L-type voltage-gated calcium channel on the plasma membrane, but is mainly from the mobilization of Ca++ reserve in sarcoplasmic reticulum via ryanodine and inositol trisphosphate receptors on the sarcoplasmic reticulum membrane. The subsequent ebbing of the intracellular Ca++ depends on large-conductance Ca++-activated K+ channel on the plasma membrane and the SERCA (Sarco-Endoplasmic Reticulum Ca++-ATPase) pump on the sarcoplasmic reticulum membrane (33,34). VSMC in the presence or absence of Efnb1 reverse signalling presented similar basal Ca++ levels and Ca++ flux after PE and AngII stimulation. This is also true regardless whether there is

extracellular Ca++ in the medium. This indicates that all the signaling components (e.g. AR, AngIIR, L-type voltage-gated calcium channels, ryanodine receptors, inositol trisphosphate receptors, large-conductance Ca++-activated K+ channels, or SERCA pumps) leading to Ca++ flux are not modulated by Efnb1 reverse signaling.

In addition to intracellular Ca++ level, VSMC contractility is regulated by their sensitivity to Ca++, and the sensitivity is regulated by the degree of MLC phosphorylation (26,27). We have found that in the absence of Efnb1, the constitutive MLC phosphorylation in artery proteins was drastically augmented. The converse is also true: with Efnb1 engagement, VSMC showed decreased MLC phosphorylation. Conceivably, such modulation of MLC phosphorylation leads to altered VSMC Ca++ sensitivity, and consequently altered VSMC contractility.

We have tried to identify components in the Efnb1 reverse signaling pathway that regulates MLC phosphorylation and VSMC contraction. We discovered that RhoA activation in the form of GTP-associated RhoA was reduced in anti-Efnb1 Ab-stimulated VSMC. Compatible with such a finding, RhoA activation was augmented in the mesenteric artery smooth muscles of KO mice, compared to that in WT mice. Activated RhoA can activate RhoA-associated kinase, which phosphorylates myosin phosphatase. The phosphorylation of the phosphatase will reduce its activity, which will then prolong the phosphorylation of MLC (28). This might be a mechanism to increase the responsiveness of MLC to Ca++ flux in the absence of Efnb1 reverse signaling.

Additional search of the components in the Efnb1 reverse signaling pathway has identified Grip1, as its knockdown partially reverses Efnb1's effect on dampening VSMC contractility. Whether and how Grip1 is connected to RhoA activation, which will in turn promote MLC phosphorylation, is not clear and we can only speculate at this point. Grip1 is an adapter protein containing 7 PDZ domains (35), which can associate with the PDZ-binding domain at the C-termini of Efnbs (28). It is possible that the remaining PDZ domains in Grip1 might interact with modulators of RhoA activity, such as GDP dissociation inhibitors (GDI) or GDP exchange factors (GEF), and influence their functions, which will in turn regulate RhoA activity. Indeed, Grip1 can associate with a

Rho-GDI (36) and a Ras-GEF [65] through its PDZ domains. Validation of such hypotheses is in progress.

Consistent with most of the in vitro and ex vivo findings, Efnb1 KO mice manifested an augmented increment of SP, DP and MAP during stress, compared to WT mice, when they were on a high-salt diet. Although the increase was only statistically significant at several time points, this finding is genuine because it was reproducible in 2 independent experiments. BP, a vital physiological parameter, is tightly regulated by multiple compensatory mechanisms at the levels of vascular tone, blood volume and cardiac output. It is not easy to override all these compensatory mechanisms to achieve an overt BP phenotype. Any molecule that could cause an overt BP phenotype, even a minimal one, has much more than a minimal role in BP regulation. This is especially true for Efnb1, which is a member of the Efnb subfamily. The Efnb subfamily has 3 Efnb members which have redundant functions and interact promiscuously with Ephs. Such redundancy might have further diminished the BP phenotype of Efnb1 KO mice, so that BP upregulation in the KO mice is not manifested on a normal diet or under stress while on a normal diet, but is only revealed with a combination of a high salt diet plus stress. Under such conditions, the compensation mechanisms are finally overwhelmed. It is very likely that other Efnbs in addition to Efnb1 and some Ephb members are also involved in VSMC contractility and BP control. Our additional study showed that this is indeed the case: we have found that Ephb6 KO mice have BP and VSMC contractility phenotypes similar to that of Efnb1 KO mice (38).

There is some discrepancy among certain findings in our study. Ex vivo, RhoA activation and constitutive phosphorylation of MLC in the smooth muscle of the mesenteric arteries from KO mice were elevated. This is consistent with augmented BP in KO mice in vivo compared with WT mice, when they were under stress and on a high salt diet. This is also compatible with the findings in cultured VSMC, in that VSMC contractility was reduced upon Efnb1 engagement. However, why don't we see increased ex vivo contraction of mesenteric arteries from KO mice compared to that from WT mice (Fig. 6B), and why could the lack of increased contraction in vessels translate into the in vivo phenotype of increased BP? It is possible that a subtle and minor increase of vasoconstriction is present in the vessel, but our vasoconstriction tests ex vivo are not sensitive enough to reveal it.

Such an increase, as it is subtle and minor, neither was revealed in vivo when mice were on a normal diet or undergone immobilization stress alone. It only manifested itself when the KO mice were assaulted with both high salt diet and immobilization stress, which overcome most of the compensation mechanisms in BP regulation.

Based on our findings, we speculate that under a physiological condition, Efnb1 (or other Efnb members) on VSMC interact(s) with Ephs in neighbouring VSMC or endothelial cells, and such interactions modulate VSMC contractility. Since the expression of Efnb1 (or other Efnb members) and its binding partner Ephs is unlikely to change instantly, the physiological role of Efnb1 (or other Efnbs) and Ephbs could be basal vascular tone regulation. These findings have enhanced our understandings of BP regulation mechanisms.

Acknowledgements

The authors sincerely thank Dr. Michael Kotlikoff for generously providing us with smMHC-Cre-IRES-eGFP transgenic mice. This work was supported by grants from the Canadian Institutes of Health Research to J.W. (MOP57697, MOP69089, and PPP85159), H.L. (IMH 79565 and MOP97829), E.T. (MOP14496) and J.T. It was also funded by grants from the Heart and Stroke Foundation of Quebec, the Quebec Ministry of Economic Development, Innovation and Export Trade (PSR-SIIRI-069) and the J.-Louis Lévesque Foundation to J.W. It was supported in addition by a group grant from the Fonds de la recherche en santé du Québec (FRSQ) for Transfusional and Hemovigilance Medical Research to J.W.; T. W was supported in part by grants from the Zhejiang Provincial Natural Science Foundation of China (Grant #Y2080374) and the National Natural Sciences Foundation of China (Project for Young Scientists #30800999).

References

1. [240] Unified nomenclature for Eph family receptors and their ligands, the ephrins. Eph Nomenclature Committee. Cell 90, 403-404

2. Pasquale, E. B. (2008) Eph-ephrin bidirectional signaling in physiology and disease. Cell 133, 38-52

3. Wilkinson, D. G. (2000) Eph receptors and ephrins: regulators of guidance and assembly. Int.Rev.Cytol. 196, 177-244

4. Flanagan, J. G., Vanderhaeghen, P. [241] The ephrins and Eph receptors in neural development. Annu.Rev.Neurosci. 21, 309-345

5. Wu, J., Luo, H. (2005) Recent advances on T-cell regulation by receptor tyrosine kinases. Curr.Opin.Hematol. 12, 292-297

6. Batlle, E., Henderson, J. T., Beghtel, H., van den Born, M. M., Sancho, E., Huls, G., Meeldijk, J., Robertson, J., van de Wetering, M., Pawson, T., Clevers, H. (2002) Beta-catenin and TCF mediate cell positioning in the intestinal epithelium by controlling the expression of EphB/ephrinB. Cell 111, 251-263

7. Dravis, C., Yokoyama, N., Chumley, M. J., Cowan, C. A., Silvany, R. E., Shay, J., Baker, L. A., Henkemeyer, M. (2004) Bidirectional signaling mediated by ephrin-B2 and EphB2 controls urorectal development. Dev.Biol. 271, 272-290

8. Wang, H. U., Chen, Z. F., Anderson, D. J. [242] Molecular distinction and angiogenic interaction between embryonic arteries and veins revealed by ephrin-B2 and its receptor Eph-B4. Cell 93, 741-753

9. Davy, A., Bush, J. O., Soriano, P. (2006) Inhibition of gap junction communication at ectopic Eph/ephrin boundaries underlies craniofrontonasal syndrome. PLoS.Biol. 4, e315

10. Zhao, C., Irie, N., Takada, Y., Shimoda, K., Miyamoto, T., Nishiwaki, T., Suda, T., Matsuo, K. (2006) Bidirectional ephrinB2-EphB4 signaling controls bone homeostasis. Cell Metab 4, 111-121

11. Konstantinova, I., Nikolova, G., Ohara-Imaizumi, M., Meda, P., Kucera, T., Zarbalis, K., Wurst, W., Nagamatsu, S., Lammert, E. (2007) EphA-Ephrin-A-mediated beta cell communication regulates insulin secretion from pancreatic islets. Cell 129, 359-370

Ref Type: Journal

12. Hashimoto, T., Karasawa, T., Saito, A., Miyauchi, N., Han, G. D., Hayasaka, K., Shimizu, F., Kawachi, H. (2007) Ephrin-B1 localizes at the slit diaphragm of the glomerular podocyte. Kidney Int. 72, 954-964

13. Dravis, C., Wu, T., Chumley, M. J., Yokoyama, N., Wei, S., Wu, D. K., Marcus, D. C., Henkemeyer, M. (2007) EphB2 and ephrin-B2 regulate the ionic homeostasis of vestibular endolymph. Hear.Res. 223, 93-104

14. Foo, S. S., Turner, C. J., Adams, S., Compagni, A., Aubyn, D., Kogata, N., Lindblom, P., Shani, M., Zicha, D., Adams, R. H. (2006) Ephrin-B2 controls cell motility and adhesion during blood-vessel-wall assembly. Cell 124, 161-173

15. Shin, D., Garcia-Cardena, G., Hayashi, S., Gerety, S., Asahara, T., Stavrakis, G., Isner, J., Folkman, J., Gimbrone, M. A., Jr., Anderson, D. J. (2001) Expression of ephrinB2 identifies a stable genetic difference between arterial and venous vascular smooth muscle as well as endothelial cells, and marks subsets of microvessels at sites of adult neovascularization. Dev.Biol. 230, 139-150

16. Gale, N. W., Baluk, P., Pan, L., Kwan, M., Holash, J., DeChiara, T. M., McDonald, D. M., Yancopoulos, G. D. (2001) Ephrin-B2 selectively marks arterial vessels and neovascularization sites in the adult, with expression in both endothelial and smooth-muscle cells. Dev.Biol. 230, 151-160

17. Ogita, H., Kunimoto, S., Kamioka, Y., Sawa, H., Masuda, M., Mochizuki, N. (2003) EphA4-mediated Rho activation via Vsm-RhoGEF expressed specifically in vascular smooth muscle cells. Circ.Res. 93, 23-31

18.Hongyu Luo, Tania Charpentier, Xuehai Wang, Shijie Qi, Bing Han, Tao Wu, Rafik Terra, Alain Lamarre, and Jiangping Wu. (2011) EFNB1 and EFNB2 proteins regulate thymocyte development, peripheral T cell differentiation and antiviral immune responses and are essential for IL-6 signaling. J. Biol. Chem. 286:41135-41152.

19. Xin, H. B., Deng, K. Y., Rishniw, M., Ji, G., Kotlikoff, M. I. (2002) Smooth muscle expression of Cre recombinase and eGFP in transgenic mice. Physiol Genomics 10, 211-215

20. Golovina, V. A., Blaustein, M. P. (2006) Preparation of primary cultured mesenteric artery smooth muscle cells for fluorescent imaging and physiological studies. Nat.Protoc. 1, 2681-2687

21. Thorin E, Huang PL, Fishman MC, Bevan JA. Nitric oxide inhibits alpha2-adrenoceptor-mediated endothelium-dependent vasodilation. Circ Res 1998;82[243]:1323-9.
22. Lavoie, J. L., Lake-Bruse, K. D., Sigmund, C. D. (2004) Increased blood pressure in transgenic mice expressing both human renin and angiotensinogen in the renal proximal tubule. Am.J.Physiol Renal Physiol 286, F965-F971
23. Dumas, P., Pausova, Z., Kren, V., Krenova, D., Pravenec, M., Dumont, M., Ely, D., Turner, M., Sun, Y., Tremblay, J., Hamet, P. (2000) Contribution of autosomal loci and the Y chromosome to the stress response in rats. Hypertension 35, 568-573
24. Carlson, S. H., Osborn, J. W., Wyss, J. M. [244] Hepatic denervation chronically elevates arterial pressure in Wistar-Kyoto rats. Hypertension 32, 46-51
25. Compagni, A., Logan, M., Klein, R., Adams, R. H. (2003) Control of skeletal patterning by ephrinB1-EphB interactions. Dev.Cell 5, 217-230
26. Somlyo, A. P., Somlyo, A. V. [245] Signal transduction and regulation in smooth muscle. Nature 372, 231-236
27. Han, Y. J., Hu, W. Y., Piano, M., de, L. P. (2008) Regulation of myosin light chain kinase expression by angiotensin II in hypertension. Am.J.Hypertens. 21, 860-865
28. Kimura K, Ito M, Amano M, Chihara K, Fukata Y, Nakafuku M, Yamamori B, Feng J, Nakano T, Okawa K, Iwamatsu A, Kaibuchi K. Regulation of myosin phosphatase by Rho and Rho-associated kinase (Rho-kinase) Science. 1996 Jul 12;273(5272):245-8.
29. Tanaka, M., Kamo, T., Ota, S., Sugimura, H. (2003) Association of Dishevelled with Eph tyrosine kinase receptor and ephrin mediates cell repulsion. EMBO J. 22, 847-858
30. Bruckner, K., Pablo, L. J., Scheiffele, P., Herb, A., Seeburg, P. H., Klein, R. [246] EphrinB ligands recruit GRIP family PDZ adaptor proteins into raft membrane microdomains. Neuron 22, 511-524
31. Lu, Q., Sun, E. E., Klein, R. S., Flanagan, J. G. (2001) Ephrin-B reverse signaling is mediated by a novel PDZ-RGS protein and selectively inhibits G protein-coupled chemoattraction. Cell 105, 69-79
32. Schulz, T. J., Glaubitz, M., Kuhlow, D., Thierbach, R., Birringer, M., Steinberg, P., Pfeiffer, A. F., Ristow, M. (2007) Variable expression of Cre recombinase transgenes precludes reliable prediction of tissue-specific gene disruption by tail-biopsy genotyping. PLoS.One. 2, e1013.

33. Ledoux, J., Werner, M. E., Brayden, J. E., Nelson, M. T. (2006) Calcium-activated potassium channels and the regulation of vascular tone. Physiology.(Bethesda.) 21, 69-78

34. Wamhoff, B. R., Bowles, D. K., Owens, G. K. (2006) Excitation-transcription coupling in arterial smooth muscle. Circ.Res. 98, 868-878

35. Dong H, O'Brien RJ, Fung ET, Lanahan AA, Worley PF, Huganir RL. GRIP: a synaptic PDZ domain-containing protein that interacts with AMPA receptors. Nature. 1997 Mar 20;386(6622):279-84.

36. Su LF, Wang Z, Garabedian MJ. Regulation of GRIP1 and CBP Coactivator activity by Rho GDI modulates estrogen receptor transcriptional enhancement. J Biol Chem. 2002 Oct 4;277(40):37037-44. Epub 2002 Jul 22.

37. Ye B, Liao D, Zhang X, Zhang P, Dong H, Huganir RLGRASP-1: a neuronal RasGEF associated with the AMPA receptor/GRIP complex. Neuron. 2000 Jun;26(3):603-17.

38.Luo H, Wu Z, Tremblay J, Thorin E., Peng J, Lavoie JL, Hu B, Stoyanova E, Cloutier G, Qi S, Wu T, Cameron M and Jiangping Wu. Receptor tyrosine kinase EphB6 regulates vascular smooth muscle contractility and modulates blood pressure in concert with sex hormone. J Biol Chem. Feb 24, 2012; 287 (9):6819-6829.

FIGURES AND LEGENDS

Figure 1 Generation of mice with SMC-specific deletion of Efnb1

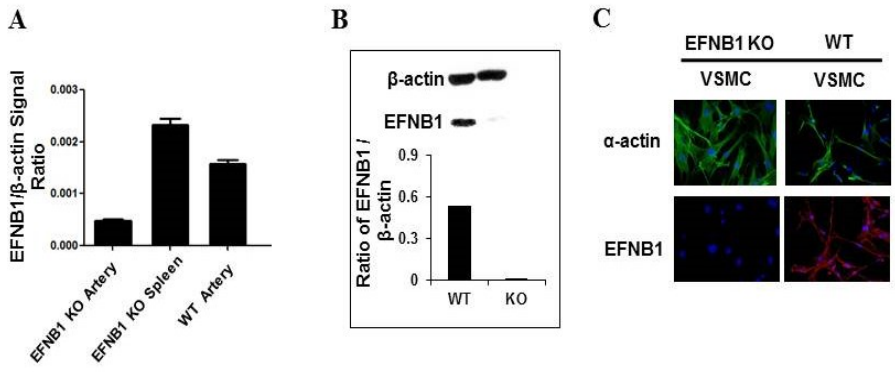

A. Deletion of Efnb1 at the mRNA level in the artery of male Efnb1 KO mice. mRNA from the VSMC and spleen cells of male Efnb1 KO and WT mice was assessed for Efnb1 mRNA by RT/qPCR. Means $\pm$ SD of the ratios of Efnb1 versus β-actin signals are presented.

B. Deletion of Efnb1 at the protein level in Efnb1 KO arteries according to immunoblotting. Proteins extracted from the mesenteric arteries of Efnb1 KO and WT mice were subjected to immunoblotting analysis. β-actin levels were used as a loading control. The signal ratios of Efnb1 and β-actin (lower panel) were determined by densitometry

C. VSMC-specific deletion of Efnb1 protein in Efnb1 KO mice according to immunofluorescence microscopy. VSMC and non-VSMC from Efnb1 KO and WT mice were isolated from mesenteric arteries, and their Efnb1 (red, lower row) and α-actin (green, upper row) expression was detected by immunofluorescence microscopy. The experiments in this figure were repeated 3 times and representative ones are shown.

Figure 2 Decreased contractility of Efnb1-engaged VSMC

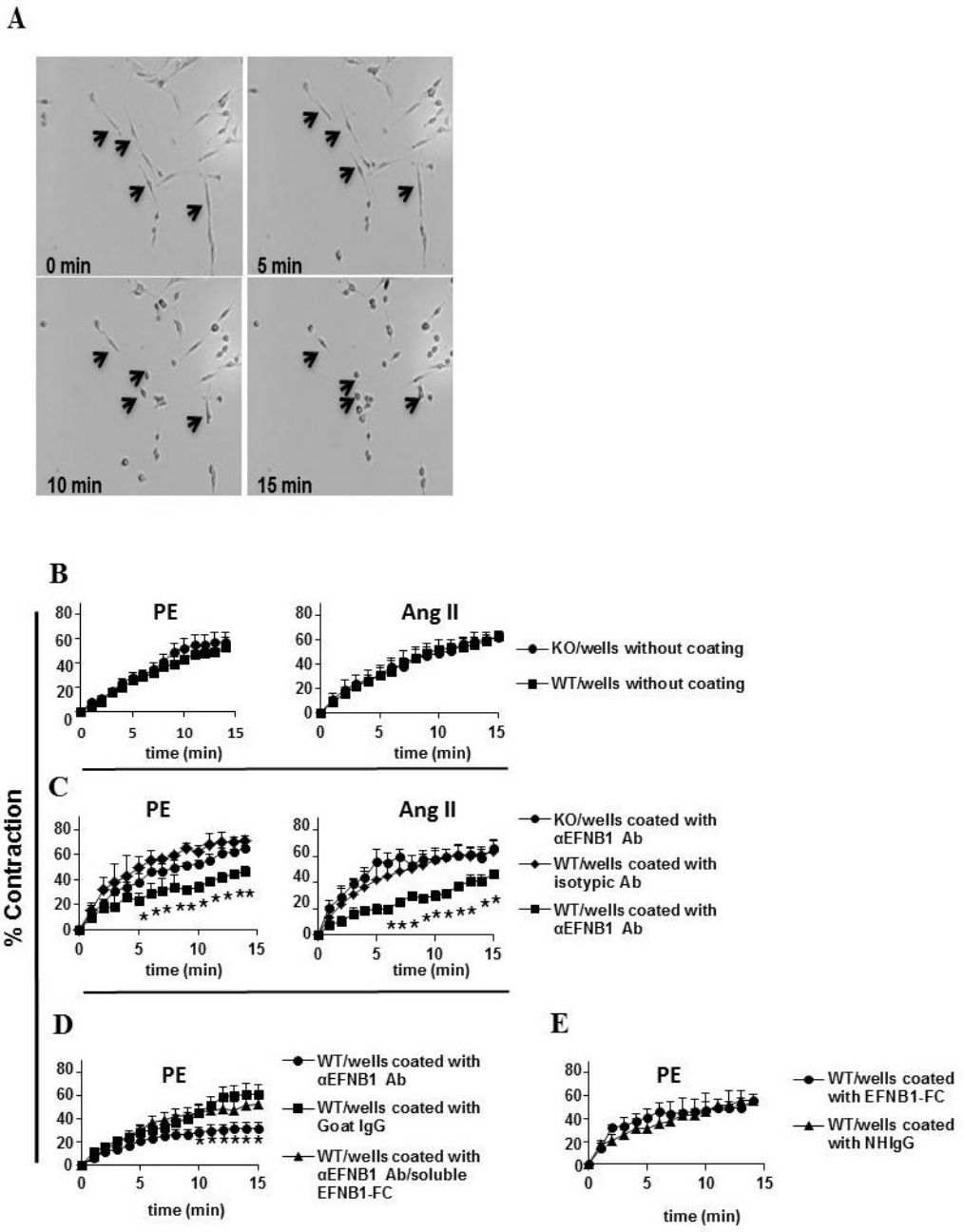

A. VSMC contraction after PE stimulation. VSMC were isolated from the mesenteric arteries of WT mice, and cultured for 4 days. The cells were stimulated with 20 μM PE and imaged every min. Images at 0 min, 5 min, 10 min and 15 min are shown. Four arrows point to the same 4 cells during the 15-min imaging period, and show their contraction. The photos also reveal that about 85% of the cells are capable of contraction, indicating the purity of VSMC in such cell preparations.

B. VSMC from Efnb1 KO and WT mice presented similar contractility upon PE and AngII stimulation when cultured in uncoated wells. VSMC from Efnb1 KO and WT mice were stimulated with 20 μM PE (left column) or 10 μM AngII (right column). The means ± SD of their percentage contraction are illustrated. Data were analyzed with paired Student's *t* test, but no significant difference was found.

C. Solid phase anti-Efnb1 Ab caused decreased contractility in WT but not Efnb1 KO VSMC Efnb1 KO or WT VSMC were cultured in wells coated with goat anti-Efnb1 Ab (αEfnb1 Ab) or goat IgG-coated wells (2 μg/ml/well for 12-well plates during coating at 4ºC overnight) for 4 days, and then stimulated with PE (20 μM; left panel) or AngII [247]. Means ± SD of percentage contraction of these VSMC are illustrated. αEfbn1 Ab: anti-Efnb1 antibody. *: significant differences between Efnb1 KO and WT VSMC on αEfnb1 Ab-coated wells, and between WT VSMC cultured on isotypic Ab-coated wells and WT VSMC cultured on wells coated with αEfnb1 Ab ($p<0.05$; paired Student's *t* test). No significant difference was found between Efnb1 KO VSMC on αEfnb1 Ab-coated wells and WT VSMC on isotypic Ab-coated wells.

D. Soluble recombinant Efnb1-Fc blocked the effect of solid phase anti-Efnb1 Ab on WT VSMC contraction upon PE stimulation. WT VSMC were cultured in α-Efnb1 Ab-coated wells, in the presence of soluble Efnb1-Fc or normal human IgG (both at 10 μg/ml). Means ± SD of percentage contraction of these VSMC stimulated with PE (20 μM) are illustrated. *: significant differences ($p<0.05$; paired Student's *t* test).

E. Solid phase Efnb1-Fc had no effect on VSMC contraction stimulated by PE. WT VSMCs were cultured in Efnb1-Fc- or normal human IgG-coated wells (both at 10 μg/ml for coating). Percentage contraction of these VSMC stimulated with PE (20 μM) are illustrated. Data were analyzed with paired Student's t test, but no significant difference was found. All experiments in this figure were conducted more than twice and data from representative experiments are shown.

Figure 3 Early Efnb1-mediated signaling events in VSMC stimulated by PE and AngII

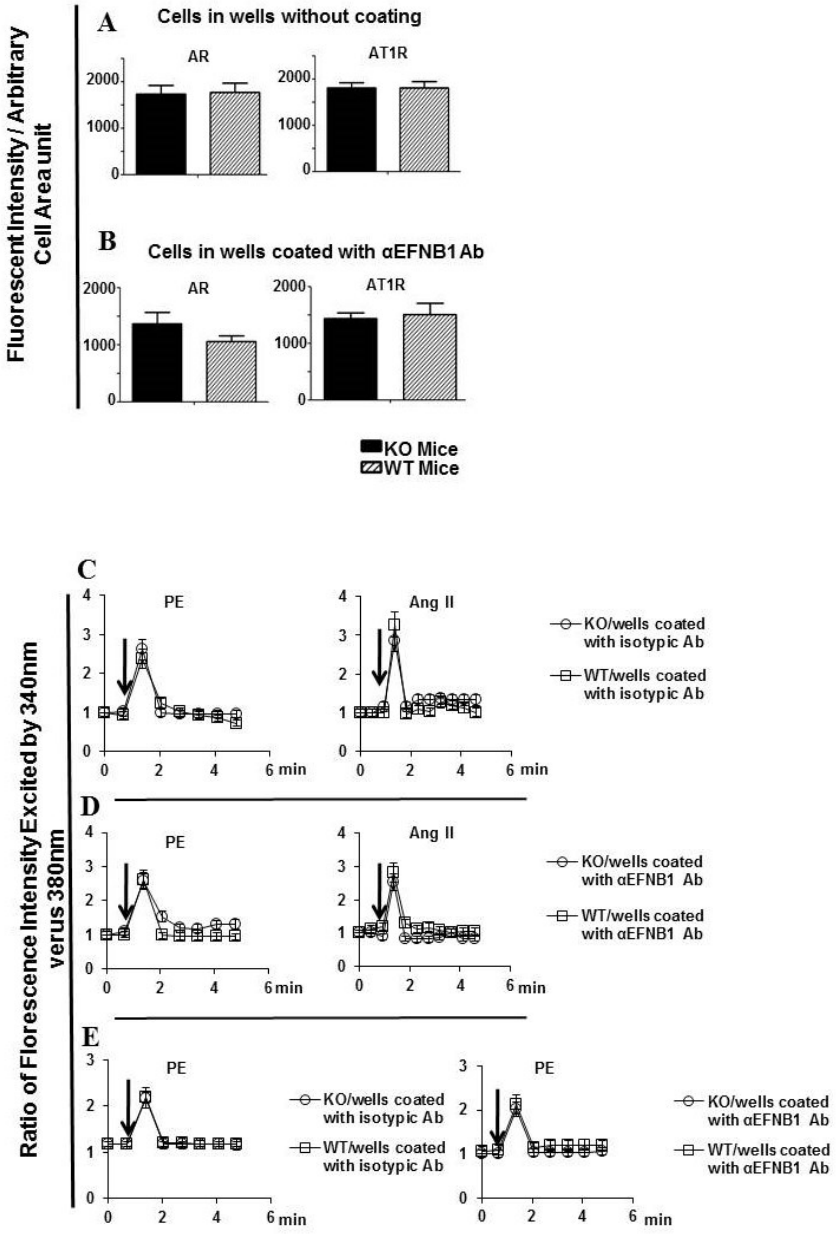

A. Normal AR and AT1R expression in Efnb1 KO VSMC. VSMC from male Efnb1 KO or WT mice were cultured in uncoated wells for 4 days and then stained with Abs against AR or AT1R as indicated. VSMC were identified with anti-α-actin Ab staining. For each experiment, more than 15 α-actin-positive cells were randomly selected and their total immune fluorescence intensity and cell size were registered. The means $\pm$ SD of the fluorescent intensity per arbitrary cell area unit [248] of all cells examined are shown. Data

were analyzed with paired Student's *t* test, but no significant difference was found. **B.** Normal AR and AT1R expression in WT VSMC with Efnb1 engagement. VSMC from male WT mice were cultured in wells coated with goat αEfnb1 Ab or normal goat IgG (2μg/ml during coating) for 4 days and then stained with Abs against AR or AT1R and analyzed as described above. Data were analyzed with paired Student's *t* test, but no significant difference was found. **C-E** Normal Ca^{++} flux in VSMC with or without Efnb1 engagement: VSMC from male Efnb1 KO or WT mice were cultured for four days and then loaded with Fura2 (5 μM). The cells were then placed in HBSS with or without 1.26 mM Ca^{++} at 37ºC and stimulated with PE (20 μM) or AngII [249]. The ratio of emissions at 510 nm triggered by 340 nm versus 380 nm excitation in each cell was registered every 10 s for a duration of 5 min and the means $\pm$ SD of the ratio of more than 15 randomly selected VSMC are shown. The arrows indicate the time point at which PE was added. **C**. VSMC from male Efnb1 KO or WT mice were cultured in normal goat IgG-coated wells for 4 days and stimulated with PE (left panel) or AngII (right panel) in Ca^{++}-free buffer **D.** VSMC from male Efnb1 KO or WT mice were cultured in goat αEfnb1 Ab-coated wells and stimulated with PE (left panel) or AngII (right panel) in Ca^{++}-free buffer. **E.** VSMC from male Efnb1 KO or WT mice were cultured in goat αEfnb1 Ab-coated or normal goat IgG-coated wells and stimulated with PE (left panel) or AngII (fight panel) in Ca^{++}-containing buffer. All experiments in this figure were conducted more than twice and data from representative experiments are shown.

Figure 4 MLC phosphorylation and RhoA activation in VSMC

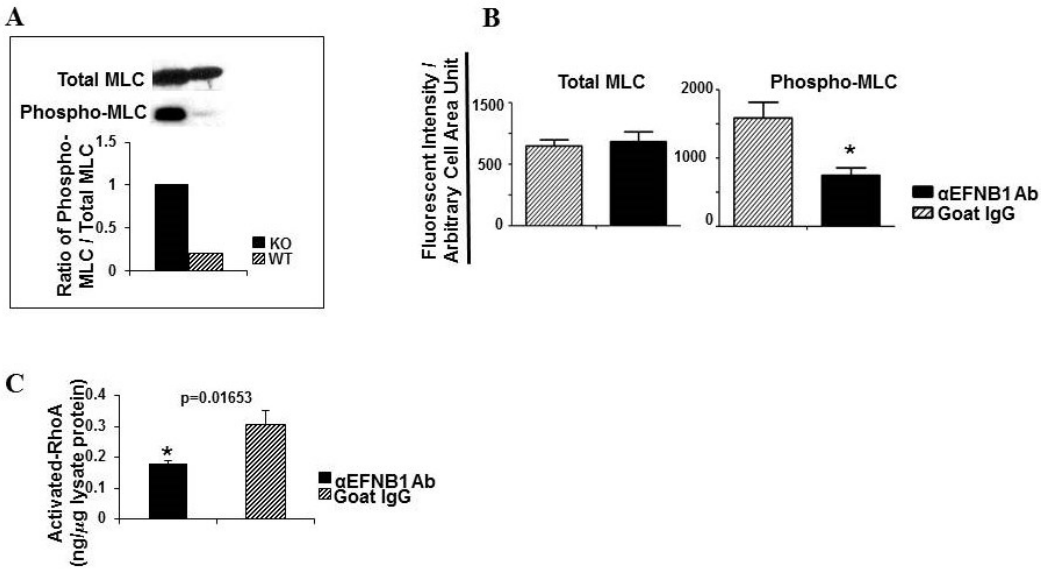

A. Increased constitutive MLC phosphorylation in Efnb1 KO VSMC ex vivo. The mesenteric arteries of Efnb1 KO and WT mice were cleared of adventitia and homogenized. The proteins of these tissues were analyzed for phosphorylated MLC (phospho-MLC) and total MLC expression by immunoblotting, as indicated. Densitometry was performed to quantify the signals, and the data are expressed as ratios of phospho-MLC versus total MLC signals (bar graph, lower panel). **B**. Reduced MLC phosphorylation in Efnb1-engaged WT VSMC: VSMC from male WT mice were cultured in wells coated with goat αEfnb1 Ab or normal goat IgG (2 μg/ml during coating) for four days. Total MLC (left panel) and phosphor-MLC, right panel) of VSMC were detected by immunofluorescence. The means $\pm$ SD of fluorescent intensity per arbitrary cell area unit of more than 15 randomly selected α-actin-positive cells examined are shown in the bar graphs. *: significant differences (p<0.05, paired Student's t test). **C.** Increased RhoA activation in Efnb1-engaged WT VSMC: VSMC from WT mice were cultured in wells coated with goat αEfnb1 Ab or normal goat IgG (2 μg/ml during coating) for four days. The cells were then harvested and the GTP-accociated RhoA in the cell lysates were determined in duplicate. The experiments were repeated twice and the results are consistent. A representative set of data are shown. *: significant differences (p<0.05, paired Student's t test).

Figure 5 Grip1 in the Efnb1 reverse signling pathway

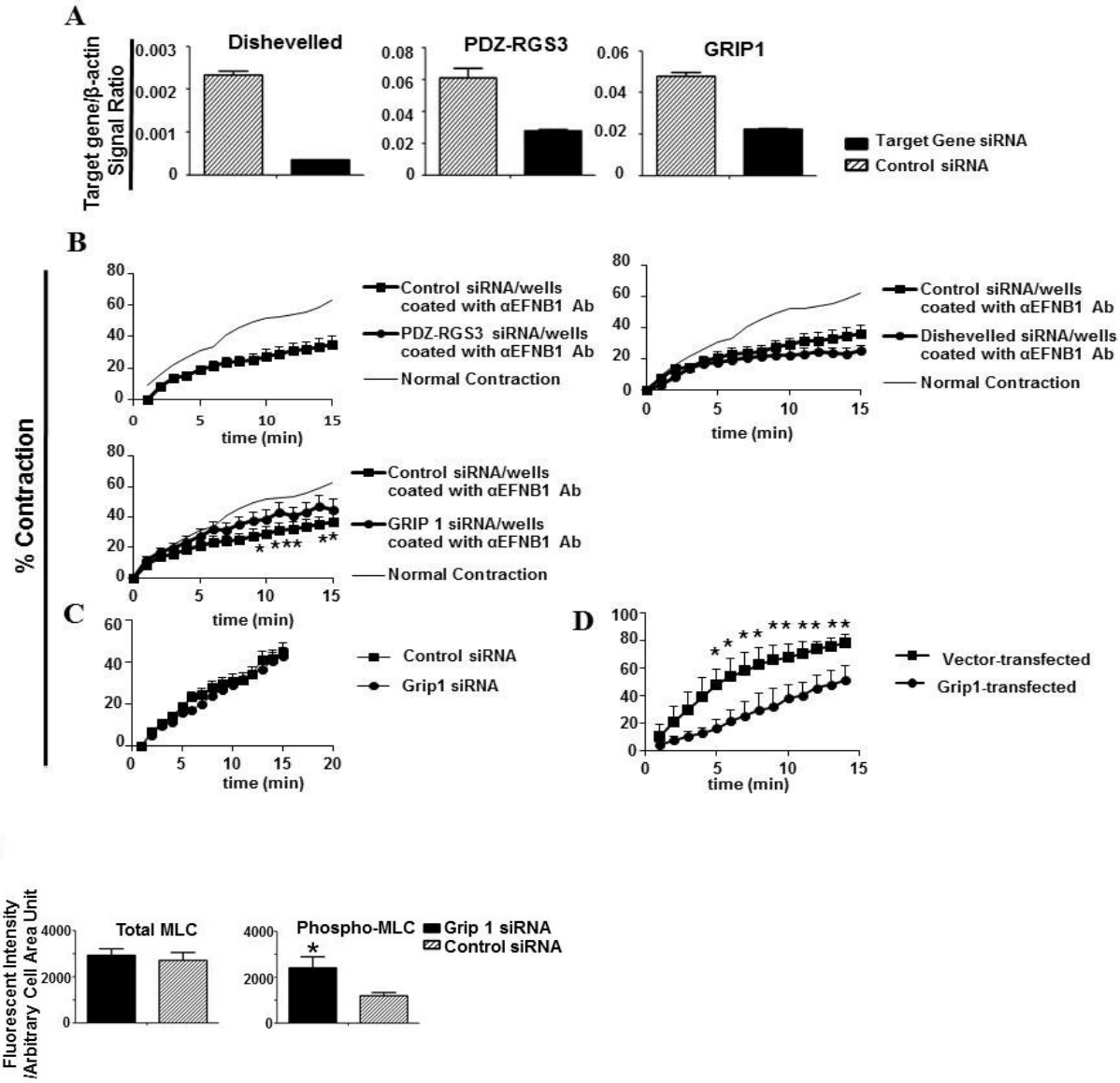

A. Effective knockdown of Grip1, Dishevelled and PDZ-RGS3 mRNA by siRNA: VSMC from WT mice were transfected with 30 nM siRNA targeting Grip1, Dishevelled or PDZ-RGS3, or with control siRNA. After additional 4-h culture, the mRNA levels of these 3 genes were measured by RT/qPCR, and the data are expressed as the means $\pm$ SD of signal ratios between the test genes and β-actin**. B.** Grip1 knockdown by siRNA partially reversed the inhibitory effect of solid phase *αEfnb1 Ab.* VSMC from WT males were cultured in wells coated with goat αEfnb1 Ab (2 μg/ml for coating). After 2 days, the cells were transfected with 30 nM siRNA targeting Grip1, Dishevelled or PDZ-RGS3, or control

siRNA. On day 4 of culture, the cells were stimulated with PE (20 μM) and their percentage contraction was registered. Means ± SD of the percentage are shown. The thin line (indicated as Normal Contraction) represents the mean percentage contraction of VSMC cultured in wells coated with normal goat IgG (2 μg/ml) without siRNA transfection (for better visual effect, the SD of each time point in this control is omitted). **C.** VSCM cultured in uncoated wells are not affected by Grip1 siRNA in their contractility: VSMC from WT males were cultured in normal wells for 4 days and then transfected with Grip1 or control siRNA. Their contraction in response to 20 μM PE was measured. Means ± SD of the percentage are shown. No significant statistical difference is found (Student's t test) between VSMC transfected with Grip1 or control siRNA. **D.** Grip1 overexpression in VSMC led to decreased contractility. WT VSMCs were cultured for 6 days and transfected with pCEP4-Grip1. Cell contraction stimulated by PE (20 μM) was conducted 24 h later and mean ± SD of percentage contraction were shown. **E.** Grip1 knockdown by siRNA resulted in increased MLC phosphorylation in EFNB1-engaged WT VSMC. VSMC from WT males were cultured in wells coated with goat αEfnb1 Ab, and transfected with Grip1 or control siRNA as described in Fig. 5D. The means ± SD of fluorescent intensity per arbitrary cell area unit of more than 15 cells are shown in the bar graphs. All experiments in this figure were conducted more than twice and data from representative experiments are shown. *: significant differences ($p<0.05$, paired Student's t test).

Figure 6 GTP-associated RhoA expression and vasoconstriction of Efnb1 KO mesenteric arteries

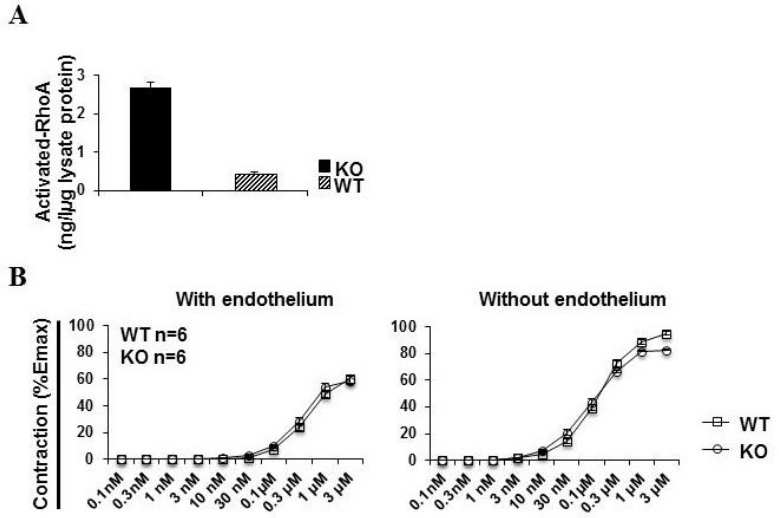

A. Activated RhoA in Efnb1 mesenteric arteries: The mesenteric arteries of Efnb1 KO and WT mice were cleared of adventitia and homogenized. The proteins of these tissues were analyzed for GTP-associated RhoA levels in duplicate. The experiment was repeated twice, and data of a representative one are shown as Mean + SD of GTP-RhoA concentration per µg total protein. *: $p< 0.05$ according to paired Student's *t* test. **B.** Contractility of mesenteric arteries from Efnb1 KO and WT mice following PE stimulation. Segments (2 mm) of the third-order branch of the mesenteric artery with endothelium or with endothelium removed were stimulated with PE. A single cumulative concentration-response curve to PE ^{250} was obtained. The maximal tension (Emax) was determined by challenging the vessels with a physiological saline containing 127 mM KCl. Vessel contractility is expressed as percentage of the Emax. Data from three mice per group were pooled and Mean $\pm$ SE are shown. There is no significant difference between KO and WT vessels (paired Student's *t* test).

Figure 7 Blood pressure and heart rate of Efnb1 KO mice

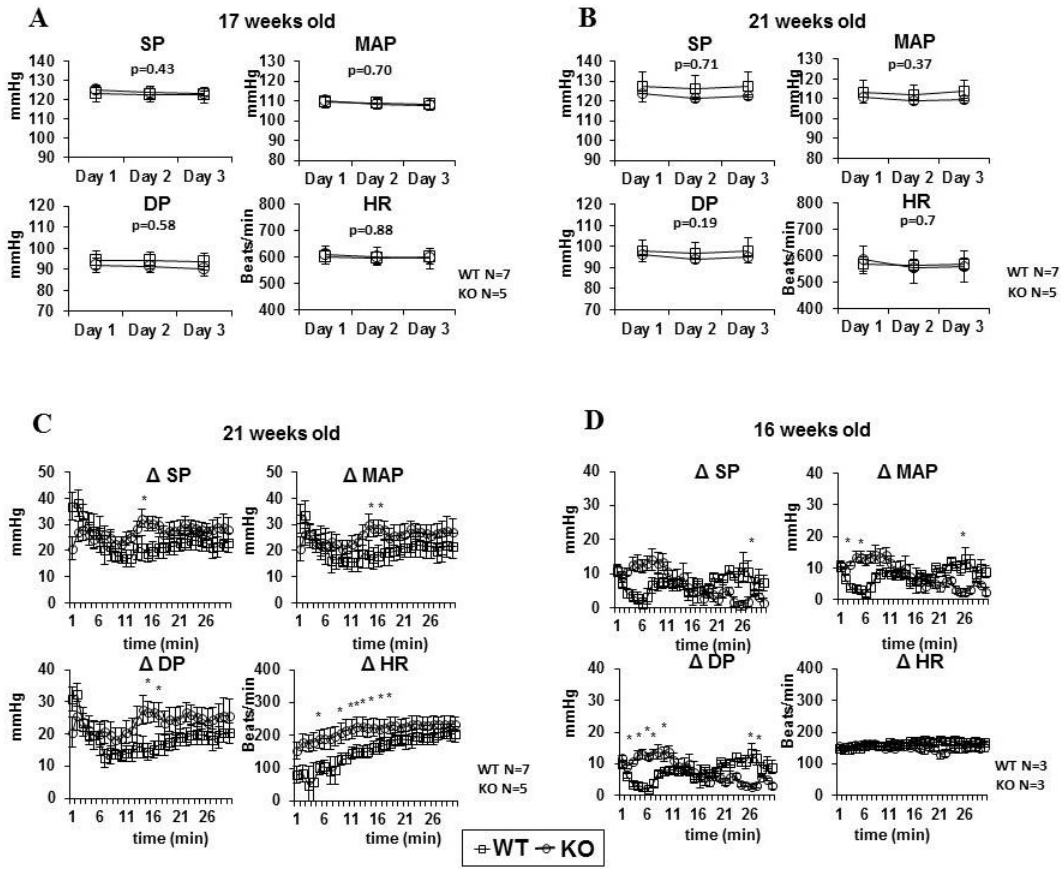

A and B. Male Efnb1 KO mice in the C57BL/6 background (F10) on a normal diet or high-salt diet presented normal BP and HR: **A**. Mice [251] were on a normal diet. **B.** Mice (21 week old) were on a high salt diet for 3 weeks. BP and HR were measured for 3 days by telemetry starting at least 7 days after transmitter implantation. For mice on a high-salt diet, BP and HR were measured 3 weeks after the initiation of the high-salt diet. Number per group is indicated. Values are expressed as mean 24-h BP and HR for each day ± SE. SP: systolic pressure; DP: diastolic pressure; MAP: mean arterial pressure; HR: heart rate. **C.** Male Efnb1 KO mice (after 10 generations of backcrossing to the C57BL/6 background) on a high-salt diet under immobilization stress presented augmented increment of BP: SP, DP, MAP and HR of 21-week-old male Efnb1 KO and WT mice (number per group is indicated) were on a high-salt diet for 3 weeks, and their BP and HR were recorded by telemetry during 30-min immobilization stress. The data are expressed as means $\pm$ SE of increments (Δ) of SP, DP, ΔMAP, and HR. ΔSP, ΔDP, ΔMAP and ΔHR are calculated as follows: Δ = value during stress – value during the resting period. **D.** Male Efnb1 KO mice (after 5

generations of backcrossing to the C57BL/6 background from the 129/sv X C57BL/6 background) on a high-salt diet under immobilization stress presented augmented increment of BP. SP, DP, MAP and HR of 16-week-old male Efnb1 KO and WT mice (number per group is indicated) on a high-salt diet for 3 weeks were recorded by telemetry during 30-min immobilization stress. ΔSP, ΔDP, ΔMAP and ΔHR are shown. Data in this figure were analyzed by unpaired *t* test and repeated-measures ANOVA, and the *p* values are shown. * indicates $p<0.05$.

Figure 8 Normal urine and plasma hormone levels in Efnb1 KO and WT mice

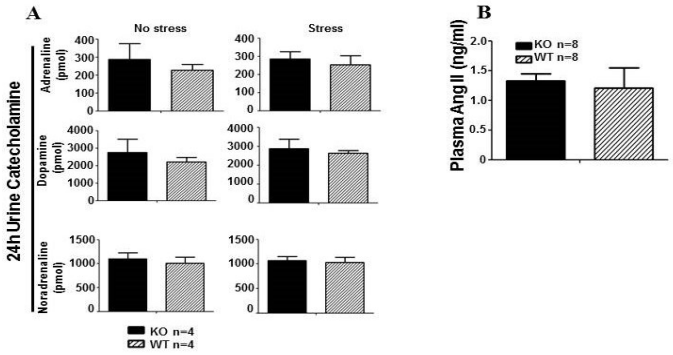

A. Twenty-four-h urine catecholamine levels after stress in male Efnb1 KO mice. Male Efnb1 KO and WT mice were placed in metabolic cages without prior stress or immediately after immobilization stress. Urine was collected during a 24-h fasting period. Urinary catecholamines were measured by ELISA. Mouse number per group and means $\pm$ SD of the hormones in 24-h urine are presented. No statistically significant difference was found (Student's *t* test) between KO and WT mice. **B.** Plasma AngII levels in male Efnb1 KO and WT mice. Plasma AngII of male Efnb1 KO and WT mice was measured by ELISA. Mouse numbers per group and mean $\pm$ SD of the hormone concentrations are shown. No statistically significant difference was found (Student's *t* test) between the KO and WT mice.

Article 3.

Blood pressure modulation by Efnb3 protein in concert with sex hormones: evidence from gene knockout mice and blood pressure-associated single nucleotide polymorphisms in *EFNB3* related genes in 69,395 human subjects

[1#]Zenghui Wu, [1#]Yujia Wang, [2]Eric Thorin, [1]Johanne Tremblay, [1]Julie L. Lavoie, [1]Hongyu Luo, [1]Junzheng Peng, [4]John Realson, The International Consortium for Blood Pressure Genome-Wide Association Studies, [5]Georg B. Ehret, [6]Patricia B. Munroe, [1]Ekatherina Stoyanova, [1]Zhao Qin, [1]Guy Cloutier, [1]Edward Bradley, [1]Pavel Hamet, [1]Shijie Qi, and [1,3]Jiangping Wu

Paper was submitted to *Circulation-Cardiovascular Genetics*

Summary: in this paper we showed elevated blood pressure in Efnb3$^{-/-}$female mice but not male knockout mice. The phosphorylation of MLC was also increased in knockout female mice. These results indicate that the Efnb3 is involved in the regulation in VSMCs.

Zenghui Wu and Yujia wang performed the experiments in VSMC and analyzed the data. Dr. Eric Thorin performed the experiments for vessel constriction in vitro Dr. Hongyu Luo did aldosterone level in sera. Drs. Johanne Tremblay, Junzheng Peng and Julie Lavoie measured the blood pressure in vivo. Drs. Raelson, Bradley, Ehret, Munroe and Hamet conducted human genetic studies. Drs. Stoyanova, Qin and Cloutier performed ultrasonic studies in the cardiovascular system. Dr. Shijie Qi carried out castration, ovariectomy and animal husbandry. Dr. Jiangping Wu and Dr Hongyu Luo directed the experimental design and data analysis.

Blood pressure modulation by Efnb3 protein in concert with sex hormones: evidence from gene knockout mice and blood pressure-associated single nucleotide polymorphisms in *EFNB3* related genes in 69,395 human subjects

[1#]Zenghui Wu, [1#]Yujia Wang, [2]Eric Thorin, [1]Johanne Tremblay, [1]Julie L. Lavoie, [1]Hongyu Luo, [1]Junzheng Peng, [4]John Realson, The International Consortium for Blood Pressure Genome-Wide Association Studies, [5]Georg B. Ehret, [6]Patricia B. Munroe, [1]Ekatherina Stoyanova, [1]Zhao Qin, [1]Guy Cloutier, [1]Edward Bradley, [1]Pavel Hamet, [1]Shijie Qi, and [1,3]Jiangping Wu

From the [1]Research Centre and [3]Nephrology Service, Centre hospitalier de l'Université de Montréal (CHUM), Montreal, Quebec H2L 4M1, Canada; [2]Montreal Heart Institute, Montreal, Quebec H1T 1C8, Canada; [4]PGX-Services, Montreal, Quebec H2T 1S1, Canada; [5]Center for Complex Disease Genomics, McKusick-Nathans Institute of Genetic Medicine, Johns Hopkins University School of Medicine, Baltimore, Maryland 21205, USA; [6]Clinical Pharmacology and The Genome Centre, William Harvey Research Institute, Barts and The London School of Medicine and Dentistry, Queen Mary University of London, London EC1M 6BQ, UK

Running title: Efnb3 regulates blood pressure

[#]These authors contributed equally to this work.

Abstract

EPH receptor tyrosine kinases and their ligands, ephrins (EFNs), fulfill vital and diverse functions in various tissues and organs. In the present study, we reported that Efnb3 plays a novel role in controlling vascular tone and blood pressure (BP) through reverse signalling. *Efnb3* gene knockout (KO) in female mice elevated BP and small artery resistance *in vivo*, enhanced small arterial contractility *ex vivo*, and augmented vascular smooth muscle cell (VSMC) contractility *in vitro*. At the molecular level, VSMC from female KO mice showed heightened myosin light chain (MLC) phosphorylation compared to their wild type (WT) counterparts, corroborating increased VSMC contractility. MLC kinase and MLC phosphatase phosphorylation in female KO VSMC was lower than in WT controls, and such reduction is known to enhance MLC phosphorylation. However, all these abnormalities were not observed in male KO mice or tissues from male KO mice, suggesting that these phenotypes are sex hormone-dependent. When female KO mice were ovariectomized, they lost their hypertensive phenotype, whereas estrogen increased VSMC contractility in male KO but not WT mice. These results indicate that estrogen promotes VSMC contractility, and hence BP, in the absence of Efnb3. Although male KO mice had normal BP, castration led to its significant elevation in KO but not in WT mice. However, castration did not increase KO vessel contractility, and exogenous testosterone did not decrease it in female KO mice. The results suggest that testosterone does not intrinsically repress BP elevation, but needs to work in concert with Efnb3 deletion to achieve such an effect, and this regulation by Efnb3/testosterone occurs in target tissues/organs other than VSMC.

We further demonstrated that cross-linking VSMC from WT mice with solid-phase anti-Efnb3 antibody (Ab) reduced their contractility, while solid-phase recombinant Efnb3 had no impact, indicating that Efnb3 acts through reverse signalling to dampen VSMC contractility. We also discerned that Grip1, an adaptor protein, was critical in mediating Enb3 reverse signalling in VSMC.

To validate the relevance of our findings in humans, we targeted 522 single nucleotide polymorphisms (SNPs) within 4 genes in the EPH/EFN signalling system, i.e., *EPHB6*, *EFNBb2*, *EFNB33* and *GRIP1*, to query the International Blood Pressure Consortium dataset, which contains SNP information on 69,395 individuals of European ancestry in 29 general population-based cohorts. The minimum p-value (0.000389) for tag SNPs within *GRIP1* gene

was 0.000389 for its association with diastolic BP. It approaches the critical p-value of 0.000302 (or 0.000151 based on overly conservative correction). GRIP1 is situated in a node where Ephb/Efnb reverse signalling pathways converge, and thus probably carries more weight for the detection of association(s) with BP phenotypes. Such a result is quite promising, considering that the analysis is not based on stratification of gender and sex hormone levels,

Our study reveals previously unknown sex hormone-dependent EFNB3 functions in hypertension.

Introduction

Eph kinases are the largest family of receptor tyrosine kinases. They are divided into A and B subfamilies according to sequence homology [252]. Ephrins (Efns), which are also cell surface molecules, are ligands of Ephs. Efns are classified as A and B subfamilies. A subfamily members attach to the cell surface through glycosylphosphatidylinositol anchoring, whereas B subfamily members attach through transmembrane tails [253-255]. Interactions among Ephs and Efns are promiscuous but, in general, Epha members interface preferentially with Efna members, and Ephb members with Efnb members [254-256]. Such redundancy suggests that these kinases are crucial in various biological contexts. Efns can stimulate Eph receptors, and this is called forward signalling. Interestingly, Ephs are also capable of stimulating Efns which then transmit signalling reversely into cells, a phenomenon known as reverse signalling.

Ephs and Efns are expressed in many tissues and organs. They play important roles in the central nervous system [254, 255], immune system [257, 258], digestive system [259, 260], bone metabolism [16,17], angiogenesis [18] and other processes [261-263].

Until recently, few studies assessed the role of Ephs and Efns in vascular smooth muscle cell (VSMC) function. VSMC with Efnb2 deletion show compromised migration [264]. In cultured rat and human VSMC, Efna1 triggers Epha4 signalling and actin stress fiber assembly [265]. Whether such signalling elicits changes in VSMC contractility has not been investigated.

We recently reported that Ephb6, in concert with sex hormones, is crucial in VSMC contraction and blood pressure (BP) regulation [266]. VSMC are a target tissue through which Ephb6 exerts its effect on BP control. Since Ephb6 and all its major ligands of the Efnb family, i.e., Efnb1, Efnb2 and Efnb3, are expressed in VSMC [24], there is a molecular framework for their function in these cells. We showed that while solid-phase recombinant Ephb6 reduces VSMC contraction

in response to phenylephrine (PE) stimulation, solid-phase anti-Ephb6 antibody (Ab) does not [266], indicating that reverse signalling from Ephb6 to Efnbs but not forward signalling from Efnbs to Ephb6 is responsible for dampening VSMC contractility. Corroborating this finding, mice expressing tailless Ephb6 (Ephb6 without intracellular domains) were normotensive, and their VSMC acted similarly to wild type (WT) VSMC upon exposure to PE [24].

Unlike males, small arteries freshly isolated from Ephb6 knockout (KO) females show increased contraction force upon PE stimulation compared to their WT counterparts. However, small arteries from castrated male Ephb6 KO mice become more contractile than those of WT controls [266], demonstrating that Ephb6 acts in concert with sex hormones to regulate blood vessel tone. Despite increased vessel contractility in female Ephb6 KO mice they remain normotensive, likely due to compensatory BP control mechanisms. On the other hand, castrated Ephb6 KO mice become hypertensive [266], probably owing to loss of male sex hormone-dependent compensatory mechanisms. Indeed, 24-h urinary catecholamine levels are diminished in non-castrated Ephb6 KO males, and such reduction is lost upon castration [266]. Thus, adrenal gland chromaffin cells are the second target tissue of Ephb6 with regard to its role in BP control.

Therefore, we identified Ephb6 and, by logical extension, its ligands (Efnbs) as novel BP regulatory factors.

Ephb6 has 3 major ligands, namely, Efnb1, Efnb2 and Efnb3. In the present study, we discovered that Efnb3 KO in mice resulted in similar but not identical BP phenotypes as those in Ephb6 KO mice, suggesting that at least a part of Ephb6's observed effect in BP regulation occurs via its reverse signalling through Efnb3. We targeted single nucleotide polymorphisms (SNPs) from the EPHB/EFNB system to query the International Blood Pressure Consortium (IBPC) dataset, which contains SNP information on 69,395 individuals, and found that a SNP in the EPHB/EFNB signalling pathway approached statistical significance for association with diastolic blood pressure (DP).

Materials and Methods

Efnb3 KO mice

Efnb3 KO mice were produced by Regeneron Pharmaceuticals, as described previously [267], and generously provided to us. They had been backcrossed to the C57BL/6 background for more than 10 generations. Age- and gender-matched WT littermates or C57BL/6 mice served as controls and are referred to as WT mice.

VSMC isolation

Mouse VSMC were isolated from aortic and mesenteric arteries, including their secondary branches as described before [266, 268].

Reverse transcription-quantitative polymerase chain reaction (RT-qPCR)

Efnb3 mRNA levels in VSMC were measured by RT-qPCR [266, 268]. β-actin mRNA served as internal control. Samples were tested in triplicate, and the data expressed as signal ratios of test gene mRNA/β-actin mRNA.

Immunofluorescence microscopy

VSMC surface Efnb3, α1-adrenergic receptor (AR) and intracellular α-actin expression were studied by immunofluorescence microscopy [266, 268]. Stained cells were examined under a Zeiss microscope. AR expression was quantified by ascertaining the fluorescence of more than 15 cells, and the data were expressed as arbitrary intensity per unit cell surface area (pixel) by Zeiss AxioVision software.

BP measurement

Systolic and diastolic BP (SP and DP) and heart rates (HR) of conscious mice were monitored by radiotelemetry [266, 268]. Raw data were processed with the Dataquest A.R.T.-Analysis program [269], and presented as means ± SE. Statistically significant differences between the experimental

groups were evaluated by unpaired t test and repeated-measures analysis of variance (ANOVA). $P<0.05$ values were considered to be statistically significant.

Echocardiography

Transthoracic echocardiography was undertaken in mice lightly anesthetized with isoflurane. Their carotid vessels and heart were imaged with a high-resolution ultrasound biomicroscope (Vevo770; Visualsonics, Toronto, ON, Canada) equipped with a 100% bandwidth 30-MHz central frequency transducer (RMV-707, 12.7 mm focal length, 6 mm aperture). Lateral and axial resolutions with this probe are ~115 μm and ~55 μm, respectively [270]. Preheated ultrasound transmission gel (Aquasonic 100, Parker Laboratories, Orange, NJ, USA) was placed on regions of interest to provide acoustic coupling medium between the transducers and animals. The left and right common carotid arteries were imaged longitudinally in B mode to guide recordings of Doppler time-varying flow velocities for 2 s. Doppler sample volume was positioned 1-2 mm prior to the carotid bifurcation at a 60o angle. Acquired angle-corrected Doppler data were analyzed to measure the mean Pourcelot index (PI) over 10 consecutive cardiac cycles, according to Stoyanova et al. [271]. The PI is a dimensionless echographic parameter that characterizes vascular hemodynamics downstream of a measurement point, i.e., the hemodynamics of vascular brain and facial networks. It depends on both arterial compliance and downstream vascular resistance.

The heart was also imaged in B mode via the parasternal long-axis view to assess aortic hemodynamics and cardiac output (CO). The M-mode sampling line was positioned perpendicularly to the ascending aorta, 0.5-1.5 mm downstream of the aortic valve, and time-varying tracings tracked changes in aortic diameter (AoD). Mean AoD was assessed over 5 consecutive cardiac cycles. Doppler velocity waveforms were then recorded in the ascending aorta by positioning sampling volume at the exact same location where M-mode tracings were obtained. The envelope of angle-corrected (60o) Doppler tracings was delineated manually to compute the velocity time integral (VTI), which was averaged over 10 cardiac cycles. Assuming a parabolic velocity profile in the ascending aorta [271], stroke volume (SV) was calculated (in ml)

as ½ (AoD / 2)2 × π × VTI, and CO (in ml/min) was estimated as SV × HR, where HR was mean HR of the animals.

Left ventricle (LV) dimensions (in mm) at end-systole and end-diastole were finally assessed to quantify fractional shortening, ejection fraction and LV mass. B-mode parasternal long-axis viewing guided the capture of M-mode tracings through the anterior and posterior LV walls at the level of the papillary muscle. For each mouse, LV end-diastolic diameter (LVEDD), LV end-systolic diameter (LVESD), LV end-diastolic posterior wall thickness (LVEDPW) and intra-ventricular septum dimension at end-diastole (IVSED) were quantified, and LV mass ascertained in mg with the following equation [272, 273]:

LV mass (mg) = 1.055 × [(LVEDD + LVEDPW + IVSED) – LVEDD]

Ex vivo vessel constriction

Vessel constriction was studied ex vivo [266, 268, 274]. Briefly, mesenteric artery segments of third-order branches were stripped off the endothelium and stretched to optimal tension at 37°C. Single cumulative concentration-response curves were charted on exposure to the AR agonist PE. At the end of the protocol, maximal tension (Emax) was quantified with a solution containing 127 mM KCl. The data are expressed as percentages of Emax. Concentration-response curves were compared by Student's t test .

VSMC contractility

VSMC contractility was measured [266, 268]. Briefly, the cells were stimulated with PE (20 M)[273], and photographed continuously for 15 min at a rate of 1 picture per min. Fifteen or more cells were randomly selected, and their length was measured at each time point with Zeiss Axiovision software. Percentage contraction was calculated as follows:
% contraction = 100 x (cell length at time 0 – cell length at time X) / cell length at time 0.
Statistically significant differences were assessed by Student's t test.

Ca++ flux

PE-stimulated Ca++ influx in VMSC was measured by immunofluorescence microscopy [266, 268]. Briefly, VSMC were loaded with Fura-2-AM, stimulated with PE (20 M)[273] at 37oC and imaged for 60 s at a rate of 1 picture per 3 s. Excitation wavelengths were switched between 340 nm and 380 nm, and emission wavelength was 510 nm. Signals from more than 15 randomly selected cells were recorded, and the results expressed as ratios of fluorescence intensity at 510 nm excited by 340 nm versus 380 nm.

Immoblotting

VSMC from the aorta and mesenteric arteries of WT and KO mice were isolated and cultured for 3-4 days. After 3 s stimulation with PE (20 M), all the VSMC were lysised by RIPA[273, 273] . Phosphorylated myosin light chain (MLC) and total MLC of VSMC were measured by immunoblotting as described in our publications [266, 268]. Phosphorylated and total MLC kinase (MLCK) and MLC phosphatase (MLCP) of the VSMC were similarly measured, using rabbit anti-MLCK mAb (clone EP1458Y; Abcam, Cambridge, UK), rabbit anti-phospho-MLCK Ab (Invitrogen, Camarillo, CA), rabbit anti-MLCP Ab (#2634; Cell Signalling, Danvers, MA), and rabbit anti-phospho-MLCP Ab (#5163; Cell Signalling). For AR detection, VSMC were used without stimulation. Rabbit Ab against 1-AR (ab3462; Abcam) was used for blotting.

Urinary catecholamines

Twenty four-hour urine under a fasting condition were collected and urinary catecholamines were assayed by catecholamine ELISA kit (Rocky Mountain Diagnostics, Colorado Springs, CO, USA) according to the manufacturer's instructions.

Plasma angiotensin II (AngII)

Plasma AngII was measured by ELISA (Phoenix Pharmaceuticals, Burlingame, CA, USA) according to the manufacturer's instructions. Samples were in duplicate.

Serum aldosterone

Mouse serum aldosterone was measured by HPLC in the CHUM Clinical Endocrinology Laboratory with certified quality control for human serum aldosterone levels.

Meta-analysis of SNPs in Eph/Efn and related genes associated with BP phenotypes in humans

The p-values for association with DP and SP were calculated for a total of 528 SNPs found within the regions of 4 genes (EPHB6, EFNB2, EFNB3 and GRIP1) and within 10 kb 5' and 3' of these genes, employing the LocusZoom genome browser [33] to query the]IBPC dataset [34], which contains SNP information on 69,395 individuals of European ancestry in 29 general population-based cohorts. These 528 SNPs represented 166 independent linkage disequilibrium (LD) blocks, as determined by the Tagger program [35] on the HapMap website [36]. Table 1A lists the genes and regions in which the SNPs are located. Query of 166 independent LD blocks resulted in a Bonferroni-corrected critical p-value of 0.0003012 for a given BP phenotype (SP or DP). Looking for the best results between DP and SP phenotypes would require a lower critical p-value; however, correcting for 2 X 166 tests (p=0.000151) would be overly conservative as these 2 measurements are not independent.

Results

Efnb3 KO mice

RT-qPCR demonstrated that Efnb3 mRNA was virtually absent in endothelium-stripped mesenteric arteries from Efnb3 KO mice (Fig. 1A). Efnb3 KO was also confirmed at the protein level in isolated Efnb3 KO VSMC by immunofluorescence microscopy (Fig. 1B).

Efnb3 regulates BP in concert with sex hormones

Our previous study showed that BP is heightened in castrated Ephb6 KO mice compared to their WT counterparts [24]. As in this case Ephb6 acts through Efnb reverse signalling [24], and Efnb3 is a ligand of Ephb6, we investigated whether Efnb3 KO mice had abnormal BP phenotype(s). The BP of *Efnb3* KO and WT mice was measured by radiotelemetry. The SP, DP, mean arterial pressure (MAP) and HR of male KO mice showed no significant differences from their WT controls (Fig. 2A). However, female KO mice presented significantly elevated SP, DP and MAP compared to WT females (Fig. 2B).

The fact that BP is increased in female but not male KO mice suggests that Efnb3 works in concert with sex hormones to achieve its BP-regulating effects. We asked whether estrogen enhanced or testosterone reduced BP in the absence of Efnb3. Male mice were castrated, and females, ovariectomized, then rested for 3 weeks to wane sex hormone levels. As illustrated in Figure 2C, after castration, the BP of male KO mice was significantly higher than that of their

WT counterparts, indicating that testosterone was repressing BP up-regulation in the absence of Efnb3. On the other hand, Efnb3 KO females became normotensive after ovariectomy (Fig. 2D), suggesting that estrogens were promoting BP up-regulation in the absence of Efnb3. It should be noted that castration and ovariectomy of WT mice did not affect BP (data not reported). Therefore, Efnb3 needs to work in concert with sex hormones to achieve its BP-regulating effects.

In these experiments, the HR of male and female KO mice was always similar to that of their WT counterparts, ruling out the possibility that BP anomalies in KO females and castrated males derive from differences in CO. This point was further verified by echography (see next section).

Small artery resistance in vivo

BP is a function of CO, blood volume and blood vessel flow resistance, the latter being mainly determined by the tone of small arteries. Echography was employed to examine CO, the PI (a parameter reflecting blood flow resistance) of carotid arteries, and LV mass in live KO and WT mice. CO in male (Table 2A) and female (Table 2B) KO mice was comparable to that in WT controls, indicating that this parameter, which could affect BP, is not under the influence of Efnb3 and is not responsible for elevated BP in female KO mice. However, the left carotid PI in female KO (Table 2B) but not male KO (Table 2A) mice was significantly boosted ($p=0.0218$), reflecting heightened resistance of these small arteries. LV mass increased significantly in female but not in male KO mice ($p=0.0397$, Table 2B). This hypertrophy might be the result of augmented cardiac workload in female KO mice to overcome the heightened blood flow resistance of their small arteries.

Increased vessel contractility of female KO mice ex vivo

The echography results of in vivo studies pointed to vessel flow resistance as an intermediate cause of elevated BP in female KO mice. We next attempted to confirm this finding ex vivo and further pin-point target cell types (e.g., endothelial cells and VSMC) through which Efnb3 exerted its effect. The ex vivo contractility of mesenteric arteries from KO and WT mice was assessed after stimulation with PE. Female but not male KO vessels showed greater contractility than their WT counterparts (Figs. 3A and 3B). This contractility phenotype remained unchanged in the presence or absence of endothelium (Figs. 3A and 3B), indicating that VSMC but not the

endothelium were the target and that nitric oxide or endothelin produced by the endothelium was not required to enhance vessel contractility in the absence of Efnb3. Castration did not change vessel contractility in male KO mice, as KO vessels remained similar to their WT counterparts in terms of contractility. On the other hand, vessels from ovariectomized female KO mice lost their hyper-contractility, becoming similar to those of WT controls. Such a change of the contractility of female KO vessels before and after ovariectomy is reminiscent of the BP phenotype of KO females. The discrepancy between unchanged vessel contractility and increased BP after castration in KO males will be discussed later.

Efnb3 modulates VSMC contractility in concert with sex hormones and through reverse signalling

Data on vasoconstriction in the previous section identified VSMC as the target tissue of Efnb3 deletion. We tried to confirm this finding in single VSMC. When VSMC were stimulated with PE, those derived from female – unlike male – Efnb3 KO mice showed increased contractility compared to their WT coiunterparts (Figs. 4A and 4B), confirming that Efnb3 deletion in females leads to augmented VSMC contractility.

Differential contractility between VSMC from female and male KO mice as well as the effect of castration and ovariectomy on BP in Efnb3 KO mice prompted us to assess whether they were the target tissues of sex hormones in the absence of Efnb3. To answer this question, VSMC from male KO and WT mice were cultured in the presence of exogenous estrogen. KO VSMC contractility increased in comparison to WT controls (Fig. 4C). On the other hand, male WT VSMC contractility remained unchanged in the presence or absence of exogenous estrogen. This result corroborates the hypertensive phenotype of female KO mice, and indicates that VSMC are a target of concerted Efnb3 and estrogen effects: Efnb3 deletion in the presence of estrogen enhances VSMC contractility and, hence, increases vascular tone and BP.

On the other hand, VSMC contractility in female KO mice was not repressed by exogenous testosterone (Fig. 4D). This finding is not compatible with the BP phenotype of castrated KO males, in which reduced testosterone levels combined with Efnb3 KO raised BP. Possible explanations are given in the Discussion.

In theory, Efnb3 deletion could affect both forward (from Efnb3 through Ephbs) and reverse (from Ephbs through Efnb3) signalling in VSMC. To distinguish these 2 possibilities, we placed

VSMC from WT females on wells coated with solid-phase anti-Efnb3 Ab (to trigger reverse signalling) and found that their contractility was significantly reduced (Fig. 4C, line with solid squares). However, solid-phase Efnb3-Fc (to trigger forward signalling) did not significantly affect VSMC contractility (Fig. 4E, line with triangles), suggesting that reverse signalling via Efnb3 but not forward signalling from Efnb3 to Ephs decreases VSMC contractility. Solid-phase anti-Efnb3 Ab also reduced VSMC contractility in male WT mice (Fig. 4F), although male KO and WT had similar values (Fig. 4B). Possible explanations of these findings are presented in the Discussion.

Normal AR expression and Ca++ flux in KO VSMC

We asked whether Efnb3 deletion modulated AR expression or Ca++ flux in VSMC, as both these events can affect VSMC contractility. AR expression in KO VSMC from male and female mice was similar to that in WT controls (Fig. 5A), according to immunofluorescence microscopy and confirmed by immunoblotting (Fig. 5B). PE-stimulated Ca++ flux in KO VSMC from males and females was not different from that in WT mice (Fig. 5C). These results indicate that Efnb3 does not affect VSMC contractility through modulation of AR expression or Ca++ flux-related ion channels.

Efnb3 KO affects signalling pathways related to VSMC contractility

Since there was no difference in Ca++ flux in VSMC from female KO mice compared to WT females, increased contractility of the small arteries and VSMC from female KO mice was likely due to heightened Ca++ responsiveness of VSMC, which is regulated by MLC phosphorylation. Female KO mice arteries indeed manifested a significantly higher degree of MLC phosphorylation than their WT counterparts immediately (3 s) after PE stimulation (Fig. 6A). On the other hand, such MLC phosphorylation in male KO arteries was similar to that in WT controls, consistent with our findings that female but not male KO small arteries presented increased contractility compared to WT.

MLC is phosphorylated by MLCK which is, in turn, phosphorylated at ser1760 by Ca++/CaM-dependent protein kinase II or protein kinase A, and such phosphorylation reduces MLCK enzymatic activity [37,38] We assessed MLCK phosphorylation at ser1760 and observed that VSMC from female but not male KO mice had significantly lower values upon PE stimulation

than WT controls (Fig. 6B). This result implies higher MLC phosphorylation in VSMC from female KO mice, compatible with the finding that female VSMC presented augmented contractility. MLC phosphorylation is also modulated by MLCP, which dephosphorylates MLC and reduces VSMC contractility [39]. MLCP phosphorylation at T695 prevents MLCP binding to MLC and thus diminishes the effect on its substrate [40]. We investigated the outcome of Efnb3 deletion on MLCP phosphorylation in VSMC. Immediately after PE stimulation (3 s), MLCP phosphorylation at T695 in VSMC from both female and male KO mice was similar to that of their WT counterparts (Fig. 6C). This observation suggests that MLCP is not influenced by Efnb3 deletion and does not participate in the contractility upregulation of female KO arteries. Efnb3 had no enzymatic activity. However, Efns engage adaptor proteins to link their intracellular tails to various signalling pathways. Small interference RNAs (siRNAs) were deployed to knock down the expression of 3 adaptor proteins, i.e., Grip1, PDZ-RGS3 and Disheveled, which are known to associate with Efnbs [41-43]. The effectiveness of mRNA knockdown was verified by RT-qPCR (Fig. 7A). VSMC from female WT mice were cultured in wells coated with anti-Efnb3 Ab to invoke Efnb3 reverse signalling, dampening VSMC contractility. With Grip1 siRNA but not PDZ-RGS3 or Dishevelled siRNA transfection into these cells, the inhibitory effect of Efnb3 reverse signalling was released and they showed increased contractility compared to those transfected with control siRNA (Fig. 7B). This result indicates that Grip1 is involved in Efnb3 reverse signalling which regulates VSMC contractility.

BP-related hormone levels in Efnb3 KO mice

We questioned whether some key hormones involved in BP regulation were affected by Efnb3 null mutation directly or as a compensatory consequence. As depicted in Figure 8A, 24-h urinary catecholamine (i.e., adrenaline, dopamine and noradrenaline) levels of male and female KO mice were similar to those in their WT counterparts during fasting, showing that ambient catecholamine secretion in KO mice is not altered. Plasma AngII levels in male and female KO mice were also comparable to those in their WT counterparts (Fig. 8B). Thus, these hormones are not the cause of increased vessel resistance and BP in female KO mice. The serum aldosterone levels of male and female KO mice were all significantly lower than those of WT controls (Fig. 8C). Decreased aldosterone levels in female KO are expected, likely a compensatory mechanism that enhances sodium excretion to reduce blood volume due to higher

BP in these mice. Possible reasons for decreased aldosterone levels in male KO mice are discussed later.

SNPs in genes of the EPH/EFN system associated with BP phenotypes

Our findings in this and previous studies [24,26]. along with some of our unpublished observations indicate that molecules in the EphB and EfnB families (e.g., EphB6, EfnB1, EfnB2, EfnB3) and a certain adaptor protein (Grip1) in their signalling pathways are novel factors that can modulate BP in mice. The relevance of these results in human BP regulation was investigated. The IBPC conducted a meta-analysis of genome-wide association scanning (GWAS) in 69,395 individuals of European ancestry in 29 cohorts from European and North American countries [34]. Two and a half million genotyped or imputed SNPs were tested for their association with SP and DP in these individuals. We queried the results of this meta-analysis for association of 528 SNPs in EPHB6, EFNB2, EFNB3 and GRIP1 genes with DP and SP in these individuals. EFNB1 was not included in the analysis because it is an X-linked gene, and its SNP information is not included in the IBPC dataset. The p-values of these SNPs for their association with SP and DP are illustrated in Supplementary Figure 1 plots. Table 1B summarizes the names of SNPs with the most significant association and their p-values. The minimum p-value (0.000389) for tag SNPs within GRIP1 gene occurs with SNP rs1495496 for its association with DP. This value approaches the critical p-value of 0.000302 (or 0.000151 based on overly conservative correction considering BP and DP as 2 totally independent phenotypes, which they are not). For the other 3 genes analyzed, i.e., EPHB6, EFNB2 and EFNB3, the minimum p-values of their SNPs did not approach the critical p-value. The implications of these findings are elaborated in the Discussion.

Discussion

Ephs and Efns perform critical functions in many tissues and organs. In our recent studies, a novel role for Ephs and Efns in BP regulation was discovered in *Ephb6* KO and *Efnb1* KO mice [266, 268]. In the current investigation, we provide additional evidence in support of the notion that Eph/Efn family members are essential in BP control. We demonstrated that, after *Efnb3* deletion, small arterial resistance is increased in these mice *in vivo*, and that VSMC and the small arteries

from female *Efnb3* KO mice showed heightened responsiveness to vasoconstrictive stimuli *ex vivo* and *in vitro*. As a result, female *Efnb3* KO mice had higher BP than WT females. At the molecular level, Efnb3 deletion in female mice decreased MLCK and MLCP phosphorylation in VSMC, both of which augmented MLC phosphorylation and, hence, VSMC contractility.

Our data consistently pointed to hyper-responsiveness of female *Efnb3* KO VSMC and small arteries, suggesting that they are target tissues for Efnb3 function in BP regulation. However, Efnb3 deletion depends on female sex hormones to achieve BP control and VSMC contractility. Reduction of female sex hormones by ovariectomy led to disappearance of the BP increase in female KO mice and return of their vessel contractility to the WT level *ex vivo*. The enhancing effect of female sex hormones, in this case estrogen, only occurs in the absence of Efnb3 with regard to VSMC contractility, in that male KO VSMC showed increased contractility in the presence of exogenous estrogen, while estrogen by itself did not affect it in WT males. How estrogen influences the Efnb3 reverse signalling pathway in VSMC is currently unknown, and is under investigation in our laboratory.

It has become clear that VSMC in male mice are not a target tissue of Efnb3 in terms of its function in BP control. Male KO mice had normal BP and vessel tone *in vivo*; their small arteries showed normal contractility and MLC phosphorylation *ex vivo*. VSMC from male KO mice presented contractility and MLCK phosphorylation similar to values of their WT counterparts. This is not due to a suppressive effect of testosterone on Efnb3 function regarding VSMC contractility, because adding exogenous testosterone to female KO VSMC did not reduce it. We also tested vessel and VSMC contractility in castrated KO mice, but these parameters did not increase in comparison to non-castrated animals (Fig. 3C and data not included), ruling out the possibility that testosterone inhibits VSMC contractility in the absence of Efnb3. The fact that castrated KO mice manifested augmented BP compared to their WT counterparts indicates that Efnb3 can indeed act in concert with testosterone to regulate BP, but the target of the duo under physiological conditions is outside VSMC. It should be mentioned that VSMC from male WT mice still responded to Efnb3 reverse signalling by reducing their contractility when they were cross-linked by solid-phase anti-Efnb3 Ab (Fig. 4F). This suggests that male VSMC could still be subject to the effect of non-physiologically strong Efnb3 reverse signalling. However, *in vivo*, stimulation from Ephs to Efnb3 on VSMC in vessels is probably not as strong as artificial *in vitro* cross-linking by solid-phase anti-Efnb3 Ab, and that is why we did not observe any

phenotype in male KO mice in BP and echographic studies *in vivo* and vessel contraction *ex vivo*.

We reported previously that chromaffin cells in the adrenal glands are a second target tissue in male *Ephb6* KO mice, after VSMC, in terms of Ephb6's effect on BP regulation. Catecholamine synthesis and/or secretion are repressed in *Ephb6* KO males. As a result, these male Ephb6 KO mice remain normotensive due to the compensatory reduction of catecholamines [24]. Once testosterone is reduced by castration, the compensation is lost, catecholamine levels return to normal, and the mice become hypertensive [266]. As Efnb3 is a ligand of Ephb6, as the latter acts through reverse signalling to achieve its BP-regulating effect, and as BP increases similarly in Ephb6 and Efnb3 KO males after castration, we wondered whether adrenal gland chromaffin cells are another target tissue of Efnb3. However, we did not detect any change in ambient catecholamine levels in male *Efnb3* KO mice based on their 24-h urinary catecholamine levels, indicating that chromaffin cells in the adrenal glands are not a target tissue of Efnb3 and that the testosterone-dependent compensation mechanism in catecholamine synthesis/secretion in male *Ephb6* KO mice is mediated by ligands other than Efnb3.

We noted a significant decrease in serum aldosterone levels in both male and female *Efnb3* KO mice, probably a feedback response to cope with increased BP tendency. Reduced aldosterone levels in female KO mice are fully understandable, because of their elevated BP. However, decreased aldosterone levels in male *Efnb3* KO mice, albeit their normal BP, suggest a trend towards heightened BP, but it did not change probably because of sufficient compensation by mechanisms such as aldosterone reduction, which then diminishes sodium and water re-absorption from distal tubules and collecting ducts of nephrons into blood. In this case, the increased BP tendency in male KO mice is likely caused by so-far uncharacterized Efnb3 target tissues/organs other than VSMC, as alluded to earlier in this discussion.

BP is a vital physiological parameter and, not surprisingly, multiple compensatory mechanisms are engaged once fluctuation tends to occur. These compensatory mechanisms have to be disabled before the BP phenotype becomes obvious. Previously, we identified catecholamine synthesis and/or release as such a mechanism in *Ephb6* KO mice. There is also one in male *Efnb3* KO mice, but its nature has not been revealed. An interesting feature of these compensatory mechanisms is that they act in concert with sex hormones, and male hormone seems to be essential for them. In other words, male hormone is protective against hypertension;

the results in both *Ephb6* KO and *Efnb3* KO mice are similar although not identical in pointing to this conclusion: in both types of KO mice, castration leads to hypertension in males. It is known that ageing male humans have higher incidence of hypertension. Our finding points to a possibility that in a subpopulation of hypertensive ageing males, the increased BP could be caused by the EPH/EFN signalling pathway defects, which only start to have BP manifestation once male sex hormone level decreases. On the other hand, estrogen is culpable for elevated BP in the absence of Efnb3. Such results suggest that if we decide to assess genes in the *EPH/EFN* family as hypertension risk factors, we need to consider not only gender but also sex hormone levels to filter out "noises".

As for the Efnb3's effect on VSMC contractility regulation, we determined that it depends on reverse signalling via Efnb3 into cells. Efnb3 intracellular tails have no enzymatic activity, but are capable of binding to several adaptor proteins, such as Grip1, PDZ-RGS3 and Dishevelled [41-43]. Among these 3 molecules, we found that Grip1 is critically required for Efnb3 function, in that Grip1 knockdown by siRNA can reverse the dampening effect of solid-phase anti-Efnb3 Ab on VSMC contractility. Grip1 has 5 PDZ domains [41] which can associate with signalling molecules that contain PDZ-binding domains and thus mediate Efn reverse signalling. This molecule, since it can physically bind to Efnb3 [41], seems to be the most proximal in the Efnb3 reverse signalling pathway. We have also pin-pointed defects in MLC phosphorylation in *Efnb3* KO VSMC, which determines the responsiveness of VSMC to Ca^{++} flux and, hence, contractility. We have identified abnormal MLCK phosphorylation, which controls MLCK activity and, subsequently, MLC phosphorylation. The connection between Grip1 or other putative proximal molecules with MLCK phosphorylation remains to be further investigated. It is not surprising that Grip1 has been found to be critical in controlling VSMC contractility in all 3 types of KO mice, i.e., *Ephb6* [24], *Efnb1* [26] and *Efnb3* KO (this study) mice, as Ephb6 regulates BP via reverse signalling, and Efnb1 and Efnb3 are both likely in this reverse signalling pathway. Moreover, Efnb1 and Efnb3 intracellular tails have a high degree of homology and can bind to Grip1. Therefore, Grip1 is situated in a node of signalling pathways emanating from the Ephb/Efnb family of molecules with regard to their roles in BP regulation, and carries more weight than each individual Ephb/Efnb member.

Collectively, we discovered a novel role for a group of genes whose known function is not associated with BP and vascular tone. This has opened a new area of knowledge in the

pathogenesis of hypertension. Under physiological conditions, Ephb6 on neighboring cells probably provides VSMC with a negative signal to dampen their contractility through reverse signalling. We have confirmed, in our previous publications [266, 268] and the current one, that Efnb1 and Efnb3 are mediating such reverse signalling. Since the interactions between Ephb6 and Efnbs are constant, such a dampening effect is not regulated rapidly and likely controls constitutive vascular tone rather than fast responses to neuroendocrine stimulation.

As of today, no genes in the *EPHB/EFNB* family have been identified as hypertension risk genes in several large-scale GWAS [275]. There are a couple of possible reasons. 1) The contribution of genes in the *EPHB/EFNB* family to the BP phenotype is relatively small, and the possible association is rendered undetectable due to heavy statistical penalties in GWAS. 2) As evidenced by our work, the effect of Ephbs and Efnbs on BP phenotypes needs concerted input of sex hormones, and is thus not only gender- but also hormone leve-dependent; however, no current GWAS study has specifically stratified cohorts based on sex hormone levels. We conducted a more focused query of the IBPC dataset and discovered that a SNP, rs1495496, located between exons 22 and 23 of *GRIP1*, had a p-value of 0.000389 for its association with DP, and such a p-value approached the Bonferroni corrected critical p-value 0.000302 or an overly conservative corrected critical p-value of 0.000151. This finding is very promising since the queried cohorts were not stratified according to sex hormone levels, and Bonferroni correction by itself was deemed to be quite conservative. Considering our observation that Ephb/Efnbs likely influence vessel tone in mice, the possible association of this SNP in GRIP1 gene with DP seems logical. Why does only a SNP from *GRIP1* approach significance and not those from 3 *EPHB6/EFNBs* queried? As discussed above, in mice Grip1 is situated in a node of Ephb6, Efnb1 and Efnb3 reverse signalling; it thus probably carries more weight than each individual Ephb or Efnb member and, hence, is easier to detect for its associations with BP phenotypes. It is possible that in a cohort stratified by gender and sex hormone levels, significant association of BP phenotypes with SNPs from *GRIP1* and *EPHB/EFNB* family members will be detected in humans, and this will fully establish the relevance of our findings from animal models to human hypertension.

Acknowledgments

This work was supported by grants from the Canadian Institutes of Health Research to J.W. (MOP57697, MOP69089 and MOP 123389), H.L. (MOP97829), E.T. (MOP14496), and G.C. (CMI72323). It was also financed by grants from the Heart and Stroke Foundation of Quebec, the Natural Sciences and Engineering Research Council of Canada (203906-2012), and the J.-Louis Levesque Foundation to J.W. This study was also made possible by a group grant from Fonds de la recherche en santé du Québec for Transfusional and Hemovigilance Medical Research to J.W. The authors thank Regeneron Pharmaceuticals for generously providing *Efnb3* KO mice.

Disclosures

The authors declare no conflict of interests.

References

1. Unified nomenclature for Eph family receptors and their ligands, the ephrins. Eph Nomenclature Committee. *Cell*. 1997;90:403-404.

2. Pasquale EB. Eph-ephrin bidirectional signaling in physiology and disease. *Cell.* 2008;133:38-52.

3. Wilkinson DG. Eph receptors and ephrins: regulators of guidance and assembly. *Int Rev Cytol*. 2000;196:177-244.

4. Flanagan JG, Vanderhaeghen P. The ephrins and Eph receptors in neural development. *Annu Rev Neurosci*. 1998;21:309-345.

5. Luo H, Wan X, Wu Y, Wu J. Crosslinking of EphB6 resulting in signal transduction and apoptosis in Jurkat cells. *J. Immunol*. 2001;167:1362-1370.

6. Luo H, Yu G, Wu Y, Wu J. EphB6 crosslinking results in costimulation of T cells. *J. Clin. Invest.* 2002;110:1141-1150.

7. Yu G, Luo H, Wu Y, Wu J. Ephrin B2 induces T cell costimulation. *J. Immunol.* 2003;171:106-114.

8. Yu G, Luo H, Wu Y, Wu J. Mouse ephrinB3 augments T-cell signaling and responses to T-cell receptor ligation. *J. Biol. Chem.* 2003;278:47209-47216.

9. Luo H, Yu G, Tremblay J, Wu J. EphB6 null mutation results in compromised T cell function. *J. Clin. Investigation.* 2004;114:1762-1773.

10. Yu G, Luo H, Wu Y, Wu J. EphrinB1 is essential in T-cell-T-cell co-operation during T-cell activation. *J. Biol. Chem*. 2004;279:55531-55539.

11. Wu J, Luo H. Recent advances on T-cell regulation by receptor tyrosine kinase. *Curr Opin Hematol*. 2005;12:292-297.

12. Yu G, Mao J, Wu Y, Luo H, Wu J. Ephrin-B1 is critical in T-cell development. *J. Biol. Chem*. 2006;281:10222-10229.

13. Luo H, Charpentier T, Wang X, Qi S, Han B, Wu T, Terra R, Lamarre A, Wu J. Efnb1 and Efnb2 proteins regulate thymocyte development, peripheral T cell differentiation, and antiviral immune responses and are essential for interleukin-6 (IL-6) signaling. *J. Biol. Chem*. 2011;286:41135-41152.

14. Luo H, Wu Z, Qi S, Jin W, Han B, Wu J. Ephrinb1 and Ephrinb2 are associated with interleukin-7 receptor α and retard its internalization from the cell surface. *J. Biol. Chem.* 2011;286:44976-44987.

15. Batlle E, Henderson JT, Beghtel H, van den Born MM, Sancho E, Huls G, Meeldijk J, Robertson J, van de Wetering M, Pawson T, Clevers H. Beta-catenin and TCF mediate cell positioning in the intestinal epithelium by controlling the expression of EphB/ephrinB. *Cell.* 2002;111:251-263.

16. Davy A, Bush JO, Soriano P. Inhibition of gap junction communication at ectopic Eph/ephrin boundaries underlies craniofrontonasal syndrome. *PLoS Biol*. 2006;4:e315.

17. Zhao C, Irie N, Takada Y, Shimoda K, Miyamoto T, Nishiwaki T, Suda T, Matsuo K. Bidirectional ephrinB2-EphB4 signaling controls bone homeostasis. *Cell Metab.* 2006;4:111-121.

18. Wang HU, Chen ZF, Anderson DJ. Molecular distinction and angiogenic interaction between embryonic arteries and veins revealed by ephrin-B2 and its receptor Eph-B4. *Cell*. 1998;93:741-753.

19. Konstantinova I, Nikolova G, Ohara-Imaizumi M, Meda P, Kucera T, Zarbalis K, Wurst W, Nagamatsu S, Lammert E. EphA-Ephrin-A-mediated beta cell communication regulates insulin secretion from pancreatic islets. *Cell*. 2007;129:359-370.

20. Hashimoto T, Karasawa T, Saito A, Miyauchi N, Han GD, Hayasaka K, Shimizu F, Kawachi H. Ephrin-B1 localizes at the slit diaphragm of the glomerular podocyte. *Kidney Int.* 2007;72:954-964.

21. Dravis C, Wu T, Chumley MJ, Yokoyama N, Wei S, Wu DK, Marcus DC, Henkemeyer M. EphB2 and ephrin-B2 regulate the ionic homeostasis of vestibular endolymph. *Hear Res.* 2007;223:93-104.

22. Foo SS, Turner CJ, Adams S, Compagni A, Aubyn D, Kogata N, Lindblom P, Shani M, Zicha D, Adams RH. Ephrin-B2 controls cell motility and adhesion during blood-vessel-wall assembly. *Cell.* 2006;124:161-173.

23. Ogita H, Kunimoto S, Kamioka Y, Sawa H, Masuda M, Mochizuki N. EphA4-mediated Rho activation via Vsm-RhoGEF expressed specifically in vascular smooth muscle cells. *Circ Res*. 2003;93:23-31.

24. Luo H, Wu Z, Tremblay J, Thorin E, Peng J, Lavoie JL, Hu B, Stoyanova E, Cloutier G, Qi S, Wu T, Cameron M, Wu J. Receptor tyrosine kinase Ephb6 regulates vascular smooth muscle contractility and modulates blood pressure in concert with sex hormones. *J. Biol. Chem*. 2012;287:6819-6829.

25. Kullander K, Croll SD, Zimmer M, Pan L, McClain J, Hughes V, Zabski S, DeChiara TM, Klein R, Yancopoulos GD, Gale NW. Ephrin-B3 is the midline barrier that prevents corticospinal tract axons from recrossing, allowing for unilateral motor control. *Genes Dev*. 2001;15:877-888.

26. Wu Z, Luo H, Thorin E, Tremblay J, Peng J, Lavoie JL, Wang Y, Qi S, Wu T, Wu J. Possible role of Efnb1 protein, a ligand of Eph receptor tyrosine kinases, in modulating blood pressure. *J. Biol. Chem.* 2012;287:15557-15569.

27. Lavoie JL, Lake-Bruse KD, Sigmund CD. Increased blood pressure in transgenic mice expressing both human renin and angiotensinogen in the renal proximal tubule. *Am J Physiol Renal Physiol.* 2004;286:F965-F971

28. Zhou YQ, Foster FS, Nieman BJ, Davidson L, Chen XJ, Henkelman RM. Comprehensive transthoracic cardiac imaging in mice using ultrasound biomicroscopy with anatomical confirmation by magnetic resonance imaging. *Physiol Genomics.* 2004;18:232-244.

29. Stoyanova E, Trudel M, Felfly H, Garcia D, Cloutier G. Characterization of circulatory disorders in beta-thalassemic mice by noninvasive ultrasound biomicroscopy. *Physiol Genomics*. 2007;29:84-90.

30. Yang XP, Liu YH, Rhaleb NE, Kurihara N, Kim HE, Carretero OA. Echocardiographic assessment of cardiac function in conscious and anesthetized mice. *Am J Physiol*. 1999;277:H1967-H1974.

31. Pollick C, Hale SL, Kloner RA. Echocardiographic and cardiac Doppler assessment of mice. *J Am Soc Echocardiogr*. 1995;8:602-610.

32. Thorin E, Huang PL, Fishman MC, Bevan JA. Nitric oxide inhibits alpha2-adrenoceptor-mediated endothelium-dependent vasodilation. *Circ Res*. 1998;82:1323-1329.

33. http://csg.sph.umich.edu/locuszoom/

34. International Consortium for Blood Pressure Genome-Wide Association Studies, Ehret GB, Munroe PB, Rice KM, Bochud M, Johnson AD, Chasman DI, Smith AV, Tobin MD,

Verwoert GC, Hwang SJ, Pihur V, Vollenweider P, O'Reilly PF, Amin N, Bragg-Gresham JL, Teumer A, Glazer NL, Launer L, Zhao JH, Aulchenko Y, Heath S, Sõber S, Parsa A, Luan J, Arora P, Dehghan A, Zhang F, Lucas G, Hicks AA, Jackson AU, Peden JF, Tanaka T, Wild SH, Rudan I, Igl W, Milaneschi Y, Parker AN, Fava C, Chambers JC, Fox ER, Kumari M, Go MJ, van der Harst P, Kao WH, Sjögren M, Vinay DG, Alexander M, Tabara Y, Shaw-Hawkins S, Whincup PH, Liu Y, Shi G, Kuusisto J, Tayo B, Seielstad M, Sim X, Nguyen KD, Lehtimäki T, Matullo G, Wu Y, Gaunt TR, Onland-Moret NC, Cooper MN, Platou CG, Org E, Hardy R, Dahgam S, Palmen J, Vitart V, Braund PS, Kuznetsova T, Uiterwaal CS, Adeyemo A, Palmas W, Campbell H, Ludwig B, Tomaszewski M, Tzoulaki I, Palmer ND; CARDIoGRAM consortium; CKDGen Consortium; KidneyGen Consortium; EchoGen consortium; CHARGE-HF consortium, Aspelund T, Garcia M, Chang YP, O'Connell JR, Steinle NI, Grobbee DE, Arking DE, Kardia SL, Morrison AC, Hernandez D, Najjar S, McArdle WL, Hadley D, Brown MJ, Connell JM, Hingorani AD, Day IN, Lawlor DA, Beilby JP, Lawrence RW, Clarke R, Hopewell JC, Ongen H, Dreisbach AW, Li Y, Young JH, Bis JC, Kähönen M, Viikari J, Adair LS, Lee NR, Chen MH, Olden M, Pattaro C, Bolton JA, Köttgen A, Bergmann S, Mooser V, Chaturvedi N, Frayling TM, Islam M, Jafar TH, Erdmann J, Kulkarni SR, Bornstein SR, Grässler J, Groop L, Voight BF, Kettunen J, Howard P, Taylor A, Guarrera S, Ricceri F, Emilsson V, Plump A, Barroso I, Khaw KT, Weder AB, Hunt SC, Sun YV, Bergman RN, Collins FS, Bonnycastle LL, Scott LJ, Stringham HM, Peltonen L, Perola M, Vartiainen E, Brand SM, Staessen JA, Wang TJ, Burton PR, Soler Artigas M, Dong Y, Snieder H, Wang X, Zhu H, Lohman KK, Rudock ME, Heckbert SR, Smith NL, Wiggins KL, Doumatey A, Shriner D, Veldre G, Viigimaa M, Kinra S, Prabhakaran D, Tripathy V, Langefeld CD, Rosengren A, Thelle DS, Corsi AM, Singleton A, Forrester T, Hilton G, McKenzie CA, Salako T, Iwai N, Kita Y, Ogihara T, Ohkubo T, Okamura T, Ueshima H, Umemura S, Eyheramendy S, Meitinger T, Wichmann HE, Cho YS, Kim HL, Lee JY, Scott J, Sehmi JS, Zhang W, Hedblad B, Nilsson P, Smith GD, Wong A, Narisu N, Stančáková A, Raffel LJ, Yao J, Kathiresan S, O'Donnell CJ, Schwartz SM, Ikram MA, Longstreth WT Jr, Mosley TH, Seshadri S, Shrine NR, Wain LV, Morken MA, Swift AJ, Laitinen J, Prokopenko I, Zitting P, Cooper JA, Humphries SE, Danesh J, Rasheed A, Goel A, Hamsten A, Watkins H, Bakker SJ, van Gilst WH, Janipalli CS, Mani KR, Yajnik CS, Hofman A, Mattace-Raso FU, Oostra BA, Demirkan A, Isaacs A, Rivadeneira F, Lakatta EG, Orru M, Scuteri A, Ala-Korpela M, Kangas AJ, Lyytikäinen LP, Soininen P,

Tukiainen T, Würtz P, Ong RT, Dörr M, Kroemer HK, Völker U, Völzke H, Galan P, Hercberg S, Lathrop M, Zelenika D, Deloukas P, Mangino M, Spector TD, Zhai G, Meschia JF, Nalls MA, Sharma P, Terzic J, Kumar MV, Denniff M, Zukowska-Szczechowska E, Wagenknecht LE, Fowkes FG, Charchar FJ, Schwarz PE, Hayward C, Guo X, Rotimi C, Bots ML, Brand E, Samani NJ, Polasek O, Talmud PJ, Nyberg F, Kuh D, Laan M, Hveem K, Palmer LJ, van der Schouw YT, Casas JP, Mohlke KL, Vineis P, Raitakari O, Ganesh SK, Wong TY, Tai ES, Cooper RS, Laakso M, Rao DC, Harris TB, Morris RW, Dominiczak AF, Kivimaki M, Marmot MG, Miki T, Saleheen D, Chandak GR, Coresh J, Navis G, Salomaa V, Han BG, Zhu X, Kooner JS, Melander O, Ridker PM, Bandinelli S, Gyllensten UB, Wright AF, Wilson JF, Ferrucci L, Farrall M, Tuomilehto J, Pramstaller PP, Elosua R, Soranzo N, Sijbrands EJ, Altshuler D, Loos RJ, Shuldiner AR, Gieger C, Meneton P, Uitterlinden AG, Wareham NJ, Gudnason V, Rotter JI, Rettig R, Uda M, Strachan DP, Witteman JC, Hartikainen AL, Beckmann JS, Boerwinkle E, Vasan RS, Boehnke M, Larson MG, Järvelin MR, Psaty BM, Abecasis GR, Chakravarti A, Elliott P, van Duijn CM, Newton-Cheh C, Levy D, Caulfield MJ, Johnson T. Genetic variants in novel pathways influence blood pressure and cardiovascular disease risk. *Nature*. 2011;478:103-109.

35. de Bakker PI, Yelensky R, Pe'er I, Gabriel SB, Daly MJ, Altshuler D. Efficiency and power in genetic association studies. *Nat Genet*. 2005;37:1217-1223.

36. http://hapmap.ncbi.nlm.nih.gov.

37. Miller JR, Silver PJ, Stull JT. The role of myosin light chain kinase phosphorylation in beta-adrenergic relaxation of tracheal smooth muscle. *Mol Pharmacol*. 1983;24:235-242.

38. Raina H, Zacharia J, Li M, Wier WG. Activation by Ca2+/calmodulin of an exogenous myosin light chain kinase in mouse arteries. *J Physiol*. 2009;587:2599-2612.

39. Kawano Y, Fukata Y, Oshiro N, Amano M, Nakamura T, Ito M, Matsumura F, Inagaki M, Kaibuchi K. Phosphorylation of myosin-binding subunit (MBS) of myosin phosphatase by Rho-kinase in vivo. *J Cell Biol*. 1999;147:1023-1038.

40. Murányi A, Derkach D, Erdodi F, Kiss A, Ito M, Hartshorne DJ. Phosphorylation of Thr695 and Thr850 on the myosin phosphatase target subunit: inhibitory effects and occurrence in A7r5 cells. *FEBS Lett*. 2005;579:6611-6615.

41. Bruckner K, Pablo LJ, Scheiffele P, Herb A, Seeburg PH, Klein R. EphrinB ligands recruit GRIP family PDZ adaptor proteins into raft membrane microdomains. *Neuron*.1999;22:511-524.

42. Tanaka M, Kamo T, Ota S, Sugimura H. Association of Dishevelled with Eph tyrosine kinase receptor and ephrin mediates cell repulsion. *EMBO J*. 2003;22:847-858.

43. Lu Q, Sun EE, Klein RS, Flanagan JG. Ephrin-B reverse signaling is mediated by a novel PDZ-RGS protein and selectively inhibits G protein-coupled chemoattraction. *Cell*. 2001;105:69-79.

44. Wellcome Trust Case Control Consortium. Genome-wide association study of 14,000 cases of seven common diseases and 3,000 shared controls. *Nature*. 2007;447:661-678.

45. Org E, Eyheramendy S, Juhanson P, Gieger C, Lichtner P, Klopp N, Veldre G, Döring A, Viigimaa M, Sõber S, Tomberg K, Eckstein G; KORA, Kelgo P, Rebane T, Shaw-Hawkins S, Howard P, Onipinla A, Dobson RJ, Newhouse SJ, Brown M, Dominiczak A, Connell J, Samani N, Farrall M; BRIGHT, Caulfield MJ, Munroe PB, Illig T, Wichmann HE, Meitinger T, Laan M. Genome-wide scan identifies CDH13 as a novel susceptibility locus contributing to blood pressure determination in two European populations. *Hum Mol Genet*. 2009;18:2288-2296.

46. Levy D, Ehret GB, Rice K, Verwoert GC, Launer LJ, Dehghan A, Glazer NL, Morrison AC, Johnson AD, Aspelund T, Aulchenko Y, Lumley T, Köttgen A, Vasan RS, Rivadeneira F, Eiriksdottir G, Guo X, Arking DE, Mitchell GF, Mattace-Raso FU, Smith AV, Taylor K, Scharpf RB, Hwang SJ, Sijbrands EJ, Bis J, Harris TB, Ganesh SK, O'Donnell CJ, Hofman A, Rotter JI, Coresh J, Benjamin EJ, Uitterlinden AG, Heiss G, Fox CS, Witteman JC, Boerwinkle E, Wang TJ, Gudnason V, Larson MG, Chakravarti A, Psaty BM, van Duijn CM. Genome-wide association study of blood pressure and hypertension. *Nat Genet.* 2009;41:677-687

47. Adeyemo A, Gerry N, Chen G, Herbert A, Doumatey A, Huang H, Zhou J, Lashley K, Chen Y, Christman M, Rotimi C. A genome-wide association study of hypertension and blood pressure in African Americans. *PLoS Genet.* 2009;5:e1000564.

48. Hiura Y, Tabara Y, Kokubo Y, Okamura T, Miki T, Tomoike H, Iwai N. A genome-wide association study of hypertension-related phenotypes in a Japanese population. *Circ J*. 2010;74:2353-2359.

49. Padmanabhan S, Melander O, Johnson T, Di Blasio AM, Lee WK, Gentilini D, Hastie CE, Menni C, Monti MC, Delles C, Laing S, Corso B, Navis G, Kwakernaak AJ, van der Harst P, Bochud M, Maillard M, Burnier M, Hedner T, Kjeldsen S, Wahlstrand B, Sjögren M, Fava C, Montagnana M, Danese E, Torffvit O, Hedblad B, Snieder H, Connell JM, Brown M, Samani NJ, Farrall M, Cesana G, Mancia G, Signorini S, Grassi G, Eyheramendy S, Wichmann HE, Laan M, Strachan DP, Sever P, Shields DC, Stanton A, Vollenweider P, Teumer A, Völzke H, Rettig R, Newton-Cheh C, Arora P, Zhang F, Soranzo N, Spector TD, Lucas G, Kathiresan S, Siscovick DS, Luan J, Loos RJ, Wareham NJ, Penninx BW, Nolte IM, McBride M, Miller WH, Nicklin SA, Baker AH, Graham D, McDonald RA, Pell JP, Sattar N, Welsh P; Global BPgen Consortium, Munroe P, Caulfield MJ, Zanchetti A, Dominiczak AF. Genome-wide association study of blood pressure extremes identifies variant near UMOD associated with hypertension. *PLoS Genet*. 2010;6:e1001177.

50. Slavin TP, Feng T, Schnell A, Zhu X, Elston RC. Two-marker association tests yield new disease associations for coronary artery disease and hypertension. *Hum Genet*. 2011;130:725-733.

51. Guo Y, Tomlinson B, Chu T, Fang YJ, Gui H, Tang CS, Yip BH, Cherny SS, Hur YM, Sham PC, Lam TH, Thomas NG. A genome-wide linkage and association scan reveals novel loci for hypertension and blood pressure traits. *PLoS One.* 2012;7:e31489.

42. International Consortium for Blood Pressure Genome-Wide Association Studies *Nature 478(103): 6 October 2011.*

Tables

Table I. Association of SNPs in the EPHB6/EFNB system with BP phenotypes in 69,396 human subjects

A. Locations of 4 genes for which 528 SNPs were tested

	Build 36		Build 37	
Gene	Location	Size (kb)	Location	size (kb)
EPHB6	chr7: 142,252,914 - 142,288,969	36.06	chr 7: 142,542,792 - 142,578,847	36.06
EFNB2	chr13: 105,930,097- 105,995,338	65.24	chr 13: 107,132,079- 107,197,388	65.31
EFNB3	chr17: 7,539,245- 7,565,418	26.17	chr 17: 7,598,520- 7,624,693	26.17
GRIP1	chr12: 65,019,066- 65,369,020	349.95	chr 12: 66,731,211- 67,082,925	351.71

B. Minimum p-values from IBPC meta-analysis among SNPs examined within EPHB6, EFNB2, EFNB3 and GRIP1 genes

Gene	Number of SNPs examined	LD Blocks r2=0.8	Diastolic Pressure		Systolic Pressure	
			SNP	p-value	SNP	p-value
EPHB6	48	4	rs1009848	0.0373	rs2299557	0.404
EFNB2	54	24	rs2057408	0.077	rs9520087	0.218
EFNB3	6	6	rs3744258	0.201	rs3744258	0.191
GRIP1	420	132	**rs1495496**	**0.000389**	**rs1495496**	**0.00144**
Total	528	166	Critical p value: 0.05/166 = 0.0003012			

Table II. Echographic analysis of CO, carotid artery resistance and left ventricle mass of KO and WT mice

BP-related echographic parameters of individual *Efnb3* KO and WT mice are reported. Means ± SD are shown at the end of each group, and *p* values (unpaired Student' *t* test) are indicated at the end of Tables 2A and 2B. PI: Pourcelot index; LV: left ventricle.

A. Echographic parameters of male Efnb3 KO mice

Mouse Type	Age	Cardiac Output (ml/min)	Left Carotid PI	Right Carotid PI	LV Mass (mg)
KO male	15wk	14.65	0.75	0.72	103.7
KO male	15wk	21.46	0.87	0.68	125.8
KO male	15wk	24.79	0.73	0.78	154.1
KO male	15wk	17.23	0.74	0.70	91.7
KO male	15wk	14.93	0.78	0.78	89.7
KO male	14wk	18.2	0.73	0.72	133.6
KO mean		**18.54**	**0.77**	**0.73**	**116.4**
SD		3.939	0.0533	0.041	25.65
WT male	14wk	21.5	0.83	0.84	116.0
WT male	15wk	15.33	0.74	0.70	140.5
WT male	15wk	23.52	0.75	0.77	115.6
WT male	15wk	18.21	0.73	0.72	133.6
WT male	14wk	31.85	0.77	0.86	115.0
WT male	14wk	28.57	0.77	0.81	145.1
WT male	14wk	24.19	0.74	0.76	152.7
WT male	14wk	30.95	0.79	0.83	175.6
WT mean		**24.265**	**0.77**	**0.78**	**126.4**
SD		5.92	0.030	0.047	12.57
p value (t test)		0.0637	0.9075	0.08200	0.4967

B. Echographic parameters of female Efnb3 KO mice

Mouse Type	Age	Cardiac Output (ml/min)	Left Carotid PI	Right Carotid PI	LV Mass (mg)
KO female	15wk	21.89	0.75	0.78	112.3
KO female	15wk	16.29	0.77	0.8	92.5
KO female	14wk	20.16	0.81	0.81	121.1
KO female	15wk	27.57	0.76	0.77	143.3
KO female	15wk	20.54	0.94	0.76	130.5
KO female	14wk	27.71	0.75	0.73	134.3
KO female	15wk	19.13	0.8	0.77	135.8
KO female	14wk	18.38	0.81	0.82	122
KO mean		**21.45**	**0.79**	**0.78**	**123.9**
SD		4.153	0.062	0.029	16.04
WT female	14wk	33.49	0.72	0.72	109
WT female	14wk	18.92	0.69	0.67	118.1
WT female	14wk	29.03	0.71	0.8	110.9
WT female	14wk	28.06	0.81	0.79	95.9
WT female	14wk	15.96	0.68	0.76	114.6
WT female	14wk	22.46	0.7	0.74	72.2
WT mean		**24.65**	**0.71**	**0.74**	**93.4**
SD		6.664	0.047	0.048	29.98
p value (t test)		0.289	***0.0218***	0.132	***0.0397***

FIGURES AND LEGENDS

Figure 1 *Efnb3 deletion in vascular cells in Efnb3 KO mice*

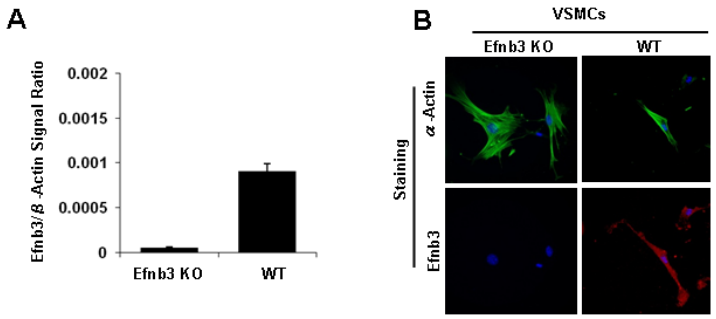

All experiments were repeated at least twice, and data from a representative experiment are reported.

A. *Efnb3 mRNA deletion in mesenteric arteries of Efnb3 KO mice*

Efnb3 mRNA expression in mesenteric arteries from WT and *Efnb3* KO mice was measured by RT-qPCR with β-actin mRNA as internal control. Means ± SD of Efnb3 signal/β-actin signal ratios are reported.

B. *Efnb3 deletion in VSMC*

WT and *Efnb3* KO VSMC cultured for 4-5 days were stained with FITC-goat anti-α-actin Ab (in pseudo-green color) and goat anti-mouse-Efnb3 Ab, followed by PE-donkey anti-goat IgG Ab (in pseudo-red color). Nuclei were identified by DAPI staining.

Figure 2 *BP and HR of Efnb3 KO mice*

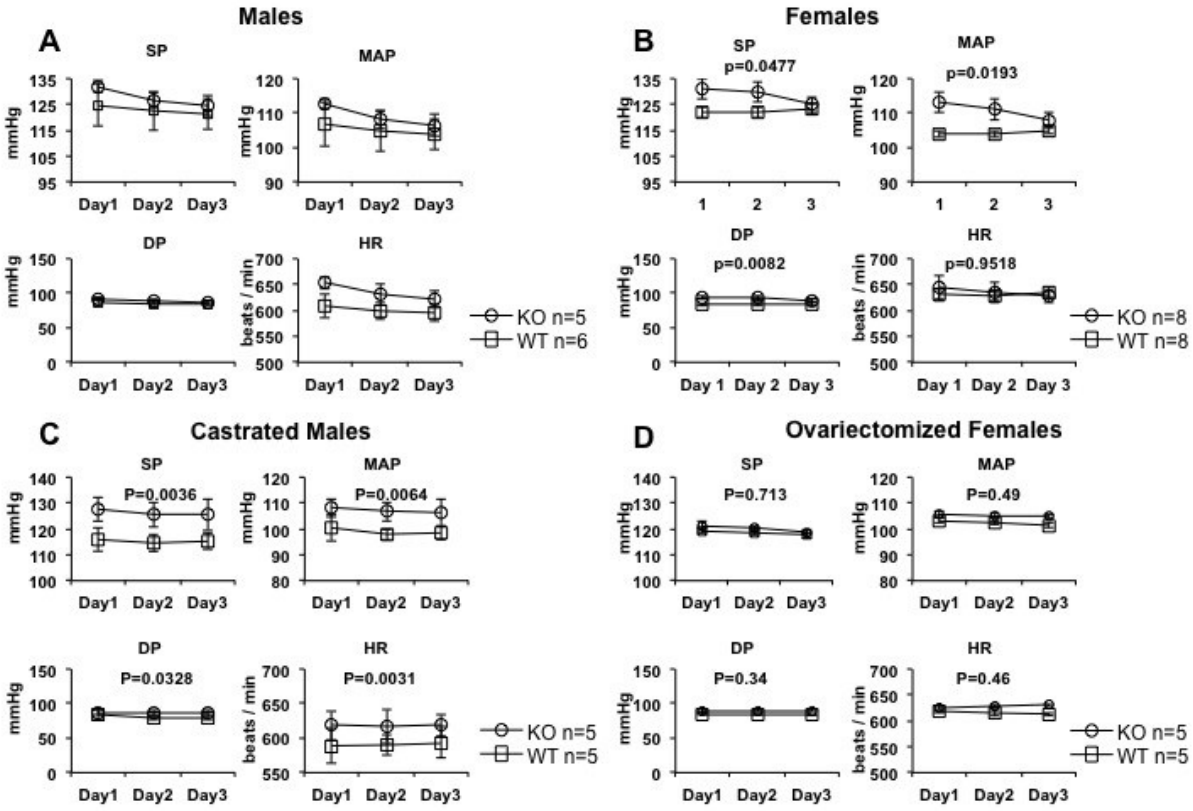

BP and HR were measured for 3 days by radiotelemetry starting at least 7 days after transmitter implantation. In castrated and ovariectomized mice, telemetry was conducted 3 weeks after surgery. Number per group is indicated. Values are expressed as mean 24-h BP and HR for each day ± SE. SP: systolic pressure; DP: diastolic pressure; MAP: mean arterial pressure; HR: heart rate. The WT and KO data were evaluated statistically by repeated-measures ANOVA. P-values are indicated.

A. *BP and HR of males*

B. *BP and HR of females*

C. *BP and HR of castrated males*

D. *BP and HR of ovariectomized females*

Figure 3 *Contractility of mesenteric arteries from Efnb3 KO mice*

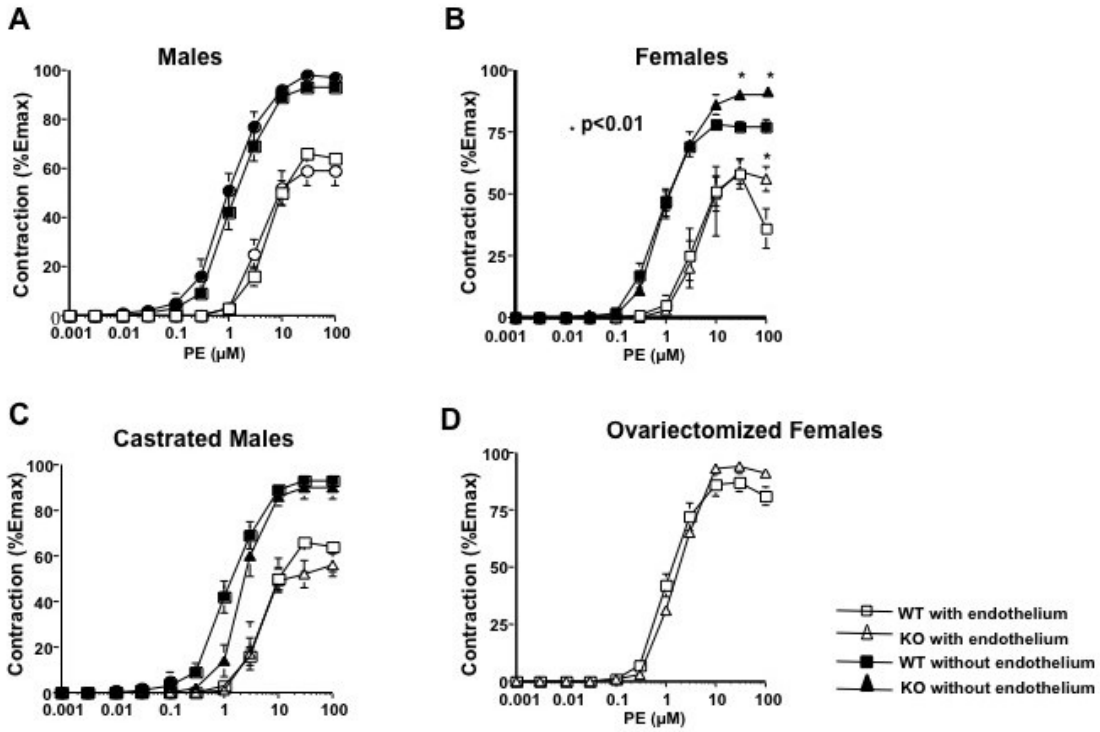

Segments of the third-order branch of the mesenteric artery with or without endothelium were stimulated with PE. A single cumulative concentration-response curve to PE (1 nM to 100 µM) was obtained. Maximal tension (Emax) was determined by challenging the vessels with physiological saline containing 127 mM KCl. Vessel contractility is expressed as the percentage of Emax. Data from 3 mice per group were pooled, and means ± SE are reported. **p*<0.01 (paired Student's *t* test).

A. *Vessel contractility in male KO and WT mice*

B. *Vessel contractility in female KO and WT mice*

C. *Vessel contractility in castrated male KO and WT mice*

D. *Vessel contractility in ovariectomized female KO and WT mice*

Figure 4 *VSMC contractility is influenced by Efnb3 deletion and reverse signalling*

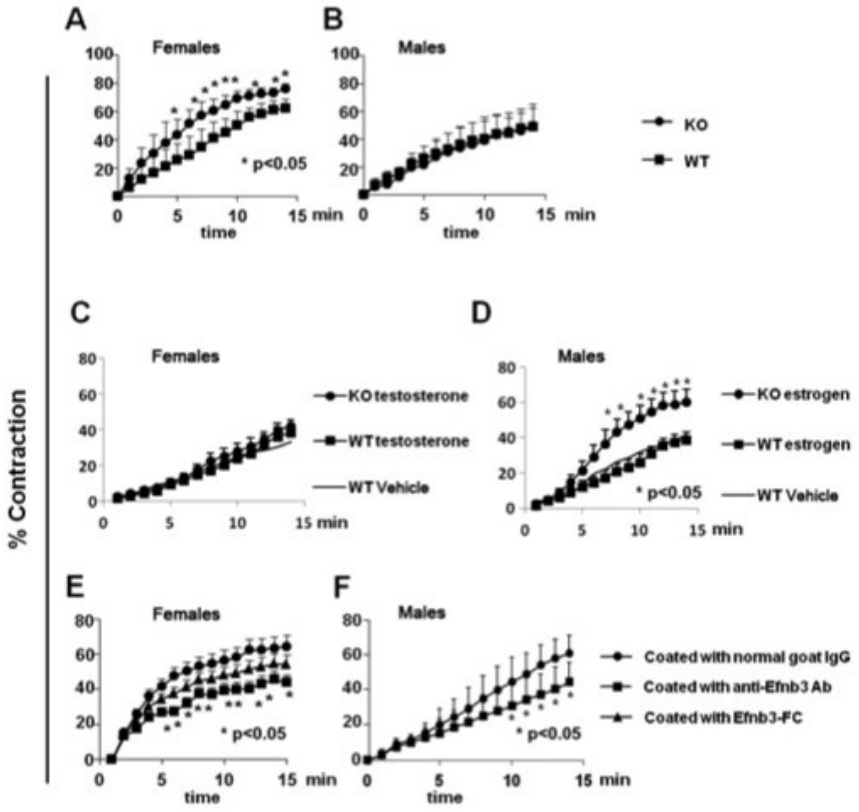

VSMC were isolated from the mesenteric arteries of WT and KO mice, and cultured for 4 days. They were stimulated with 20 μM PE at 37°C and imaged every min for 15 min. Means ± SD of percentage contraction of more than 15 cells are reported. Statistically significant differences were assessed by Student's *t* test. *p<0.05 (unpaired Student's *t* test). All experiments were conducted more than twice, and data from representative experiments are presented.

A *and* ***B****. Increased contractility of VSMC from female but not male Efnb3 KO mice*

VSMC from WT and KO females (A) and males (B) were cultured for 4 days, then stimulated with PE.

C*. Estrogen augments contractility of VSMC from male KO but not WT mice*

VSMC from WT and KO males were cultured in wells coated with anti-Efnb3 Ab (2 μg/ml during coating) for 4 days in the presence (10 μg/ml) estrogen, then stimulated with PE. The thin line (indicated as WT Vehicle) represents the mean percentage contraction of female WT

VSMC cultured in wells coated with anti-Efnb3 Ab in the presence of vehicle in lieu of testoterone (for a better visual effect, the SD of each time point in this control is omitted).

D. *Testosterone does not suppress contractility of VSMC from female KO or WT mice*

VSMC from WT and KO females were cultured in wells coated with anti-Efnb3 Ab for 4 days in the presence (10 μg/ml) of testosterone, then stimulated with PE. The thin line (indicated as WT Vehicle) represents the mean percentage contraction of male WT VSMC cultured in wells coated with anti-Efnb3 Ab in the presence of vehicle in lieu of estrogen (for a better visual effect, the SD of each time point in this control is omitted).

E *and* ***F***. *Reverse signalling through Efnb3 reduces VSMC contractility*

Wells were coated with goat-anti-Efnb3 Ab, normal goat IgG or Efnb3-Fc (2 μg/ml during coating). VSMC from WT females (E) and WT males (F) were cultured in these wells for 4 days, then stimulated with PE.

Figure 5 *Normal α_1-adrenoreceptor (AR) expression and Ca^{++} flux in Efnb3 KO VSMC*

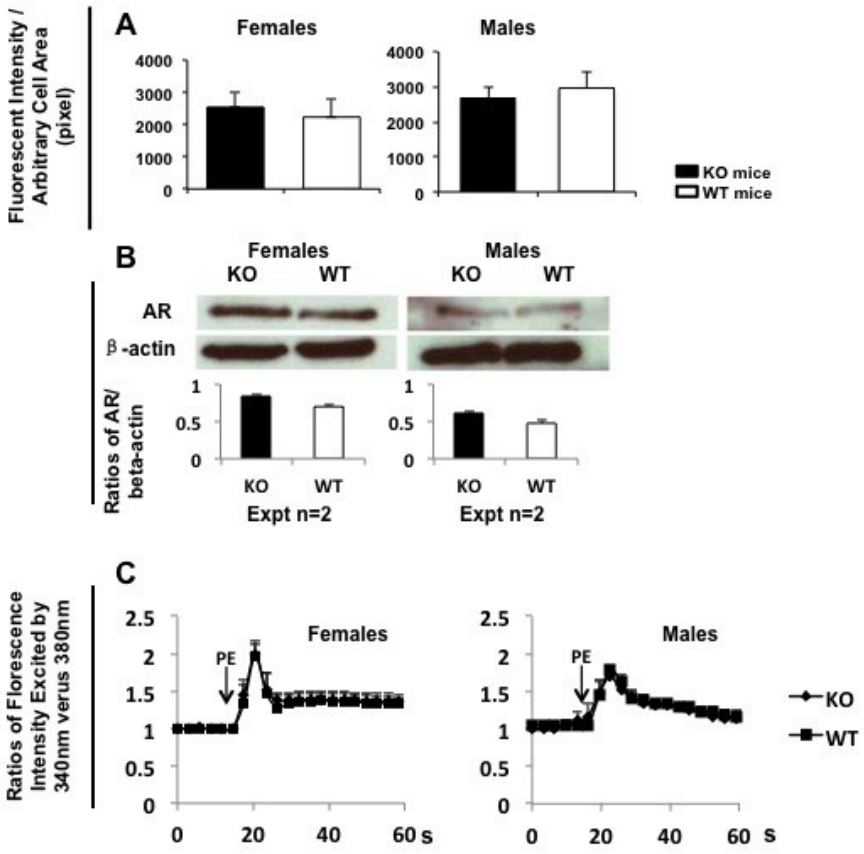

A. *Normal AR expression in Efnb3 KO VSMC according to immunofluorescence microscopy*
VSMC from male (right panel) and female (left panel) *Efnb3* KO or WT mice were cultured for 4 days, then stained with Ab against AR, as indicated. They were identified by anti-α-actin Ab staining. For each experiment, more than 15 α-actin-positive cells were randomly selected, and their total immunofluorescence intensity and cell size were recorded. Means ± SD of fluorescence intensity per unit of arbitrary cell area (pixel) of all cells in a group examined are reported.

B. *Normal AR expression in Efnb3 KO VSMC according to immunoblotting*
VSMC from male (right panel) and female (left panel) *Efnb3* KO and WT mice were cultured for 4 days, then harvested. Cell lysates were analyzed for AR expression by immunoblotting. A representative immunoblotting is shown. Densitometry data from two independent experiments were pooled and presented as bar graphs in the lower panel.

C. *Normal Ca^{++} flux in VSMC from Efnb3 KO mice*

VSMC from male (right panel) and female (left panel) *Efnb3* KO or WT mice were cultured for 4 days and loaded with Fura2. They were then placed in HBSS with or without 1.26 mM Ca^{++} at 37^{o}C and stimulated with PE. The ratio of emissions at 510 nm triggered by 340 nm versus 380 nm excitation in each cell was registered every 3 s for 1 min. Means $\pm$ SD of the ratio of more than 15 randomly-selected VSMC are reported. Arrows indicate the time points at which PE was added.

All experiments were conducted more than twice, and data from representative experiments are reported. They were analyzed by paired Student's *t* test, but no significant difference was found.

Figure 6 *MLC, MLCK and MLCP phosphorylation of small arteries and VSMC from WT and KO mice*

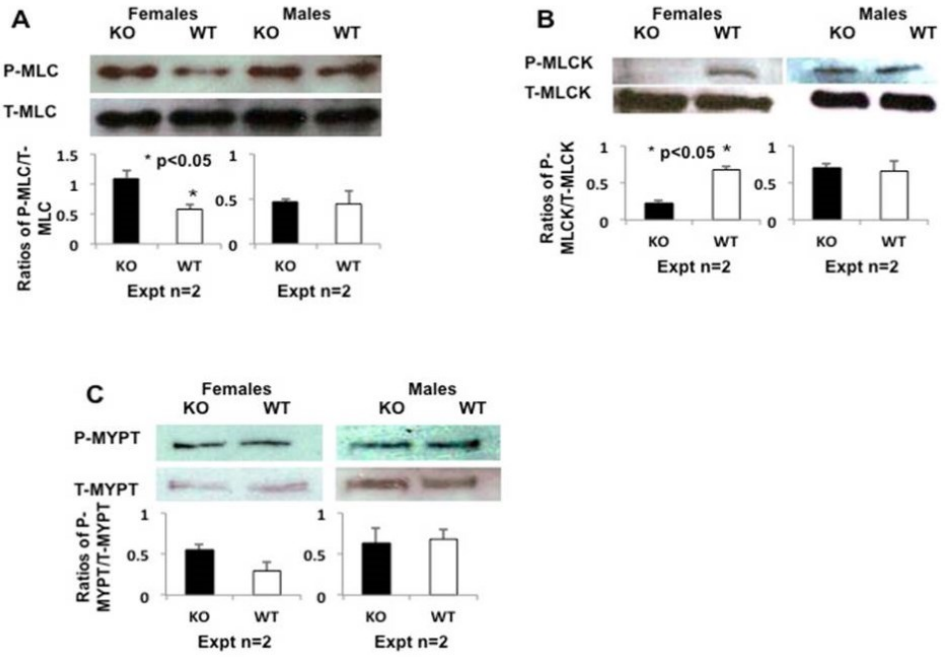

VSMC from female and male KO and WT mice were cultured for 4 days, then stimulated with 20 μM PE for 3 s and immediately lysed. Total and phosphorylated MLC, MLCK and MLCP were analyzed by immunoblotting. Immoblotting images from representative experiments are illustrated. The signal ratios of phosphorylated versus total MLC, MLCK and MLCP were quantified by densitometry. Densitometry data from two or more independent experiments (as indicated) were pooled and presented as bar graphs in the panels below the immunoblotting images. Paired Student's *t* tests were employed to examine statistical significant differences. "*" indicates $p<0.05$.

A. *Increased MLC phosphorylation in VSMC from female but not male Efnb3 KO mice*

B. *Reduced MLCK phosphorylation in VSMC from female but not male Efnb3 KO mice*

C. *Reduced MLCP phosphorylation in VSMC from female but not male Efnb3 KO mice*.

Figure 7 *Grip1 in the Efnb reverse signalling pathway in VSMC*

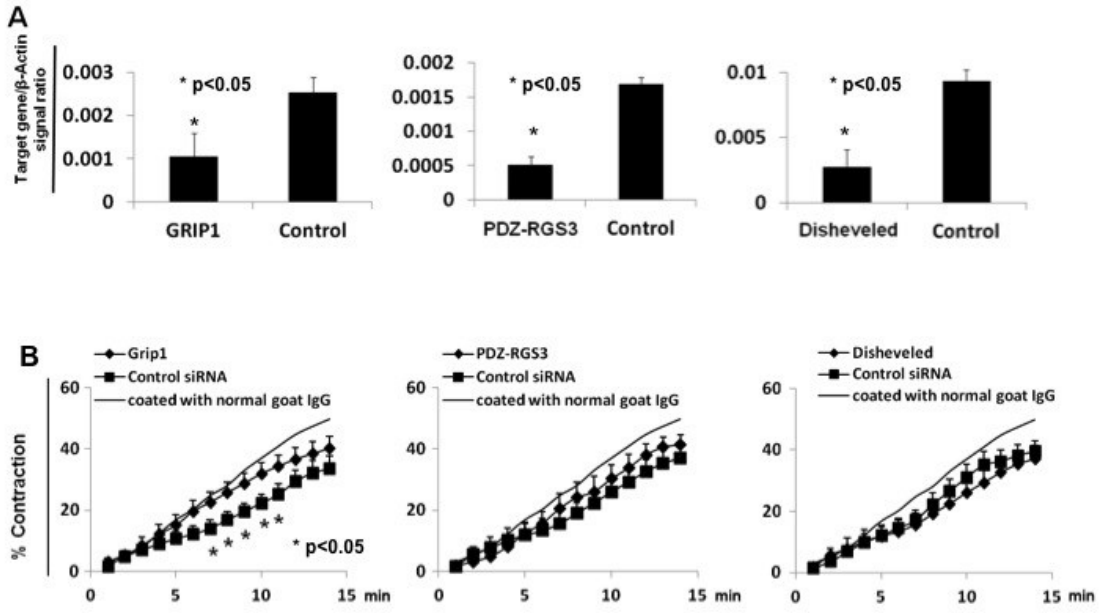

Experiments in this figure were repeated more than twice, and representative data are reported.

A. *Effective mRNA knockdown of Dishevelled, PDZ-RGS3 and Grip1 by siRNA*

Cultured WT VSMC were transfected with a mixture of siRNAs of a particular gene or control siRNA, as indicated. After 24-h culture, the cells were harvested and the mRNA expression of each gene was determined by RT-qPCR. The data are expressed as means ± SD of the ratios of the target gene signal versus the β-actin signal.

B. *Grip1 knockdown by siRNAs partially reverses the inhibitory effect of solid-phase Ephb6-Fc*

VSMC from WT males were cultured in wells coated with goat anti-mouse Efnb3 Ab (2 μg/ml). After 2 days, they were transfected with siRNAs targeting *Dishevelled, PDZ-RGS3* or *Grip1*, or with control siRNA. On day 4 of culture, they were stimulated with PE (20 μM), and their percentage contraction was recorded. Means ± SD of the percentage are reported. The thin lines (indicated as "coated with normal goat IgG") represent the mean percentage contraction of VSMC cultured in wells coated with normal goat IgG (2 μg/ml) without siRNA transfection (for a better visual effect, the SD of each time point in this control is omitted). *p< 0.05 according to paired Student's t test, between Grip1 siRNA- and control siRNA-transfected VSMC.

Figure 8 *BP-related hormone levels in Efnb3 KO mice*

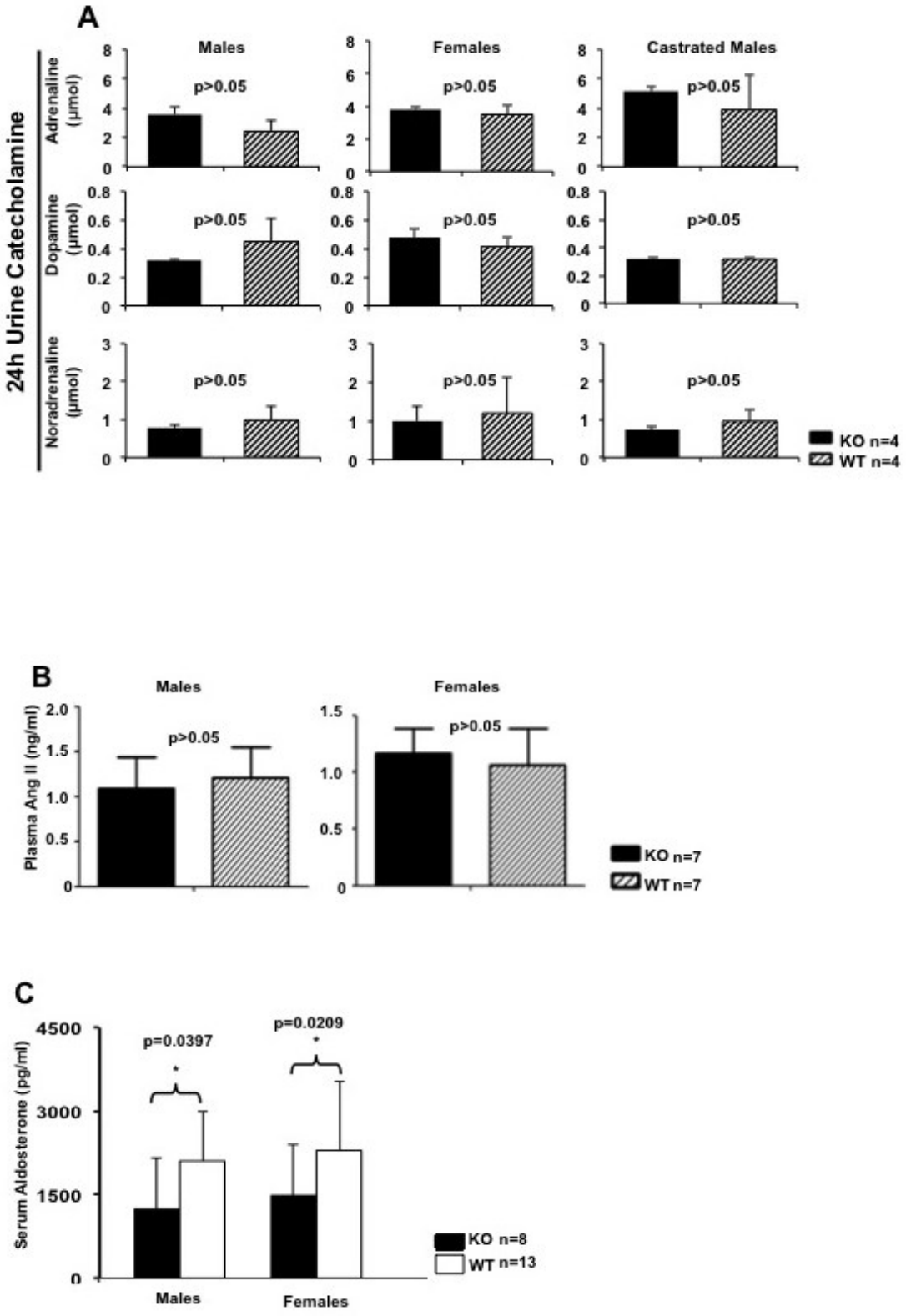

A. *Twenty-four-h urinary catecholamine levels in Efnb3 KO mice*

Male and female *Efnb3* KO and WT mice were placed in metabolic cages. Urine was collected during a 24-h fasting period. Urinary catecholamines were measured by ELISA, and means ± SD of hormones excreted during the 24-h period and mouse number per group (n) are presented. No statistically significant differences were found (unpaired Student's *t* test).

B *and* ***C***. *Plasma AngII and serum aldosterone levels in Efnb3 KO mice*

Plasma Ang II (B) and serum aldosterone (C) in male and female *Efnb3* KO and WT mice were measured by ELISA. Mouse numbers per group (n) are indicated. Means ± SD of hormone concentrations are reported. P-values are presented. *Significantly different ($p<0.05$, unpaired Student's *t* test).

Supplementary figure1. LocusZoom plots of –log$_{10}$ p-values (left hand vertical axis) from IBPC meta-analysis for specific queried genes

Supplementary Figure 1. LocusZoom plots of -log$_{10}$ p-values (left hand vertical axis) from IBPC meta-analysis of specific queried genes

The positions of all SNPs in the query are indicated at the top of the plot as short, thin vertical lines, and as diamonds and circles in the plots. Diamonds represent reference SNPs with the highest -log$_{10}$ p-value in the region, and their names are indicated above the diamonds. R^2 refers to LD between the reference SNP and respective SNPs within the region. Blue lines refer to recombination rates (right hand vertical axis) in centimorgans/megabase at each position. Thus, peaks in blue lines indicate low LD regions of high recombination rates or recombination hotspots.

Efnb2 region for diastolic BP

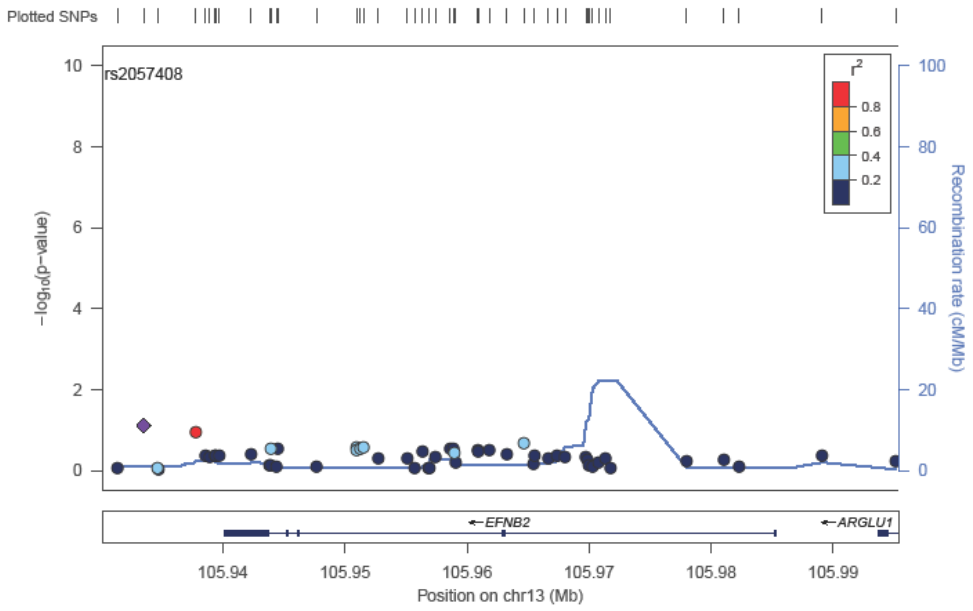

Efnb2 region for systolic BP

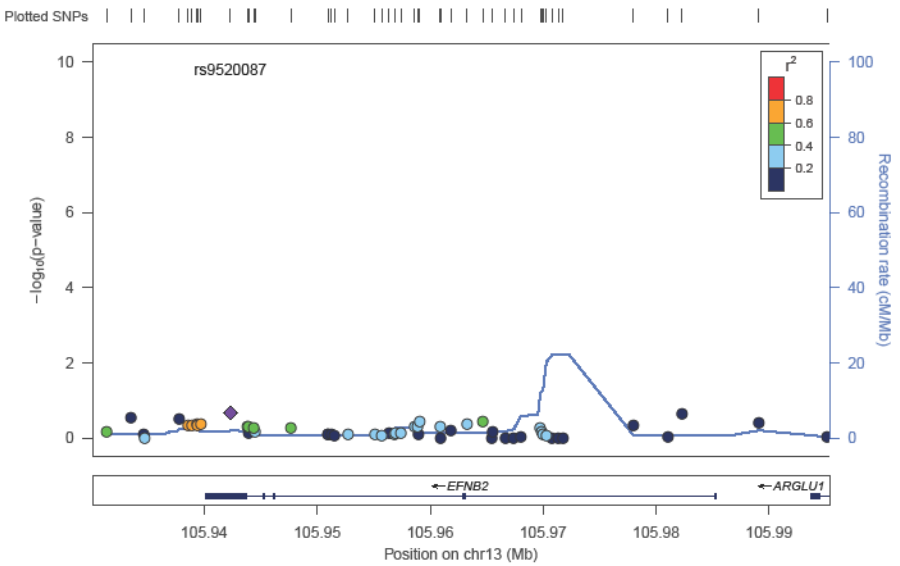

Efnb3 region for diastolic BP

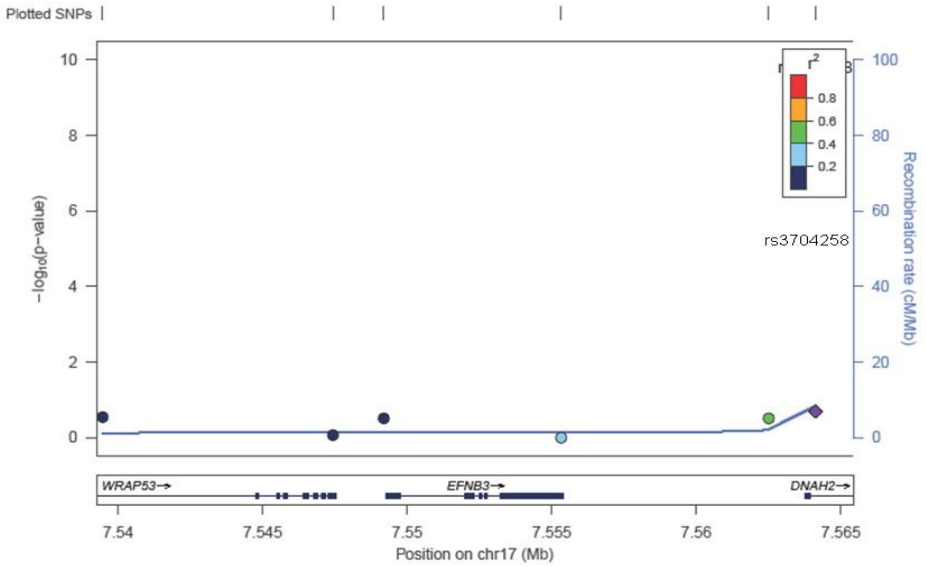

Efnb3 region for systolic BP

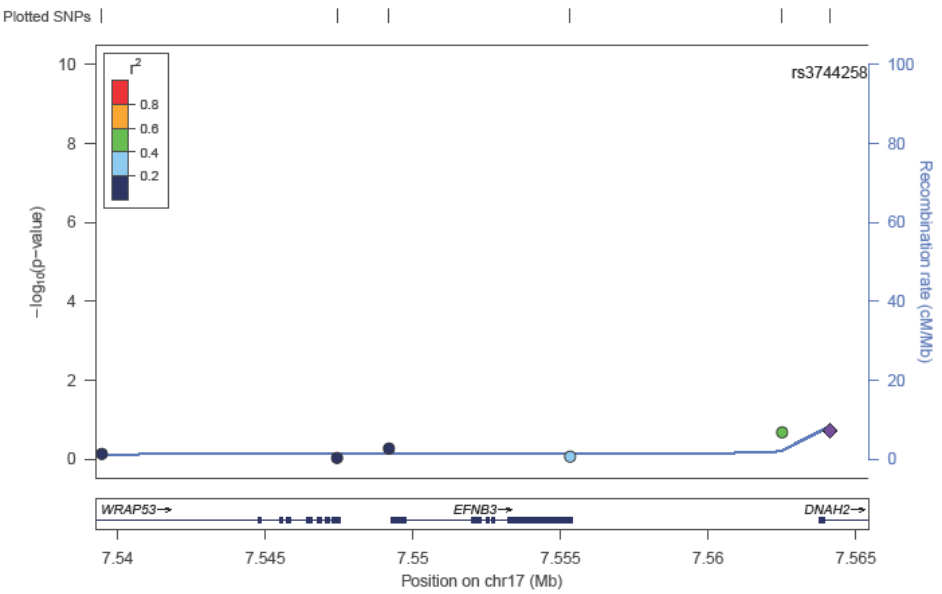

Ephb6 region for diastolic BP

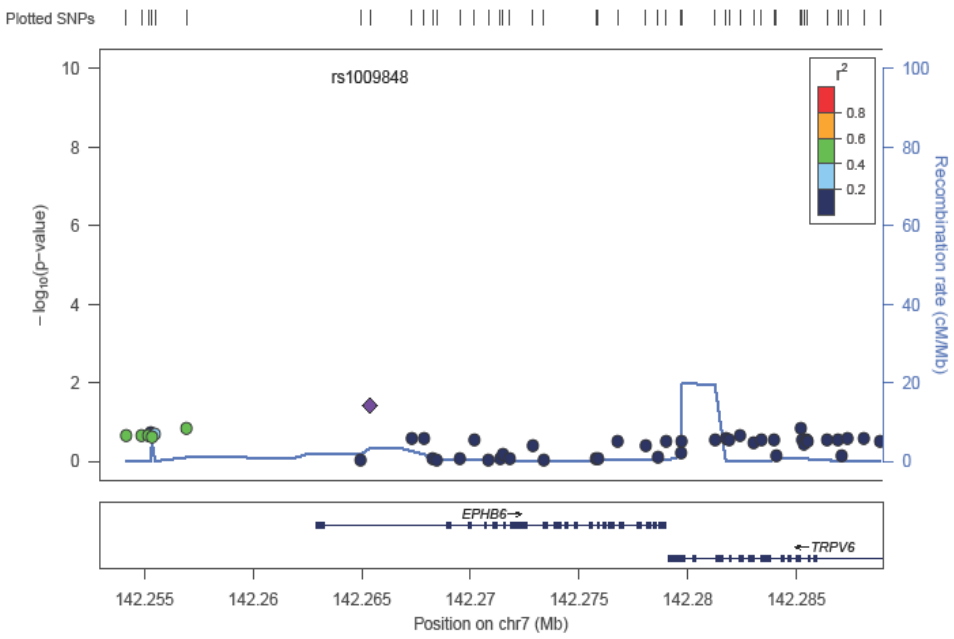

Ephb6 region for systolic BP

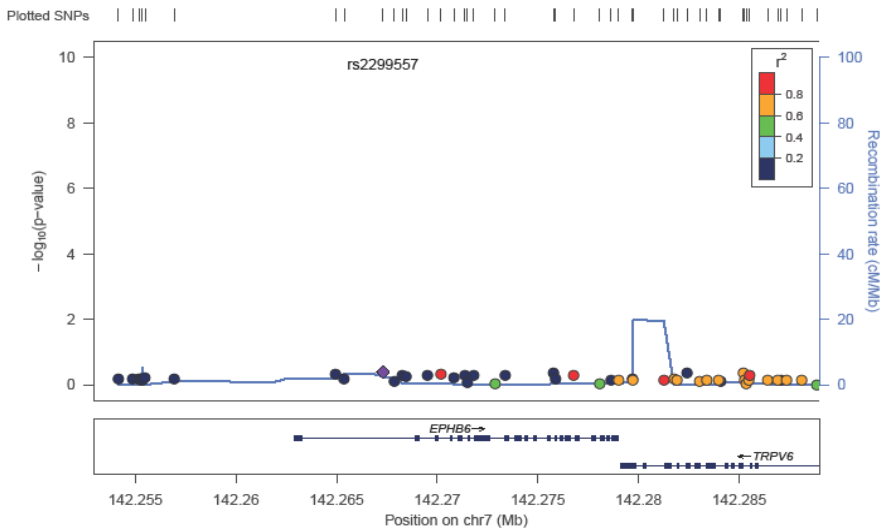

Grip1 region for diastolic BP

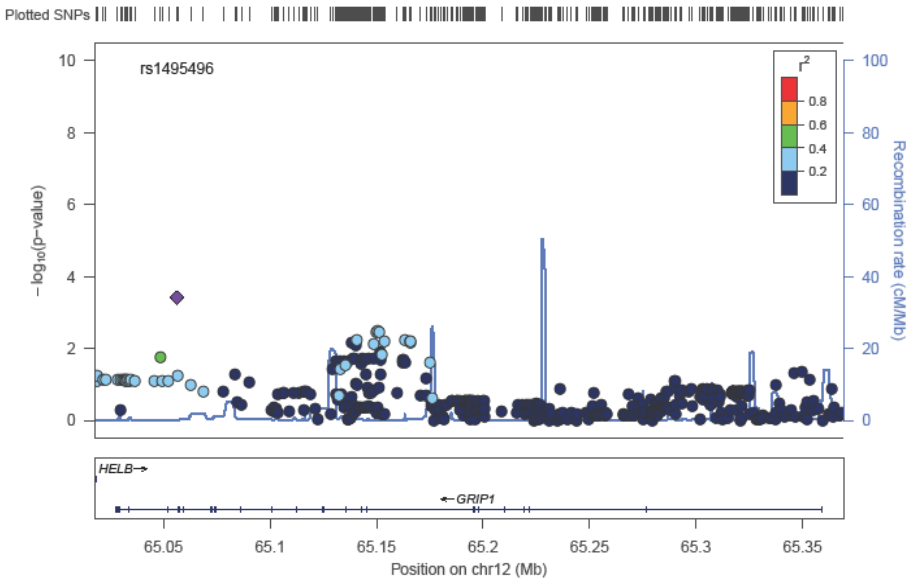

Grip1 region for systolic BP

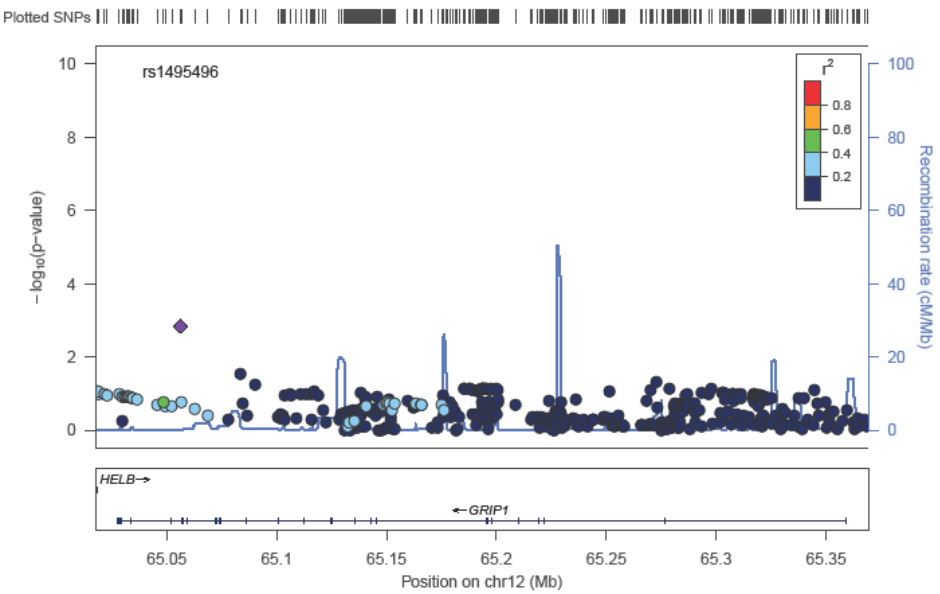
Plotted SNPs
rs1495496
r²
0.8
0.6
0.4
0.2
10
8
6
4
2
0
100
80
60
40
20
0
− log10(p−value)
Recombination rate (cM/Mb)
HELB→
←GRIP1
65.05
65.1
65.15
65.2
65.25
65.3
65.35
Position on chr12 (Mb)

III. Discussion

The etiology of essential hypertension remains unclear. Several models have been built for studying the mechanism of hypertension. The VSMC tone plays a basic role in regulating blood pressure[1,2].

Eph/Efnb family is the largest tyrosine kinase family, which plays many functions in physiological and pathological processes in cells[3] such as the cell migration, cancer pathogenesis, synapse development et al[4-6]. However, little work has been done in studying their roles in blood pressure control[7,8]. Thanks to the availability of different Ephs/Efnbs knockout mouse models, our studies could explore how Ephs and Efnbs influence the function of VSMCs with regard to blood pressure regulation[7,8].

Our study for the first time shows that certain Eph and Efnbs are involved in blood pressure by affecting the VSMC contractility[7,8]. We demonstrate that 1) the reverse signaling pathways from Ephb6 to Efnb1 and Efnb3 lead to the hyporesponsiveness of VSMC; 2) Ephb6 and Efnb3 act in concert with sex hormones to regulate blood ambient catecholamine levels, which are related to small artery vessel tone control; 3) Grip1 is the downstream signaling molecule of Ephb6/Efnb1/Efnb3 in regulating of VSMC contractility. A discussion is conducted below in an attempt to reconcile some seemingly controversial results, and to explain the overall physiological relevance necessity of the Eph/Efn system in the BP regulation.

1. Signaling pathways to regulate VSMC contractility

It is known that the contractility of VSMC is regulated by many signaling events[9]. The following diagram is based on available literature, our results and some reasoned speculations.

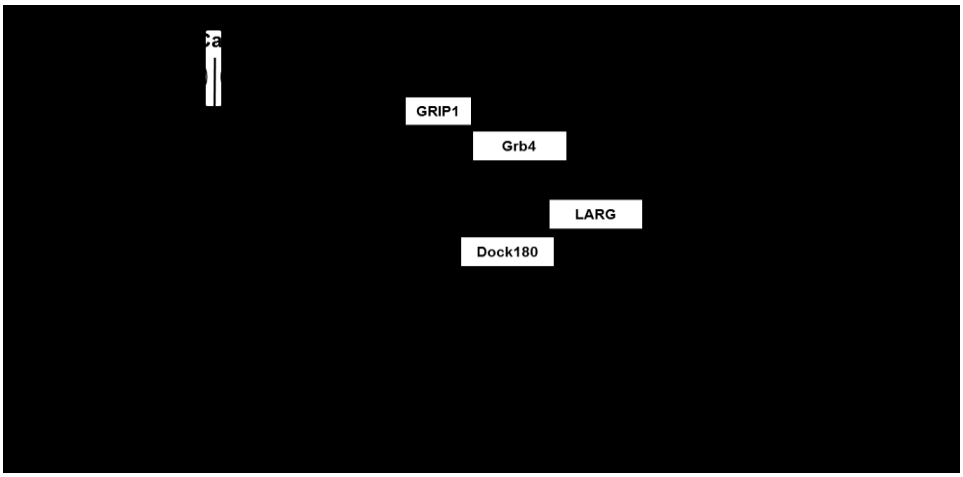

Figure 1 the contractile signaling pathway of VSMC

The diagram shows general signaling pathways, which are involved in the regulation of VSMCs contractility. Our results add two major new components to the known literature: the first is the reverse signaling pathway through Efnbs, which interact with Grip1 to regulate phosphorylation of MLC; the second is testosterone, which can regulate the expression of RhoA and Rho kinase. As the membrane-anchored protein, Efnb contains phosphorylation site[10] and PDZ-binding motif at its intracellular carboxyl terminus[4], which could interact with downstream proteins, such as Grb4, Dishevelled, DPZ-RGS3 and Grip1[11,12]. As an adapter protein, Grb4 associates Dock180, FAK through SH domains[11,13,14]. Cell migration is related to phosphorylated FAK through $p130^{CAS}$/Dock180/Rac1 signaling pathway[15], in which Dock180 serves as nucleotide exchange factors (GEFs) for Rho GTPase activation. RhoA takes the initial step of FAK, Dock180[16] to regulate cytoskeletal reorganization, actin polymerization and force generation in smooth muscle[17]. G-protein[18] is also essential in regulation of VSMC contractility[19,20]. Receptors couple with the G_q-G_{11} and G_{12}-G_{13} to stimulate phosphorylated MLC via Ca^{2+}/MLCK and Rho/ROCK respectively[21]. G_q-G_{11} stimulates cAMP production and PKA activation to maintain basal BP[22]; G_{12}-G_{13} promotes activated RhoA to enhance phosphorylation level of MLCP to regulate VSMC[23].

2. The hypotheses of how Eph/Efnb in concert with testosterone regulate VSMC functions

Under physiological conditions, the function of VSMC is tightly regulated[24,25]. The major function of VSMC is to generate tension to regulate blood circulation. The tension state of VSMC is mainly related to the phosphorylated MLC. The elevated phosphorylation level of MLC directly enhances the VSMC contractility. Our hypothesis is that EphB6 triggered-reverse signaling of Efnbs governs the VSMC contractility by regulating the phosphorylated MLC through RhoA-ROCK-MLCP signaling pathway; and Grip1 is the downstream protein in this process.

We also found that the effects of Ephb6 and Efnb3 deletion on males and females and on males and castrated males are different in terms of VSMC function and BP. Based on these findings and some literature, we come to the second hypothesis that the effect of testosterone is via its regulatory function on ROCK synthesis and activity[26], and consequently the RhoA activity to influence Phosphorylated MLC through RhoA-ROCK-MLCP signaling pathway.

3. Evidences supporting the hypothesis that the reverse signaling regulates the contractile phenotype

In EphB6 knockout mouse model, we found that the vasoconstriction, activated RhoA, and phosphorylated MLC were elevated in EphB6 female KO mice and castrated male KO mice, but no difference was observed in male KO mice. The EphB6-FC binds to all three Efnb ligands to active reverse signaling pathway, and the α-EphB6 induces the EphB6 forward signaling. In order to study each Eph/Efnb effects, α-EphB6 Ab, EphB6-FC and α-Efnb Abs were used in vitro. α-Ephb6 Ab or Ephb6-Fc were used for exploring the consequences of forward and reverse signaling. We demonstrated that 1) the Ephb6-Fc can significantly reduce the contraction of VSMC. 2) α-Ephb6 Ab stiumlation did not affect the contraction of VSMC.

In Efnb1, 3 KO mouse models, the vasoconstriction, activated RhoA and phosphorylated MLC were increased in Efnb3 female KO mice and Efnb1 castrated male KO mice (the female Efnb1KO mice die at embryonic stage[27]); the activated RhoA and phosphorylated MLC were increased in Efnb1 male KO mice. The α-Efnb1 Ab, α-Efnb3 Ab reduce the activated RhoA and VSMC contractility. These results demonstrate: 1) deletion of EphB6 causes the malfunction of VSMC; 2) the reverse signaling, but nor forward signaling, plays the dominant role in regulation of VSMC contractility[28] and RhoA promotes phosphorylation of MLC [7,8]; 3) there is gender difference.

4. Efnbs regulate RhoA-ROCK-MLCP signaling pathway

The vascular tone is generated by the phosphorylation of MLC, which conducts the myosin to interact with actin. Generally the MLC phosphorylation can be increased by two signaling pathways: 1) the activation of MLC kinase through the Ca^{2+} and calmodulin-dependent pathway[29]; 2) the inhibition of MLCP via the RhoA/ROCK pathway[30].

To address the role of MLCK and MLCP-mediated signaling pathways in regulation of vascular tone in Eph/Efnb KO mice, we examined the Ca^{2+} flux of EphB6, Efnb1 and Efnb3 KO VSMC. Our data showed that Ca^{2+} flux had not changed in EphB/Efnbs KO VSMC, suggesting the Ca^{2+} signaling was unaltered.

The phosphorylation of MYPT1 by RhoA/ROCK is well established. ROCK phosphorylates the MYPT1 at threonine 696, serine 854 and threonine 853 to inhibit MLCP activity[30]. In Efnb1, Efnb3 knockout mouse models, we found that activated RhoA and phosphorylated MLC were

elevated in male Efnb1 KO and female Efnb3 KO VSMC; phosphorylated MYPT1 was increased in Efnb3 KO mice. The α-Efnb1, α-Efnb3 stimulation showed the reduction of activated RhoA, phosphorylated MYPT1 and contractility in VSMCs. The work demonstrates that Efnb1, 3 reduce activated RhoA, which influences phosphorylation level of MLCP, leading to the reduction of phosphorylated MLC.

To conclude, these results support our hypothesis that reverse signaling of Efnb1, 3 governs the VSMC contractility by regulating the phosphorylated MLC through RhoA-ROCK-MLCP signaling pathway.

5. The effect of Grip1 in VSMC

To validate the relevance of Grip1 in humans, we targeted single nucleotide polymorphisms (SNPs) with *grip1* gene to compare the international blood pressure consortium dataset, showing that the p-value of *Grip1* gene (p=0.000389) reaches to critical point (p=0.000302), suggesting that Grip1 is related to the BP. To address whether Grip1 influences VSMC contraction, we examined the VSMC treated with *Grip1* siRNA. We found that cell contraction, activated RhoA, phosphorylated MLC and phosphorylated MLCP was elevated, suggesting that Grip1 is involved in regulation of VSMC. However, how Grip1 interacts with Efnbs to regulate VMSC is unclear. The Efnb contains PDZ-binding motif at its intracellular carboxyl terminus, which is the function domain to interact with Grip1. As a cytoplasmic scaffolding protein containing of seven PDZ domains, the Grip1 interacts with PDZ-binding motif of Efnbs to contribute Efnb clustering and trafficking[10]. The deletion of Grip1 weakens the reverse signaling of Efnbs, augments phosphorylated MLC and hence VSMC contractility[10].

6. The role of EphB forward signaling in VSMC

The effect of forward signaling is unclear in regulation of vasoconstriction. We found that EphB6 female KO mice show the elevated BP; EphB6Δ KO mice (lack forward signaling function of EphB6) show normal BP, suggesting that forward signaling of EphB6 does not alter the BP. However the EphB4 KO mice showed decreased BP and vasoconstriction (data unpublished), suggesting that forward signaling of EphB4 promotes the BP. We also demonstrated that α-Ephb6 Ab did not change VSMC contractility and α-Ephb4 Ab reduced VSMC constrictility. The EphB4 inhibitor suppresses VSMC contractility and phoshporylated

MLC in vitro (unpublished). Data indicates that EphBs exhibit different functions in VSMC. Further study will explore the different functions between EphBs.

7. The hypothesis that the effect of testosterone on VSMC is via its regulatory function on RhoA synthesis and activity

We confirmed that sex hormone is crucial in EphB/Efnb KO mice in regulation of BP that phenotypes are different between male, female and castrated male KO mice[7,8]. As mentioned before, the castrated EphB6 KO male, Efnb3 KO female mice showed elevation of BP, vasoconstriction, phosphorylated MLC and activated RhoA. However Efnb3 KO male and Efnb1 KO male mice showed normal BP, even EphB6 KO male mice showed lower BP comparing with WT control mice. The following table presents the phenotypes in accordance with differnet gender.

	EphB6 KO			**Efnb3 KO**		**Efnb1 KO**	
	Male	Female	Castrated-male	Male	Female	Male	Castrated-male
Blood pressure	-	-	+	-	+	-	-
Vasoconstriction	↓	+	+	-	+	-	+
Phosphorylated MLC	-	+	+	-	+	+	+
Activated RhoA	-	+	+	-	+	+	+

↓ Decrease - Normal + Increase

In EphB6 KO mice, only castrated males have high blood pressure, indicating that sex hormones act in concert with Ephb6 to regulate blood pressure. Why do only EphB6 KO castrated male mice show increased BP? In theory, the deletion of EphB6 receptor will enhance the VSMC contractile phenotype and result in increased BP in EphB6 KO mice. However, BP is a tightly-controlled physiological parameter with many compensatory feedback mechanisms. In EphB6 KO female mice, there might be some in vivo compensatory mechanisms to maintain the normal BP. In EphB6 KO male mice, we found that the ambient catecholamine release by the adrenal glands is reduced after Ephb6 deletion. This is at least one of the reasons why the EphB6 KO male mice does not show increased phosphorylated-MLC, vessel constriction and avtivated RhoA. In Efnb1, 3 KO mice, the elevated BP was found only in female Efnb3 KO mice (the female Efnb1 KO is embryonic lethal), suggesting that testosterone play the important role in

regulation of BP[28]. We also demonstrate that EphB6, Efnb3 KO VSMC shows significant less contraction in the presence of exogenous testosterone but not estrgen.

Previous data confirms that the EphB6, Efnb1, Efnb3 KO mice model are associated with an upregulation of RhoA/ROCK/MLCP signaling. In diabete mouse model, testosterone showed the suppression of activated RhoA and expression of ROCK. We speculate that testosterone plays the similar function in Eph/Efnb KO mice to maintain the normal BP. However much work should be done to explore the role of testosterone in VSMC how the deletion of Eph/Efnb influence the testosteone function? What is the exact signaling pathway between Eph/Efnb and testosterone ?

8. An attempt to reconcile some controversial findings in our study

In our studies, VSMC from Efnb1 KO but not EphB6 male mice show elevated MLC phosphorylation; in spite that testosterone should have the same effect on these KO male mice in terms of maintaining MLC phosphorylation and RhoA activity. There could be 2 possible explanations. Firstly, the Enfb1 plays a dominant role in regulating VSMC among three different Efnbs. We demonstrated that VSMC respond differently depending on antibodies against different Efnbs. The α-Efnb1 Ab is more potent than α-Efnb3 Ab in reducing the contractility of VSMC. In EphB6 KO male mice, a reduced reverse signaling through Efnb1 could be compensated by other EphBs. So, the BP phenotype is not overt. In the Efnb1 KO male mice, the major reverse signaling is affected; hence the elevated BP. Secondly, the reverse but nor forward signaling is important in regulating contractile of VSMC. The deletion of Efpb6 causes the removal of forward signaling (through EphB6) but still retains the reverse signaling caused by other EphBs. On the contrary, the deletion of Efnb1 leads to the removal of reverse signaling through Efnb1 but remains the forward signaling caused by other Efnbs. So, without the suppressive effect of Efnb1 via reverse signaling in Efnb1 KO VSMC, MLC phosphorylation and RhoA activation are elevated in Efnb1 KO VSMC, which leads to increased BP.

VSMC show elevated contractility after Grip1 knock down. The exact signaling pathway remains to be defined. A possible mechanism is that Grip1 interacts with Efnb1, 3 by its PDZ domain. The interaction leads to the enhanced phosphorylation of Efnb1, 3 and causes the redistribution on cell membrane. The phosphorylation and redistribution of Efnb1, 3 could form larger clusters, which could produce stronger reverse signaling to downstream proteins[31-33].

Therefore, the silence of Grip1 equals to blocking the reverse signaling pathway and enhances the VSMC contractility phenotype.

9. A brief summary

Hypertension is a complex, multifactorial and polygenic disease. Over last decade many genetic determinants have been dissected. However the understanding of mechanism still needs further exploration. This study identified a new function of Eph/Efn in vasoconstriction and BP regulation. The successful disclosure of the relationship between Eph/Efnb and testosterone enhances the understanding of BP regulation mechanisms.

10. Contribution to sciences and future research directions

The major contributions to sciences from my Ph.D. program are as follows:

1. For the first time we revealed that in EphB/Efnb can regulate blood pressue.
2. We demonstrated that Eph/Efnb reverse signaling is dominant in the regulation of vascular smooth muscle cell contractility. The phosphorylation of MLC is increased in the absent of Ephb6 or Efnb1 in vivo. The Grip1 is involved in this process.

Some interesting questions remain to be further investigated.

1. Can antagonists of Eph/Efnb be employed to treat or prevent hypertension?
2. What are the downstream target proteins, which directly link Efn to MLC phosphorylation?
3. Does testosterone involve signaling pathways other than ROCK/RhoA-MLCP-MLC and act in concert with Eph/Efn to regulate blood pressure?

Reference list

1. Carretero, O. A. & Oparil, S. Essential Hypertension: Part I: Definition and Etiology. *Circulation* **101,** 329–335 (2000).
2. Takahashi, H., Yoshika, M., Komiyama, Y. & Nishimura, M. The central mechanism underlying hypertension: a review of the roles of sodium ions, epithelial sodium channels, the renin-angiotensin-aldosterone system, oxidative stress and endogenous digitalis in the brain. *Hypertens. Res.* **34,** 1147–1160 (2011).
3. Pasquale, E. B. Eph receptors and ephrins in cancer: bidirectional signalling and beyond. *Nat. Rev. Cancer* **10,** 165–180 (2010).
4. Miao, H. & Wang, B. Eph/ephrin signaling in epithelial development and homeostasis. *The International Journal of Biochemistry & Cell Biology* **41,** 762–770 (2009).
5. Côté, J.-F. & Vuori, K. GEF what? Dock180 and related proteins help Rac to polarize cells in new ways. *Trends in Cell Biology* **17,** 383–393 (2007).
6. Kullander, K. & Klein, R. Mechanisms and functions of Eph and ephrin signalling. *Nat Rev Mol Cell Biol* **3,** 475–486 (2002).
7. Wu, Z. *et al.* Possible role of Efnb1 protein, a ligand of Eph receptor tyrosine kinases, in modulating blood pressure. *J. Biol. Chem.* **287,** 15557–15569 (2012).
8. Luo, H. *et al.* Receptor tyrosine kinase Ephb6 regulates vascular smooth muscle contractility and modulates blood pressure in concert with sex hormones. *J. Biol. Chem.* **287,** 6819–6829 (2012).
9. Sobue, K., Hayashi, K. & Nishida, W. Expressional regulation of smooth muscle cell-specific genes in association with phenotypic modulation. *Mol. Cell. Biochem.* **190,** 105–118 (1999).
10. Bong, Y.-S. *et al.* Tyr-298 in ephrinB1 is critical for an interaction with the Grb4 adaptor protein. *Biochem. J.* **377,** 499–507 (2004).
11. Cowan, C. A. & Henkemeyer, M. The SH2/SH3 adaptor Grb4 transduces B-ephrin reverse signals. *Nature* **413,** 174–179 (2001).
12. Pasquale, E. B. Eph-Ephrin Bidirectional Signaling in Physiology and Disease. *Cell* **133,** 38–52 (2008).
13. Xu, N.-J. & Henkemeyer, M. Ephrin-B3 reverse signaling through Grb4 and cytoskeletal

regulators mediates axon pruning. *Nature Neuroscience* **12,** 268–276 (2009).

14. Coutinho, S. *et al.* Characterization of Ggrb4, an adapter protein interacting with Bcr-Abl. *Blood* **96,** 618–624 (2000).
15. Deramaudt, T. B. *et al.* FAK phosphorylation at Tyr-925 regulates cross-talk between focal adhesion turnover and cell protrusion. *Mol. Biol. Cell* **22,** 964–975 (2011).
16. Siu, M. K. *et al.* The β1-integrin-p-FAK-p130Cas-DOCK180-RhoA-vinculin is a novel regulatory protein complex at the apical ectoplasmic specialization in adult rat testes. *Spermatogenesis* **1,** 73–86 (2011).
17. Zhang, W., Huang, Y. & Gunst, S. J. The small GTPase RhoA regulates the contraction of smooth muscle tissues by catalyzing the assembly of cytoskeletal signaling complexes at membrane adhesion sites. *J. Biol. Chem.* **287,** 33996–34008 (2012).
18. Chiba, Y. & Misawa, M. Increased expression of G12 and G13 proteins in bronchial smooth muscle of airway hyperresponsive rats. *Inflamm. Res.* **50,** 333–336 (2001).
19. Wirth, A. *et al.* G12-G13–LARG–mediated signaling in vascular smooth muscle is required for salt-induced hypertension. *Nature Medicine* **14,** 64–68 (2007).
20. McGraw, D. W. *et al.* Crosstalk between Gi and Gq/Gs pathways in airway smooth muscle regulates bronchial contractility and relaxation. *J. Clin. Invest.* **117,** 1391–1398 (2007).
21. 56343 629..635. *Sandrine* 1–7 (2002).
22. Wirth, A. Rho kinase and hypertension. *BBA - Molecular Basis of Disease* **1802,** 1276–1284 (2010).
23. Hajicek, N. *et al.* Identification of critical residues in G(alpha)13 for stimulation of p115RhoGEF activity and the structure of the G(alpha)13-p115RhoGEF regulator of G protein signaling homology (RH) domain complex. *J. Biol. Chem.* **286,** 20625–20636 (2011).
24. Carmeliet, P. & Jain, R. K. Molecular mechanisms and clinical applications of angiogenesis. *Nature* **473,** 298–307 (2011).
25. Walsh, D. A. Pathophysiological mechanisms of angiogenesis. *Adv Clin Chem* **44,** 187–221 (2007).
26. Zhang, X.-H., Melman, A. & Disanto, M. E. Update on corpus cavernosum smooth

muscle contractile pathways in erectile function: a role for testosterone? *J Sex Med* **8,** 1865–1879 (2011).

27. Davy, A., Aubin, J. & Soriano, P. Ephrin-B1 forward and reverse signaling are required during mouse development. *Genes & Development* **18,** 572–583 (2004).
28. Wingard, C. J., Johnson, J. A., Holmes, A. & Prikosh, A. Improved erectile function after Rho-kinase inhibition in a rat castrate model of erectile dysfunction. *Am. J. Physiol. Regul. Integr. Comp. Physiol.* **284,** R1572–9 (2003).
29. Jackson, W. F. Ion Channels and Vascular Tone. *Hypertension* **35,** 173–178 (2000).
30. Puetz, S., Lubomirov, L. T. & Pfitzer, G. Regulation of Smooth Muscle Contraction by Small GTPases. *Physiology* **24,** 342–356 (2009).
31. Bochenek, M. L., Dickinson, S., Astin, J. W., Adams, R. H. & Nobes, C. D. Ephrin-B2 regulates endothelial cell morphology and motility independently of Eph-receptor binding. *Journal of Cell Science* **123,** 1235–1246 (2010).
32. TORRES, R. PDZ Proteins Bind, Cluster, and Synaptically Colocalize with Eph Receptors and Their Ephrin Ligands. *Neuron* **21,** 1453–1463 (1998).
33. Im, Y. J. Crystal Structure of GRIP1 PDZ6-Peptide Complex Reveals the Structural Basis for Class II PDZ Target Recognition and PDZ Domain-mediated Multimerization. *Journal of Biological Chemistry* **278,** 8501–8507 (2002).